# International Journal on Advances in Networks and Services


2014 vol. 7 nr. 1&2

The *International Journal on Advances in Networks and Services* is published by IARIA.
ISSN: 1942-2644
journals site: http://www.iariajournals.org
contact: petre@iaria.org



Sponsored by IARIA
www.iaria.org

**International Journal on Advances in Networks and Services**
**Volume 7, Number 1 & 2, 2014**

Christos Bouras, University of Patras, Greece
David Boyle, Tyndall National Institute, University College Cork, Ireland
Mahmoud Brahimi, University of Msila, Algeria
Marco Bruti, Telecom Italia Sparkle S.p.A., Italy
Dumitru Burdescu, University of Craiova, Romania
Diletta Romana Cacciagrano, University of Camerino, Italy
Maria-Dolores Cano, Universidad Politécnica de Cartagena, Spain
Juan-Vicente Capella-Hernández, Universitat Politècnica de València, Spain
Eduardo Cerqueira, Federal University of Para, Brazil
Patryk Chamuczyński, Radytek, Poland
Bruno Chatras, Orange Labs, France
Marc Cheboldaeff, T-Systems International GmbH, Germany
Kong Cheng, Telcordia Research, USA
Dickson Chiu, Dickson Computer Systems, Hong Kong
Andrzej Chydzinski, Silesian University of Technology, Poland
Hugo Coll Ferri, Polytechnic University of Valencia, Spain
Noelia Correia, University of the Algarve, Portugal
Noël Crespi, Institut Telecom, Telecom SudParis, France
Paulo da Fonseca Pinto, Universidade Nova de Lisboa, Portugal
Philip Davies, Bournemouth and Poole College / Bournemouth University, UK
Carlton Davis, École Polytechnique de Montréal, Canada
Claudio de Castro Monteiro, Federal Institute of Education, Science and Technology of Tocantins, Brazil
João Henrique de Souza Pereira, University of São Paulo, Brazil
Javier Del Ser, Tecnalia Research & Innovation, Spain
Behnam Dezfouli, Universiti Teknologi Malaysia (UTM), Malaysia
Daniela Dragomirescu, LAAS-CNRS, University of Toulouse, France
Jean-Michel Dricot, Université Libre de Bruxelles, Belgium
Wan Du, Nanyang Technological University (NTU), Singapore
Matthias Ehmann, Universität Bayreuth, Germany
Wael M El-Medany, University Of Bahrain, Bahrain
Imad H. Elhajj, American University of Beirut, Lebanon
Gledson Elias, Federal University of Paraíba, Brazil
Joshua Ellul, University of Malta, Malta
Rainer Falk, Siemens AG - Corporate Technology, Germany
Károly Farkas, Budapest University of Technology and Economics, Hungary
Huei-Wen Ferng, National Taiwan University of Science and Technology - Taipei, Taiwan
Gianluigi Ferrari, University of Parma, Italy
Mário F. S. Ferreira, University of Aveiro, Portugal
Bruno Filipe Marques, Polytechnic Institute of Viseu, Portugal
Ulrich Flegel, HFT Stuttgart, Germany
Juan J. Flores, Universidad Michoacana, Mexico
Ingo Friese, Deutsche Telekom AG - Berlin, Germany
Sebastian Fudickar, University of Potsdam, Germany
Stefania Galizia, Innova S.p.A., Italy
Ivan Ganchev, University of Limerick, Ireland
Miguel Garcia, Universitat Politecnica de Valencia, Spain

Emiliano Garcia-Palacios, Queens University Belfast, UK
Gordana Gardasevic, University of Banja Luka, Bosnia and Herzegovina
Marc Gilg, University of Haute-Alsace, France
Debasis Giri, Haldia Institute of Technology, India
Markus Goldstein, DFKI (German Research Center for Artificial Intelligence GmbH), Germany
Luis Gomes, Universidade Nova Lisboa, Portugal
Anahita Gouya, Solution Architect, France
Mohamed Graiet, Institut Supérieur d'Informatique et de Mathématique de Monastir, Tunisie
Christos Grecos, University of West of Scotland, UK
Vic Grout, Glyndwr University, UK
Yi Gu, Middle Tennessee State University, USA
Angela Guercio, Kent State University, USA
Xiang Gui, Massey University, New Zealand
Mina S. Guirguis, Texas State University - San Marcos, USA
Tibor Gyires, School of Information Technology, Illinois State University, USA
Keijo Haataja, University of Eastern Finland, Finland
Gerhard Hancke, Royal Holloway / University of London, UK
R. Hariprakash, Arulmigu Meenakshi Amman College of Engineering, Chennai, India
Go Hasegawa, Osaka University, Japan
Eva Hladká, CESNET & Masaryk University, Czech Republic
Hans-Joachim Hof, Munich University of Applied Sciences, Germany
Razib Iqbal, Amdocs, Canada
Abhaya Induruwa, Canterbury Christ Church University, UK
Muhammad Ismail, University of Waterloo, Canada
Vasanth Iyer, Florida International University, Miami, USA
Peter Janacik, Heinz Nixdorf Institute, University of Paderborn, Germany
Robert Janowski, Warsaw School of Computer Science, Poland
Imad Jawhar, United Arab Emirates University, UAE
Aravind Kailas, University of North Carolina at Charlotte, USA
Mohamed Abd rabou Ahmed Kalil, Ilmenau University of Technology, Germany
Kyoung-Don Kang, State University of New York at Binghamton, USA
Omid Kashefi, Iran University of Science and Technology, Iran
Sarfraz Khokhar, Cisco Systems Inc., USA
Vitaly Klyuev, University of Aizu, Japan
Jarkko Kneckt, Nokia Research Center, Finland
Dan Komosny, Brno University of Technology, Czech Republic
Ilker Korkmaz, Izmir University of Economics, Turkey
Tomas Koutny, University of West Bohemia, Czech Republic
Evangelos Kranakis, Carleton University - Ottawa, Canada
Lars Krueger, T-Systems International GmbH, Germany
Kae Hsiang Kwong, MIMOS Berhad, Malaysia
KP Lam, University of Keele, UK
Birger Lantow, University of Rostock, Germany
Hadi Larijani, Glasgow Caledonian Univ., UK
Annett Laube-Rosenpflanzer, Bern University of Applied Sciences, Switzerland
Angelos Lazaris, University of Southern California (USC), USA

Gyu Myoung Lee, Institut Telecom, Telecom SudParis, France
Ying Li, Peking University, China
Shiguo Lian, Orange Labs Beijing, China
Chiu-Kuo Liang, Chung Hua University, Hsinchu, Taiwan
Wei-Ming Lin, University of Texas at San Antonio, USA
David Lizcano, Universidad a Distancia de Madrid, Spain
Chengnian Long, Shanghai Jiao Tong University, China
Jonathan Loo, Middlesex University, UK
Edmo Lopes Filho, Algar Telecom, Brazil
Pascal Lorenz, University of Haute Alsace, France
Albert A. Lysko, Council for Scientific and Industrial Research (CSIR), South Africa
Pavel Mach, Czech Technical University in Prague, Czech Republic
Elsa María Macías López, University of Las Palmas de Gran Canaria, Spain
Damien Magoni, University of Bordeaux, France
Ahmed Mahdy, Texas A&M University-Corpus Christi, USA
Zoubir Mammeri, IRIT - Paul Sabatier University - Toulouse, France
Gianfranco Manes, University of Florence, Italy
Sathiamoorthy Manoharan, University of Auckland, New Zealand
Moshe Timothy Masonta, Council for Scientific and Industrial Research (CSIR), Pretoria, South Africa
Hamid Menouar, QU Wireless Innovations Center - Doha, Qatar
Guowang Miao, KTH, The Royal Institute of Technology, Sweden
Mohssen Mohammed, University of Cape Town, South Africa
Miklos Molnar, University Montpellier 2, France
Lorenzo Mossucca, Istituto Superiore Mario Boella, Italy
Jogesh K. Muppala, The Hong Kong University of Science and Technology, Hong Kong
Katsuhiro Naito, Mie University, Japan
Deok Hee Nam, Wilberforce University, USA
Sarmistha Neogy, Jadavpur University- Kolkata, India
Rui Neto Marinheiro, Instituto Universitário de Lisboa (ISCTE-IUL), Instituto de Telecomunicações, Portugal
David Newell, Bournemouth University - Bournemouth, UK
Armando Nolasco Pinto, Universidade de Aveiro / Instituto de Telecomunicações, Portugal
Jason R.C. Nurse, University of Oxford, UK
Kazuya Odagiri, Yamaguchi University, Japan
Máirtín O'Droma, University of Limerick, Ireland
Rainer Oechsle, University of Applied Science, Trier, Germany
Henning Olesen, Aalborg University Copenhagen, Denmark
Jose Oscar Fajardo, University of the Basque Country, Spain
Constantin Paleologu, University Politehnica of Bucharest, Romania
Eleni Patouni, National & Kapodistrian University of Athens, Greece
Harry Perros, NC State University, USA
Miodrag Potkonjak, University of California - Los Angeles, USA
Yusnita Rahayu, Universiti Malaysia Pahang (UMP), Malaysia
Yenumula B. Reddy, Grambling State University, USA
Oliviero Riganelli, University of Milano Bicocca, Italy
Patrice Rondao Alface, Alcatel-Lucent Bell Labs, Belgium
Teng Rui, National Institute of Information and Communication Technology, Japan

Antonio Ruiz Martinez, University of Murcia, Spain
George S. Oreku, TIRDO / North West University, Tanzania/ South Africa
Sattar B. Sadkhan, Chairman of IEEE IRAQ Section, Iraq
Husnain Saeed, National University of Sciences & Technology (NUST), Pakistan
Addisson Salazar, Universidad Politecnica de Valencia, Spain
Sébastien Salva, University of Auvergne, France
Ioakeim Samaras, Aristotle University of Thessaloniki, Greece
Luz A. Sánchez-Gálvez, Benemérita Universidad Autónoma de Puebla, México
Teerapat Sanguankotchakorn, Asian Institute of Technology, Thailand
José Santa, University of Murcia, Spain
Rajarshi Sanyal, Belgacom International Carrier Services, Belgium
Mohamad Sayed Hassan, Orange Labs, France
Thomas C. Schmidt, HAW Hamburg, Germany
Hans Scholten, Pervasive Systems / University of Twente, The Netherlands
Véronique Sebastien, University of Reunion Island, France
Jean-Pierre Seifert, Technische Universität Berlin & Telekom Innovation Laboratories, Germany
Sandra Sendra Compte, Polytechnic University of Valencia, Spain
Dimitrios Serpanos, Univ. of Patras and ISI/RC ATHENA, Greece
Xu Shao, Institute for Infocomm Research, Singapore
Roman Y. Shtykh, Rakuten, Inc., Japan
Salman Ijaz Institute of Systems and Robotics, University of Algarve, Portugal
Adão Silva, University of Aveiro / Institute of Telecommunications, Portugal
Florian Skopik, AIT Austrian Institute of Technology, Austria
Karel Slavicek, Masaryk University, Czech Republic
Vahid Solouk, Urmia University of Technology, Iran
Peter Soreanu, ORT Braude College, Israel
Pedro Sousa, University of Minho, Portugal
Vladimir Stantchev, SRH University Berlin, Germany
Radu Stoleru, Texas A&M University - College Station, USA
Lars Strand, Nofas, Norway
Stefan Strauβ, Austrian Academy of Sciences, Austria
Álvaro Suárez Sarmiento, University of Las Palmas de Gran Canaria, Spain
Masashi Sugano, School of Knowledge and Information Systems, Osaka Prefecture University, Japan
Young-Joo Suh, POSTECH (Pohang University of Science and Technology), Korea
Junzhao Sun, University of Oulu, Finland
David R. Surma, Indiana University South Bend, USA
Yongning Tang, School of Information Technology, Illinois State University, USA
Yoshiaki Taniguchi, Osaka University, Japan
Anel Tanovic, BH Telecom d.d. Sarajevo, Bosnia and Herzegovina
Olivier Terzo, Istituto Superiore Mario Boella - Torino, Italy
Tzu-Chieh Tsai, National Chengchi University, Taiwan
Samyr Vale, Federal University of Maranhão - UFMA, Brazil
Dario Vieira, EFREI, France
Natalija Vlajic, York University - Toronto, Canada
Lukas Vojtech, Czech Technical University in Prague, Czech Republic
Michael von Riegen, University of Hamburg, Germany

**International Journal on Advances in Networks and Services**
**Volume 7, Numbers 1 & 2, 2014**

## CONTENTS

# Analysis of the Performance for SFBC-OFDM and FSTD-OFDM Schemes in LTE Systems over MIMO Fading Channels

Mohammad Torabi, Ali Jemmali, and Jean Conan
Department of Electrical Engineering,
École Polytechnique de Montréal,
Montréal, QC, Canada,
{mohammad.torabi, ali.jemmali, jean.conan}@polymtl.ca

***Abstract*— In this paper, a performance analysis is presented for space-frequency block coded orthogonal frequency division multiplexing (SFBC-OFDM) and Frequency Switched Transmit Diversity OFDM (FSTD-OFDM) schemes in the 3GPP Long Term Evolution (LTE) system over MIMO fading channels. Analytical expressions for the average BER, average channel capacity and the average throughput of the system are derived for two different MIMO schemes, SFBC-OFDM and FSTD-OFDM, defined in LTE, and are evaluated numerically. Monte-Carlo simulation results are also provided to verify the accuracy of the mathematical analysis. It is shown that the results obtained from Monte-Carlo simulations match closely with those obtained from the derived mathematical formulas.**

***Keywords*- Performance Analysis, MIMO, LTE, M-QAM Modulation, Capacity, Throughput.**

## I. Introduction

To increase the capacity and speed of wireless communication systems, a new wireless data networks has been emerged and has been standardized by the 3rd Generation Partnership Project (3GPP). This new standard is a natural evolution to the existing second (2G) and third (3G) generation wireless networks in order to respond to the growing demand in terms of data rates and speed and marketed as 4G Long Term Evolution (LTE). In LTE, data throughput and the speed of wireless data are increased by using a combination of new methods and technologies like Orthogonal Frequency Division Multiplexing (OFDM) and Multiple-Input Multiple-Output (MIMO) techniques.

In the downlink, LTE transmission is based on Orthogonal Frequency Division Multiple Access (OFDMA), known as a technique for encoding digital data on multiple carrier frequencies. It was shown that OFDMA is an efficient technique to improve the spectral efficiency of wireless systems. By converting the wide-band frequency selective channel into a set of several flat fading subchannels, OFDM technique becomes more resistant to frequency selective fading than single carrier systems. As OFDM signals are in time and frequency domain, they allow adding frequency domain scheduling to time domain scheduling. In LTE, for a given transmission power, the system data throughput and the coverage area can be optimized by employing Adaptive Modulation and Coding (AMC) techniques. The role of a user scheduler at the transmitter side is to assign the data rate for each user according to the channel conditions from the serving cell, the interference level from other cells, and the noise level at the receiver side.

In LTE standard, the use of MIMO has been considered as an essential technique in order to achieve the target in terms of data throughput and reliability. MIMO is known to be a very powerful technique to improve the system performance of wireless communication systems. The diversity and multiplexing modes are the two main modes of operation of multiple antennas systems. The principle of diversity mode is based on transmitting the same signal over multiple antennas and hence to improve the reliability of the system by a diversity gain. In this mode, the mapping function of transmit symbols used at the transmit antennas is called Space Time Block Coding (STBC). On the other hand, multiplexing mode uses two or more different spatial streams and sends them through two different antennas, consequently, the data rate can be improved.

In [1] an analysis is performed for evaluating the average bit error rate (BER) of MIMO schemes in LTE systems employing the classical M-ary quadrature amplitude modulation (M-QAM) scheme. In this paper, we provide more details about the system model and about the considered transmit diversity schemes in LTE and we extend the results in [1] and in addition to the average BER analysis, we present the average capacity analysis as well as the average throughput analysis for two different MIMO schemes as defined in LTE. Then, the results obtained from analytical formulas are provided, showing the performance of the considered schemes. From those results one can simply compare the benefits of using considered MIMO schemes. In addition, the results obtained from Monte-Carlo simulations are also provided to verify the accuracy of the analysis for each performance metric.

To study the performance of LTE systems a MATLAB based downlink physical layer simulator for Link Level Simulation (LLS) has been developed in [2], [3]. A System Level Simulation of the Simulator is also available [4]. The goal of developing the LTE simulator was to facilitate comparison with the works of different research groups and it is publicly available for free under academic non-commercial use license [3]. The main features of the simulator are adaptive coding and modulation, MIMO transmission and scheduling. As the simulator includes many physical layer features, it can be used for different applications in research [4]. In [5], the simulator was used to study the channel estimation of OFDM systems and the performance evaluation of a fast fading channel estimator was presented. In [6] and [7], a method for calculating the Precoding Matrix Indicator (PMI), the Rank Indicator (RI), and the Channel Quality Indicator (CQI) were studied and analyzed with the simulator.

In this paper, analyses of the performance for two transmit diversity schemes, known as Space Frequency Block Coding (SFBC) and Frequency Switched Transmit Diversity (FSTD) MIMO schemes in LTE system, are presented for different performance metrics. Those performance metrics are the average BER, the average capacity and the average throughput. The average BER results obtained from the analysis are then compared to the results of Monte-Carlo simulation using the Link Level LTE simulator [2], [3].

The remainder of this paper is organized as follows. In Section II, we present the system model used in the paper. In Section III, we present performance analyses for the average BER, the average capacity and the average throughput of SFBC and FSTD MIMO schemes. The numerical and simulation results and discussions are presented in Section IV. Finally, Section V concludes the paper.

## II. System Model

In this section, the structure of the OFDM LTE signal and LTE transmit diversity schemes are described. However, more details can be found in [8]. The OFDM signal has a time and a frequency domains. In the time domain, the LTE signal is composed of successive frames. Each frame has a duration of $T_{\text{frame}} = 10$ *msec*. Each frame is divided into $10$ subframes with equal length of $1$ *msec*. Each subframe consists of two equal length time-slots with a time duration of $T_{\text{slot}} = 0.5$ *msec*. For a normal cyclic prefix length, each time-slot consists of $N_s = 7$ OFDM symbols. In the frequency domain, the OFDM technique converts the LTE wideband signal into several narrowband signals. Each narrowband signal is transmitted on one subcarrier frequency.

In LTE, the spacing between subcarriers is fixed to $15$ KHz. Twelves adjacent subcarriers, occupying a total of $180$ KHz, of one slot forms the so-called Resource Block (RB). The number of Resource Blocks in an LTE slot depends on the allowed system bandwidth. The minimum number of RB is equal to 6 corresponding to $1.4$ MHz system bandwidth. For $20$ MHz system bandwidth (Maximum Allowed bandwidth in LTE) the number of RB is equal to $100$. In a MIMO system with $M_R$ receive antennas and $M_T$ transmit antennas, the relation between the received and the transmitted signals on subcarrier frequency $k$ ($k \in 1, \cdots, K$), at sampling instant time $n$ ($n \in 1, \cdots, N$) is given by

$$\mathbf{y}_{k,n} = \mathbf{H}_{k,n}\mathbf{x}_{k,n} + \mathbf{n}_{k,n} \tag{1}$$

where $\mathbf{y}_{k,n} \in C_{M_R \times 1}$ is the received vector, $\mathbf{H}_{k,n} \in C_{M_R \times M_T}$ represents the channel matrix on subcarrier $k$ at instant time $n$, $\mathbf{x}_{k,n} \in C_{M_R \times 1}$ is the transmit symbol vector and $\mathbf{n}_{k,n} \sim \mathcal{CN}(0, \sigma_n^2.\mathbf{I})$ is a white, complex valued Gaussian noise vector with variance $\sigma_n^2$.

Assuming perfect channel estimation, the channel matrix and noise variance are considered to be known at the receiver. A linear equalizer filter given by a matrix $\mathbf{F}_{k,n} \in C_{M_R \times M_R}$ is applied on the received symbol vector $\mathbf{y}_{k,n}$ to determine the post-equalization symbol vector $\mathbf{r}_{k,n}$ as follows [7]

$$\mathbf{r}_{k,n} = \mathbf{F}_{k,n}\mathbf{y}_{k,n} = \mathbf{F}_{k,n}\mathbf{H}_{k,n}\mathbf{x}_{k,n} + \mathbf{F}_{k,n}\mathbf{n}_{k,n}. \tag{2}$$

The Zero Forcing (ZF) or Minimum Mean Square Error (MMSE) design criterion [9] are typically used for the linear receiver and the input signal vector is normalized to unit power. In MIMO-OFDM systems, the key factor of link error prediction and performances is the signal to noise ratio (SNR) which represents the measurement for the channel quality information. In this study, the SNR is defined by

$$\gamma_{k,n} = \frac{\overline{\gamma}}{N_T}\|\mathbf{H}_{k,n}\|_{\text{F}}^2 \tag{3}$$

where $\overline{\gamma} = E_s/N_0$ is the average SNR per symbol and $\|.\|_F^2$ is the squared Frobenius norm of a matrix.

### A. LTE Frame Structure

Two types of LTE frame structures are defined depending on the duplexing mode of the transmission. Two duplexing methods are defined in LTE, namely Time Division Duplex (TDD) and Frequency Division Duplex (FDD). In the FDD mode, the downlink path (DL), from the eNodeB to user equipment (UE), and the uplink path (UL), from the UE to eNodeB, operate on different carrier frequencies. In the TDD mode, the downlink and the uplink paths operate on the same carrier frequency but in different time slots. In other word, in FDD, the downlink and uplink transmissions are separated in the frequency domain, whereas in TDD the downlink and uplink transmissions are separated in the time domain. Type 1 frame structure of LTE is associated with the FDD duplexing mode whereas Type 2 frame structure of LTE is associated with the TDD duplexing mode. For both types of LTE frame structures, the DL and UL transmissions in LTE systems are arranged into radio frames. The duration of a radio frame is fixed at 10 *msec*. The radio frame is comprised of ten 1 *msec* subframes, which represents the shortest Transmission Time Interval (TTI). Each subframe consists of two slots of duration 0.5 *msec*.

Frame structure of Type 1 LTE FDD and Type 2 TDD are shown in Figure 1(a) and Figure 1(b), respectively. In Type 2 TDD frame structure, as shown in Figure 1(b), each radio frame includes 2 half frames of 5 subframes each. Subframes can be either uplink subframes, downlink subframes or special subframes. Special subframes include the following fields: Downlink Pilot Time Slot (DwPTS) and Uplink Pilot Time Slot (UpPTS). Depending on the length of the Cyclic Prefix (CP) and the subcarriers spacing, each time slot consists of 6 or 7 OFDM symbols. In fact, the cyclic prefix represents

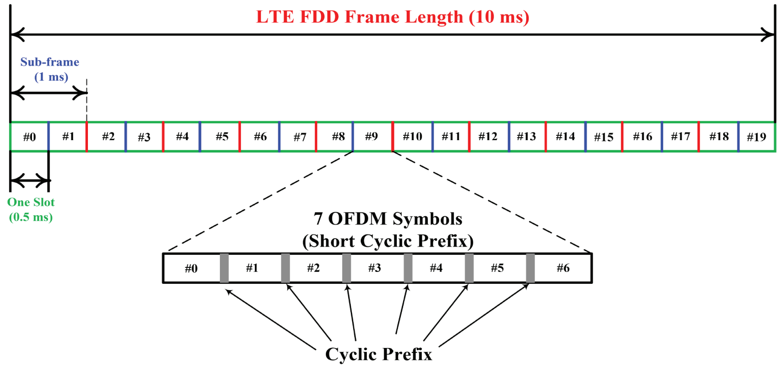


(a) Type 1 LTE FDD Frame Structure.

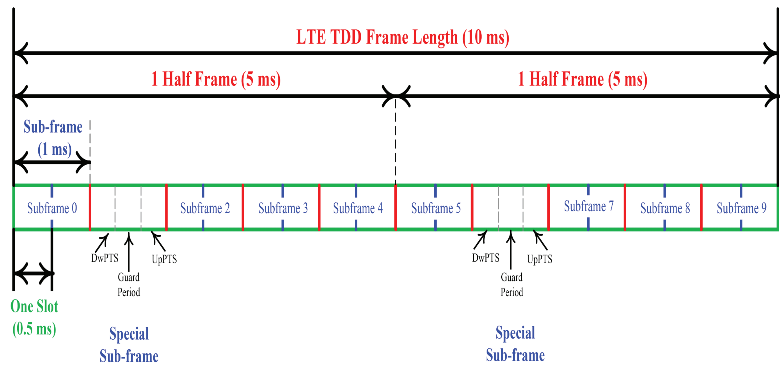


(b) Type 2 LTE TDD Frame Structure.

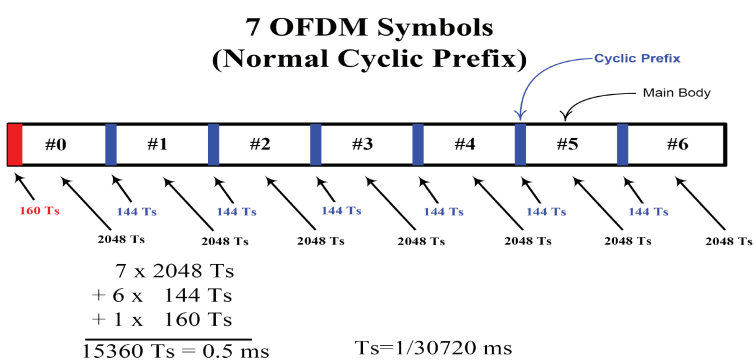


(c) Structure of the symbols in one slot with Normal Cyclic Prefix.

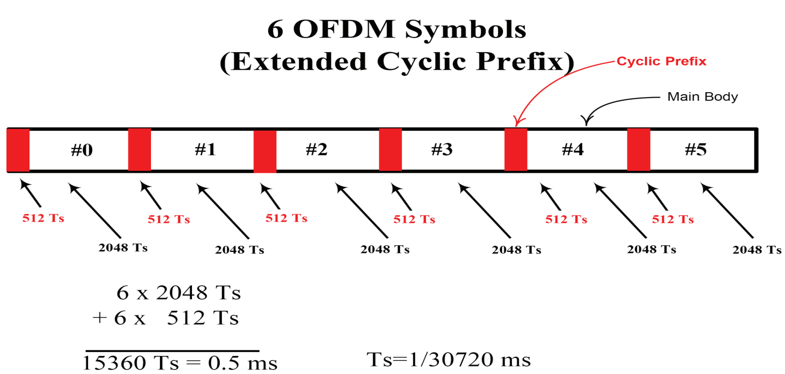


(d) Structure of the symbols in one slot with Extended Cyclic Prefix.

Fig. 1. LTE Frame Structure.

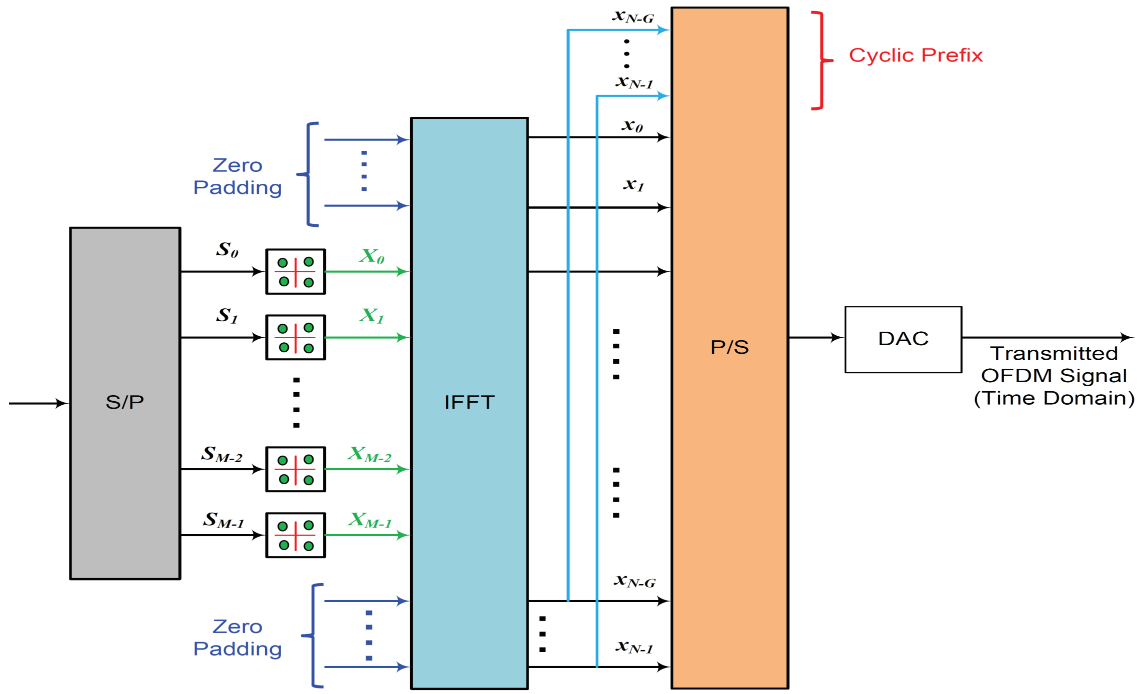


Fig. 2. OFDM Signal Generation.

a guard period at the beginning of each OFDM symbol which provides protection against multi-path delay spread. To effectively combat the delay spread of the channel, the duration of the cyclic prefix should be greater than the duration of the multi-path delay spread. At the same time, cyclic prefix also yields an overhead which should be minimized.

Two types of CP were specified in LTE, namely the normal CP and the extended CP. The structure of the symbols in a 0.5 *msec* time slot with *normal cyclic prefix* and *extended cyclic prefix* are shown in Figure 1(c) and Figure 1(d), respectively. As shown, in normal CP, each slot includes 7 OFDM symbols, whereas in extended CP each slot includes only 6 OFDM symbols. The duration of the first cyclic prefix and the subsequent prefixes in terms of sampling time ($T_s$) are also shown in Figure 1(c). $T_s$ represents the basic time unit and is given by $T_s = 1/(15000 \times 2048)$ seconds. It can be noticed that the duration of the first cyclic prefix is larger than the subsequent cyclic prefixes. For the normal cyclic prefix the duration of the first cyclic prefix is defined as $160 \times T_s$, whereas the duration of subsequent cyclic prefixes is only $144 \times T_s$. For extended cyclic prefix, all prefixes have the same length of $512 \times T_s$. The normal cyclic prefix length is proposed to be sufficient for the majority of radio environment scenarios, while the extended cyclic prefix is intended for radio environment with particularly high delay spreads. As we will see later, the cyclic prefix of size $G$ is the copy of $G$ last elements from an OFDM block including $N$ elements.

## B. OFDM Symbol Generation

An OFDM symbol can be generated using the Inverse Fast Fourier Transform (IFFT), which is an operation of a transformation from frequency domain to time domain. Accordingly, the transmitted signal is defined in the frequency domain. This means that the complex modulated symbols are considered as the coefficients in the frequency domain. The block diagram of an OFDM signal generation is shown in Figure 2. The serial input data stream of size $M$ are converted into $M$ parallel data elements denoted a block given by $\mathbf{S} = (S_0, S_1, S_2, ..., S_{M-1})^T$. Then, $M$ parallel data streams ($S_i$, $i = 0, 1, ..., M-1$) are independently modulated (e.g., M-QAM modulation) to form a vector of complex modulated symbols given by $\mathbf{X} = (X_0, X_1, X_2, ..., X_{M-1})^T$.

The vector $\mathbf{X}$ is then applied to the input of an $N$-point Inverse Fast Fourier Transform (IFFT). The output of this operation is a set of $N$ complex time-domain samples, given by $\mathbf{x} = (x_0, x_1, x_2, ..., x_{N-1})^T$ . In practical implementation of an OFDM system, $N$ the size of IFFT is greater than $M$ the number of modulated symbols (i.e., $N \geq M$).

As shown in Figure 2, for the remaining subcarriers ($N-M$ subcarriers) are being padded with zeros. The next important operation in the generation of an OFDM signal is the creation of a guard period at the beginning of each OFDM symbol by inserting a Cyclic Prefix (CP). This CP is simply generated by taking the last $G$ samples of the IFFT output and appending them at the beginning of vector $\mathbf{x}$. This yields the OFDM symbol in the time domain, as a vector of size $G + N$, given by $(x_{N-G}, ..., x_{N-1}, x_0, x_1, x_2, ..., x_{N-1})^T$ as shown in Figure 2. The last step in the OFDM signal generation is the parallel to serial conversion of the IFFT output an then its transmissions through the transmit antennas. The generated OFDM signal will be transmitted over multiple transmit antennas using the transmit diversity schemes to be explained in the following.

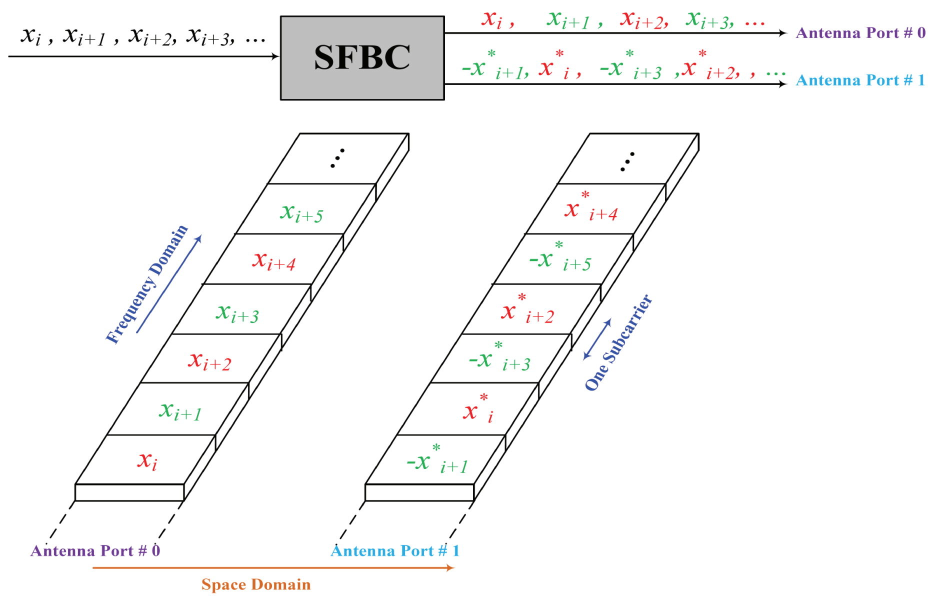


Fig. 3. Space Frequency Block Coding (SFBC) Scheme in LTE [11].

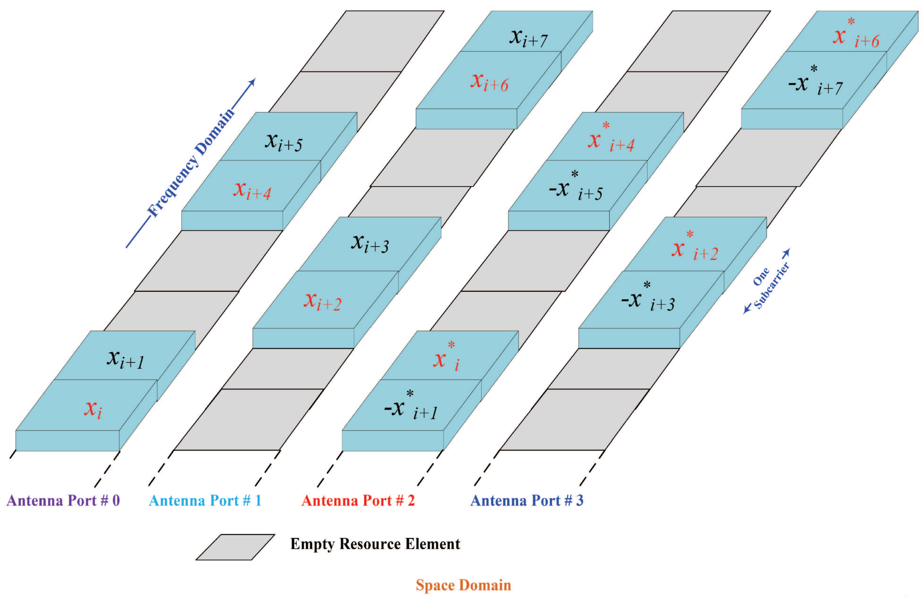


Fig. 4. Frequency Switched Transmit Diversity (FSTD) Scheme in LTE [11].

### *C. Transmit Diversity Schemes in LTE*

In LTE, two main transmit diversity schemes are employed; the first one (SFBC scheme) with 2 transmit antennas and the second one (FSTD scheme) with 4 transmit antennas [10]. Both schemes use only one data stream (one signal) [11]. In LTE, one data signal (also called data stream) is referred as one codeword because only one transport block (TB) is used per data stream. In order to ensure uncorrelated channels between different antennas and hence maximizing the diversity gain, the antennas should be well separated relative to the wavelength.

*1) SFBC scheme in LTE:* When a physical channel in LTE is configured for transmit diversity operation using two eNodeB antennas, the diversity scheme is called Space Frequency Block Coding. The principle of SFBC transmission is shown in Figure 3, similarly to the one reported in [11]. As can be seen from Figure 3, the SFBC diversity scheme is, in fact, the frequency domain implementation of the well known Space Time Block Coding technique, developed by Alamouti [12]. The fundamental characteristic of this family of coding is that the transmitted diversity streams are orthogonal and they can be simply decoded at the receiver.

STBC operates on pairs of adjacent symbols in the time domain. Since the signal in LTE is two dimensional (time and frequency domains) and the number of available OFDM symbols in a subframe is not always an even number, the direct application of STBC is not straightforward. Therefore, SFBC scheme is proposed to be employed.

In LTE, for SFBC transmission, the symbols are transmitted from two eNodeB antenna ports on each pair of adjacent subcarriers as follows [10]:

$$\begin{bmatrix} y^{(0)}(2j) & y^{(0)}(2j+1) \\ y^{(1)}(2j) & y^{(1)}(2j+1) \end{bmatrix} = \begin{bmatrix} x_{2j} & x_{2j+1} \\ -x^*_{2j+1} & x^*_{2j} \end{bmatrix} \quad (4)$$

where $y^{(p)}(k)$ denotes the symbols transmitted on the $k$-th subcarrier from antenna port $p$. $x_{2j}$ and $x_{2j+1}$ ($j = 0, 1, 2, ..., \frac{N}{2} - 1$) are two adjacent subcarriers in the OFDM modulated signals, explained earlier. An important characteristic of such codes is that the transmitted signal streams are orthogonal and a simple linear receiver can be used for detection and decoding of the signal.

*2) FSTD scheme in LTE:* The diversity scheme in case of four transmit antennas (operating on port 0 to port 3) is called Switched Transmit Diversity [10]. The transmission structure for FSTD diversity scheme is shown in Figure 4, similarly to the one explained in [11]. In the FSTD scheme a pair of modulated symbols are transmitted using SFBC scheme over two antennas, whereas the other two antennas are not transmitting. In other words, in the FSTD scheme, the transmission is switched between a pair of transmit antennas at each frequency slot. This means that in the first frequency slot the first two symbols are transmitted through antenna port 0 and antenna port 2, whereas nothing is transmitted on antennas ports 1 and 3. Then, in the next frequency slot for transmission of next two symbols, antenna ports 1 and 3 are used, where antenna ports 0 and 2 are not transmitting. In LTE, the space frequency block code, designed for FSTD employing 4 transmit antennas is defined as follows:

$$\begin{bmatrix} y^{(0)}(4j) & y^{(0)}(4j+1) & y^{(0)}(4j+2) & y^{(0)}(4j+3) \\ y^{(1)}(4j) & y^{(1)}(4j+1) & y^{(1)}(4j+2) & y^{(1)}(4j+3) \\ y^{(2)}(4j) & y^{(2)}(4j+1) & y^{(2)}(4j+2) & y^{(2)}(4j+3) \\ y^{(3)}(4j) & y^{(3)}(4j+1) & y^{(3)}(4j+2) & y^{(3)}(4j+3) \end{bmatrix} =$$

$$\begin{bmatrix} x_{4j} & x_{4j+1} & 0 & 0 \\ 0 & 0 & x_{4j+2} & x_{4j+3} \\ -x^*_{4j+1} & x^*_{4j} & 0 & 0 \\ 0 & 0 & -x^*_{4j+3} & x^*_{4j+2} \end{bmatrix} \quad (5)$$

where $y^{(p)}(k)$ denotes the symbols transmitted on the $k$-th subcarrier from antenna port $p$. $x_{4j}$, $x_{4j+1}$, $x_{4j+2}$, and $x_{4j+3}$, ($j = 0, 1, 2, ..., \frac{N}{4} - 1$) are 4 adjacent subcarriers in the OFDM modulated signals, explained earlier.

In the following, we present a performance analysis and evaluation for three important metrics, namely the average BER, the average capacity, and the average throughput of the considered MIMO systems in LTE.

## III. Performance Analysis

In the following, we first present a performance analysis for the average BER of $2 \times 1$ MIMO SFBC and $4 \times 2$ MIMO FSTD systems, over slow fading channels. Then an analysis for the channel capacity of the considered systems is presented, followed by the average throughput evaluation. The channel capacity and throughput results can be considered as a performance limit in terms of bits/sec/Hz for the LTE system. Finally, the numerical results, obtained from closed-form expressions as well as the results obtained from Monte-carlo simulations, are presented to verify the accuracy of our analysis.

### *A. Average BER Performance Analysis*

In the following, we present the average BER analysis for the SFBC and SFTD systems. For each case, we first briefly describe the transmit diversity and space frequency coding scheme. Then, using the Moment Generating Function (MGF)-based approach, closed-form expressions are obtained for the average BER performance of the system for $2 \times 1$ SFBC and $4 \times 2$ FSTD MIMO schemes.

*1) BER Analysis of SFBC:* As explained earlier for Figure 3, SFBC-OFDM transmit diversity scheme is in fact a $2 \times 1$ MIMO system employing space frequency block coding over $N$ OFDM subcarriers.

Since OFDM converts the multipath fading channel into $N$ frequency flat fading sub-channels, we first derive the BER expressions over flat Rayleigh fading sub-channels, given by $P_b(E)$. Then, the overall average BER over $N$ sub-channels, in each case can be calculated from

$$BER_{avg} = \frac{1}{N} \sum_{k=1}^{N} P_{b,k}(E) \quad (6)$$

where the index $k$ (subcarrier/sub-channel index) is ignored for the sake of brevity. In addition, the impact of cyclic prefix in OFDM is assumed to be negligible.

For the $2 \times 1$ MIMO system employing SFBC scheme, the probability density function of the SNR for each subcarrier is given by a chi-square distribution function as follows [13]

$$f_\gamma(\gamma) = \frac{2}{\bar{\gamma}^2} \gamma e^{-\frac{2}{\bar{\gamma}}\gamma} \quad (7)$$

where $\bar{\gamma}$ is the average SNR per symbol given by $\bar{\gamma} = E_s/N_0$.

The moment generating function (MGF) can be determined using the following equation:

$$M_{\bar{\gamma}}(s) = \int_0^\infty e^{-s\gamma} f(\gamma) d\gamma. \quad (8)$$

Inserting (7) into (8) and solving the integral yields

$$M_{\bar{\gamma}}(s) = \frac{4}{\bar{\gamma}^2 (s + \frac{2}{\bar{\gamma}})^2}. \quad (9)$$

The average BER expression for M-QAM modulation scheme can be obtained from [14] (equation (8.111; Page 255))

$$P_b(E) \cong B \sum_{i=1}^{\sqrt{M}/2} \frac{1}{\pi} \int_0^{\pi/2} M_{\bar{\gamma}}(A_{i,\theta}) \, d\theta \quad (10)$$

where $A_{i,\theta} = \frac{(2i-1)^2}{2\sin^2\theta}\frac{3}{(M-1)}$ and $B$ is defined by

$$B = 4\left(\frac{\sqrt{M}-1}{\sqrt{M}}\right)\left(\frac{1}{\log_2 M}\right). \tag{11}$$

Then, using the MGF expression in (9), we obtain

$$M_{\bar{\gamma}}(A_{i,\theta}) = \frac{4}{\bar{\gamma}^2\left(\left[\frac{(2i-1)^2}{2\sin^2\theta}\frac{3}{(M-1)}\right]+\frac{2}{\bar{\gamma}}\right)^2}. \tag{12}$$

Substituting (12) into (10) and after some manipulations, we obtain

$$P_b\left(E\right) \cong B\sum_{i=1}^{\sqrt{M}/2}\frac{1}{\pi}\int_0^{\pi/2}\left(\frac{\sin^2\theta}{\sin^2\theta+c_i}\right)^2 d\theta \tag{13}$$

where $c_i = \frac{3(2i-1)^2}{2(M-1)}\frac{\bar{\gamma}}{2}$.

The average BER performance as a function of $\bar{\gamma} = E_s/N_0$ can be evaluated by numerical evaluation of the integral in (13) for M-QAM modulation schemes.

Alternatively, by solving the integral, we obtain a closed-form expression for the average BER of M-QAM modulation as follows

$$P_b\left(E\right) \cong B\sum_{i=1}^{\sqrt{M}/2}\mathcal{I}_2\left(\pi/2, c_i\right) \tag{14}$$

where the closed-form expression for $\mathcal{I}_2(.,.)$ can be obtained from [14](eq.5A.24) as follows

$$\mathcal{I}_n\left(\phi, D\right) = \frac{1}{\pi}\int_0^{\phi}\left(\frac{\sin^2\theta}{\sin^2\theta+D}\right)^n d\theta, \qquad -\pi\leq\phi\leq\pi \tag{15}$$

$$= \frac{\phi}{\pi}-\frac{\beta}{\pi}\left\{\left(\frac{\pi}{2}+\tan^{-1}\alpha\right)\sum_{q=0}^{n-1}\binom{2q}{q}\frac{1}{\left(4\left(1+D\right)\right)^q}\right.$$

$$\left.+\sin\left(\tan^{-1}\alpha\right)\sum_{q=1}^{n-1}\sum_{p=1}^{q}\frac{T_{p\,q}}{(1+D)^q}\left[\cos\left(\tan^{-1}\alpha\right)\right]^{2(q-p)+1}\right\} \tag{16}$$

where $T_{p\,q} = \binom{2q}{q}\left[\binom{2(q-p)}{q-p}4^p\left[2(q-p)+1\right]\right]^{-1}$, $\beta = \sqrt{\frac{D}{1+D}}\,\mathrm{sgn}\phi$, and $\alpha = -\beta\cot\phi$.

*2) BER Analysis of FSTD:* As discussed earlier for Figure 4, FSTD-OFDM transmit diversity scheme is a $4\times 2$ MIMO system employing space frequency block coding over $N$ OFDM subcarriers, in which only 2 transmit antennas out of 4 antennas are used at each transmission slot. In this case, considering two consecutive slots, in the first slot only antenna ports 0 and 2 are used for transmissions and in the second slot only antenna ports 1 and 3 are employed for transmissions.

For the $4\times 2$ MIMO system employing FSTD-OFDM scheme, we can show that the instantaneous SNR of the system, for $k$-th subcarrier, is equivalent to that for a $2\times 2$ STBC MIMO system. Therefore, the probability density function of the SNR is given by a chi-square distribution function as follows [13]

$$f_\gamma(\gamma) = \frac{8}{3\bar{\gamma}^4}\gamma^3 e^{-\frac{2}{\bar{\gamma}}\gamma}. \tag{17}$$

In this case, the MGF expression can be obtained by substituting (17) into (8), which yields

$$M_{\bar{\gamma}}(s) = \frac{16}{\bar{\gamma}^4(s+\frac{2}{\bar{\gamma}})^4}. \tag{18}$$

Similarly to the SFBC case discussed earlier, inserting (18) into (10), the average BER expression with M-QAM modulation for FSTD can be written as

$$P_b\left(E\right) \cong B\sum_{i=1}^{\sqrt{M}/2}\frac{1}{\pi}\int_0^{\pi/2}\left(\frac{\sin^2\theta}{\sin^2\theta+c_i}\right)^4 d\theta \tag{19}$$

where $c_i = \frac{3(2i-1)^2}{2(M-1)}\frac{\bar{\gamma}}{2}$, and the integral can be calculated numerically.

Alternatively, by solving the integral, we obtain a closed-form expression for the average BER of M-QAM modulation for FTSD as follows

$$P_b\left(E\right) \cong B\sum_{i=1}^{\sqrt{M}/2}\mathcal{I}_4\left(\pi/2, c_i\right) \tag{20}$$

where the closed-form expression for $\mathcal{I}_4(.,.)$ can be obtained from (16).

Finally, for the sake of comparisons, we express the average BER of the single-input single-output (SISO) system, that has been derived for Rayleigh fading channels for M-QAM signals [14] (eq. 8.112; Page 256), as follows:

$$P_b(E) \cong B/2\sum_{i=1}^{\sqrt{M}/2}\left(1-\sqrt{\frac{1.5(2i-1)^2\overline{\gamma}\log_2 M}{M-1+1.5(2i-1)^2\overline{\gamma}\log_2 M}}\right) \tag{21}$$

where $B$ is defined earlier.

### *B. Average Channel Capacity Analysis*

The channel capacity of the MIMO-OFDM system employing a space-frequency code for the $k$-th subcarrier at $n$-th time instant can be written as [15], [16]:

$$C_{k,n} = R_c\,\log_2\left(1+\frac{\overline{\gamma}}{N_{\mathrm{T}}R_c}\|\mathbf{H}_{k,n}\|_F^2\right). \tag{22}$$

It can be also expressed as

$$C_{k,n} = R_c\,\log_2(1+\gamma_{k,n}) \tag{23}$$

where $\gamma_{k,n} = \frac{\overline{\gamma}}{N_T R_c} \|\mathbf{H}_{k,n}\|_F^2$ and $R_c$ is the SFBC code rate, that is equal to one ($R_c = 1$) for Alamouti space-time coding used in SFBC and FSTD schemes.

The average capacity averaged over time instant $n$ for $k$ subcarrier can be written as

$$\overline{C}_k = E\left\{C_{k,n}\right\} = \int_0^\infty R_c \, \log_2(1+\gamma_{k,n}) \; f_{\gamma_{k,n}}(\gamma_{k,n}) \, d\gamma_{k,n}. \tag{24}$$

Finally, by averaging over $N$ subchannels, the overall average channel capacity can be obtained from

$$\mathrm{C}_{\mathrm{avg}} = \frac{1}{N}\sum_{k=0}^{N-1} \overline{C}_k. \tag{25}$$

*1) Channel Capacity of SFBC MIMO-OFDM:* For the $2 \times 1$ SFBC MIMO-OFDM scheme, the probability density function of the SNR for each subcarrier is given by (7). Inserting (7) into (24), we obtain

$$\begin{aligned}\overline{C}_k &= \int_0^\infty R_c \, \log_2(1+\gamma) \, \frac{2}{\bar{\gamma}^2}\gamma e^{-\frac{2}{\bar{\gamma}}\gamma} \, d\gamma \\ &= R_c \, \log_2(e) \int_0^\infty \frac{2}{\bar{\gamma}^2} \ln(1+\gamma) \; \gamma e^{-\frac{2}{\bar{\gamma}}\gamma} \, d\gamma. \end{aligned} \tag{26}$$

To solve the above integral, we use the following result [17]

$$\begin{aligned}&\frac{\mu}{(M-1)!}\int_0^\infty \ln\left(1+x\right)(\mu\, x)^{M-1}\, e^{-\mu\, x}\, dx \\ &= \mathcal{P}_M(-\mu)\, E_1(\mu) + \sum_{j=1}^{M-1}\frac{1}{j}\,\mathcal{P}_j(\mu)\,\mathcal{P}_{M-j}(-\mu)\end{aligned} \tag{27}$$

where $\mathcal{P}_M(.)$ is the Poisson distribution defined by $\mathcal{P}_M(x) = \sum_{v=0}^{M-1} \frac{x^v}{v!}\, e^{-x}$, and where $E_1(.)$ is the exponential integral of first order, defined by $E_1\left(x\right) = \int_x^\infty t^{-1}e^{-t}dt$ for $x > 0$.

Therefore, using (27) and after performing changes of variables together with some simplifications, we obtain the solution of integral in (26) as

$$\overline{C}_k = A_1\left[\mathcal{P}_1(-\mu)\, E_1(\mu) + \mathcal{P}_1(\mu)\,\mathcal{P}_1(-\mu)\right] \tag{28}$$

where $A_1 = R_c \, \log_2(e)$ and $\mu = \frac{2}{\bar{\gamma}}$. Then the overall average channel capacity can be obtained from (25).

*2) Channel Capacity of FSTD MIMO-OFDM:* As mentioned earlier, for the $4 \times 2$ FSTD MIMO-OFDM scheme, we can show that the instantaneous SNR of the system, for $k$-th subcarrier, is equivalent to that for a $2 \times 2$ SFBC MIMO-OFDM scheme. For the $2 \times 2$ SFBC MIMO-OFDM scheme, the probability density function of the SNR for each subcarrier is given by (17).

Similar to the $2 \times 1$ SFBC MIMO-OFDM case, substituting (17) into (24), we can obtain

$$\overline{C}_k = A_2\left[\mathcal{P}_4(-\mu)\, E_1(\mu) + \sum_{j=1}^{3}\frac{1}{j}\,\mathcal{P}_j(\mu)\,\mathcal{P}_{4-j}(-\mu)\right] \tag{29}$$

where $A = R_c \, \log_2(e)/3$ and $\mu = \frac{2}{\bar{\gamma}}$. Then the overall average channel capacity can be obtained from (25).

## C. Throughput Analysis

In a frequency selective fading channel, the subchannels corresponding the OFDM subcarriers have different amplitudes. To obtain a better throughput or a spectral efficiency, the transmission mode on each subcarrier can be chosen according the subchannels state information. Using the known channel state information (CSI), the transmitter can choose the best modulation mode and can adapt the transmission rate and/or transmit power on each OFDM subcarrier. Here, we consider an adaptive modulation with constant-power and adaptive-rate transmission while satisfying a quality of service (QoS) indicator such as a predefined target BER or a target Block error rate (BLER). We use a rate adaptive modulation assuming $L$-mode square M-QAM modulations.

To perform adaptive modulation we divide the entire SNR region into $L+1$ fading regions. Then, according the instantaneous SNR value on each subchannel in each SNR region, we assign the best modulation mode. This method can provide the largest throughput while satisfying a target BER value [15].

In this case, the throughput (in Bits/Sec/Hz) for the considered MIMO-OFDM systems is defined as [15], [16], [18]:

$$T_{avg} = \frac{R_c}{N}\sum_{k=0}^{N-1}\sum_{l=1}^{L} \beta_{l}[k]\left[F_\gamma(\alpha_{l+1}) - F_\gamma(\alpha_{l})\right] \tag{30}$$

where $\beta_l[k]$ is the number of bits assigned in $l$-th SNR region for $k$-th OFDM subcarrier, $\alpha_l$ and $\alpha_{l+1}$ are the switching SNR thresholds for $l$-th SNR region. $F_\gamma(\gamma)$ is the cumulative distribution function (CDF) defined as $F_\gamma(\alpha_j) = \int_{-\infty}^{\alpha_j} f_\gamma(\gamma)\, d\gamma$, where $f_\gamma(\gamma)$ is defined earlier for each MIMO-OFDM scheme. We can simply show that substituting the $f_\gamma(\gamma)$ expressions for $2\times1$ SFBC MIMO-OFDM and $4\times2$ FSTD MIMO-OFDM respectively given by (7) and (17) in it we obtain

$$F_\gamma(\gamma) = 1 - e^{-\frac{2}{\bar{\gamma}}\gamma}\left(1 + \frac{2}{\bar{\gamma}}\right) \tag{31}$$

and

$$F_\gamma(\gamma) = 1 - e^{-\frac{2}{\bar{\gamma}}\gamma}\left(1 + \frac{2}{\bar{\gamma}} + \frac{2}{\bar{\gamma}^2} + \frac{8}{3\bar{\gamma}^3}\right). \tag{32}$$

Finally, closed-form expressions for the average throughput of $2\times1$ SFBC MIMO-OFDM and $4\times2$ FSTD MIMO-OFDM systems can be obtained by inserting the corresponding CDF expressions (31) and (32) into (30), respectively.

TABLE I
SIMULATION SETTINGS

| Parameter | Setting |
|---|---|
| Transmission Schemes | SISO; $2 \times 1$ SFBC; $4 \times 2$ FSTD |
| Bandwidth | 5 MHz |
| Simulation length | 5000 subframes |
| Channel Type | Rayleigh Fading |
| Channel knowledge | Perfect |
| CQI | 6 (QPSK), 9 (16-QAM), and 16 (64-QAM) |

## IV. SIMULATION AND ANALYTICAL RESULTS

In this section, we provide the performance results obtained from the mathematical expressions derived in this paper for the average BER, the average capacity and the average throughput of the considered MIMO systems in LTE, and assuming $\overline{\gamma} = E_s/N_0$ and $R_c = 1$. Monte-Carlo simulation results are also provided to show the accuracy of the analysis.

The common simulation settings for Monte-Carlo simulations are summarized in Table I.

### A. Average BER Performance results

The average BER performance as a function of $\overline{\gamma} = Es/N_0$ for SISO and MIMO schemes are shown in Figure 5, Figure 6, and Figure 7. In Figure 5, the average BER results are provided assuming 4-QAM, i.e., QPSK modulation. Figure 6 shows the results for 16-QAM modulation and Figure 7 presents the results for 64-QAM modulation.

It can be seen that the average BER performances of QPSK, 16-QAM, and 64-QAM schemes at high SNRs decrease by factors $\overline{\gamma}^1$, $\overline{\gamma}^2$, and $\overline{\gamma}^4$, for SISO, $2 \times 1$, and $4 \times 2$ MIMO cases, respectively. Thus, the diversity order (slope of the curves) are equal to $1$, $2$ and $4$, respectively, for the considered cases. As stated earlier, since in $4 \times 2$ FSTD, at each time-slot/frequency-slot $2$ out of $4$ transmit antennas are in use, therefore the diversity order will be $2 \times 2 = 4$. In fact, the corresponding average BER curve for $4 \times 2$ FSTD is somehow like the classical $2 \times 2$ STBC system, when the channel is not a time-varying channel.

From the figures it is clear that the BER performance improves as the number of transmit or receive antennas increases, as expected. It can be observed that the negative slope of the BER curve for the SISO case is equal to $1$, meaning that the diversity order for the SISO case is equal to $1$, as expected.

The second curves in Figure 5, Figure 6, and Figure 7 represent the BER results of the $2 \times 1$ SFBC diversity scheme. Asymptotically, the slope of these curves can be observed to be equal to $2$, which corresponds to the diversity order of $2 \times 1$ SFBC system. An SNR ($Es/N_0$) gain improvement can also be observed compared to the SISO scheme. From Figure 6, it can be observed that to achieve the BER value of $10^{-3}$, the $2 \times 1$ diversity scheme needs about $10$ dB less in $Es/N_0$, compared to the SISO case.

In Figure 7 for 64-QAM modulation, the average BER of $10^{-3}$ is achieved at $Es/N_0 = 39$ dB in SISO configuration, however, the same value of BER is achieved with only at $Es/N_0 = 29$ dB in the $2 \times 1$ diversity scheme. Thus an SNR gain of $10$ dB is clearly observed for the $2 \times 1$ diversity

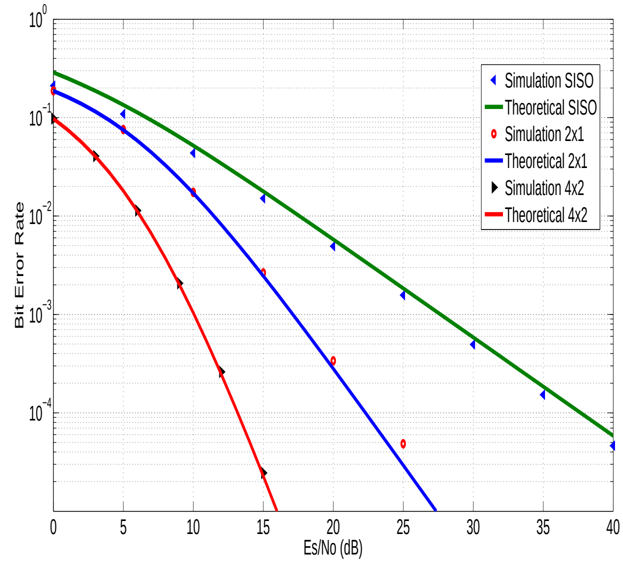


Fig. 5. Numerical Evaluation and Monte-Carlo Simulations of the average BER for QPSK modulation.

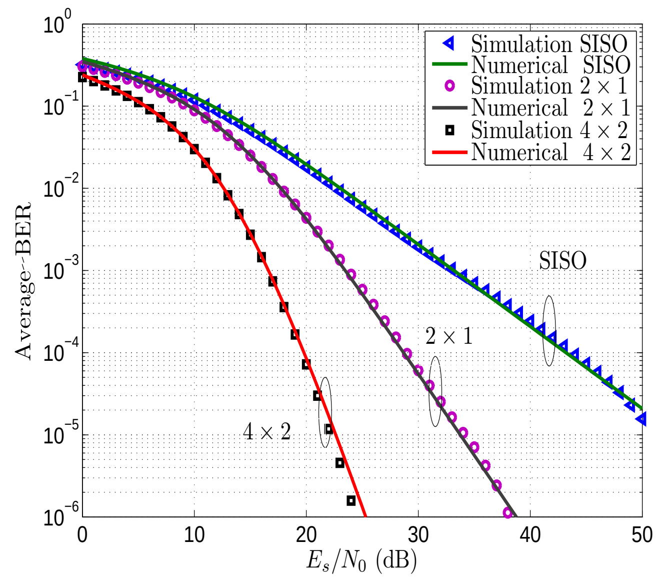


Fig. 6. Numerical Evaluation and Monte-Carlo Simulations of the average BER for 16-QAM modulation.

scheme. The BER results of the $4 \times 2$ diversity scheme for both modulation schemes, i.e., 16-QAM and 64-QAM are also shown. As described earlier, in high SNRs region the slope of that curve tends to be equal to $4$. This value corresponds to the diversity order of a $2 \times 2$ system.

Finally, it can be observed from Figure 5, Figure 6 and Figure 7 that numerical evaluation results obtained from average BER formulas match closely to the average BER results obtained from Monte-Carlo simulations. This verifies the accuracy of the analysis.

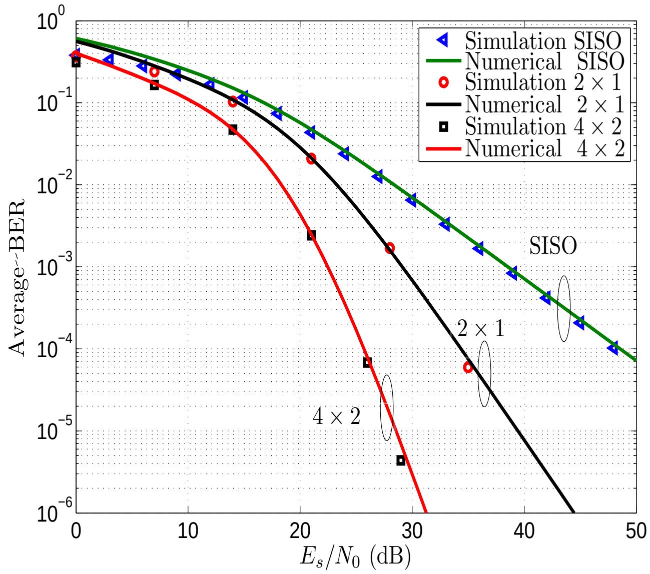

Fig. 7. Numerical Evaluation and Monte-Carlo Simulations of the average BER for 64-QAM modulation.

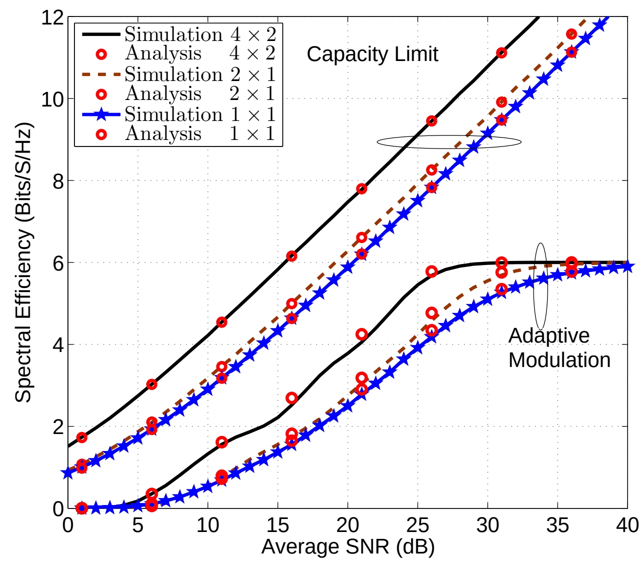

Fig. 9. Numerical Evaluation and Monte-Carlo Simulations of the average spectral efficiency of the system for different cases.

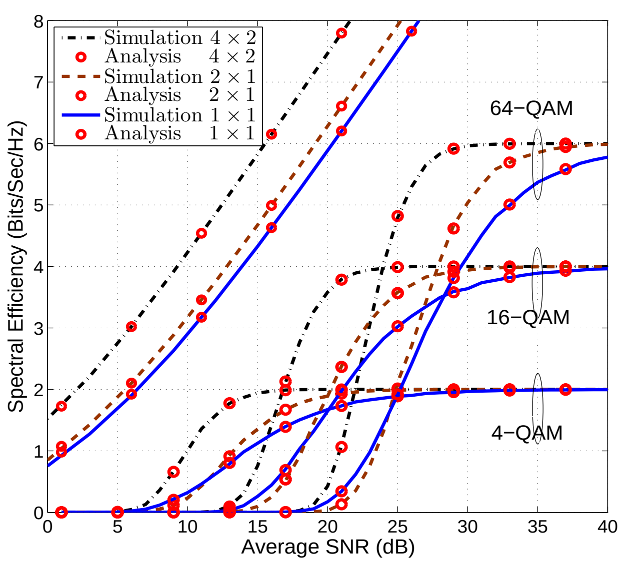

Fig. 8. Numerical Evaluation and Monte-Carlo Simulations of the average spectral efficiency of the system for different cases.

### B. Average Channel Capacity and Throughput Results

In the following, we show the results for the average capacity and the average throughput (average spectral efficiency) results for the considered systems. The results are obtained from the mathematical formulas presented in previous section as well as from Monte-Carlo simulations. Figure 8 and Figure 9 show the channel capacity limits as well as the throughput of $2 \times 1$ SFBC MIMO-OFDM, $4 \times 2$ FSTD MIMO-OFDM, and SISO-OFDM systems. For evaluating the throughout, we assume several cases considering a target BER of $10^{-5}$.

In Figure 8, we assume a case using two transmission modes, i.e., one M-QAM transmission mode ($M \in \{4, 16, 64\}$) and a no-transmission mode. For example, when 16-QAM modulation and no-transmission modes are considered, when the SNR of the subchannel is below a certain threshold we use 16-QAM for transmission, otherwise no data is transmitted, i.e., no-transmission mode. The SNR threshold is obtained according the target BER value. It can be observed in Figure 8 that the capacity for $4 \times 2$ FSTD MIMO-OFDM system is superior than those of $2 \times 1$ SFBC MIMO-OFDM, and SISO cases, as expected.

It is also shown that $2 \times 1$ SFBC MIMO-OFDM system can provide superior capacity performance compared to the SISO system. It can be observed that in a two-mode transmission case, using a higher modulation mode (e.g., 16-QAM instead of 4-QAM) yields a throughput increase at high SNRs. However, at low SNR values, for example between 8 to 20 dB, 4-QAM transmission can provide a higher throughput than 64-QAM case. This is due to the fact that the SNR threshold for 4-QAM is much less than that for 64-QAM, and a two-mode transmission using 4-QAM starts the transmission at a lower SNR than for a two-mode transmission using 64-QAM.

To obtain a better throughput, we use more modulation modes in the transmission. In Figure 9, we assume a case using several transmission modes, including a no-transmission mode, and a four-transmission mode using BPSK, 4-QAM, 16-QAM, 64-QAM schemes. In this case, we obtain 4 SNR thresholds $\alpha_l$ ($l = 1, 2, 3, 4$) corresponding to the considered modulation schemes and satisfying the target BER of $10^{-5}$. It can be seen that transmissions occur in a wide range of SNR values. In $1 \times 1$ SISO system, and in $2 \times 1$, and $2 \times 4$ MIMO systems, the throughput values reach a maximum rate of 6 bits/sec/Hz that is equal to the average bits transmitted by 64-QAM, the highest mode considered. To verify the analysis the results obtained from Monte-carlo simulations are also provided. It can be seen that the numerical results obtained from the formulas match closely to the simulation results.

## V. Conclusion

In this paper, we have presented performance analyses for the average BER, the average channel capacity and the throughput of MIMO schemes in the 3GPP Long Term Evolution (LTE). The theoretical analysis for two different MIMO schemes in a $5$ MHz bandwidth LTE system were presented. To verify the accuracy of the analysis the results of Monte-Carlo simulation for the studied schemes were provided and compared with the results obtained from theoretical analysis. To show the performance improvement in the MIMO schemes, the performance of a SISO configuration was also presented. The results show a good agreement between numerical results and Monte-Carlo simulation results.

## References

[1] A. Jemmali, J. Conan, and M. Torabi, "Bit Error Rate Analysis of MIMO Schemes in LTE Systems," in *Proc. International Conference on Wireless and Mobile Communications (ICWMC-2013)*, July 2013, pp. 190–194.

[2] C. Mehlführer, M. Wrulich, J. C. Ikuno, D. Bosanska, and M. Rupp, "Simulating the long term evolution physical layer," in *Proc. European Signal Processing Conference (EUSIPCO 2009)*, 2009.

[3] Online, "LTE link level simulator," 2009, available http://www.nt.tuwien.ac.at/ltesimulator.

[4] J. Ikuno, M. Wrulich, and M. Rupp, "System level simulation of LTE networks," in *Proc. IEEE Vehicular Technology Conference (VTC 2010-Spring)*, May 2010, pp. 1–5.

[5] M. Simko, C. Mehlfuhrer, M. Wrulich, and M. Rupp, "Doubly dispersive channel estimation with scalable complexity," in *Proc. International ITG Workshop on Smart Antennas (WSA)*, Feb. 2010, pp. 251–256.

[6] S. Schwarz, M. Wrulich, and M. Rupp, "Mutual information based calculation of the precoding matrix indicator for 3GPP UMTS/LTE," in *2010 International ITG Workshop on Smart Antennas (WSA)*, Feb. 2010, pp. 52–58.

[7] S. Schwarz, C. Mehlfuhrer, and M. Rupp, "Calculation of the spatial preprocessing and link adaption feedback for 3GPP UMTS/LTE," in *Proc. 6th Conference on Wireless Advanced (WiAD)*, June 2010, pp. 1–6.

[8] A. Jemmali, *Performance Evaluation and Analysis of MIMO Schemes in LTE Networks Environment*. PhD Thesis, Université De Montréal, École Polytechnique De Montréal, Quebec, Canada., 2013.

[9] D. Tse and P. Viswanath, *Fundamnetals of Wireless Communications*. Cambridge University Press, 2008.

[10] S. Sesia, T. Issam, and M. Backer, *LTE The UMTS Long Term Evolution From Theory To Practice*. John Wiley, 2011.

[11] E. Dahlman, S. Parkvall, and J. Skld, *4G LTE/LTE-Advanced for Mobile Broadband*. Academic Press, Elsevier, 2011.

[12] S. Alamouti, "A simple transmit diversity technique for wireless communications," *IEEE Journal on Selected Areas in Communications*, vol. 16, no. 8, pp. 1451–1458, Oct. 1998.

[13] M. Torabi and D. Haccoun, "Performance Analysis of Joint User Scheduling and Antenna Selection Over MIMO Fading Channels," *IEEE Signal Process. Lett.*, vol. 18, no. 4, pp. 235–238, April 2011.

[14] M. S. Alouini and M. K. Simon, *Digital Communications over Fading Channels: A Unified Approach to Performance Analysis*. Wiley, 2000.

[15] M. Torabi, D. Haccoun, and W. Ajib, "Performance Analysis of Scheduling Schemes for Rate-Adaptive MIMO OSFBC-OFDM Systems," *IEEE Trans. Veh. Technol.*, vol. 59, no. 5, pp. 2363–2379, June 2010.

[16] L. Hanzo, C. H. Wong, and M. S. Yee, *Adaptive wireless transceivers: Turbo-Coded, Turbo-Equalised and Space-Time Coded TDMA, CDMA and OFDM Systems*. John Wiley & Sons Ltd, 2002.

[17] C. G. Günther, "Comment on estimate of channel capacity in Rayleigh fading environment," *IEEE Trans. Veh. Technol.*, vol. 45, no. 2, pp. 401–403, May 1996.

[18] M. S. Alouini and A. J. Goldsmith, "Adaptive modulation over Nakagami fading channels," *Wireless Personal Communications*, vol. 13, no. 1, pp. 119–143, 2000.

# Erlang-Engset Multirate Retry Loss Models for Elastic and Adaptive Traffic under the Bandwidth Reservation Policy

Ioannis D. Moscholios*, Vassilios G. Vassilakis†, Michael D. Logothetis‡, and John S. Vardakas§
*Dept. of Informatics & Telecommunications, University of Peloponnese, 221 00 Tripolis, Greece. Email: idm@uop.gr
†Dept. of Electronic Engineering, University of Surrey, GU2 7XH Guildford, U.K. Email: v.vasilakis@surrey.ac.uk
‡Dept. of Electrical and Computer Engineering, University of Patras, 265 04 Patras, Greece. Email: mlogo@upatras.gr
§Iquadrat, Barcelona, Spain. Email: jvardakas@iquadrat.com

***Abstract*—In this paper, we consider a single-link multirate loss system, which accommodates different service-classes with different traffic and peak-bandwidth requirements. Calls of each service-class arrive in the system according to a random (Poisson) or a quasi-random process, and have an exponentially distributed service time. Poisson or quasi-random arriving calls belong to service-classes of infinite or finite number of traffic sources, respectively. The service-classes are also distinguished, according to the behaviour of calls under service, in elastic and adaptive service-classes. Elastic calls can compress their bandwidth by simultaneously increasing their service time, while, adaptive calls do not affect their service time. A new call (either elastic or adaptive) is accepted in the system with its peak-bandwidth requirement, if there is available link bandwidth. If not, the call retries one or more times (single and multi-retry loss model, respectively) with a reduced bandwidth. If the available link bandwidth is lower than the call's last bandwidth requirement, the call can still compress its last bandwidth requirement (down to a certain bandwidth), together with the bandwidth of all in-service calls. Call blocking occurs, if, after compression, the call's bandwidth still exceeds the available link bandwidth. The system incorporates the Bandwidth Reservation (BR) policy, whereby we can achieve certain Quality of Service (QoS) for each service-class, through a proper bandwidth allocation defined by the BR parameters. To calculate in an approximate but efficient way, time and call congestion probabilities, as well as link utilization, we propose recurrent formulas for the determination of the link occupancy distribution. The accuracy of the proposed formulas is verified by simulation, and is found to be very satisfactory. We show the consistency and the necessity of the proposed models.***

***Keywords*—Poisson process, quasi-random, time-call congestion probability, elastic/adaptive traffic, reservation, Markov chains, retrials, recurrent formula.**

## I. Introduction

Elastic and adaptive traffic of multirate service-classes grows rapidly in modern networks, a fact that necessitates the development of efficient analytical tools for the call-level network performance analysis [1]. The term "elastic traffic" refers to in-service calls that have the ability to compress/expand their bandwidth and simultaneously increase/decrease their service time, during their lifetime in a system. On the other hand, the term "adaptive traffic" refers to in-service calls that tolerate bandwidth compression without altering their service time. Examples of elastic traffic are generally TCP-based applications (FTP, HTTP, STMP), while examples of adaptive traffic are mostly real-time applications, like audio and video streaming, which can be transmitted with an acceptable QoS after bandwidth compression.

Assuming that the call arrival process is Poisson, the calculation of various performance measures, such as call blocking probabilities and system's utilization, can be based on the classical Erlang Multirate Loss Model (EMLM) [2] - [3], which has been extensively used for the call-level performance evaluation of wired (e.g., [4] - [14]), wireless (e.g., [15] - [21]) and optical networks (e.g., [22] - [26]). If the call arrival process is quasi-random, i.e., calls come from a finite number of users, then the Engset Multirate Loss Model (EnMLM) arises [27].

In both the EMLM and the EnMLM, calls compete for the available link bandwidth according to the complete sharing policy (i.e., calls compete for all bandwidth resources) and have fixed bandwidth requirements. The latter means that in-service calls do not compress their bandwidth during their lifetime in the system. A new call is blocked and lost, if its required bandwidth is not available. In both models, the steady state probabilities have a Product Form Solution (PFS), which leads to an accurate calculation of call blocking probabilities (see e.g., [2], [3] and [27]).

In [28] and [29], the EMLM and the EnMLM, respectively, have been extended to include retrials. Blocked calls retry one or more times (Single-Retry Model (SRM) or Multi-Retry Model (MRM), respectively) to be accepted in the link by requiring less bandwidth. A retry call is blocked and lost, if the available link bandwidth is lower than the call's last bandwidth requirement. In [30], an approximate method has been proposed for both single and multi retries in the EnMLM that simplifies the calculation of call blocking probabilities.

In [31], the authors have extended [28] by incorporating the notion of elastic traffic. Instead of rejecting immediately a retry call, the link may accept this call by compressing its bandwidth, together with the bandwidth of all in-service calls of all service-classes. Elastic calls increase their service time so that the product *bandwidth* by *service time* remains constant. After compression, the retry call is accepted in the system, if the resultant bandwidth is not higher than the available link bandwidth; otherwise the retry call is blocked and lost. When a call with compressed bandwidth leaves the system, then the remaining in-service calls expand their bandwidth.

In [32], [33], the authors have extended [31] to include adaptive traffic, as well as the Bandwidth Reservation (BR) policy. Adaptive calls compress or expand their bandwidth without altering their service time. On the other hand, the BR policy can achieve equalization of blocking probabilities among service-classes (either elastic or adaptive), or guarantee a certain QoS for each service-class, by a proper selection of the BR parameters so that each service-class meets a certain link bandwidth capacity. Note that the aforementioned models are consistent; that is, if blocked calls of all service-classes are not allowed to retry, then the model of [33] results in the model proposed in [1].

The consideration of the BR policy is of paramount importance in multirate communication networks, given that the absence of the BR policy leads to an unfair service (the less required bandwidth, the better call blocking probability). The system under the BR policy becomes non-PFS, because the Markov chain that describes the system, loses its reversibility.

In this paper, we extend [29], [30] to include elastic and adaptive traffic with retrials under the BR policy. Due to the existence of retrials, the BR policy and bandwidth compression, the proposed elastic/adaptive single-retry and multi-retry loss models for quasi-random input do not have a PFS. However, we propose approximate but recursive formulas for the calculation of the link occupancy distribution and, consequently, time and call congestion probabilities, as well as link utilization. Note that the proposed models are also consistent: if calls are generated by an infinite number of users and blocked calls are not allowed to retry, then the proposed models result in the model of [1].

The remainder of this paper is as follows: In Section II, we present application areas for teletraffic multirate loss models that support elastic traffic. In Section III, for the integrity of the paper, we review the model of [1], named herein Extended EMLM/BR (E-EMLM/BR). In Section IV, we review the models of [33], named herein Extended SRM/BR and Extended MRM/BR (E-SRM/BR and E-MRM/BR, respectively). In Section IV.A, we review the E-SRM/BR, while in Section IV.B, we consider the E-MRM/BR. In Section V, we assume that calls arrive according to a quasi-random process and propose the Extended Finite SRM/BR and the Extended Finite MRM/BR (EF-SRM/BR and EF-MRM/BR, respectively). We prove the recursive formulas for the link occupancy distribution and provide formulas for the calculation of time and call congestion probabilities, as well as link utilization. Section VI is the evaluation section. We present analytical and simulation results of the various performance measures for the proposed models. We also provide analytical results of existing models for comparison. We conclude in Section VII. Finally, we tabulate as Appendix A and B, all the symbols and acronyms, respectively, used in this paper.

## II. Applications of Multirate Elastic Loss Models

Application areas for multirate loss models that include the case of elastic traffic and the notion of bandwidth compression are numerous (see e.g., [34] - [41] and the references therein). These areas can also be considered relevant to our proposed models, which include the notion of retrials, the BR policy and the case of adaptive traffic. However, the proposed models are mostly applicable in wireless networks, where calls may come from finite sources (it is justified by the limited coverage of a cell) and their bandwidth can be compressed, while the BR policy can protect handover calls.

In [34] and [35], an EMLM based model for the recursive calculation of flow throughput and packet loss rate in IP networks is proposed. A link of certain capacity accommodates elastic calls of different service-classes. Arriving calls follow a Poisson process. The link capacity is shared among calls according to a balanced fairness criterion: if the occupied link bandwidth does not exceed the capacity of the link, then all calls use their peak-bandwidth requirement; otherwise, all calls share the capacity in proportion to their peak-bandwidth requirement and the link operates at its full capacity. The main difference of the compression mechanism between [34], [35] and the E-EMLM/BR lies on the fact that in [34] and [35], there is no parameter for admission control. The application of balanced fairness in multirate tree networks and its comparison with other classical bandwidth allocation policies (e.g., max-min fairness) are examined in [36], [37].

In [38], a Code Division Multiple Access cell is considered, which accommodates multirate elastic service-classes. Elastic calls arrive in the link according to a Poisson process and have an exponentially distributed service time. The main target of this paper is the calculation of upper and lower bounds for call blocking probabilities based on an extension of [9] (named herein E-EMLM). In [39], the co-existence of stream traffic (calls cannot compress their assigned bandwidth) and elastic traffic in IEEE802.16e mobile WiMAX subject to adaptive modulation and coding is considered. Calls of both stream and elastic service-classes arrive in the system according to a Poisson process and have an exponentially distributed service time. Stream calls have priority over elastic calls and, in that sense, elastic calls share the left-over capacity of the system. This means that the blocking probability of stream service-classes does not depend on the amount of traffic generated by elastic service-classes. The co-existence of stream and elastic traffic results in an analytical model which can not be described by recursive formulas (see also [40] for a more general multirate loss model) and, therefore, the calculation of blocking probabilities is based on the solution of the steady-state probabilities equations. Such a solution is inefficient for systems with large capacity and many service-classes, due to the extremely large number of equations that arise. Another extension of the EMLM that studies the co-existence of stream and elastic traffic (with similar problems with those described for [39]) in the downlink of Orthogonal Frequency-Division Multiple Access wireless cellular networks is proposed in [41].

## III. Review of The E-EMLM/BR

Consider a single link of capacity $C$ bandwidth units (b.u.) that accommodates calls of $K$ service-classes. Let $K_e$ and $K_a$ be the set of elastic and adaptive service-classes ($K_e + K_a = K$), respectively. A call of service-class $k$ ($k = 1, \ldots, K$) follows a Poisson process with arrival rate $\lambda_{k,inf}$ and has a peak-bandwidth requirement of $b_k$ b.u. (integer value), as well as a BR parameter of $t(k)$ b.u. The latter refers to the number of b.u. reserved so that service-class $k$ meets a link bandwidth capacity of $C - t(k)$ b.u. By assigning a bigger BR parameter $t(k)$ to a service-class $k$ requiring less bandwidth per call than another service-class, this, benefits all service-class calls of a higher bandwidth per call. Let $j$ be the occupied link bandwidth when a new service-class $k$ call arrives in the link. Bandwidth compression is introduced in the model by assuming that $j$ may exceed $C$ up to a value of $T$ b.u.; $T$ is called virtual capacity of the link. If $j + b_k \leq C$, the call is accepted in the system with its $b_k$ b.u. and remains in the system for an exponentially distributed service time with mean $\mu_k^{-1}$. The new service-class $k$ call is blocked and lost if $j + b_k > T - t(k)$. If $T - t(k) \geq j + b_k > C$, the new call is accepted in the system. However, the assigned bandwidth of all in-service calls, together with the peak-bandwidth requirement of the new call is compressed. After the bandwidth compression of all calls (new and in-service) the system state becomes $j = C$. The compressed bandwidth of the new service-class $k$ call is calculated by:

$$b_k^{'} = r b_k = \frac{C}{j^{'}} b_k \tag{1}$$

where $r \equiv r(\mathbf{n}) = C/j$ is the compression factor (common to all service-classes), $j^{'} = j + b_k = \mathbf{nb} + b_k$, $\mathbf{n} = (n_1, \ldots, n_k, \ldots, n_K)$, $n_k$ is the number of in-service calls of service-class $k$, $\mathbf{b} = (b_1, \ldots, b_K)$ and $j = \sum_{k=1}^{K} n_k b_k = \mathbf{nb}$.

Similarly, the compressed bandwidth of all in-service calls is equal to $b_i^{'} = \frac{C}{j^{'}} b_i$ for $i = 1, \ldots, K$. The minimum bandwidth of a service-class $k$ call is given by:

$$b_{k,\min}^{'} = r_{\min} b_k = \frac{C}{T} b_k \tag{2}$$

After the bandwidth compression, all elastic calls increase their service time so that the product (*service time*) by (*bandwidth*) remains constant. A simple tutorial example that describes in detail the bandwidth compression mechanism can be found in [13]. The mechanism of bandwidth compression/expansion and the existence of the BR policy destroy reversibility in the E-EMLM/BR and therefore no PFS exists. However, in [1] an approximate recursive formula is proposed, which determines the link occupancy distribution, $G(j)$, (unnormalized values):

$$G(j) = \begin{cases} 1 & \text{for } j = 0 \\ \frac{1}{\min(j,C)} \sum\limits_{k \in K_e} \alpha_{k,\inf} D_k(j - b_k) G(j - b_k) + \\ \frac{1}{j} \sum\limits_{k \in K_a} \alpha_{k,\inf} D_k(j - b_k) G(j - b_k) & \\ & \text{for } j = 1, \ldots, T \\ 0 & \text{for } j < 0 \end{cases} \tag{3}$$

$$D_k(j - b_k) = \begin{cases} b_k & for \;\; j \leq T - t(k) \\ 0 & for \;\; j > T - t(k) \end{cases} \tag{4}$$

where $\alpha_{k,\inf} = \lambda_{k,\inf} / \mu_k$ is the offered traffic-load (in erl) of service-class $k$.

As far as the computational complexity of (3) is concerned is in the order of O($KT$).

The BR policy ensures equalization of blocking probabilities among different service-classes by a proper selection of the BR parameters. If, for example, blocking equalization is required between calls of three service-classes with $b_1$=1, $b_2$=7 and $b_3$=10 b.u., respectively, then $t(1) = 9$ b.u, $t(2) = 3$ and $t(3) = 0$ b.u., so that $b_1 + t(1) = b_2 + t(2) = b_3 + t(3)$.

The application of the BR policy in the E-EMLM/BR is based on the assumption that the number of service-class $k$ calls is negligible in states $j > T - t(k)$ and is incorporated in (3) by the variable $D_k(j - b_k)$ given in (4). The states $j > T - t(k)$ belong to the so-called reservation space. Note that the population of calls of service-class $k$ in the reservation space may not be negligible. In [8] and [42], a complex procedure is implemented in order to take into account this population and increase the accuracy of the resultant blocking probability in the EMLM and Engset multirate state-dependent loss models, respectively. However, according to [42], this procedure may not always increase the accuracy of blocking probability results compared to simulation.

Based on (3), (4), we can calculate time and call congestion probabilities, and the link utilization, as follows:

1) The time congestion probabilities of service-class $k$, denoted as $P_{b_k}$, is the probability that at least $T - b_k + 1$ bandwidth units are occupied:

$$P_{b_k} = \sum_{j=T-b_k-t(k)+1}^{T} G^{-1} G(j) \tag{5}$$

where: $G = \sum_{j=0}^{T} G(j)$ is a normalization constant.
Time congestion probabilities are determined by the proportion of time the system is congested.

2) The call congestion probabilities of service-class $k$, denoted as $C_{b_k}$, is the probability that a new service-class $k$ call is blocked and lost:

$$C_{b_k} = \sum_{j=T-b_k-t(k)+1}^{T} G^{-1} G(j) \tag{6}$$

Call congestion probabilities are determined by the proportion of arriving calls that find the system congested. Time and call congestion probabilities coincide in the case of Poisson arrivals (due to the Poisson Arrivals See Time Averages (PASTA) property [43]), but not in the case of quasi-random arrivals.

3) The link utilization, denoted as $U$:

$$U = \sum_{j=1}^{C} j G^{-1} G(j) + \sum_{j=C+1}^{T} C G^{-1} G(j) \tag{7}$$

Note that if the BR policy is not applied in the system, i.e., $t(k)$ = 0 for all $k$ $(k = 1,\dots,K)$, then the link occupancy distribution is given by the E-EMLM [9]:

$$G(j)=\begin{cases}1 & \text{for } j=0\\ \frac{1}{\min(j,C)}\sum\limits_{k\in K_e}\alpha_{k,\inf}b_kG(j-b_k)+ & \\ \frac{1}{j}\sum\limits_{k\in K_a}\alpha_{k,\inf}b_kG(j-b_k) & \text{for } j=1,\dots,T\\ 0 & \text{for } j<0\end{cases} \quad (8)$$

In that case, the calculation of time and call congestion probabilities is given by (5), (6), respectively, where $t(k) = 0$ for all $k$ $(k = 1,\dots,K)$. Furthermore, if $T = C$, then the link accommodates only stream traffic (i.e., calls of all service-classes cannot compress their bandwidth) and the EMLM results. In the EMLM, the link occupancy distribution is given by the classical Kaufman-Roberts recursion [2], [3]:

$$G(j)=\begin{cases}1 & \text{for } j=0\\ \frac{1}{j}\sum\limits_{k\in K}\alpha_{k,\inf}b_kG(j-b_k) & \text{for } j=1,\dots,C\\ 0 & \text{for } j<0\end{cases} \quad (9)$$

## IV. Review of The E-SRM/BR And The E-MRM/BR

### A. The E-SRM/BR

Consider again the link of capacity $C$ b.u. that accommodates $K_e$ and $K_a$ elastic and adaptive service-classes, respectively. Service-class $k$ calls $(k = 1,\dots,K)$ follow a Poisson process with rate $\lambda_{k,\inf}$, request $b_k$ b.u. (peak-bandwidth requirement), have a BR parameter of $t(k)$ b.u. and an exponentially distributed service time with mean $\mu_k^{-1}$.

Let $j$ be the occupied link bandwidth, $j = 0,1,\dots,T$, when a service-class $k$ call arrives in the link. Now, we consider the following cases:

a) If $j + b_k \le C$, the call is accepted in the link with $b_k$ b.u.

b) If $j+b_k > C$, then the call is blocked with $b_k$ and retries immediately to be connected in the link with $b_{kr} < b_k$. Now if:

  b1) $j + b_{kr} \le C$ the retry call is accepted in the system with $b_{kr}$ and $\mu_{kr}^{-1} > \mu_k^{-1}$, so that $b_{kr}\mu_{kr}^{-1} = b_k\mu_k^{-1}$,

  b2) $j + b_{kr} > T - t(k)$ the retry call is blocked and lost, and

c) $C < j+b_{kr} \le T-t(k)$ the retry call is accepted in the system by compressing its bandwidth requirement $b_{kr}$ together with the bandwidth of all in-service calls of all service-classes. In that case, the compressed bandwidth of the retry call becomes $b_{kr}^{'} = rb_{kr} = \frac{C}{j+b_{kr}}b_{kr}$ where $r$ is the compression factor, common to all service-classes. Similarly, all in-service calls, which have been accepted in the link with $b_k$ (or $b_{kr}$), compress their bandwidth to $b_k^{'} = rb_k$ (or $b_{kr}^{'} = rb_{kr}$) for $k = 1,\dots,K$. After the compression of all calls the link state is $j = C$. The minimum value of the compression factor is $r_{\min} = C/T$.

Similar to the E-EMLM/BR, when a service-class $k$ call, with bandwidth $b_k^{'}$ (or $b_{kr}^{'}$), departs from the system, the remaining in-service calls of each service-class $i$ $(i = 1,\dots,K)$, expand their bandwidth in proportion to their initially assigned bandwidth $b_i$ (or $b_{ir}$). After bandwidth compression/expansion, only elastic service-class calls increase/decrease their service time so that the product *service time* by *bandwidth* remains constant.

The existence of retrials, the BR policy and the bandwidth compression mechanism destroy reversibility in the model and therefore no PFS exists. However, in [33] an approximate recursive formula is proposed for the calculation of the unnormalized values of the link occupancy distribution, $G(j)$:

$$G(j)=\begin{cases}1 & \text{for } j=0\\ \frac{1}{j}\sum\limits_{k\in K_a}\alpha_{k,\inf}D_k(j-b_k)\gamma_k(j)G(j-b_k)+ & \\ \frac{1}{j}\sum\limits_{k\in K_a}\alpha_{kr,\inf}D_{kr}(j-b_{kr})\gamma_{kr}(j)G(j-b_{kr})+ & \\ \frac{1}{\min(C,j)}\sum\limits_{k\in K_e}\alpha_{k,\inf}D_k(j-b_k)\gamma_k(j)G(j-b_k)+ & \\ \frac{1}{\min(C,j)}\sum\limits_{k\in K_e}\alpha_{kr,\inf}D_{kr}(j-b_{kr})\gamma_{kr}(j)G(j-b_{kr}) & \\ & \text{for } j=1,\dots,T\\ 0 & \text{otherwise}\end{cases} \quad (10)$$

where: $\alpha_{k,\inf} = \lambda_{k,\inf}\,\mu_k^{-1}$ is the offered traffic-load (in erl) of service-class $k$ calls,
$\alpha_{kr,\inf} = \lambda_{k,\inf}\,\mu_{kr}^{-1}$,

$$\gamma_k(j) = \begin{cases}1 & \text{for } 1\le j\le C \text{ and } b_{kr}>0\\ 1 & \text{for } 1\le j\le T \text{ and } b_{kr}=0\\ 0 & \text{otherwise}\end{cases},$$

$$\gamma_{kr}(j) = \begin{cases}1 & \text{for } C-b_k+b_{kr} < j \le T\\ 0 & \text{otherwise}\end{cases},$$

$$D_k(j-b_k) = \begin{cases}b_k & \text{for } j\le T-t(k)\\ 0 & \text{for } j>T-t(k)\end{cases},$$

$$D_{kr}(j-b_{kr}) = \begin{cases}b_{kr} & \text{for } j\le T-t(k)\\ 0 & \text{for } j>T-t(k)\end{cases},$$

and $t(k)$ is the reserved bandwidth in favor of calls other than service-class $k$ calls.

The proof of (10) is based on:

i) the application of local balance between adjacent states, which exists only in PFS models,

ii) an approximation in (10), expressed by $\gamma_{kr}(j)$, which assumes that the occupied link bandwidth from retry calls of service-class $k$ is negligible, when $j \le C - (b_k - b_{kr})$,

iii) an approximation in (10), expressed by $\gamma_k(j)$ that refers only to those service-class $k$ calls whose $b_{kr} > 0$; this approximation assumes that the occupied link bandwidth from service-class $k$ calls accepted in the system with $b_k$ b.u. is negligible when $j > C$.

Having determined $G(j)$'s, we can calculate time and call congestion probabilities, as well as link utilization. The final time congestion probability of a retry service-class $k$ call, $P_{bk_r}$, is given by [33]:

$$P_{bk_r} = \sum_{j=T-b_{kr}-t(k)+1}^{T} G^{-1}G(j) \quad (11)$$

where $G = \sum_{j=0}^{T} G(j)$ is the normalization constant.

Note that time and call congestion probabilities coincide in the case of Poisson arrivals. As far as the link utilization is concerned, it is calculated according to (7), where the values of $G(j)$'s are given by (10).

### B. The E-MRM/BR

In the E-MRM/BR, a service-class $k$ call that is not accepted in the system with its peak-bandwidth requirement, $b_k$, may have many retry parameters $(b_{kr_l}, \mu_{kr_l}^{-1})$ for $l = 1, \ldots, s(k)$, with $b_{kr_{s(k)}} < \ldots < b_k$ and $\mu_{kr_{s(k)}}^{-1} > \ldots > \mu_k^{-1}$. Similar to the E-SRM/BR, the E-MRM/BR does not have a PFS and therefore the calculation of $G(j)$'s is based on an approximate but recursive formula [33]:

$$G(j)=\begin{cases} 1 & \text{for } j=0 \\ \frac{1}{j}\sum\limits_{k\in K_a} a_{k,\inf} D_k(j-b_k)\gamma_k(j)G(j-b_k) \\ +\frac{1}{j}\sum\limits_{k\in K_a}\sum\limits_{s=1}^{s(k)} a_{kr_s,\inf} D_{kr_s}(j-b_{kr_s})\cdot \\ \gamma_{kr_s}(j)G(j-b_{kr_s})+ \\ \frac{1}{\min(C,j)}\sum\limits_{k\in K_e} a_{k,\inf} D_k(j-b_k)\gamma_k(j)G(j-b_k) \\ +\frac{1}{\min(C,j)}\sum\limits_{k\in K_e}\sum\limits_{s=1}^{s(k)} a_{kr_s,\inf} D_{kr_s}(j-b_{kr_s})\cdot \\ \gamma_{kr_s}(j)G(j-b_{kr_s}) & \text{for } j=1,\ldots,T \\ 0 & \text{otherwise} \end{cases} \quad (12)$$

where: $\alpha_{kr_s,\inf} = \lambda_{k,\inf}\mu_{kr_s}^{-1}$

$$\gamma_k(j) = \begin{cases} 1 \ \text{for } 1 \le j \le C \text{ and } b_{kr_s} > 0 \\ 1 \ \text{for } 1 \le j \le T \text{ and } b_{kr_s} = 0 \\ 0 \ \text{otherwise} \end{cases}$$

$$\gamma_{kr_s}(j) = \begin{cases} 1 \ \text{for } C-b_{kr_{s-1}}+b_{kr_s} < j \le C \ \text{ and } s \ne s(k) \\ 1 \ \text{for } C-b_{kr_{s-1}}+b_{kr_s} < j \le T \ \text{ and } s = s(k) \\ 0 \ \text{otherwise} \end{cases}$$

$$D_k(j-b_k) = \begin{cases} b_k & \text{for } j \le T-t(k) \\ 0 & \text{for } j > T-t(k) \end{cases},$$

$$D_{kr_s}(j-b_{kr_s}) = \begin{cases} b_{kr_s} & \text{for } j \le T-t(k) \\ 0 & \text{for } j > T-t(k) \end{cases}$$

The computational complexity of (12) is $O(KT + \sum_{k=1}^{K}(s(k)(b_k - b_{kr_1}))$, assuming that the difference $b_{kr_{s-1}} - b_{kr_s}$ is constant.

If the BR policy is not applied, then we have the E-MRM and (12) takes the form [32]:

$$G(j)=\begin{cases} 1 & \text{for } j=0 \\ \frac{1}{j}\sum\limits_{k\in K_a}\alpha_{k,\inf} b_k\gamma_k(j)G(j-b_k)+ \\ \frac{1}{j}\sum\limits_{k\in K_a}\sum_{s=1}^{s(k)}\alpha_{kr_s,\inf} b_{kr_s}\gamma_{kr_s}(j)G(j-b_{kr_s})+ \\ \frac{1}{\min(C,j)}\sum\limits_{k\in K_e}\alpha_{k,\inf} b_k\gamma_k(j)G(j-b_k)+ \\ \frac{1}{\min(C,j)}\sum\limits_{k\in K_e}\sum\limits_{s=1}^{s(k)}\alpha_{kr_s,\inf} b_{kr_s}\gamma_{kr_s}(j)G(j-b_{kr_s}) \\ \quad \text{for } j=1,\ldots,T \\ 0 & \text{otherwise} \end{cases} \quad (13)$$

If only elastic service-classes are accommodated by the link, then (12) becomes [33]:

$$G(j)=\begin{cases} 1 & \text{for } j=0 \\ \frac{1}{\min(C,j)}\sum\limits_{k\in K_e}\alpha_{k,\inf} D_k(j-b_k)\gamma_k(j)G(j-b_k) \\ +\frac{1}{\min(C,j)}\sum\limits_{k\in K_e}\sum\limits_{s=1}^{s(k)}\alpha_{kr_s,\inf} D_{kr_s}(j-b_{kr_s})\cdot \\ \gamma_{kr_s}(j)G(j-b_{kr_s}) & \text{for } j=1,\ldots,T \\ 0 & \text{otherwise} \end{cases} \quad (14)$$

If the link accommodates elastic and adaptive service-classes whose blocked calls are not allowed to retry, then (12) takes the form of (3) and the E-EMLM/BR results [1].

If calls of all service-classes may retry but are not allowed to compress their bandwidth during their service time, then the MRM under the BR policy results and (12) takes the form [44]:

$$G(j)=\begin{cases} 1 & \text{for } j=0 \\ \frac{1}{j}\sum\limits_{k\in K}\alpha_{k,\inf} D_k(j-b_k)G(j-b_k)+ \\ \frac{1}{j}\sum\limits_{k\in K}\sum\limits_{s=1}^{s(k)}\alpha_{kr_s,\inf} D_{kr_s}(j-b_{kr_s})\gamma_{kr_s}(j)G(j-b_{kr_s}) \\ \quad \text{for } j=1,\ldots,C \\ 0 & \text{otherwise} \end{cases} \quad (15)$$

Furthermore, if blocked calls of all service-classes are not allowed to retry, then the EMLM under the BR policy results and (15) takes the form [45]:

$$G(j)=\begin{cases} 1 & \text{for } j=0 \\ \frac{1}{j}\sum\limits_{k\in K}\alpha_{k,\inf} D_k(j-b_k)G(j-b_k) \\ \quad \text{for } j=1,\ldots,C \\ 0 & \text{otherwise} \end{cases} \quad (16)$$

Having determined $G(j)$'s in the E-MRM/BR according to (12), we can calculate the time (and call) congestion probabilities of a retry service-class $k$ call with its last bandwidth requirement, $P_{bkr_{s(k)}}$, according to the formula [33]:

$$P_{bkr_{s(k)}} = \sum_{j=T-b_{kr_{s(k)}}-t(k)+1}^{T} G^{-1}G(j) \quad (17)$$

The calculation of the link utilization in the E-MRM/BR is based on (7) where the values of $G(j)$'s are given by (12).

## V. The Proposed EF-SRM/BR And EF-MRM/BR

In this section, we extend the retry multirate loss models of [29], [30] (which do not examine elastic and adaptive traffic) to include elastic and adaptive traffic under the BR policy. Blocked calls of quasi-random arrivals have the ability to retry one or more times (EF-SRM/BR or EF-MRM/BR, respectively) to be connected in the system with reduced bandwidth. If the available link bandwidth is still higher than the last bandwidth requirement of a retry call, then the call can still try to be connected in the system by compressing its requirement together with the bandwidth of all in-service calls.

### A. The EF-SRM/BR

The proposed EF-SRM/BR is a non-PFS model. In order to prove an approximate but recursive formula for the determination of $G(j)$'s we present the following example.

Consider a link of capacity $C$ b.u. that accommodates calls of two service-classes. The $1^{st}$ service-class is adaptive and the $2^{nd}$ is elastic. Calls of both service-classes are generated by a finite source population $N_k$ $(k = 1, 2)$. The mean call arrival rate of service-class $k$ idle sources is $\lambda_k = (N_k - n_k)v_k$, where $v_k$ is the arrival rate per idle source and $n_k$ is the number of in-service calls. This call arrival process is a quasi-random process [43]. A Poisson process arises from a quasi-random process if $N_k \to \infty$ for $k = 1, \dots, K$, while the total offered traffic-load remains constant.

Assuming that only calls of the $2^{nd}$ service-class can retry, the traffic parameters of both service-classes are: $(N_1, v_1, \mu_1^{-1}, b_1)$ for the $1^{st}$ service-class and $(N_2, v_2, \mu_2^{-1}, \mu_{2r}^{-1}, b_2, b_{2r})$ for the $2^{nd}$ service-class, with $b_{2r} < b_2$ and $\mu_{2r}^{-1} > \mu_2^{-1}$. Initially, let assume that the BR parameters: $t(1) = t(2) = 0$. Bandwidth compression is permitted for calls of both service-classes up to a limit $T$.

The description of call admission is based on a new service-class $k$ call $(k = 1, 2)$ that arrives in the system, when the occupied link bandwidth is $j$ b.u. Then:

i) If $j + b_k \le C$, the call is accepted in the system with $b_k$ b.u. for an exponentially distributed service time with mean $\mu_k^{-1}$.

ii) If $j + b_k > C$ we consider the following sub-cases:

a) If $T \ge j + b_1 > C$, a $1^{st}$ service-class call is accepted in the system by compressing $b_1$, as well as the assigned bandwidth of all in-service calls. The compressed bandwidth of the $1^{st}$ service-class call is given by $b_1^{'} = rb_1 = (C/j^{'})b_1$, where $r = C/j^{'}$, $j^{'} = j + b_1 = \mathbf{nb} + b_1$. Similarly, the bandwidth of all in-service calls will be compressed (by the same factor $r$) and become $b_k^{'} = (C/j^{'})b_k$ for $k = 1, 2$. After compression has taken place, all calls share the $C$ b.u. in proportion to their bandwidth requirement, while the link operates at its full capacity $C$. The minimum bandwidth that a $1^{st}$ service-class call can tolerate is $b_{1,\min}^{'} = r_{\min} b_1 = (C/T)b_1$.

b) If $j + b_1 > T$, the $1^{st}$ service-class call is blocked and lost.

c) If $j + b_2 > C$, a $2^{nd}$ service-class call is blocked and retries with $b_{2r} < b_2$. Now, we consider three cases:

c1) If $j + b_{2r} \le C$, the retry call is accepted in the system with $b_{2r}$.

c2) If $j + b_{2r} > T$, the call is blocked and lost.

c3) If $C < j + b_{2r} \le T$ the call is accepted in the system by compressing $b_{2r}$ together with the bandwidth of all in-service calls. The compressed bandwidth of the call is $b_{2r}^{'} = rb_{2r} = (C/j^{'})b_{2r}$ where $j^{'} = j + b_{2r}$. Similarly, the bandwidth of all in-service calls are compressed (by the same factor $r$) and become $b_k^{'} = (C/j^{'})b_k$ for $k = 1, 2$. The minimum bandwidth that a $2^{nd}$ service-class call tolerates is $b_{2r,\min}^{'} = (C/T)b_{2r}$.

Although the steady state probabilities in the proposed model do not have a PFS, we assume that local balance exists between the adjacent states of the $1^{st}$ service-class:

$$(N_1 - n_1 + 1)v_1 P(\mathbf{n}_1^-) = n_1 \mu_1 \phi_1(\mathbf{n}) P(\mathbf{n}), \quad 1 \le \mathbf{nb} \le T \quad (18)$$

where: $\mathbf{n}_1^- = (n_1 - 1, n_2, n_{2r})$, $\mathbf{n} = (n_1, n_2, n_{2r})$, $\mathbf{b} = (b_1, b_2, b_{2r})$, $n_1 \ge 1$, $P(\mathbf{n})$ is the probability distribution of state $\mathbf{n}$, and

$$\phi_1(\mathbf{n}) = \begin{cases} 1 & , \text{ when } \mathbf{nb} \le C \\ x(\mathbf{n}_1^-)/x(\mathbf{n}), & \text{when } C < \mathbf{nb} \le T \\ 0 & , \text{ otherwise} \end{cases} \quad (19)$$

where: $\mathbf{nb} = j = n_1 b_1 + n_2 b_2 + n_{2r} b_{2r}$ and $n_{2r}$ is the number of in-service retry calls of the $2^{nd}$ service-class.

Note that $\phi_k(\mathbf{n})$ is a state dependent factor which describes: i) bandwidth compression and ii) the increase factor of service time of service-class $k$ calls in state $\mathbf{n}$. In other words, $\phi_k(\mathbf{n})$ has the same role with $r$, but it may be different for each service-class.

By multiplying both sides of (18) with $b_1$ and $r(\mathbf{n})$, and based on (19), we have:

$$(N_1 - n_1 + 1)\alpha_1 b_1 x(\mathbf{n}) r(\mathbf{n}) P(\mathbf{n}_1^-) = n_1 b_1 x(\mathbf{n}_1^-) r(\mathbf{n}) P(\mathbf{n}) \quad (20)$$

where $\alpha_1 = v_1 \mu_1^{-1}$is the offered traffic-load per idle source of $1^{st}$ service-class, $r(n) = \min(1, C/j)$ and $1 \le \mathbf{nb} \le T$.

Based on the call admission control mechanism described for $2^{nd}$ service-class calls, the following local balance equations can be derived:

a) For $1 \le \mathbf{nb} \le C$, $\mathbf{n}_2^- = (n_1, n_2 - 1, n_{2r})$, and $n_2 \ge 1$:

$$(N_2 - n_2 + 1)v_2 P(\mathbf{n}_2^-) = n_2 \mu_2 \phi_2(\mathbf{n}) P(\mathbf{n}) \quad (21)$$

where:

$$\phi_2(\mathbf{n}) = \begin{cases} 1 & , \text{ when } \mathbf{nb} \le C \\ x(\mathbf{n}_2^-)/x(\mathbf{n}), & \text{when } C < \mathbf{nb} \le T \\ 0 & , \text{ otherwise} \end{cases} \quad (22)$$

By multiplying both sides of (21) with $b_2$, and based on (22), we obtain:

$$(N_2 - n_2 + 1)\alpha_2 b_2 x(\mathbf{n}) P(\mathbf{n}_2^-) = n_2 b_2 x(\mathbf{n}_2^-) P(\mathbf{n}) \quad (23)$$

where: $1 \le \mathbf{nb} \le C$, and $\alpha_2 = v_2 \mu_2^{-1}$.

b) If $P(\mathbf{n}_{2r}^-)$ is the probability distribution of state $\mathbf{n}_{2r}^- = (n_1, n_2, n_{2r} - 1)$,

$$(N_2 - n_2 - n_{2r} + 1)v_2 P(\mathbf{n}_{2r}^-) = n_{2r} \mu_{2r} \phi_{2r}(\mathbf{n}) P(\mathbf{n}) \quad (24)$$

where: $C - b_2 + b_{2r} < \mathbf{nb} \le T$, and

$$\phi_{2r}(\mathbf{n}) = \begin{cases} 1 & , \text{ when } \mathbf{nb} \le C \\ x(\mathbf{n}_{2r}^-)/x(\mathbf{n}), & \text{when } C < \mathbf{nb} \le T \\ 0 & , \text{ otherwise} \end{cases} \quad (25)$$

By multiplying both sides of (24) with $b_{2r}$, and based on (25), we obtain for $C - b_2 + b_{2r} < \mathbf{nb} \le T$:

$$(N_2 - n_2 - n_{2r} + 1)\alpha_{2r} b_{2r} x(\mathbf{n}) P(\mathbf{n}_{2r}^-) = n_{2r} b_{2r} x(\mathbf{n}_{2r}^-) P(\mathbf{n}) \quad (26)$$

where: $\alpha_{2r} = v_2\mu_{2r}^{-1}$.

Equations (20), (23) and (26) lead to a system of equations:

$$\begin{aligned}&(N_1-n_1+1)\alpha_1 b_1 x(\mathbf{n})r(\mathbf{n})P(\mathbf{n}_1^-)+\\&(N_2-n_2+1)\alpha_2 b_2 x(\mathbf{n})P(\mathbf{n}_2^-)\\&=(n_1 b_1 x(\mathbf{n}_1^-)r(\mathbf{n})+n_2 b_2 x(\mathbf{n}_2^-))P(\mathbf{n})\\&\text{for } 1\le \mathbf{nb}\le C-b_2+b_{2r}\end{aligned} \quad (27)$$

$$\begin{aligned}&(N_1-n_1+1)\alpha_1 b_1 x(\mathbf{n})r(\mathbf{n})P(\mathbf{n}_1^-)+\\&(N_2-n_2+1)\alpha_2 b_2 x(\mathbf{n})P(\mathbf{n}_2^-)+\\&(N_2-n_2-n_{2r}+1)\alpha_{2r} b_{2r} x(\mathbf{n})P(\mathbf{n}_{2r}^-)=\\&(n_1 b_1 x(\mathbf{n}_1^-)r(\mathbf{n})+n_2 b_2 x(\mathbf{n}_2^-)+n_{2r}b_{2r}x(\mathbf{n}_{2r}^-))P(\mathbf{n})\\&\text{for } C-b_2+b_{2r}< \mathbf{nb}\le C\end{aligned} \quad (28)$$

$$\begin{aligned}&(N_1-n_1+1)\alpha_1 b_1 x(\mathbf{n})r(\mathbf{n})P(\mathbf{n}_1^-)+\\&(N_2-n_2-n_{2r}+1)\alpha_{2r} b_{2r} x(\mathbf{n})P(\mathbf{n}_{2r}^-)=\\&(n_1 b_1 x(\mathbf{n}_1^-)r(\mathbf{n})+n_{2r}b_{2r}x(\mathbf{n}_{2r}^-))P(\mathbf{n})\\&\text{for } C< \mathbf{nb}\le T\end{aligned} \quad (29)$$

By assuming that retry calls with $b_{2r}$ are negligible when $1 \le nb \le C - b_2 + b_{2r}$ and that the population of calls with $b_2$ is negligible when $C < \mathbf{nb} \le T$, we can combine (27), (28) and (29) into the following equation:

$$\begin{aligned}&(N_1-n_1+1)\alpha_1 b_1 x(\mathbf{n})r(\mathbf{n})P(\mathbf{n}_1^-)+\\&(N_2-n_2+1)\gamma_2(\mathbf{nb})\,\alpha_2 b_2 x(\mathbf{n})P(\mathbf{n}_2^-)+\\&(N_2-n_2-n_{2r}+1)\gamma_{2r}(\mathbf{nb})\alpha_{2r} b_{2r} x(\mathbf{n})P(\mathbf{n}_{2r}^-)=\\&(n_1 b_1 x(\mathbf{n}_1^-)r(\mathbf{n})+n_2 b_2 x(\mathbf{n}_2^-)+n_{2r}b_{2r}x(\mathbf{n}_{2r}^-))P(\mathbf{n})\\&\text{for } 1\le nb\le T\end{aligned} \quad (30)$$

where: $\gamma_2(\mathbf{nb}) = 1$ for $1 \le \mathbf{nb} \le C$, otherwise $\gamma_2(\mathbf{nb}) = 0$, and: $\gamma_{2r}(\mathbf{nb}) = 1$ for $C-b_2+b_{2r}< \mathbf{nb} \le T$, otherwise $\gamma_{2r}(\mathbf{nb}) = 0$.

In order to derive a formula for $x(\mathbf{n})$, we make the following assumptions:

1) When $C < \mathbf{nb} \le T$, the bandwidth of all in-service calls are compressed by $\phi_k(\mathbf{n})$, $k = 1, 2$, so that:

$$n_1 b_1^{'} + n_2 b_2^{'} + n_{2r} b_{2r}^{'} = C \quad (31)$$

2) We keep the product *service time* by *bandwidth* of service-class $k$ calls (elastic or adaptive) in state $\mathbf{n}$ of the irreversible Markov chain equal to the corresponding product in the same state $\mathbf{n}$ of the reversible Markov chain:

$$\begin{aligned}&\frac{b_1 r(\mathbf{n})}{\mu_1} = \frac{b_1^{'}}{\mu_1\phi_1(\mathbf{n})} \ \text{ or } b_1^{'} = b_1\phi_1(\mathbf{n})r(\mathbf{n})\\&\frac{b_2 r(\mathbf{n})}{\mu_2 r(n)} = \frac{b_2^{'}}{\mu_2\phi_2(\mathbf{n})} \ \textit{ or } b_2^{'} = b_2\phi_2(\mathbf{n})\\&\frac{b_{2r} r(\mathbf{n})}{\mu_{2r} r(\mathbf{n})} = \frac{b_{2r}^{'}}{\mu_{2r}\phi_{2r}(\mathbf{n})} \ \textit{ or } b_{2r}^{'} = b_{2r}\phi_{2r}(\mathbf{n})\end{aligned} \quad (32)$$

By substituting (32) in (31), we have:

$$n_1 b_1\phi_1(\mathbf{n})r(\mathbf{n}) + n_2 b_2\phi_2(\mathbf{n}) + n_{2r} b_{2r}\phi_{2r}(\mathbf{n}) = C \quad (33)$$

where $\phi_1(\mathbf{n})$, $\phi_2(\mathbf{n})$ and $\phi_{2r}(\mathbf{n})$ are given by (19), (22) and (25), respectively.

Equation (33), due to (19), (22) and (25) is written as:

$$x(\mathbf{n})=\begin{cases}1 & \text{for } \mathbf{nb}\le C,\ \mathbf{n}\in\mathbf{\Omega}\\ \frac{1}{C}n_1 b_1 x(\mathbf{n}_1^-)r(\mathbf{n})+\frac{1}{C}n_2 b_2 x(\mathbf{n}_2^-)+\\ \frac{1}{C}n_{2r}b_{2r}x(\mathbf{n}_{2r}^-) & \text{for } C<\mathbf{nb}\le T\\ 0 & \text{otherwise}\end{cases} \quad (34)$$

Based on (34), we consider again (30). Since $x(\boldsymbol{n}) = 1$, when $0 \le j \le C$, it is proved in [7] that:

$$\begin{aligned}&(N_1-n_1+1)\alpha_1 b_1 G(j-b_1)+\\&(N_2-n_2+1)\alpha_2 b_2 G(j-b_2)+\\&(N_2-n_2-n_{2r}+1)\alpha_{2r}b_{2r}\gamma_{2r}(j)G(j-b_{2r}) = jG(j)\\&\text{for } 1\le j\le C\end{aligned} \quad (35)$$

where: $G(j)$ is the link occupancy distribution, $\gamma_{2r}(j) = 1$ for $C-b_2+b_{2r} < j$, otherwise $\gamma_{2r}(j) = 0$.

When $C < j \le T$, we have $\gamma_2(j)$=0, and due to (34), we may write (30) as follows:

$$\begin{aligned}&\tfrac{C}{j}(N_1-n_1+1)\alpha_1 b_1 P(\mathbf{n}_1^-)+\\&(N_2-n_2-n_{2r}+1)\gamma_{2r}(\mathbf{nb})\alpha_{2r}b_{2r}P(\mathbf{n}_{2r}^-) = CP(\mathbf{n})\end{aligned} \quad (36)$$

since $r(\mathbf{n}) = C/j$, when $C < j \le T$.

In order to introduce the link occupancy distribution ($G(j)$) in (36), we sum both sides of (36) over the set of states $\{\mathbf{n}\in\mathbf{\Omega}\,|\mathbf{nb} = j\}$, where $\mathbf{\Omega} = \{\mathbf{n} : 0 \le \mathbf{nb} \le T\}$:

$$\begin{aligned}&\tfrac{C}{j}(N_1-n_1+1)\alpha_1 b_1 \sum_{\{\mathbf{n}|\mathbf{nb}=j\}} P(\mathbf{n}_1^-)+\\&(N_2-n_2-n_{2r}+1)\gamma_{2r}(\mathbf{nb})\alpha_{2r}b_{2r} \sum_{\{\mathbf{n}|\mathbf{nb}=j\}} P(\mathbf{n}_{2r}^-)\\&= C\textstyle\sum_{\{\mathbf{n}|\mathbf{nb}=j\}} P(\mathbf{n})\end{aligned} \quad (37)$$

Since by definition $G(j) = \sum_{n\in\Omega_j} P(n)$, we may write (37) as follows:

$$\begin{aligned}&\tfrac{C}{j}(N_1-n_1+1)\alpha_1 b_1 G(j-b_1)+\\&(N_2-n_2-n_{2r}+1)\gamma_{2r}(j)\alpha_{2r}b_{2r}G(j-b_{2r}) = CG(j)\end{aligned} \quad (38)$$

where $\gamma_{2r}(j) = 1$ for $C-b_2+b_{2r} < j \le T$.

The combination of (35) and (38) gives an approximate recursive formula for the determination of $G(j)$'s, when calls of the $1^{st}$ service-class are adaptive while calls of the $2^{nd}$ service-class are elastic and have retry parameters:

$$\begin{aligned}&G(j) = \tfrac{1}{j}(N_1-n_1+1)\alpha_1 b_1 G(j-b_1)+\\&\tfrac{1}{\min(j,C)}\left[(N_2-n_2+1)\alpha_2 b_2\gamma_2(j)G(j-b_2)\right]+\\&\tfrac{1}{\min(j,C)}\left[(N_2-n_2-n_{2r}+1)\alpha_{2r}b_{2r}\gamma_{2r}(j)G(j-b_{2r})\right]\\&\text{for } 1\le j\le T\end{aligned} \quad (39)$$

where: $\gamma_2(j)$=1 for $1 \le j \le C$, otherwise $\gamma_2(j)$=0 and $\gamma_{2r}(j)$=1 for $C - b_2 + b_{2r} < j \le T$, otherwise $\gamma_{2r}(j)$=0.

In the general case of *K* different service-classes, where all calls may retry, (39) takes the form:

$$G(j)=\begin{cases}1 \quad \text{for } j=0\\[4pt] \frac{1}{j}\sum\limits_{k\in K_a}(N_k-n_k+1)\alpha_k b_k\gamma_k(j)G(j-b_k)+\\ \frac{1}{j}\sum\limits_{k\in K_a}(N_k-n_k-n_{kr}+1)\alpha_{kr}b_{kr}\gamma_{kr}(j)G(j-b_{kr})\\ +\frac{1}{\min(C,j)}\sum\limits_{k\in K_e}(N_k-n_k+1)\alpha_k b_k\gamma_k(j)G(j-b_k)\\ +\frac{1}{\min(C,j)}\sum\limits_{k\in K_e}(N_k-n_k-n_{kr}+1)\alpha_{kr}b_{kr}\\ \gamma_{kr}(j)G(j-b_{kr}) \qquad \text{for } j=1,...,T\\[4pt] 0 \quad \text{otherwise}\end{cases} \quad (40)$$

where: $\alpha_{kr} = v_k \mu_{kr}^{-1}$

$$\gamma_k(j) = \begin{cases} 1 & \text{for } 1 \le j \le C \text{ and } b_{kr} > 0 \\ 1 & \text{for } 1 \le j \le T \text{ and } b_{kr} = 0 \\ 0 & \text{otherwise} \end{cases},$$

$$\gamma_{kr}(j) = \begin{cases} 1 & \text{for } C - b_k + b_{kr} < j \le T \text{ and } b_{kr} > 0 \\ 0 & \text{otherwise} \end{cases}$$

If the BR parameters are positive, then (40) takes the form:

$$G(j) = \begin{cases} 1 \quad \text{for } j = 0 \\ \frac{1}{j} \sum\limits_{k \in K_a} (N_k - n_k + 1) \alpha_k D_k(j - b_k) \gamma_k(j) G(j - b_k) \\ + \frac{1}{j} \sum\limits_{k \in K_a} (N_k - n_k - n_{kr} + 1) \alpha_{kr} D_{kr}(j - b_{kr}) \gamma_{kr}(j) \\ G(j - b_{kr}) + \frac{1}{\min(C,j)} \sum\limits_{k \in K_e} (N_k - n_k + 1) \alpha_k D_k(j - b_k) \\ \gamma_k(j) G(j - b_k) + \frac{1}{\min(C,j)} \sum\limits_{k \in K_e} (N_k - n_k - n_{kr} + 1) \\ \alpha_{kr} D_{kr}(j - b_{kr}) \gamma_{kr}(j) G(j - b_{kr}) \\ \quad \text{for } j = 1, \ldots, T \\ 0 \quad \text{otherwise} \end{cases} \tag{41}$$

where: $D_k(j - b_k) = \begin{cases} b_k & \text{for } j \le T - t(k) \\ 0 & \text{for } j > T - t(k) \end{cases}$

and $D_{kr}(j - b_{kr}) = \begin{cases} b_{kr} & \text{for } j \le T - t(k) \\ 0 & \text{for } j > T - t(k) \end{cases}$

Furthermore, if calls of all service-classes are elastic, then (41) takes the form:

$$G(j) = \begin{cases} 1 \quad \text{for } j = 0 \\ \frac{1}{\min(C,j)} \sum\limits_{k \in K} (N_k - n_k + 1) \alpha_k D_k(j - b_k) \gamma_k(j) G(j - b_k) \\ + \frac{1}{\min(C,j)} \sum\limits_{k \in K} (N_k - n_k - n_{kr} + 1) \alpha_{kr} D_{kr}(j - b_{kr}) \cdot \\ \gamma_{kr}(j) G(j - b_{kr}) \quad \text{for } j = 1, \ldots, T \\ 0 \quad \text{otherwise} \end{cases} \tag{42}$$

The calculation of $G(j)$'s in (40), (41) or (42) requires the values of $n_k$ and $n_{kr}$, which are unknown. In other finite multirate loss models (e.g., [11], [27], [29]) there exist methods for the determination of these values through an equivalent stochastic system, with the same traffic description parameters and set of states. However, the state space determination of the equivalent system is complex, especially for large systems that serve many service-classes. Thus, we avoid such methods and approximate $n_k$ and $n_{kr}$ in state $j$, i.e., $n_k(j)$ and $n_{kr}(j)$, as the mean number of service-class *k* calls in state *j*, $y_k(j)$ and $y_{kr}(j)$, respectively, when Poisson arrivals are considered. Such approximations are common in the literature and induce little error (e.g., [30], [46] - [47]). In that case, we may rewrite (41) as follows:

$$G(j) = \begin{cases} 1 \quad \text{for } j = 0 \\ \frac{1}{j} \sum\limits_{k \in K_a} (N_k - y_k(j - b_k)) \alpha_k D_k(j - b_k) \gamma_k(j) G(j - b_k) \\ + \frac{1}{j} \sum\limits_{k \in K_a} (N_k - y_k(j - b_{kr}) - y_{kr}(j - b_{kr})) \cdot \\ \alpha_{kr} D_{kr}(j - b_{kr}) \gamma_{kr}(j) G(j - b_{kr}) + \\ \frac{1}{\min(C,j)} \sum\limits_{k \in K_e} (N_k - y_k(j - b_k)) \alpha_k D_k(j - b_k) \gamma_k(j) G(j - b_k) \\ + \frac{1}{\min(C,j)} \sum\limits_{k \in K_e} (N_k - y_k(j - b_{kr}) - y_{kr}(j - b_{kr})) \alpha_{kr} \cdot \\ D_{kr}(j - b_{kr}) \gamma_{kr}(j) G(j - b_{kr}) \quad \text{for } j = 1, \ldots, T \\ 0 \quad \text{otherwise} \end{cases} \tag{43}$$

where the values of $y_k(j)$ and $y_{kr}(j)$ are given by:

$$y_k(j) = \alpha_{k,\inf} \gamma_k(j) G_{\inf}(j - b_k) / G_{\inf}(j) \tag{44}$$

$$y_{kr}(j) = \alpha_{kr,\inf} \gamma_{kr}(j) G_{\inf}(j - b_{kr}) / G_{\inf}(j) \tag{45}$$

where: $\alpha_{k,\inf}$, $\alpha_{kr,\inf}$ and $G_{\inf}(j)$ are the offered traffic-load (in erl) of service-class *k* and the link occupancy distribution, respectively, of the corresponding infinite model (E-SRM/BR) [33], i.e., the values of $G_{\inf}(j)$ will be determined by (10).

Having determined $G(j)$'s in the EF-SRM/BR according to (43), we calculate the time congestion probabilities according to (11), and the link utilization according to (7). As far as the call congestion probabilities are concerned, we may again use (11), but the values of $G(j)$'s in (43) should be determined for a system with $N_k - 1$ traffic sources.

### B. *The EF-MRM/BR*

Similar to the EF-SRM/BR, the corresponding multi-retry model does not have a PFS and therefore the $G(j)$'s calculation is based on an approximate but recursive formula. In the EF-MRM/BR, a blocked service-class *k* call retries *s*(*k*) times with parameters: $(b_{kr_s}, \mu_{kr_s}^{-1})$ for $s = 1, \ldots, s(k)$, where $b_{kr_{s(k)}} < \ldots < b_{kr_1} < b_k$ and $\mu_{kr_{s(k)}}^{-1} > \ldots > \mu_{kr_1}^{-1} > \mu_k^{-1}$. The determination of $G(j)$'s is based on (46) whose proof is similar to that of (41) and therefore is not presented:

$$G(j) = \begin{cases} 1 \quad \text{for } j = 0 \\ \frac{1}{j} \sum\limits_{k \in K_a} (N_k - n_k + 1) \alpha_k D_k(j - b_k) \gamma_k(j) G(j - b_k) + \\ \frac{1}{j} \sum\limits_{k \in K_a} \sum\limits_{s=1}^{s(k)} (N_k - (n_k + n_{kr_1} + \ldots + n_{kr_{s(k)}}) + 1) \cdot \\ \alpha_{kr_s} D_{kr_s}(j - b_{kr_s}) \gamma_{kr_s}(j) G(j - b_{kr_s}) + \\ \frac{1}{\min(C,j)} \sum\limits_{k \in K_e} (N_k - n_k + 1) \alpha_k D_k(j - b_k) \gamma_k(j) G(j - b_k) + \\ \frac{1}{\min(C,j)} \sum\limits_{k \in K_e} \sum\limits_{s=1}^{s(k)} (N_k - (n_k + n_{kr_1} + \ldots + n_{kr_{s(k)}}) + 1) \cdot \\ \alpha_{kr_s} D_{kr_s}(j - b_{kr_s}) \gamma_{kr_s}(j) G(j - b_{kr_s}) \\ \quad \text{for } j = 1, \ldots, T \\ 0 \quad \text{otherwise} \end{cases} \tag{46}$$

where: $\alpha_{kr_s} = v_k \mu_{kr_s}^{-1}$,

$D_k(j - b_k) = \begin{cases} b_k & \text{for } j \le T - t(k) \\ 0 & \text{for } j > T - t(k) \end{cases}$

$$D_{kr_s}(j-b_{kr_s}) = \begin{cases} b_{kr_s} & \text{for } j \le T - t(k) \\ 0 & \text{for } j > T - t(k) \end{cases}$$

$$\gamma_k(j) = \begin{cases} 1 & \text{for } 1 \le j \le C \text{ and } b_{kr_s} > 0 \\ 1 & \text{for } 1 \le j \le T \text{ and } b_{kr_s} = 0 \\ 0 & \text{otherwise} \end{cases}$$

$$\gamma_{kr_s}(j) = \begin{cases} 1 & \text{for } C - b_{kr_{s-1}} + b_{kr_s} < j \le C \text{ if } s \ne s(k) \\ 1 & \text{for } C - b_{kr_{s-1}} + b_{kr_s} < j \le T \text{ if } s = s(k) \\ 0 & \text{otherwise} \end{cases}$$

As in the EF-SRM/BR, we approximate $n_k(j)$ and $n_{kr_s}(j)$ for $s = 1, \ldots, s(k)$ with the corresponding values of the infinite model [33]. In that case, (46) takes the form:

$$G(j) = \begin{cases} 1 & \text{for } j = 0 \\ \frac{1}{j}\sum\limits_{k\in K_a}(N_k - y_k(j-b_k))\alpha_k D_k(j-b_k)\gamma_k(j)G(j-b_k) \\ +\frac{1}{j}\sum\limits_{k\in K_a}\sum\limits_{s=1}^{s(k)}(N_k - Y_k(j-b_{kr_s}))\alpha_{kr_s} D_{kr_s}(j-b_{kr_s}) \\ \cdot\gamma_{kr_s}(j)G(j-b_{kr_s}) + \\ \frac{1}{\min(C,j)}\sum\limits_{k\in K_e}(N_k - y_k(j-b_k))\alpha_k D_k(j-b_k)\cdot \\ \gamma_k(j)G(j-b_k) + \frac{1}{\min(C,j)}\sum\limits_{k\in K_e}\sum\limits_{s=1}^{s(k)}(N_k - Y_k(j-b_{kr_s})) \\ \cdot\alpha_{kr_s} D_{kr_s}(j-b_{kr_s})\gamma_{kr_s}(j)G(j-b_{kr_s}) \\ & \text{for } j = 1, \ldots, T \\ 0 & \text{otherwise} \end{cases} \tag{47}$$

where: $Y_k(j - b_{kr_s}) = y_k(j - b_{kr_s}) + y_{kr_1}(j - b_{kr_s}) + \ldots + y_{kr_{s(k)}}(j - b_{kr_s})$ and the values of $y_k(j)$ and $y_{kr_s}(j)$ are given by:

$$y_k(j) = a_{k,\inf}\gamma_k(j)G_{\inf}(j - b_k)/G_{\inf}(j) \tag{48}$$

$$y_{kr_s}(j) = \alpha_{kr,\inf}\gamma_{kr_s}(j)G_{\inf}(j - b_{kr_s})/G_{\inf}(j) \tag{49}$$

where $G_{\inf}(j)$ refers to the link occupancy distribution of the corresponding infinite model (E-MRM/BR) [33], i.e., the values of $G_{\inf}(j)$ will be given by (12).

If the BR policy is not applied, then we have the EF-MRM and (47) takes the form:

$$G(j) = \begin{cases} 1 & \text{for } j = 0 \\ \frac{1}{j}\sum\limits_{k\in K_a}(N_k - y_k(j-b_k))\alpha_k b_k \gamma_k(j)G(j-b_k) \\ +\frac{1}{j}\sum\limits_{k\in K_a}\sum\limits_{s=1}^{s(k)}(N_k - Y_k(j-b_{kr_s}))\alpha_{kr_s} b_{kr_s}\gamma_{kr_s}(j) \\ G(j-b_{kr_s}) + \frac{1}{\min(C,j)}\sum\limits_{k\in K_e}(N_k - y_k(j-b_k))\alpha_k b_k \cdot \\ \gamma_k(j)G(j-b_k) + \frac{1}{\min(C,j)}\sum\limits_{k\in K_e}\sum\limits_{s=1}^{s(k)}(N_k - Y_k(j-b_{kr_s})) \\ \alpha_{kr_s} b_{kr_s}\gamma_{kr_s}(j)G(j-b_{kr_s}) & \text{for } j = 1, \ldots, T \\ 0 & \text{otherwise} \end{cases} \tag{50}$$

where: $Y_k(j - b_{kr_s})$ is determined again through (48) and (49), but the values of $G_{\inf}(j)$ will be given by (13), because of the absence of the BR policy.

Having determined $G(j)$'s in the EF-MRM/BR according to (47), we calculate the time congestion probabilities according to (17) and the link utilization according to (7). Call congestion probabilities are determined again by (17) but the values of $G(j)$'s in (47) should be calculated for a system with $N_k - 1$ traffic sources.

## VI. Application Example – Evaluation

We consider an application example in order to compare the analytical Time Congestion (TC) probabilities with those obtained by simulation, in the case of the proposed EF-MRM and EF-MRM/BR of quasi-random input. Simulation is based on SIMSCRIPT III [48]. For a better evaluation, we comparatively present the corresponding analytical results of the E-MRM and the E-MRM/BR [33], i.e., assuming Poisson arrivals. We also show the analytical and simulation results of the proposed EF-MRM for the link utilization; they are compared with the corresponding analytical results obtained by the E-MRM. The simulation results of this section are mean values of 7 runs with 95% confidence interval. The resultant reliability ranges of the simulation measurements are very small and, therefore, we present only mean values.

To facilitate the reader, in what follows, we summarize the order of calculations per model, regarding the analytical TC probabilities and link utilization:

(A) EF-MRM/BR: Determine $G(j)$'s according to (47) with the aid of (48), (49) and (12). Then, determine link utilization according to (7) and TC probabilities according to (17).

(B) EF-MRM: Determine $G(j)$'s according to (50) with the aid of (48), (49) and (13). Then, determine link utilization according to (7) and TC probabilities according to (17) by assuming that $t(k) = 0$ for all $k = 1, \ldots, K$.

(C) E-MRM/BR: Determine $G(j)$'s according to (12), link utilization according to (7) and TC probabilities according to (17).

(D) E-MRM: Determine $G(j)$'s according to (13). Then, determine link utilization according to (7) and TC probabilities according to (17) by assuming that $t(k) = 0$ for all $k = 1, \ldots, K$.

Let us consider a link of capacity $C = 80$ b.u. that accommodates three service-classes of elastic calls. All calls arrive in the system according to a quasi-random process. The traffic characteristics of each service-class are the following:

$1^{st}$ service-class: $N_1 = 100$, $v_1 = 0.20$, $b_1 = 1$ b.u.
$2^{nd}$ service-class: $N_2 = 100$, $v_2 = 0.06$, $b_2 = 2$ b.u.
$3^{rd}$ service-class: $N_3 = 100$, $v_3 = 0.02$, $b_3 = 6$ b.u.

The call holding time is exponentially distributed with mean value $\mu_1^{-1} = \mu_2^{-1} = \mu_3^{-1} = 1$. Calls of the $3^{rd}$ service-class may retry two times with reduced bandwidth requirement: $b_{3r_1} = 5$ b.u. and $b_{3r_2} = 4$ b.u. and increased service time so that $\alpha_3 b_3 = \alpha_{3r_1} b_{3r_1} = \alpha_{3r_2} b_{3r_2}$, where $\alpha_k = v_k \mu_k^{-1}$, $k = 1, 2, 3$. The corresponding Poisson traffic-loads are: $\alpha_{1,\inf} = 20$, $\alpha_{2,\inf} = 6$, $\alpha_{3,\inf} = 2$ erl. In the x-axis of all figures (below), we assume that $v_3$ remains constant while $v_1$, $v_2$ increase in steps of 0.01 and 0.005, respectively. The last value of $v_1 = 0.28$, while that of $v_2 = 0.10$. The corresponding last values of the Poisson traffic-loads are: $\alpha_{1,\inf} = 28$, $\alpha_{2,\inf} = 10$, $\alpha_{3,\inf} = 2$ erl.

Two different values of $T$ are considered: a) $T = C = 80$ b.u., where no bandwidth compression takes place. In that case, the proposed model gives exactly the same results with the model of [30], b) $T = 82$ b.u., where bandwidth compression takes place and $r_{\min} = C/T = 80/82$. As far as the BR parameters are concerned, we choose $t(1) = 3$ b.u., $t(2) = 2$ b.u. and $t(3) = 0$ b.u., so that $b_1 + t(1) = b_2 + t(2) = b_{3r_2} + t(3)$. The selection of these BR parameters achieves equalization of TC probabilities for calls of all service-classes.

In Figs. 1-3 we present the TC probabilities of the EF-MRM and E-MRM, i.e., we consider the case whereby the BR policy is not applied. In Fig. 1, we show the analytical and simulation TC probabilities results of the $1^{st}$ service-class for both values of $T$. Similar results are presented in Figs. 2 and 3, for the $2^{nd}$ and $3^{rd}$ service-class, respectively (TC probabilities of calls with $b_{3r_2}$). The results of these three figures show that:

i) The model's accuracy is absolutely satisfactory compared to simulation (because of the very small differences of the results).
ii) The TC probabilities are lower, when the compression/expansion mechanism is introduced. A small increase of $T$ resulted in a great effect on TC probabilities.
iii) The proposed model is important (necessary), since the results obtained by the existing infinite model (E-MRM) fail to approximate the results of the proposed finite model (EF-MRM).

Successive increases of $T$ will result in even lower TC probabilities but at the cost of increasing the service time of all calls. Such behaviour has been observed in various papers that propose multirate loss models of elastic and/or adaptive traffic (e.g., [9], [32], [33]). Similarly, the increase of retrials for a particular service-class will cause the decrease of TC probabilities for that service-class and a possible increase of TC probabilities for the rest service-classes. This behaviour has been observed in various papers that study multirate loss models with retrials (e.g., [28]-[30]).

In Fig. 4 we present the equalized TC probabilities, when the BR policy is applied. In addition to the aforementioned comments for Figs. 1-3, the results of Fig. 4 show an increase of the TC probabilities of the $1^{st}$ and $2^{nd}$ service-classes in comparison to the corresponding curves of Fig. 1 and Fig. 2, respectively, and a decrease of the TC probabilities of the $3^{rd}$ service-class in comparison to the corresponding curves of Fig. 3.

Finally, in Fig. 5 we show the analytical and simulation results of the link utilization in the case of the E-MRM and the EF-MRM. Similar results are obtained in the case of the BR policy, and therefore they are not presented. These results also show that: i) The model's accuracy is absolutely satisfactory compared to simulation. ii) The introduction of the compression/expansion mechanism slightly increases the link utilization; the increase of $T$ above $C$ results in a slight increase of the link utilization, which is anticipated due to the decrease of TC probabilities. iii) The results obtained by the E-MRM cannot approximate the results of the proposed EF-MRM.

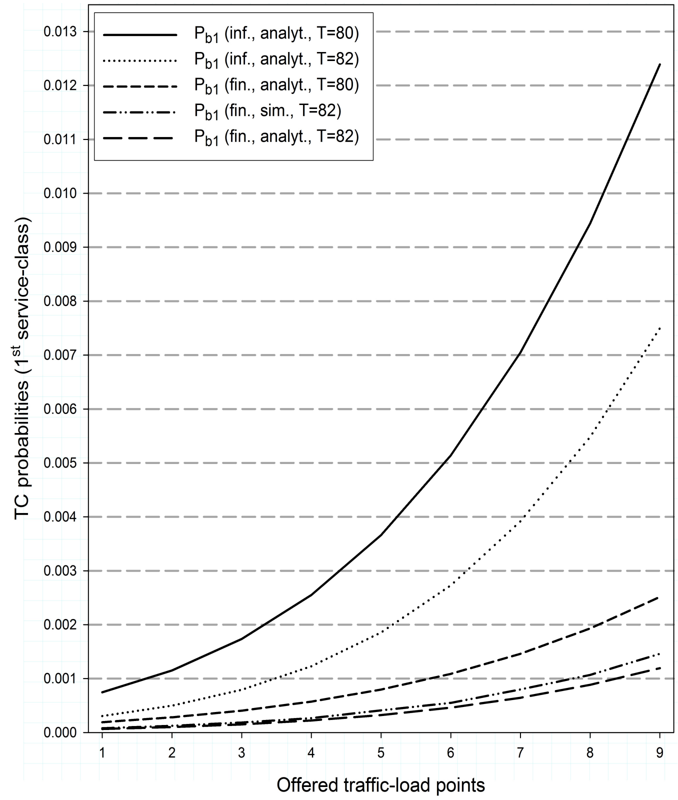


Fig. 1. TC probabilities – $1^{st}$ service-class (without BR).

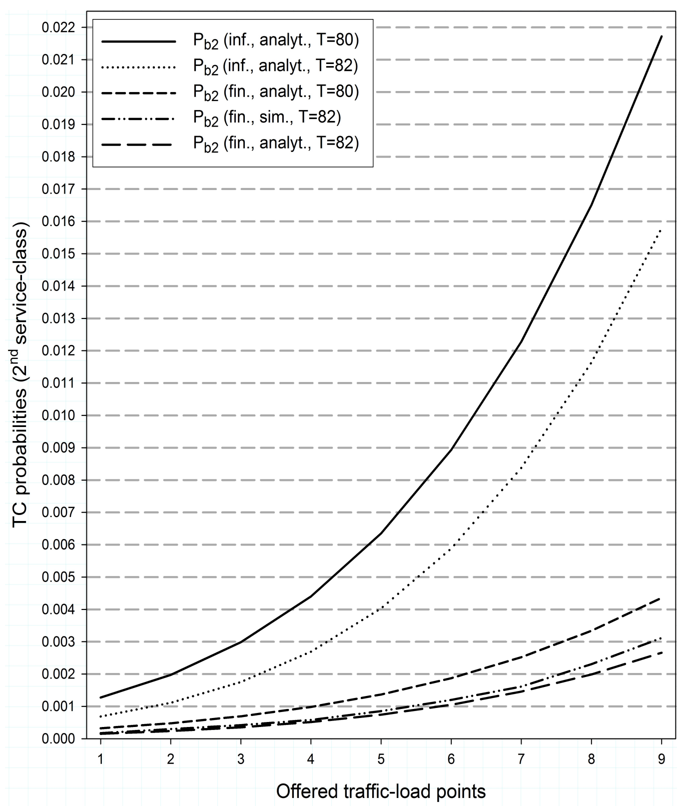


Fig. 2. TC probabilities – $2^{nd}$ service-class (without BR).

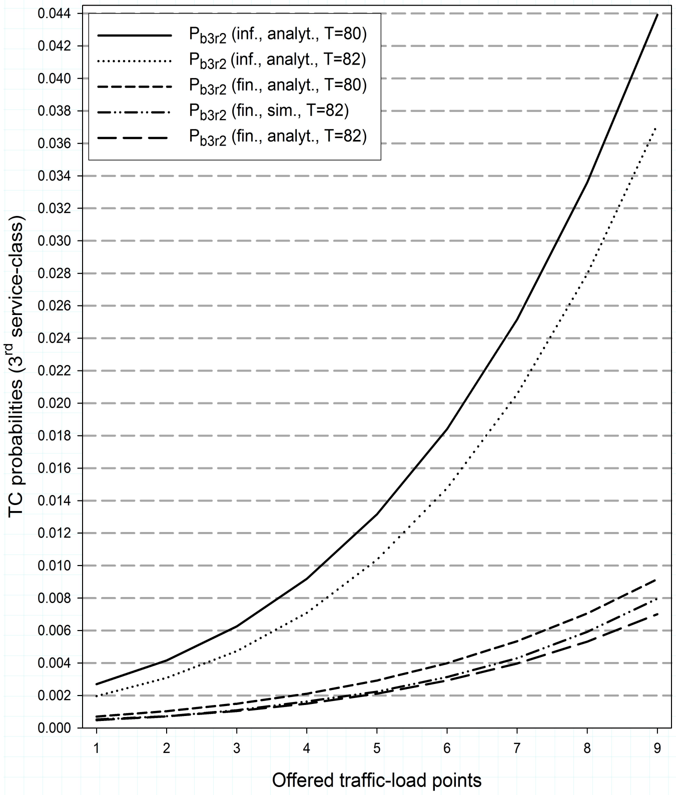


Fig. 3. TC probabilities – $3^{rd}$ service-class (without BR).

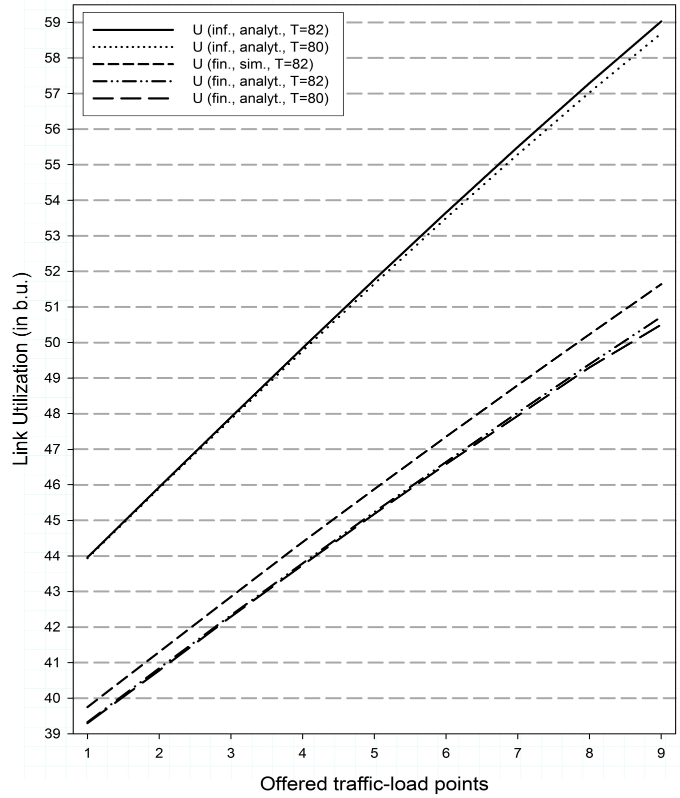


Fig. 5. Link Utilization (without BR).

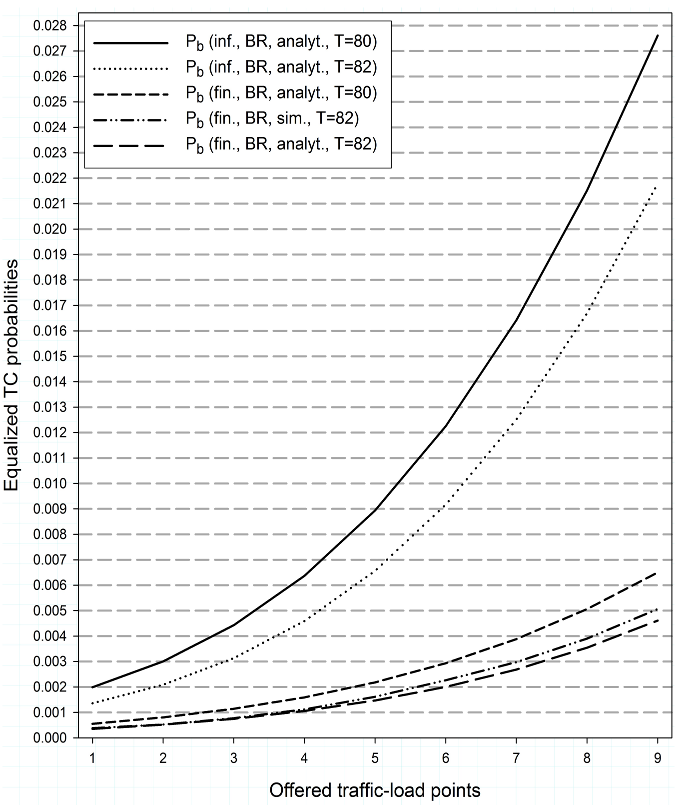


Fig. 4. Equalized TC probabilities (with BR).

## VII. CONCLUSION

We propose multirate retry loss models that support elastic and adaptive traffic assuming that calls arrive to the link according to a quasi-random process and have an exponentially distributed service time. Blocked calls have the ability to retry to be connected in the system one or more times with reduced bandwidth and increased service time requirements. Furthermore, if a retry call is blocked with its last bandwidth requirement, it can still be accepted in the system by compressing its bandwidth together with the bandwidth of all in-service calls. In addition, we incorporate into our models the bandwidth reservation policy (whereby a part of the link's available bandwidth is reserved to benefit calls of higher bandwidth requirements) and study its effects on the performance measures. The proposed models do not have a PFS. However, we propose approximate but recursive formulas for the calculation of the link occupancy distribution and, consequently, time and call congestion probabilities, as well as link utilization. Simulation results verify the analytical results. As a future work, we intend to study the application of these models in CDMA networks, and to consider also other bandwidth allocation policies, such as the threshold policy, whereby calls of a service-class are not allowed to enter the system (even if there is available bandwidth), if the number of in-service calls of that service-class exceeds a predefined threshold.

## APPENDIX A
## LIST OF SYMBOLS

| *Symbol* | *Meaning* |
|---|---|
| $C$ | Capacity of the link (in bandwidth units) |
| $T$ | Virtual capacity of the link (in bandwidth units) |
| $j$ | Occupied link bandwidth (in bandwidth units), $j = 0, \dots, T$. |
| $G(j)$ | Link occupancy distribution |
| $G$ | Normalization constant |
| $K_e$ | Set of elastic service-classes |
| $K_a$ | Set of adaptive service-classes |
| $K$ | Set of service-classes, $K = K_e + K_a$. |
| $k$ | Service-class $k$ $(k = 1, \dots, K)$ |
| $N_k$ | Finite number of sources of service-class $k$ |
| $b_k$ | Peak-bandwidth requirement of service-class $k$ calls |
| $\mathbf{b}$ | Vector of the required peak-bandwidth per call of all service-classes, $\mathbf{b} = (b_1, b_2, \dots, b_K)$. |
| $b_{kr}$ | Retry bandwidth requirement of service-class $k$ calls – single retry |
| $b_{kr_s}$ | The $s^{\mathrm{th}}$ retry bandwidth requirement of service-class $k$ calls – multi retrials, $s = 1, \dots, s(k)$. |
| $s(k)$ | Number of retrials of service-class $k$ calls |
| $\lambda_k$ | Mean arrival rate of service-class $k$ idle sources |
| $\lambda_{k,\mathrm{inf}}$ | Mean arrival rate of Poisson service-class $k$ calls |
| $v_k$ | Arrival rate per idle source of service-class $k$ |
| $\mu_k^{-1}$ | Mean of the exponentially distributed service time of service-class $k$ calls |
| $\mu_{kr}^{-1}$ | Mean of the exponentially distributed service time of service-class $k$ calls – single retry |
| $\mu_{kr_s}^{-1}$ | Mean of the exponentially distributed service time of service-class $k$ calls – multi retrials, $s = 1, \dots, s(k)$. |
| $\alpha_k$ | Offered traffic-load (in erl) per idle source of service-class $k$, $\alpha_k = v_k/\mu_k$. |
| $\alpha_{kr}$ | Offered traffic-load (in erl) per idle source of service-class $k$ – single retry, $\alpha_{kr} = v_k/\mu_{kr}$. |
| $\alpha_{kr_s}$ | Offered traffic-load (in erl) per idle source of service-class $k$ – multi retrials, $\alpha_{kr_s} = v_k/\mu_{kr_s}$. |
| $\alpha_{k,\mathrm{inf}}$ | Offered traffic-load (in erl) of Poisson service-class $k$ calls, $\alpha_{k,\mathrm{inf}} = \lambda_{k,\mathrm{inf}}/\mu_k$. |
| $\alpha_{kr,\mathrm{inf}}$ | Offered traffic-load (in erl) of Poisson service-class $k$ calls – single retry, $\alpha_{kr,\mathrm{inf}} = \lambda_{k,\mathrm{inf}}/\mu_{kr}$. |
| $\alpha_{kr_s,\mathrm{inf}}$ | Offered traffic-load (in erl) of Poisson service-class $k$ calls – multi retrials, $\alpha_{kr_s,\mathrm{inf}} = \lambda_{k,\mathrm{inf}}/\mu_{kr_s}$. |
| $n_k$ | Number of in-service calls of service-class $k$ |
| $\mathbf{n}$ | Vector of all in service calls of all service-classes, $\mathbf{n} = (n_1, n_2, \dots, n_K)$. |
| $P(\mathbf{n})$ | Steady state distribution |
| $b_k^{'}$ | Compressed bandwidth of service-class $k$ calls |
| $r$ | Compression factor |
| $b_{kr}^{'}$ | Compressed bandwidth of service-class $k$ calls with single retry |
| $t(k)$ | Bandwidth reservation parameter of service-class $k$ |
| $\phi_k(\mathbf{n})$ | State-dependent multiplier of service-class $k$ |
| $x(\mathbf{n})$ | State-dependent variable |
| $y_k(j)$ | Mean number of Poisson service-class $k$ calls in state $j$ |
| $P_{b_k}$ | Time Congestion probabilities of service-class $k$ |
| $C_{b_k}$ | Call Congestion probabilities of service-class $k$ |
| $U$ | Link utilization |

## APPENDIX B
## LIST OF ACRONYMS

| *Acronym* | *Meaning* |
|---|---:|
| EMLM | Erlang Multirate Loss Model |
| EnMLM | Engset Multirate Loss Model |
| PFS | Product Form Solution |
| SRM | Single – Retry Model |
| MRM | Multi – Retry Model |
| BR | Bandwidth Reservation |
| QoS | Quality – of – Service |
| E – EMLM/BR | Extended – EMLM/BR |
| E – SRM/BR | Extended – SRM/BR |
| E – MRM/BR | Extended – MRM/BR |
| EF – SRM/BR | Extended Finite – SRM/BR |
| EF – MRM/BR | Extended Finite – MRM/BR |
| TC | Time Congestion |
| PASTA | Poisson Arrivals See Time Averages |

## ACKNOWLEDGMENT

The authors would like to thanks the anonymous reviewers for their constructive comments.

## REFERENCES

[1] I. Moscholios, V. Vassilakis, M. Logothetis, and J. Vardakas, "Bandwidth Reservation in the Erlang Multirate Loss Model for Elastic and Adaptive Traffic," Proc. of 9th Advanced Int. Conf. on Telecommunications, AICT 2013, Rome, Italy, 23-28 June 2013, pp. 148-153.

[2] J. Kaufman, "Blocking in a shared resource environment," IEEE Trans. Commun. vol. 29, no. 10, pp. 1474-1481, October 1981.

[3] J. Roberts, "A service system with heterogeneous user requirements," *in: G. Pujolle (Ed.), Performance of Data Communications systems and their applications*, North Holland, Amsterdam, 1981, pp. 423-431.

[4] Z. Dziong, and J. Roberts, "Congestion probabilities in a circuit switched integrated services network," Performance Evaluation, vol. 7, issue 4, pp. 267-284, November 1987.

[5] D. Tsang, and K. Ross, "Algorithms to Determine Exact Blocking Probabilities for Multirate Tree Networks," IEEE Trans. Commun., vol. 38, issue 8, pp. 1266-1271, August 1990.

[6] J. Kaufman, and K. Rege, "Blocking in a shared resource environment with batched Poisson arrival processes," Performance Evaluation, vol. 24, issue 4, pp. 249-263, February 1996.

[7] G. Stamatelos, and V. Koukoulidis, "Reservation – Based Bandwidth Allocation in a Radio ATM Network," IEEE/ACM Trans. Networking, vol. 5, pp.420-428, June 1997.

[8] M. Stasiak, and M. Glabowski, “A simple approximation of the link model with reservation by a one-dimensional Markov chain,” Performance Evaluation, vol. 41, pp.195–208, July 2000.
[9] S. Rácz, B. Gerő, and G. Fodor, “Flow level performance analysis of a multi-service system supporting elastic and adaptive services,” Performance Evaluation, vol. 49, issues 1-4, pp. 451-469, September 2002.
[10] I. Moscholios, P. Nikolaropoulos, and M. Logothetis, “Call level blocking of ON-OFF traffic sources with retrials under the complete sharing policy,” Proc. of 18th ITC, Berlin, Germany, 31 August – 5 September 2003, pp. 811-820.
[11] I. Moscholios, M. Logothetis, and M. Koukias, “An ON-OFF Multi-Rate Loss Model of Finite Sources,” IEICE Trans. Commun., vol. E90-B, no. 7, pp.1608-1619, July 2007.
[12] Q. Huang, King-Tim Ko, and V. Iversen, “Approximation of loss calculation for hierarchical networks with multiservice overflows,” IEEE Trans. Commun., vol. 56, issue 3, pp. 466-473, March 2008.
[13] I. Moscholios, J. Vardakas, M. Logothetis, and M. Koukias, “A Quasi-random Multirate Loss Model supporting Elastic and Adaptive Traffic under the Bandwidth Reservation Policy,” Int. Journal on Advances in Networks and Services, vol. 6, no. 3 & 4, pp. 163-174, December 2013.
[14] M. Glabowski, and M. D. Stasiak, “Internal Blocking Probability calculation in switching networks with additional inter-stage links and mixture of Erlang and Engset Traffic,” Image Processing & Communication, vol. 17, no. 1-2, pp. 67-80, January 2013.
[15] D. Staehle, and A. Mäder, “An Analytic Approximation of the Uplink Capacity in a UMTS Network with Heterogeneous Traffic,” Proc. 18th ITC, Berlin, pp. 81-90, September 2003.
[16] V. Iversen, V. Benetis, N. Ha, and S. Stepanov, “Evaluation of Multi-service CDMA Networks with Soft Blocking,” Proc. of ITC Specialist Seminar, Antwerp, Belgium, pp. 223-227, August/September 2004.
[17] F. Cruz-Pérez, J. Vázquez-Ávila, and L. Ortigoza-Guerrero, “Recurrent Formulas for the Multiple Fractional Channel Reservation Strategy in Multi-Service Mobile Cellular Networks,” IEEE Communications Letters, vol. 8, no. 10, pp. 629-631, October 2004.
[18] V. Vassilakis, G. Kallos, I. Moscholios, and M. Logothetis, “Call-Level Analysis of W-CDMA Networks Supporting Elastic Services of Finite Population,” IEEE ICC 2008, Beijing, China, 19-23 May 2008.
[19] M. Glabowski, M. Stasiak, A. Wisniewski, and P. Zwierzykowski, “Blocking Probability Calculation for Cellular Systems with WCDMA Radio Interface Servicing PCT1 and PCT2 Multirate Traffic,” IEICE Trans. Commun., vol. E92-B, pp. 1156-1165, April 2009.
[20] M. Stasiak, and S. Hanczewski, “A new analytical model of UMTS cell,” Image Processing & Communication, vol. 17, no. 1-2, pp. 81-90, January 2013.
[21] M. Stasiak, M. Glabowski, A.Wisniewski, and P. Zwierzykowski, Modeling and Dimensioning of Mobile Networks, Wiley, 2011.
[22] K. Kuppuswamy, and D. Lee, “An analytic approach to efficiently computing call blocking probabilities for multiclass WDM networks,” IEEE/ACM Trans. Netw., vol. 17, issue 2, pp. 658-670, April 2009.
[23] J. Vardakas, I. Moscholios, M. Logothetis, and V. Stylianakis, “An Analytical Approach for Dynamic Wavelength Allocation in WDM-TDMA PONs Servicing ON-OFF Traffic,” IEEE/OSA Journal of Optical Commun. Netw., vol. 3, no. 4, pp. 347-358, April 2011.
[24] N. Jara, and A. Beghelli, “Blocking probability evaluation of end-to-end dynamic WDM networks,” Photonic Network Communications, vol. 24, issue 1, pp. 29-38, August 2012.
[25] J. Vardakas, I. Moscholios, M. Logothetis, and V. Stylianakis, “Blocking Performance of Multi-rate OCDMA PONs with QoS Guarantee,” Int. Journal on Advances in Telecommunications, vol. 5, no. 3 - 4, December 2012, pp. 120-130.
[26] J. Vardakas, I. Moscholios, M. Logothetis, and V. Stylianakis, “Performance Analysis of OCDMA PONs Supporting Multi-Rate Bursty Traffic,” IEEE Trans. Commun., vol. 61, no. 8, pp. 3374-3384, August 2013.
[27] G. Stamatelos, and J. Hayes, “Admission control techniques with application to broadband networks,” Comput. Commun., vol. 17, no. 9, pp. 663-673, 1994.
[28] J. Kaufman, “Blocking with retrials in a completely shared resource environment,” Performance Evaluation, vol. 15, issue 2, pp. 99-113, June 1992.
[29] I. Moscholios, M. Logothetis, and P. Nikolaropoulos, “Engset Multi-Rate State-Dependent Loss Models,” Performance Evaluation, vol. 59, issues 2-3, February 2005, pp. 247-277.
[30] I. Moscholios, M. Logothetis, and G. Kokkinakis, “A Simplified Blocking Probability Calculation in the Retry Loss Models for Finite Sources,” Proc. of Communication Systems, Networks and Digital Signal Processing, Patras, Greece, 19-21 July 2006.
[31] I. Moscholios, V. Vassilakis, J. Vardakas, and M. Logothetis, “Retry loss models supporting elastic traffic,” Advances in Electronics and Telecommunications, Poznan University of Technology, Poland, vol. 2, no. 3, September 2011, pp. 8-13.
[32] I. Moscholios, V. Vassilakis, J. Vardakas, and M. Logothetis, “Call Blocking Probabilities of Elastic and Adaptive Traffic with Retrials,” Proc. of AICT 2012, Stuttgart, Germany, 27 May-1 June 2012.
[33] I. Moscholios, V. Vassilakis, M. Logothetis, and M. Koukias, “QoS Equalization in a Multirate Loss Model of Elastic and Adaptive Traffic with Retrials,” Proc. of EMERGING 2013, Porto, Portugal, 29 September – 4 October 2013.
[34] T. Bonald, and J. Virtamo, “A recursive formula for multirate systems with elastic traffic,” IEEE Commun. Letters, vol. 9, no. 8, pp. 753-755, August 2005.
[35] T. Bonald, “A Recursive Formula for Estimating the Packet Loss Rate in IP Networks,” Proc. of Valuetools, Pisa, Italy, October 2009.
[36] T. Bonald, and J. Virtamo, “Calculating the flow level performance of balanced fairness in tree networks,” Performance Evaluation, vol. 58, issue 1, pp. 1-14, October 2004.
[37] T. Bonald, L. Massoulie, A. Proutiere, and J. Virtamo, “A queueing analysis of max-min fairness, proportional fairness and balanced fairness,” Queueing Systems, vol. 53, issues 1-2, pp. 65-84, June 2006.
[38] G. Fodor, and M. Telek, “Bounding the Blocking Probabilities in Multirate CDMA Networks Supporting Elastic Services,” IEEE/ACM Trans. Netw., vol. 15, issue 4, pp. 944-956, August 2007.
[39] C. Tarhini, and T. Chahed, “QoS-oriented resource allocation for streaming flows in IEEE802.16e Mobile WiMAX,” Telecommunication Systems, vol.51, issue 1, pp. 65-71, September 2012.
[40] B. Gerő, P. Pályi, and S. Rácz, “Flow-level performance analysis of a multi-rate system supporting stream and elastic services,” Int. Journal of Communication Systems, vol. 26, issue 8, pp. 974-988, August 2013.
[41] M. Karrey, “Analytical Evaluation of QoS in the Downlink of OFDMA Wireless Cellular Networks Serving Streaming and Elastic Traffic,” IEEE Trans. on Wireless Communications, vol. 9, no. 5, pp. 1799 1807, May 2010.
[42] I. Moscholios, and M. Logothetis, “Engset multi-rate state-dependent loss models with QoS guarantee,” Int. J. Commun. Syst., vol. 19, pp. 67-93, February 2006.
[43] H. Akimaru, and K. Kawashima, Teletraffic – Theory and Applications, 2nd edition, Springer-Verlag, Berlin, 1999.
[44] I. Moscholios, M. Logothetis, and G. Kokkinakis, “Connection Dependent Threshold Model: A Generalization of the Erlang Multiple Rate Loss Model,” Performance Evaluation, vol.48, issues 1-4, pp. 177-200, May 2002.
[45] J. Roberts, “Teletraffic models for the Telecom 1 Integrated Services Network,” Proceedings of ITC-10, Mondreal, Canada, 1983.
[46] M. Glabowski, and M. Stasiak, “An approximate model of the full-availability group with multi-rate traffic and a finite source population,” in Proc. of 12th MMB&PGTS, Dresden, Germany, pp. 195-204, Sept. 2004.
[47] M. Glabowski, M. Stasiak, and J. Weissenberg, “Properties of recurrent equations for the full-availability group with BPP traffic,” Mathematical Problems in Engineering, vol. 2012, Article ID 547909, 17 pages, 2012. doi:10.1155/2012/547909.
[48] Simscript III, http://www.simscript.com (retrieved: May 2014).

# Cooperative Internet Access Sharing in Wireless Mesh Networks

Vision, Implementation, and Experimentation of the CARMNET Project

Mariusz Glabowski, Andrzej Szwabe
Poznan University of Technology
Poznan, Poland
e-mail: mariusz.glabowski@put.poznan.pl,
andrzej.szwabe@put.poznan.pl

Dario Gallucci, Salvatore Vanini, Silvia Giordano
Institute for Information Systems and Networking
University of Applied Sciences and Arts of Southern Switzerland, Manno, Switzerland
e-mail: dario.galluci@supsi.ch, salvatore.vanini@supsi.ch,
silvia.giordano@supsi.ch

*Abstract*— **The paper presents the vision, as well as the main results of the implementation and the experimentation performed within CARMNET – a Swiss-Polish project aimed at investigating "CARrier-grade delay-aware resource management for wireless multi-hop/Mesh NETworks". The project focuses on solutions that motivate telecom operators to reconsider their view on user-operated IEEE 802.11-compliant wireless mesh networks. It is driven by the vision of networks operated cooperatively by telecom operators and a community of users. While the former may appreciate the CARMNET's compliance with IP Multimedia Subsystem (IMS) infrastructure, the latter likely enjoy the pervasiveness of the CARMNET-based Internet access. The project aims at providing, both telecom operators and end users, with solutions that will create appropriately strong incentives – technological, functional and economical – for a widespread adoption of CARMNET-like networks within an expanding group of users. Project results obtained so far indicate, that despite the originality of the project vision, its solutions are applicable to the telecom operator's infrastructure, in particular in Internet access sharing scenarios that become widespread in the recent years.**

***Keywords – wireless mesh networks; wireless mesh testbeds; user-operated Internet access sharing; IMS; mobility.***

## I. INTRODUCTION

The core idea of the CARMNET project [1], [2] is to make the user-provided Internet access an important alternative to the currently widespread 3G/4G-based mobile Internet access, in particular this provided in the femtocell scenario [3]. The main assumption of the project is that wireless mesh networks [4], while effectively enhanced by the introduction of advanced resource management mechanisms [5] and the compliance with the core of the telecom operators' IMS-based Authentication, Authorization, Accounting (AAA) infrastructure [6], [7], may serve as an appropriate basis for a real-world realization of the core CARMNET idea.

However, the realization of the vision of CARMNET networks – as operated jointly by telecom operators and an informal community of Internet access-sharing users – has raised several scientific and technological challenges that had not yet been investigated in a satisfactory detailed way [8], [9]. The scenario-driven research efforts of CARMNET have resulted in a set of solutions for ensuring satisfactory levels of reliability and sustainability of the user-provided Internet access sharing. The completed and the ongoing research is focused on algorithms for reliable servicing of multi-service traffic, with different packet delay tolerance, including algorithms related to: traffic stream classification, packet scheduling, buffer memory management, routing and nodes mobility management [10], [11].

Targeting the CARMNET objectives has implied the need for addressing several technological challenges, in particular those related to the compatibility with the key relevant standards, such as Optimized Link State Routing (OLSR) protocol for the reliable multi-criteria routing within wireless mesh networks [12], [13], [14], or relevant to IMS-based AAA [15] technologies used by telecom operators [16]. Moreover, as far as the long-term sustainability of CARMNET is concerned, some user-centric features have proved to be of the key importance, as well. They correspond to functional aspects of a CARMNET network use, such as the user-perceived network utility and the user-friendliness of mobile applications running on smartphones that constitute such a network.

The further part of the paper is organized as follows. In Section II, the CARMNET research motivation is presented. Section III describes the central role that scenarios play in the project. In Section IV, selected technological solutions developed for CARMNET-like networks are presented. Section V presents the multi-testbed experimentation approach for evaluating project's outcomes. The summary of the key practical results of the CARMNET research and the presentation of the conclusions close the article.

## II. RESEARCH MOTIVATION

Internet access sharing via customers' WiFi access points is a service recently deployed by several world's leading telecom operators, including Orange and British Telecom (BT). For example, in Poland such a service is offered by Orange as FunSpot [17]. The service known as FON [18] is offered in several countries by partners of BT, e.g., by Polish operator Netia [19].

However, the attractiveness of wireless mesh networks to telecom operators, despite a significant research effort that has been put in the last decade [8], remains quite limited. The following issues related to the CARMNET vision may be recognized as potentially postponing the wide adoption of existing wireless networking solutions:

- The lack of integration between the wireless network resource management and the AAA mechanism of telecom operators IMS-compliant networks,
- The lack of carrier-grade systems enabling telecom operators to measure the usage of shared Internet access in wireless mesh networks,
- The lack of solutions enabling end users to request the same level of Quality of Service (QoS) parameters as in 3G/4G networks,
- The lack of integration of the wireless network resource management oriented on the Network Utility Maximization (NUM) with 'utility-aware' accounting, in particular in a scenario in which users are provided with 'society-building' incentives similar to those familiar to users of popular Internet file-sharing applications based on the Peer-to-Peer (P2P) protocols [20],
- The lack of seamless mobility support for multimedia services with QoS requirements [11].

It is worth mentioning that the scope of CARMNET research corresponds to the recent trend of intensive studies on various wireless Internet access sharing methods [21]. Moreover, similar scientific projects have been recently conducted, including EU CARMEN [9]. However, to the best of our knowledge, all such initiatives differ from CARMNET in one of its core assumptions: they are based on the use of non-standard hardware and they are dependent on the access technologies.

## III. CARMNET SCENARIOS

The CARMNET research methodology follows the approach of the user-centered scenario-based design, focused on functional specification of the system in correspondence to the user requirements and activities [22]. Firstly, descriptions of CARMNET application scenarios constitute the core of the project vision by focusing on the user-centric view on added-value functionalities and the user-perceived incentives for cooperative use of CARMNET-based networks – both potentially enabled by the use of CARMNET technological solutions. Secondly, the CARMNET network topology scenarios [1] have served as the basis for a more detailed specification of CARMNET research scope, and serve as a starting point for network topology definitions followed in multi-testbed experimentation-oriented activities [23].

There are two main CARMNET Application Scenarios. The first one assumes the cooperative Internet access sharing as being realized via CARMNET access points, while the second one assumes the use of CARMNET mobile nodes for the same purpose. Each of the scenarios includes the 'phase' of earning virtual currency units (called denarii) by a user sharing his/her home network resources and the 'phase' of spending denarii for using the resources of a visited network. An example in which Alice earns denarii by sharing her home network with Charlie (Scenario 1) and then spends her denarii by using Bob's home network (Scenario 2) is depicted in Figure 1 and Figure 2, respectively.

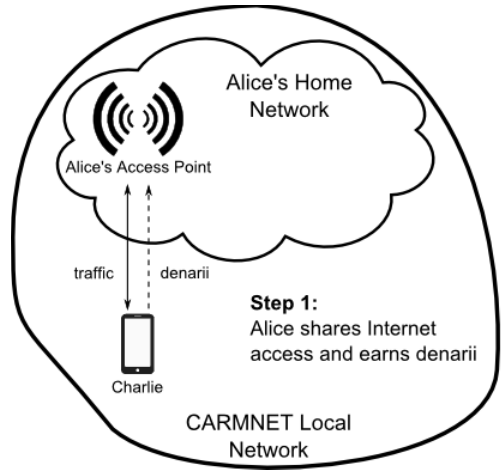


Figure 1. The first step of the first CARMNET Application Scenario: Alice 'earns' denarii by sharing her home network with Charlie.

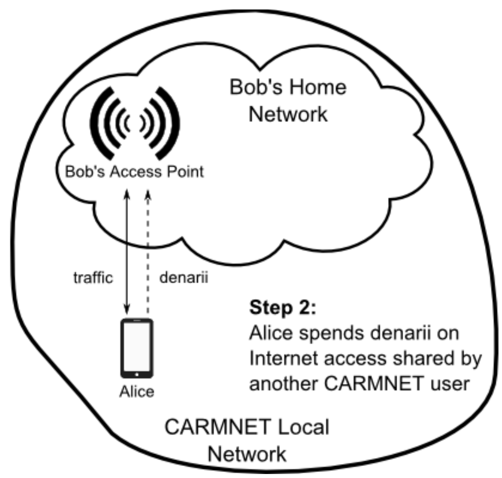


Figure 2. The second step of the first CARMNET Application Scenario: Alice 'spends' her denarii by using Bob's home network.

It may be noticed that the CARMNET Scenario 1 is architecturally similar to scenarios of currently offered services, as it is based on the assumption that the core functions of Internet access sharing are realized by means of WiFi access points (appropriately equipped and configured), i.e., the WiFi access point is the border node of the network with shared resources. However, CARMNET provides a utility-based charging based on the application of virtual units of utility (called denarii) as added value [5], [7].

In both the basic CARMNET scenarios, the scope of the 'utility-sensitive' traffic management [5], [24], which is realized in the home user's WiFi network, is naturally limited to the WiFi network's range. However, in the case of CARMNET Scenario 2, illustrated in Figure 3 and Figure 4, the scope of the Internet access sharing may be extended by means of CARMNET traffic-relaying mobile nodes. As a

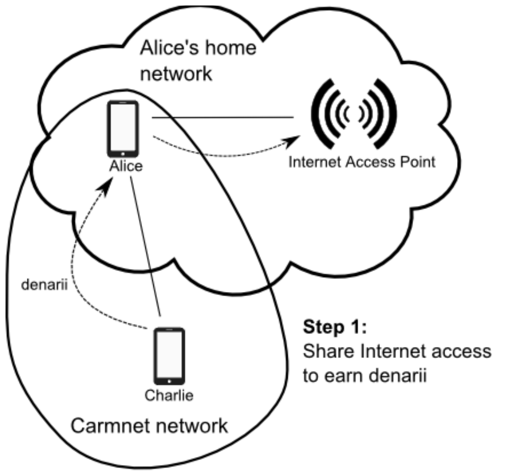


Figure 3. The first step of the second CARMNET Application Scenario: Alice 'earns' denarii by sharing her mobile Internet access with Charlie.

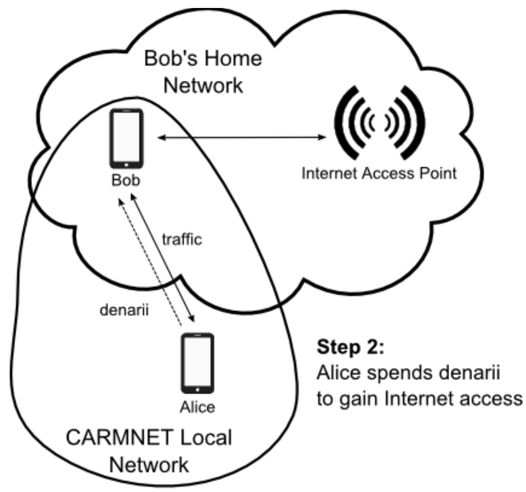


Figure 4. The second step of the second CARMNET Application Scenario: Alice 'spends' her denarii by using Bob's mobile Internet access.

result, the network coverage may be widened without additional investments on the telecom operator's side [7].

CARMNET supports both the WiFi-mobile and the WiFi-WiFi traffic relaying modes. However, as WiFi connectivity is much more power-consuming than a mobile Internet access (3G or 4G access provided by a telecom operator), the real-world applicability of the CARMNET multi-hop WiFi-to-WiFi traffic relaying - as shown in Figure 5 presenting the CARMNET multi-hop application scenario - is practically limited to cases in which the user has an easy access to a power supply, e.g., when he/she shares his/her mobile Internet access with drivers of other cars staying in the same traffic jam area.

Currently, a typical multi-hop WiFi-to-WiFi traffic relaying scenario can be used by mobile operators in order to extend the range of their networks. However, one of the key problems in multi-hop wireless networks, especially in networks that serve heterogeneous traffic, is optimal resource management and routing. In order to make multi-hop networks attractive for telecom operators, within the CARM-

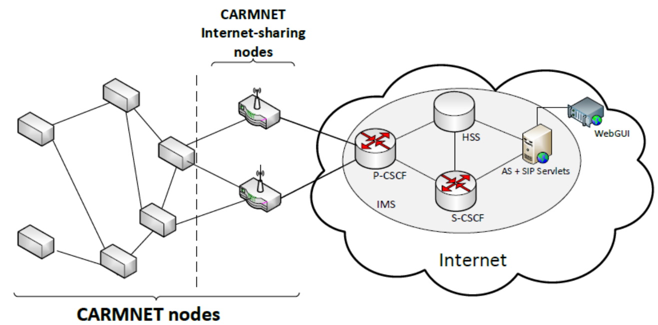


Figure 5. CARMNET multi-hop application scenario.

NET project the development of a resource management system and a multi-criteria routing were undertaken.

## IV. Key Areas of CARMNET Research

The implementation of the CARMNET vision required integrated studies in several research areas that are usually investigated independently, such as multi-criteria routing, wireless network resource management and integration of a NUM system with IMS core infrastructure aimed at providing SIP-Based AAA Support [6].

### A. *Multi-Criteria Routing*

Within the activities related to CARMNET project, a new routing protocol (based on the OLSR protocol), which allows for multi-criteria path selection, is proposed. The protocol is capable to build the routing table (at each node), including not only the best path but a set of paths that lead to the specified destination network. The paths in the set are selected as the subsequent shortest paths to the specified destination, based on one of the *k*-shortest paths algorithms [25], [26], [27]. The paths are determined according to main criterion, e.g., delay, and they include additional criteria (metrics). The additional metrics are useful in order to choose the best path that fulfils the criteria for a given traffic stream. The criteria correspond to the QoS requirements for all traffic classes offered in the CARMNET network. An example of the criteria can be delay, a number of hops, link reliability or link load. Thus, the proposed QoS routing protocol is able to use different traffic profiles and for each of them proposes the best path, i.e., the path that fulfils recommended (for the considered traffic profile) QoS values in the best possible way.

The multi-criteria routing is dedicated primarily to the multi-hop scenario, but it can be also used in the single-hop scenario, to select the best CARMNET Internet-sharing node. Additionally, the routing protocol introduced in the CARMNET system may be also used as one of the possible methods for mobility management: one or more of the criteria can be used by a mobile node to select the best path (next-hop node) for a traffic stream of a given class.

### B. *Wireless Network Resource Management based on Delay-Aware Network Utility Maximization (DANUM) Approach*

The aim of the DANUM model is to provide an optimal packet scheduling policy regarding the maximisation of the network users' satisfaction. It targets the maximum of the network utility (a sum of utility of all flows within the network):

$$\max \sum_{r \in S} U_r \left( x_r , d_r \right), \qquad (1)$$

where $S$ denotes a set of flows within the network; $x_r$ – rate of flow $r$; $d_r$ – delay of flow $r$; $U_r$ – the utility function of flow $r$. In other words, DANUMS aims at solving the NUM problem in a delay-aware way. The relation between measurable flow transmission quality parameters and its utility is modelled by means of a utility function. Each function corresponds to flows of a given type or, more precisely, to flows with specific network requirements [5].

In DANUMS the utility is determined not only according to the flow's throughput, but also to its end-to-end delay. Each flow may have a distinct utility function since it may prioritise different network performance parameters. Assigning utility functions to flows is a task of the Flow Classifier [10].

It has been proven that the Max-Weight Scheduling (MWS) algorithm is a solution to the standard throughput-oriented NUM problem formulation [28]. The DANUMS applies the MWS algorithm to virtual queue levels in order to determine the next flow queue to transmit a packet from. A virtual queue is defined as a product of flow's packet backlog level and a virtual price of a single packet. Packet's virtual price is a value of the derivative of a utility function assigned to the flow. In other words, the more utility a flow would gain from improving its network performance parameters (e.g., by lowering its delay), the higher is the virtual price. The virtual price plays an important role in packet scheduling as well as influences the cost of CARMNET network usage [10].

### C. Wireless Network Resource Management Based on Multiservice State-Dependent Queueing Models

Another key objective of the CARMNET project in the area of resource management is to elaborate a model of a multiservice queuing system. A careful review of the available literature reveals that no satisfactory models of multiservice queueing systems have been developed as yet. The proposed solutions [29], [30], [31], [32] concern a certain number of boundary cases only and do not provide methods for individual evaluation of queue parameters for individual classes of calls. The advantage of the proposed in CARMNET project model will be opportunities to evaluate analytically the average parameters of queues for individual classes of calls, which may prove to be of particular importance in engineering applications, especially in solutions concerning the analysis, dimensioning and optimization of mobile networks.

Within the CARMNET project, an accurate model of a state-dependent queuing system with limited queue and state-dependent dynamic resource sharing between individual classes of streams was proposed. The assumption was that the queueing system had a server with the capacity $C$ and the queue with the capacity $U$, expressed in AUs (Allocation Unit) [33], [34]. The assumption in the model was that the allocation unit had the value 1 bit/s, (or 1 Kbit/s, 1 Mbit/s and so on, depending on the adopted bit rate units appropriate for a considered system). In the proposed queueing system, the number of AUs that service streams of class $i$ ($1 \le i \le M$, where $M$ is the number of classes of offered streams) in the server depends on the number of streams of individual classes in the system at a given moment of the service process. This defined system can be also treated as $M$ virtual queueing systems in which bit rates, allocated in the server to service streams of particular classes, depend on the number of currently serviced streams and streams placed in $M$ queues (see Figure 6).

Figure 6 shows a diagram of a queueing system to which two classes of traffic streams are offered. The figure shows two virtual queues, though, in real circumstances, there is only one queue for all classes of streams. This particular presentation of the system results from the fact that the resources allocated in the server to service particular classes depend on the total number of streams in the system, while they are independent of the actual order of call arrival to the system [33], [34].

It is proved in [34] that the distribution of the number of streams $[p(X)]_{C+U}$ currently in thus defined queueing system (being serviced in the server and waiting in the queue) can be written as follows:

$$[p(X)]_{C-U} = \begin{cases} \dfrac{1}{n_X} \displaystyle\sum_{i=1}^{M} A_i \left[ p(X - 1_i) \right]_{C+U} & \text{for} \quad X : 0 \le n = \displaystyle\sum_{i=1}^{M} x_i(X) c_i < C, \\ \dfrac{1}{C} \displaystyle\sum_{i=1}^{M} A_i \left[ p(X - 1_i) \right]_{C+U} & \text{for} \quad X : C \le n = \displaystyle\sum_{i=1}^{M} x_i(X) c_i < C + U, \end{cases} \qquad (2)$$

where $X$ is the state of the service process defined by the number of streams $x_i(X)$ of particular classes currently being in the system: $X = \{x_1(X), x_2(X), \ldots, x_M(X)\}$, $A_i$ is the traffic intensity of class $i$, defined relative to AU [33], [34], $c_i$ is the bit rate of a stream of class $i$, the $n_X$ parameter denotes the total number of allocation units in the system in state $X$, whereas $1_i$ denotes one stream of class $i$.

On the basis of (2) it is possible to determine all important averaged characteristics for streams of individual classes, e.g., the average value $Q_i$ of the number of streams

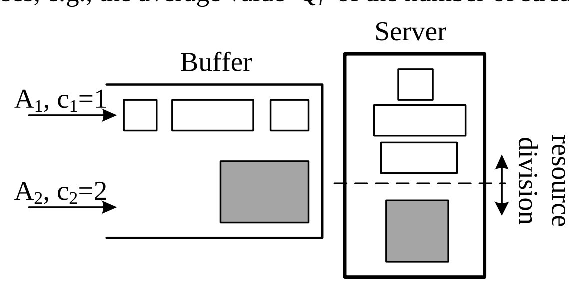


Figure 6. Multiservice queueing system with state-dependent dynamic distribution of server resources.

of class $i$ waiting in the queue can be expressed by the following formula:

$$Q_i = \sum_{\Omega} \left[ x_i(X)[p(X)]_{C+U} - \frac{A_i}{c_i}[p(X-1_i)]_{C+U} \right], \qquad (3)$$

where $\Omega$ is the set of all states in which the queue is not empty:

$$\Omega = \left\{ X : C \le \sum_{i=1}^{M} x_i(X)c_i \le C+U \right\}. \qquad (4)$$

The proposed model of the state-dependent queuing system with limited queue and state-dependent dynamic resource sharing between individual classes of streams is the first accurate multiservice queueing model that makes it possible to evaluate queues for individual classes of calls. Within this context, the opportunities offered by its practical applicability exceed the scope of the CARMNET project. The model can be particularly important in engineering applications, particularly those that are related to the analysis of 4G mobile networks and other telecommunications systems that use buffers.

### *D. Integration of Wireless Network Resource Management with Routing and AAA Functions*

One of the key objectives of CARMNET is to integrate IMS-based AAA support with the utility-oriented resource management for wireless mesh networks, in particular the one based on DANUM System (DANUMS) [6], [7]. DANUMS is an application-layer system providing a delay-aware indirect flow control mechanism based on a system transporting virtual utility units and a packet forwarding component aimed at providing an approximation of Max-Weight Scheduling (MWS) [24].

The DANUMS is a part of an architecture (see Figure 7) that consists of a routing component in the form of Optimised Link State Routing Protocol daemon (OLSRd) [12], a custom SIP User Agent integrated with a Linux Loadable Kernel Module (LKM), a user interface (WebUI) and an IP Multimedia Subsystem (IMS) platform [16]. SIP User Agent is responsible for asynchronous communication between LKM and the IMS. The user interface is a WWW application that allows users to bind utility functions to various types of traffic. The WebUI also provides insight into statistics about transmitted traffic and network usage cost.

The DANUMS is implemented as a Linux LKM [5] and has to be installed and running on all of the client devices, that wish to participate in the CARMNET network. The implementation as a kernel module gives access to low-level networking stack. This is a crucial ability, as DANUMS manages the flow of packets with respect to their delay-aware Max-Weight Scheduling (MWS) weights [24] by

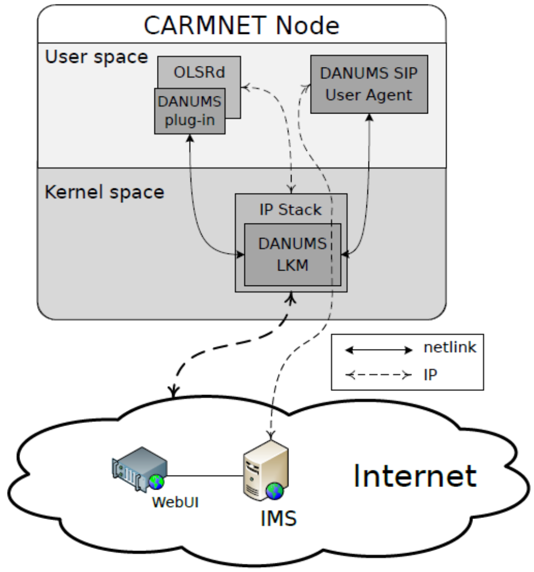


Figure 7. Overview of CARMNET system architecture.

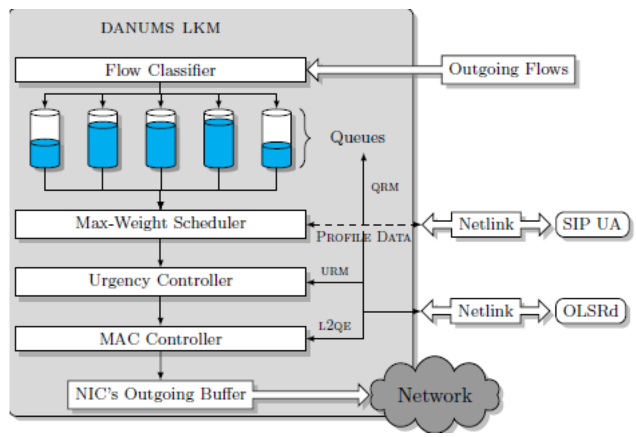


Figure 8. A single CARMNET mobile node subsystem implemented as LKM [35].

means of custom queues and the corresponding scheduling system – as depicted in Figure 8. For the MWS algorithm to function correctly, information about queue levels is signalled throughout the CARMNET network by means of CARMNET-specific Layer-2 Queue-Level Estimation (L2QE) protocol.

Other protocols are used internally in the CARMNET network to measure network delay (Delay Reporting Protocol, DRP), exchange information about currently forwarded flows (Queue Reporting Protocol, QRM) and for exchanging information on urgency scheduling weights (Urgency Reporting Messages, URM).

### *E. IMS-Based Support for Utility-Based Charging*

Typically, CARMNET users are the ones that do not have the direct and acceptably cheap access to 3G/4G network. It is assumed that virtual utility units, after being earned by users sharing their mobile Internet access with other users of CARMNET-based wireless networks, may be spent by these users ('potentially altruistic', i.e., risking the lack of a reward for sharing the Internet connection) for accessing mobile Internet connection shared by other users.

The original CARMNET concept of the utility-based charging is based on a combination of charging per traffic volume and traffic volume virtualization based on the mechanism of explicit transfer of virtual units that has been proposed as the key element of the Delay-Aware NUM System (DANUM) framework [5]. The realization of the concept is supported by efforts put on the integration of the DANUM system with an IMS-compliant AAA system [6], [15].

The CARMNET architecture assumes extending an open implementation of the IMS server infrastructure (OpenIMSCore) by the SIP servlet located on the Application Server (AS). The communication between the network nodes and the IMS Server is realized with the use of SIP User Agent (a lean SIP client application).

CARMNET-DANUM system has been made fully compatible with the interfaces of the IMS core servers [6]. Information on flows' utility is signalled in the network by the SIP User Agent and sent to the accounting server on the IMS platform. Implementing a fully featured IMS server based on OpenIMSCore [36] eliminated the need for developing a core telecom infrastructure from scratch, at least as long it is understood as a combination of user management, session handling and AAA functions [15].

### F. CARMNET-XML Protocol

According to the vision of CARMNET, the standard session management functionalities provided by IMS core servers are used in a non-typical way - for the management of user-shared Internet access sessions (so called "CARMNET sessions") rather than, e.g., for the management of VoIP sessions. On the other hand, the standard AAA functionalities provided by IMS core are extended by additional CARMNET-specific features of utility monitoring that enable utility-based charging. These additional functionalities are provided in an IMS-complaint way, as a result of an implementation of SIP servlet and a special "CARMNET over SIP protocol" used for exchanging the information for the purpose of the utility-based charging. What is specific for CARMNET is that the IMS infrastructure is used to manage users profiles and to store the configuration of end-users' utility functions.

As shown in Figure 9 SIP protocol, as one of the basic constituents of the IMS architecture, has been selected for the CARMNET-XML protocol encapsulation [15]. On the server side, a SIP servlet that receives CARMNET XML messages has been implemented. The architecture of the IMS platform makes the set of CARMNET servlets easily extendable. The CARMNET-specific implementation of IMS assumes the use of a Representational State Transfer (REST) Web Service for the interaction between the AS and a CARMNET-specific user database, e.g., performed to update the amount of denarii 'possessed' by a given user. Functions of the CARMNET-XML protocol are illustrated in Figure 10.

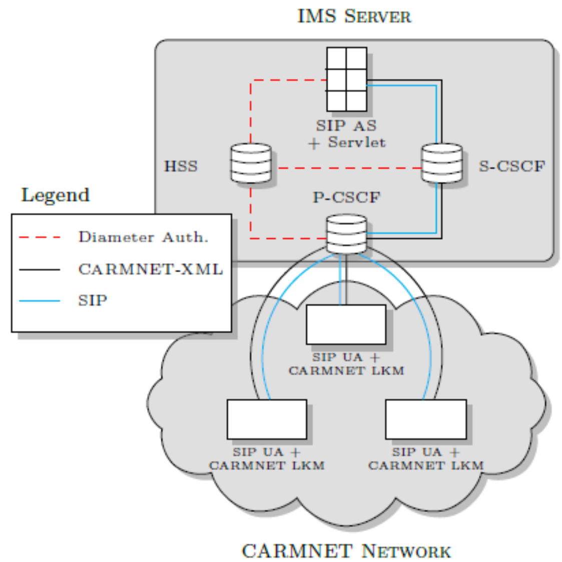


Figure 9. Integration of CARMNET system with IMS architecture [35].

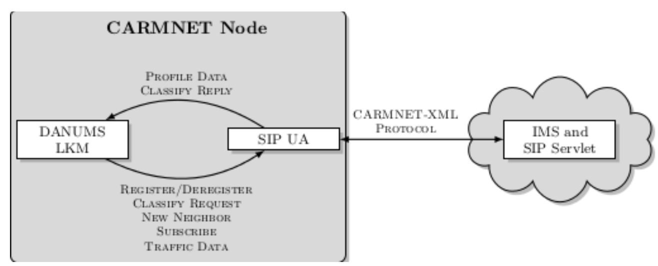


Figure 10. Functions of CARMNET-XML Protocol [35].

### G. Integration of Wireless Network Resource Management with Mobility Support

Since DANUM uses the OLSR protocol to send DRM messages [24], it cannot measure the delay of flows endpoints that are beyond a CARMNET network. DANUMS can measure the delay of such flows up to the Internet sharing node. Similarly, the accuracy of rate measurement for such flows is reduced. To fix these problems, the DANUMS Loadable Kernel Module (LKM) allows injection of measurements from external sources through procfs interface [11]. This interface is represented in Linux systems as a regular file, allowing both read and write operations [37]. DANUM system operates on per-flow basis, i.e., it measures the network performance parameters for each flow separately. Consequently, each line of the procfs file corresponds to a single flow managed by DANUM. In addition, DANUM allows supplying information regarding routes as well.

In a CARMNET network, mobility support is provided by the WiOptiMo [11], [38] framework. A CNAPT installed on any CARMNET wireless node provides mobility services to users who subscribed for them. It intercepts traffic flows associated to the mobility service and relays them to a SNAPT according to their requirements in terms of bandwidth and delay, in order to provide the desired Quality of Service (QoS). Multiple SNAPTs are located on the Internet to manage scalability and avoid concentrating traffic flows in a single spot.

WiOptiMo monitors the route between CNAPT and a SNAPT with a separate control traffic flow. Each CNAPT also periodically measures delay (one-trip time) and throughput (amount of received data over a time period) towards the different SNAPTs using this socket. The information gathered in the process can be passed to the DANUM LKM by writing it to the procfs file as flow measurement lines with reduced flow identifier consisting of source and destination IP addresses only. Implementation details about the format of each line can be found in [11].

Thanks to the procfs interface, WiOptiMo can provide measurements DANUM cannot perform. For example, a delay between a gateway and a SNAPT, measured by a CNAPT, can be added to the delay of flows destined to that SNAPT and leaving the CARMNET network through that gateway, in order to enhance the accuracy of measurements used in utility calculation. Furthermore, since a SNAPT can be installed on the same device of the flow endpoint or on a different device of the same network, the accuracy of measurements used by DANUM in the calculation of utility for flows that are outside a CARMNET network can be exactly estimated. A CNAPT on the source node can also overwrite throughput measurements for flows which it is responsible for, to account for losses encountered outside of the CARMNET network.

The WiOptiMo framework also allows a mobile node of a CARMNET network to change gateway transparently (e.g., when node moves out of the reach of the initial gateway due to the mobility of the associated user), without suffering service disruption (mobility support). In typical use cases of wireless mesh networks, only Internet gateways have public IP addresses and use NAT to share this connection. If an Internet gateway changes, the already established connections will break. To avoid this, the most common practice is to route traffic through the old gateway, which is inefficient. WiOptiMo overcomes this limitation and allows public IP to be changed seamlessly. DANUM allows to use the best available route to the selected SNAPT, at all times, regardless of the currently selected gateway. This feature is implemented by DANUM without modifying the OLSR protocol and its implementation by introducing a "virtual" host entity into Topology Control OLSR messages, representing a connection between an Internet sharing node and a SNAPT as a link state information [7].

## V. MULTI-TESTBED EXPERIMENTATION

CARMNET solutions are being extensively evaluated in multiple experiments performed in several realistic testbeds, in particular in the ones located at CARMNET partners' facilities: the wnPUT testbed [39], the Polanka-net [23] and the SUPSI testbed. The experimentation efforts involve the remote use of a large-scale wireless testbed, the DES-Testbed. Experiments within the facilities of a public metropolitan WiFi operator have been performed as well [7].

### A. *wnPUT Testbed*

The wnPUT Testbed has been built mainly for the development and the experimentation related to carrier-grade resource management for heterogeneous traffic based on the DANUM approach [5]. The focus of this work is put on the core CARMNET software, such as DANUMS Loadable Linux Kernel Module, which requires more control over each node than development of applications run in the so-called Linux userspace [37].

The wnPUT testbed consists of a software framework for centralised control of the testbed, and hardware upon which experimental and management networks are built. The hardware part consists of 13 dedicated nodes allowing to conduct multiple uninterrupted iterations of experiments remotely, without additional assistance.

Each node is connected to a Power-over-Ethernet switch, allowing to remotely power-cycle the node, even if built-in watchdog fails to detect system failure. This feature is crucial for low-level Linux kernel development, such as implementation of routing and packet scheduling modules of the DANUM system [40]. Nodes themselves are built upon ALIX platform, very similar to the one used in one of the largest wireless experimental networks – the DES-Testbed [41], [42].

The software framework accompanying the hardware part of wnPUT testbed includes online monitoring and graphical analysis tools that allow for the real-time graphical analysis of each experiment. The system consists of two core elements:

- the reader of unified experiment data,
- the tool for graphical visualization of the data.

An example of the network topology observable in an experiment conducted in the wnPUT testbed is presented in Figure 11 - it has the form provided by the wnPUT Monitor. Plots representing changes of the key DUNUMS variables during one of experiments executed in the wnPUT testbed are shown in Figure 12. The set of the variables includes:

- queue level,
- flow rate,
- virtual traffic price,
- flow utility,
- flow utility change.

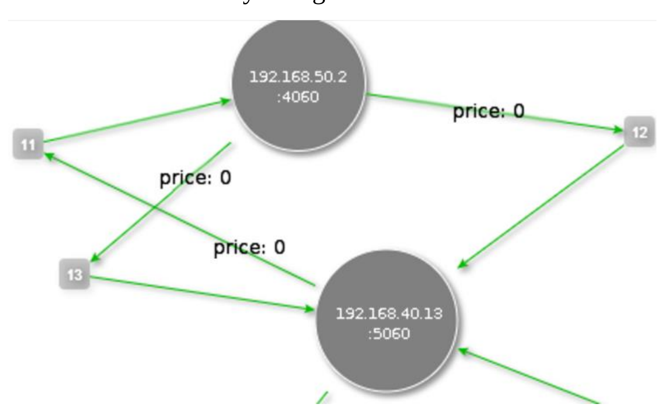


Figure 11. A view on the topology of an exemplary network shown in the wnPUT Monitor.

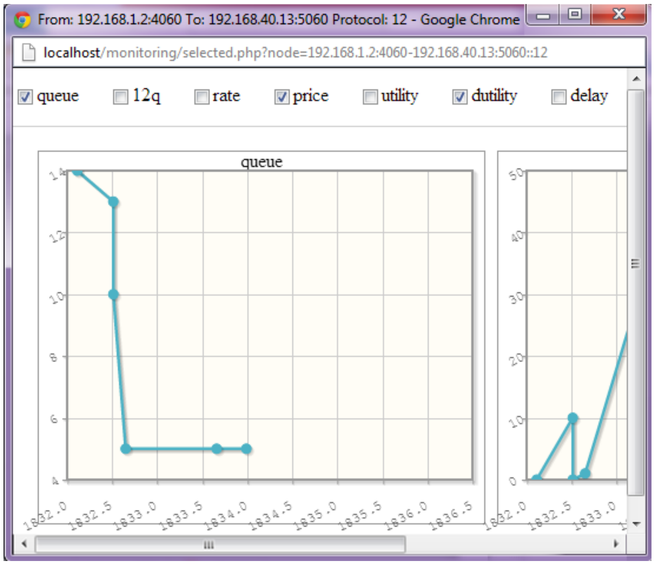


Figure 12. Graphs presenting the experiment results in wnPUT Monitor.

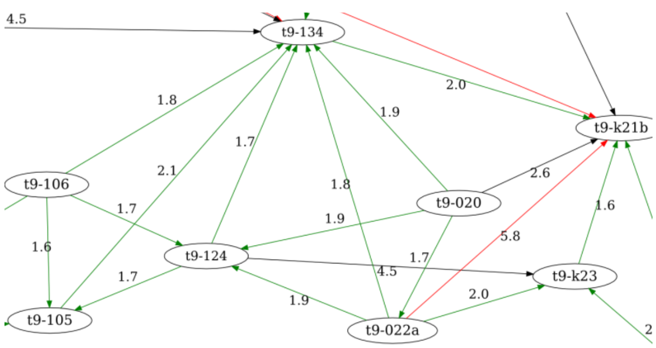


Figure 13. Sample topology fragment, generated based on ETX metric by wnPUT topology monitoring tool.

Figure 13 shows a part of wireless network topology generated by the wnPUT topology monitoring tool on the basis of the ETX metric supplied by OLSRd and monitored on one of the testbed nodes [40].

The wnPUT testbed uses an extended DES-Cript — a domain specific language for the testbed experimentation developed at Freie Universitat Berlin [43]. Instead of developing another experiment description, we have opted to use the already established DES-Cript. Thanks to DES-Cript being based on XML, we were able to further extend capabilities of the experiment description while preserving the ability of executing pure DES-Cript scenarios. For additional features, such as remote power-cycling of nodes, we use in-house extensions of the experiment description syntax.

### B. *Polanka-net Testbed*

The Polanka-net testbed was designed for testing the modified OLSR protocol based on the proposed multi-criteria *k*-shortest path algorithm [26]. The architecture of Polanka-net testbed is shown in Figure 14. The main part of the testbed consists of 12 nodes equipped with dual-core Intel ATOM processors. Each of them is equipped with: a solid state drive with the capacity of 24 GB, 4 GB of RAM and double core ATOM CPU (Central Processing Unit). The presented node's configuration allows for installing Linux in both "server" and "desktop" versions. The nodes are of small size, comparable to the dimensions of the nodes used in wnPUT testbed.

The main advantage of x86 nodes with ATOM CPUs is reasonable computing power and the fact that the developing software for this kind of nodes does not require cross-compilation. The source code can be compiled directly on the developer's workstation or within the node. The simplest solution for x86 nodes is the native compilation of the software at the nodes. In the case of native compilation, it is only required to provide the node with a source code.

The use of the nodes that were built using x86 processors (hereinafter referred to as x86 nodes) facilitates the implementation of the software. However, such nodes are more expensive and consume more energy with respect to the nodes using Reduced Instruction Sets Computer (RISC) processor. This fact was taken into account when the Polanka-net testbed was designed. Consequently, the testbed allows using low-cost nodes based on RISC CPUs (RISC nodes in Figure 14). The concept of using low-cost nodes was presented in the article [23].

The RISC nodes, used in Polanka-net testbed, support OpenWRT [44]. Open WRT is a Linux distribution dedicated for routers. It is characterized by small hardware requirements, since a firmware image (including kernel but without WiFi support) often does not occupy more than 2 MB of memory. One of the main advantages of the Open WRT is its ability to run on wide variety of processor architectures. This is possible owing to the fact that the software has an open code, which can be compiled into binary code designed for a specific platform.

In order to facilitate the implementation of multi-criteria algorithm, a special approach was applied: new discovered routes are added to the system routing table via a separate module. This module uses Zebra protocol to communicate with the OLSR protocol and its path computing algorithm. The Zebra protocol's messages are exchanged using TCP connections. The extension of Zebra's functionalities allows us to use RISC node without implemented OLSR protocol software. The OLSR protocol may be supported by the dedicated server. Consequently, the functionality of RISC nodes is limited to two tasks only. The first task is related to forwarding IPv4 packets according to the rules written in the routing table. This task is performed by the Data Plane. The second task is related to sending, receiving, forwarding and processing OLSR messages. In the proposed solution, the control plane OLSR server does not have direct access to the nodes' interfaces. In order to send or receive OLSR protocol messages via specified interface, the control plane OLSR server has to send them to the nodes, via appropriately modified Zebra protocol.

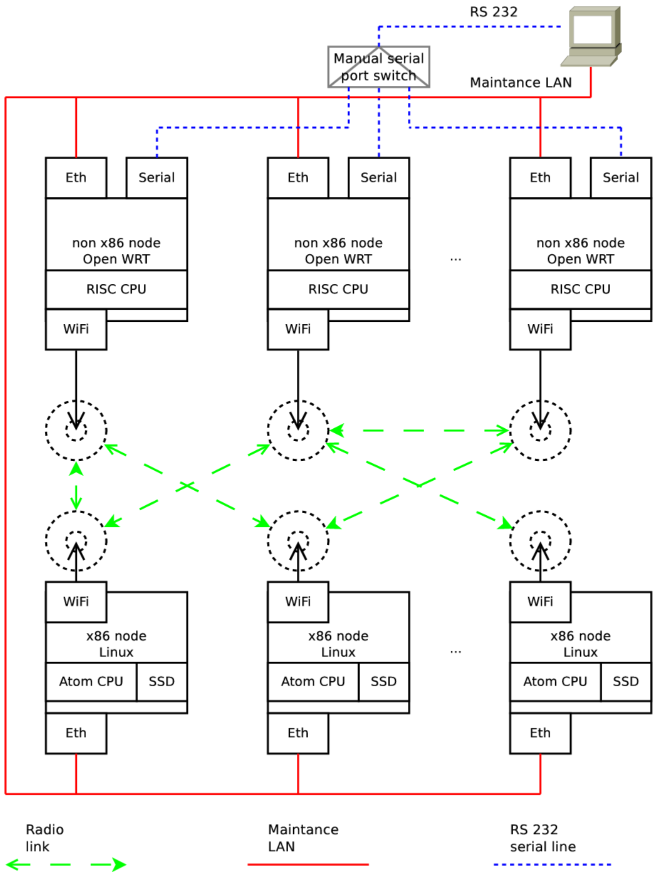


Figure 14. Polanka-net Testbed.

## C. SUPSI Testbed

The SUPSI testbed was designed to test the performance of the CARMNET mobility module based on the WiOptiMo framework. It contains three static (two of which are Internet-sharing) nodes and two wireless mobile network nodes. Each static node consists of an ALIX.2D2 system board, which supports two mini-PCI radios. We used one Wistron DNMA92 miniPCI card for each board, which is in turn connected to a two 802.11n antennas. Each board has a 500 MHz AMD Geode LX800 processor and 256 MB DDR DRAM. We installed Debian Wheezy (7.0) on each node with Linux Kernel 3.12.6 and used driver ath9k for Wi-Fi. The two mobile nodes are two ASUS EeePC 900 with a Atheros 5008Wireless Card, a 900MHz Celeron Processor and 1GB DDR RAM. They run Debian Wheezy 7.0 as well, while the Wi-Fi driver is ath5k.

To complete the hardware setup, we installed WiOptiMo SNAPT on a Dell Optiplex 760 (server), while WiOptiMo CNAPT was installed on a Lenovo ThinkPad T410a. Both machines run a Linux distribution (Ubuntu 12.04). Two of the static nodes (gateways) and the server are connected to the Internet with an Ethernet 100Mbit/s connection, while the rest of the nodes are participating in the mesh network. Both the gateways perform NAT between the mesh network and the Internet. Optimised Link S tate Routing Protocol

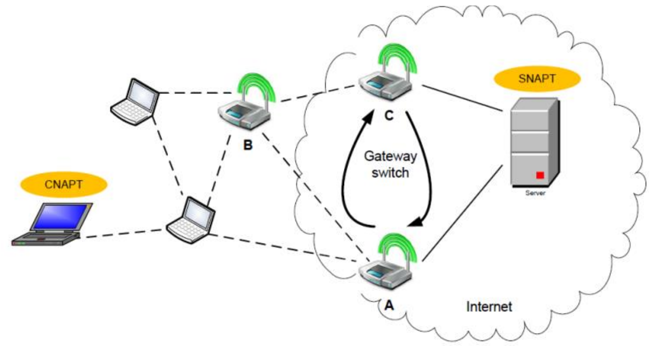


Figure 15. SUPSI testbed.

daemon (OLSRd, version 0.6.2) [12] runs on each node of the network for network path resolution. The final testbed architecture is illustrated in Figure 15.

## D. Experimental Application in a Public Wireless Network

Experiments presented in [7] describe the case of a CARMNET system being integrated with an existing, real-world public wireless network (WiFi Lugano network). As it has been demonstrated in the experiments, CARMNET solutions may be used to extend the network coverage and provide the unique features of network coverage extension and utility-aware seamless handover [7]. In particular, as presented in Figure 16 (depicting the network topology) and Figure 17, in the network coverage experiment, the nodes $n_1$ and $n_2$ (featuring the CARMNET DANUMS LKM) have enabled a mobile user to preserve the access to the Internet despite being out of WiFi Lugano's range.

The balance of virtual utility units (called denarii) presented in Figure 17 indicates how 'cooperation-oriented' each node was in sharing/using the Internet connection during the experiment. It may be seen that the user node, being the one initiating all the traffic was thus simply 'paying' for it: this can be seen in its constantly dropping denarii balance. The virtual unit balance of node $n_2$ oscillated around zero, since it was only forwarding the traffic originated in another node. The node $n_1$ has been immediately 'rewarded' for sharing its Internet access connectivity [7]. Moreover, the nodes $n_1$ and the user's node have provided the IMS Core servers with the CARMNET-specific data indicating the fairness of the user traffic relaying realized by the node $n_2$. On the basis of this data, the 'reputation' of the node $n_2$ may be automatically 'evaluated' and 'taken into account' by other nodes - not necessarily the same as those taking part in the session providing the data.

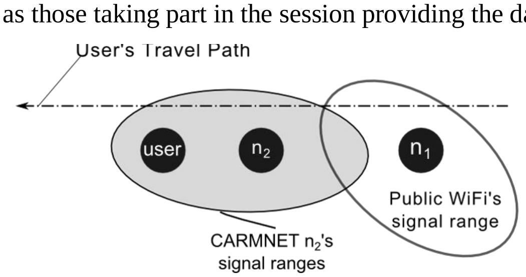


Figure 16. Network topology in the Internet access coverage extension experiment.

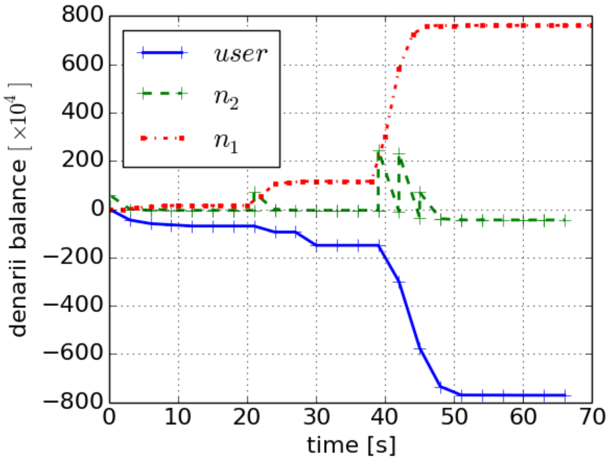


Figure 17. Denarii balance for the three CARMNET nodes during the Internet access coverage extension experiment [7].

## VI. Key Practical Results

To the authors' knowledge, the DANUMS system developed in CARMNET is the first delay-aware NUM solution practically interoperable with widely used protocols such as Transmission Control Protocol (TCP), User Datagram Protocol (UDP), Internet Protocol (IP), and 802.11 Media Access Control (MAC) [11]. The system is also the first NUM system integrated with the core IMS infrastructure [6], [15] and the first one that is capable to effectively operate in a public wireless network [7].

As demonstrated in experiments conducted in a physical testbed [15], the integration with the DANUMS (i.e., with a system responsible for wireless network resource management) has not compromised the performance of the IMS-compliant AAA functions. It may also be seen that the idea of developing a new protocol (i.e., CARMNET-XML protocol for the CARMNET specific registering and signalling) as an extension of SIP protocol, has proven to be a good choice, as far as the key user-perceived performance metrics are concerned [15], [35]. In particular, the addition of CARMNET-specific functions based on SIP communication, has not introduced a significant user registration delay, nor a significant protocol encapsulation overhead, necessary for the CARMNET-specific transmission quality reporting (allowing to maximize the network utility in a delay aware way) [15]. On the basis of such observations, it may be concluded that the proposed SIP-based approach to the access management and the user information exchange, while being compliant with the widespread IMS technology used in many telecom operators' networks [35], is indeed a viable mean for utility-maximizing local wireless network management [15].

## VII. Conclusion

In our opinion, CARMNET is a project worth a significant interest of researchers working in – so far rather distinct – areas of wireless mesh networking and IMS-based session and user management. Moreover, the practical importance of the project research objectives seems to be in line with the recent trend of deploying wireless Internet access sharing by commercial service providers and telecom operators [35]. CARMNET-like networking provides many benefits for service providers, e.g., increases network coverage without the need for extending the hardware infrastructure [7]. CARMNET architecture makes no assumptions regarding the kind of the Internet access connection, although naturally it is more likely to be deployed in a network with a fixed line Internet access, as it is usually cheaper and provides higher throughput than mobile Internet access.

It is worth being noted that in contrast to existing services, the implementation of CARMNET technological solutions, in particular the Delay-Aware Network Utility Maximization framework [5], enables to share the Internet access within a community of users truly delay-aware and QoS-oriented. In particular, a visiting user may be served in accordance to both his/her current demands (meeting of which is reflected by the rate of spending of virtual currency units) and the access point owner's willingness to share his/her WiFi network and the Internet connection.

Mainly as a result of the scenario-based design methodology [22] most of CARMNET solutions, although at a glance possibly appearing as purely technological, stay in a close correspondence to the project vision. In particular, a one-to-one correspondence appears between the delay-dependent traffic transport utility perceived by the visiting user (innovatively reflecting both the average effective throughput and the transmission delay characteristics) and the rate at which virtual currency units are earned by the owner of the local network infrastructure. In other words, we assume that each user should be awarded (in terms of virtual currency earnings) for his/her network resources sharing, and that this should be done in a way reflecting the user's subjective experience of the network access fairness. We believe that this is the right way in which the owners of high-quality and/or conveniently located network facilities may be motivated to share a significant part of their resources with many satisfied members of the CARMNET-enabled network access sharing community.

## Acknowledgment

This work was supported by a grant CARMNET financed under the Polish-Swiss Research Programme by Switzerland through the Swiss Contribution to the enlarged European Union.

## References

[1] M. Glabowski and A. Szwabe, "Carrier-grade Internet access sharing in wireless mesh networks: the vision of the CARMNET project," Proc. The Ninth Advanced International Conference on Telecommunications (AICT 2013), pp. 113-116, 2013.

[2] "CARMNET project website," [Online]. Available from: http://www.carmnet.eu 2014.05.30.

[3] V. Chandrasekhar, J. Andrew, and A. Gatherer, "Femtocell networks: A survey," IEEE Comm. Magazine, vol. 46, no. 9, pp. 59-67, Sep. 2008.

[4] I. Akyildiz, X. Wang, and W. Wang, “Wireless mesh networks: A survey,” Computer Networks, vol. 47, no. 4, pp. 445-487, 2005.

[5] A. Szwabe, P. Misiorek, and P. Walkowiak, “Delay-aware NUM system for wireless multi-hop networks,” Proc. 17th IEEE European Wireless 2011, EW2011, Vienna, 2011.

[6] P. Walkowiak, M. Urbanski, A. Figaj, and P. Misiorek, “Integration of DANUM-based carrier-grade mesh networks and IMS infrastructure,” Proc. Ad-hoc, Mobile, and Wireless Networks, Lecture Notes in Computer Science, vol. 7960, pp. 185-196, 2013.

[7] P. Walkowiak, R. Szalski, S. Vanini, and A. Walt, “Integrating CARMNET system with public wireless networks,” Proc. The Thirteenth International Conference on Networks, Nice, February 2014.

[8] S. Rayment and J. Bergstrom, “Achieving carrier-grade Wi-Fi in the 3GPP world,” Ericsson Review, 2012.

[9] A. Banchs et al., “CARMEN: Delivering carrier grade services over wireless mesh networks,” Proc. PIMRC 2008, Sep. 2008.

[10] P. Walkowiak, M. Urbanski, M. Poszwa, and R. Szalski, “Flow classification in delay-aware NUM-oriented wireless mesh networks,” Proc. The Sixth International Conference on Advances in Mesh Networks, Barcelona, 2013.

[11] S. Vanini, D. Gallucci, S. Giordano, and A. Szwabe, “A delay-aware NUM-driven framework with terminal-based mobility support for heterogeneous wireless multi-hop networks,” Proc. ICTF 2013 Information and Communication Technology Forum, I-scover, IEICE, 2013.

[12] “An ad-hoc wireless mesh routing daemon,” 2009. [Online]. Available from: http://www.olsr.org. 2014.05.30.

[13] A. Szwabe, P. Misiorek, A. Nowak, and J. Marchwicki, “Implementation of backpressure-based routing integrated with Max-Weight Scheduling in a wireless multi-hop network,” Proc. IEEE 35th Conference on Local Computer Networks (LCN), Oct. 2010.

[14] T. Clausen and P. Jacquet, “Optimized Link State Routing Protocol (OLSR),” Internet Engineering Task Force, 2003. [Online]. Available from: http://www.ietf.org/rfc/rfc3626.txt 2014.05.30.

[15] P. Misiorek, P. Walkowiak, S. Karlik, and S. Vanini., “SIP-Based AAA in delay-aware NUM-oriented wireless mesh networks,” Image Processing and Communications, vol. 18, no. 4, pp. 45-58, 2013.

[16] H. Khartabil, A. Niemi, M. Poikselka, and G. Mayer, “The IMS: IP multi-media concepts and services in the mobile domain,” Wiley, 2004.

[17] “Orange FunSpot,” [Online]. Available from: http://www.funspot.orange.pl/ 2014.05.30.

[18] “Fon,” fon, [Online]. Available from: https://corp.fon.com 2014.05.30.

[19] “Netia,” Netia, [Online]. Available from: http://www.netia.pl/ 2014.05.30.

[20] M. Chen, M. Ponec, S. Sengupta, J. Li, and P. A. Chou, “Utility maximization in peer-to-peer systems,” Proc. The 2008 ACM SIGMETRICS International Conference on Measurement and Modeling of Computer Systems, Annapolis, MD, USA, June 02-06, 2008.

[21] C. Middleton and A. Potter, “Is it good to share? A case study of FON and Meraki approaches to broadband provision,” Proc. International Telecommunications Society 17th Biennial Conference, Montreal, 2008.

[22] J. Carroll and R.H.J. Sprague, “Five reasons for scenario-based Design,” Proc. The 32nd Annual Hawaii International Conference on Systems Sciences, 1999.

[23] A. Kaliszan and M. Głąbowski, “An environment for implementing and testing routing protocols in CARMNET architecture,” Proc. The The Ninth Advanced International Conference on Telecommunications (AICT 2013), Rome, 2013.

[24] A. Szwabe, P. Misiorek, and P. Walkowiak, “DANUM system for single-hop wireless mesh networks,” Proc. The 2010 International Conference on Future Information Technology (ICFIT 2010), Changsha, China, Dec. 2010.

[25] A. Brander and M.C. Sinclair, “A comparative study of k-shortest path algorithms,” Proc. 11th UK Performance Engineering Workshop, 1995.

[26] D. Eppstein, “Finding the k shortest paths,” SIAM Journal on Computing, vol. 28, no. 2, pp. 652-673, 1998.

[27] C. Clímaco, M. Pascoal, M. Craveirinha, M. Eugénia, and V. Captivo, “Internet packet routing: Application of a K-quickest path algorithm,” European Journal of Operational Research, vol. 181, no. 3, pp. 1045-1054, Sep. 2007.

[28] A. Szwabe and P. Misiorek, “Integration of Multi-path Optimized Link State Protocol with Max-Weight,” Proc. IEEE International Conference on Information and Multimedia, Jeju Island, South Korea, 2009.

[29] M. de Vega Rodrigo and R. Pleich, “Validation and extension of the M/G/R Processor Sharing to dimension elastic traffic in TCP/IP networks,” Proc. The 2nd Polish-German Teletraffic Symposium, Gdansk, 2002.

[30] J. Roberts and T. Bonald, “Internet and the Erlang Formula,” ACM Computer Communications Review, vol. 42, no. 1, pp. 23-30, 2012.

[31] T. Bonald and J. Virtamo, “A recursive formula for multirate systems with elastic traffic,” IEEE Comm. Letters, vol. 9, no. 8, pp. 753-755, 2005.

[32] G. Stamatelos and V. Koukoulidis, “Reservation-based bandwidth allocation in a radio ATM network,” IEEE/ACM Transactions on Networking, vol. 5, no. 3, pp. 420-428, 1997.

[33] S. Hanczewski, M. Stasiak, and J. Weissenberg, “The queueing model of a multiservice system with dynamic resource sharing for each class of calls,” Proc. Computer Networks, Springer, 2013, pp. 436-445.

[34] S. Hanczewski, M. Stasiak, and J. Weissenberg, “A queueing model of a multi-service system with state-dependent distribution of resources for each class of calls,” IEICE Transactions on Communications, in press, 2014.

[35] R. Szalski, A. Szwabe, and P. Misiorek, “Flow utility estimation and signaling in a CARMNET network,” Institute of Control and Information Engineering, Poznan University of Technology, Technical Report no 657, Poznan, 2014.

[36] “OpenIMSCore,” [Online]. Available from: http://www.openimscore.org/. 2014.05.30.

[37] B. Wang, B. Wang, and Q. Xiong, “The comparison of communication methods between user and kernel space in embedded Linux,” Proc. International Conference on Computational Problem Solving, 2010.

[38] S. Giordano, D. Lenzarini, A. Puiatti, and S. Vanini, “WiSwitch: seamless handover between multi-provider networks,” Proc. WONS 2005, 2005.

[39] A. Nowak, P. Walkowiak, A. Szwabe, and P. Misiorek, “wnPUT Testbed experimentation framework,” Distributed Computing and Networking, Lecture Notes in Computer Science, vol. 7129, pp. 367-381, 2012.

[40] R. Szalski, et al. “D3.1: The report on testbed set-up and performance measures specification, CARMNET project deliverable (internal report),” 2013.

[41] M. Gunes, F. Juraschek, B. Blywis, and J. S. Q. Mushtaq, "Testbed for next generation wireless network research," Special Issue PIK on Mobile Ad-hoc Networks, vol. 34, no. 4, 2009.
[42] "DES-Testbed," [Online]. Available from: http://www.des-testbed.net/ 2014.05.30.
[43] M. Gunes, F. Juraschek, B. Blywis, and W. Olaf, "DES-CRIPT - a domain specific language for network experiment descriptions," Proc. The International Conference on Next Generation Wireless Systems, Melbourne, 2009.
[44] "OpenWRT," [Online]. Available from: https://openwrt.org/ 2014.05.30.

# MAC Protocols and Mobility Management Module for Healthcare Applications Using Wireless Sensor Networks

Muhsin Atto and Chris Guy

University of Reading, Reading, United Kingdom
{kp003919, c.g.guy}@reading.ac.uk

*Abstract*— **Using Wireless Sensor Networks (WSNs) in healthcare systems has had a lot of attention in recent years. In much of this research tasks like sensor data processing, health states decision making and emergency message sending are done by a remote server. Many patients with lots of sensor data consume a great deal of communication resources, bring a burden to the remote server and delay the decision time and notification time. A healthcare application for elderly people using WSN has been simulated in this paper. A WSN designed for the proposed healthcare application needs efficient Medium Access Control (MAC) and routing protocols to provide a guarantee for the reliability of the data delivered from the patients to the medical centre. Based on these requirements, the GinMAC protocol including a mobility module has been chosen, to provide the required performance such as reliability for data delivery and energy saving. Simulation results show that this modification to GinMAC can offer the required performance for the proposed healthcare application.**

*Keywords*—**WSN;Healthcare Applications; GinMAC; Mobility; Castalia.**

## I. Introduction

Wireless Sensor Networks (WSNs) have been widely used in a variety of applications dealing with monitoring, such as healthcare monitoring, environment monitoring, fire detection and so on. A WSN is composed of tiny, battery powered devices, called sensor nodes. The design and implementation of WSNs face several challenges, mainly due to the limited resources and limited capabilities of sensor nodes, such as power and storage. To accomplish their task, sensor nodes are required to communicate with each other and act as intermediate nodes to forward data on behalf of others so that this data can reach the sink, which is responsible for taking the required decision. Different applications using WSNs have different requirements so no generic results can be used [1], [2].

The initial applications supported by WSNs were mostly in environment monitoring, such as temperature monitoring for a specific area, house alarms, and so on. The main objectives in such applications only involved simple data processing. Energy consumption needed to be considered for specific applications, so little attention was taken on data delivery and reliability related issues such as in [1], [3].

WSNs have been extended and their designs have been advanced to support more complex applications, such as security, military, fire detection and health care related issues. In these applications, data delivery and reliability must be taken as important parameters in addition to energy efficiency, because data must be collected from the sources of events and be forwarded to the sink in real time with high reliability, otherwise the application may not fulfil its purpose [4].

In this paper, an implementation of GinMAC [1] including a proposed mobility management module is described and simulated for a healthcare application, where energy saving, delay and reliability for end to end data delivery over multi hop WSNs needs to be considered. Some scenarios are given to simulate GinMAC for the proposed healthcare application, where mobility of nodes and reliability of the data are big issues.

The rest of the paper is structured as follow. Related work and motivations for the paper are given in Sections II and III, respectively. The implementation of GinMAC for both static and mobility applications are described in Section IV. The proposed healthcare application is described in Section V. Simulation scenarios and the required parameters with figures showing the results for GinMAC implementation for the proposed applications are given in Section VI. The simulation results and some discussion is in Section VII. A conclusion and proposals for future work are presented in Section VIII.

## II. Related work

Wireless Sensor Networks consist of a set of nodes where each node has a number of sensors with the capability of collecting data about events and sending them back to a Base Station (BS). In order to ensure the successful operation of WSNs, efficient MAC and routing protocols need to be designed. The MAC protocol in a WSN controls the accessing of channels in a network, so the highest number of nodes can share the communication capability, without affecting the integrity of the data delivered to the indicated destination. Due to the wireless communication and insufficient resources and hard challenges in WSN, an efficient MAC protocol is one of the most important factors that needs to be considered before designing any applications, to enhance the life time and improve the performance of the proposed applications [5], [6].

### A. MAC Protocols for WSNs

Designing a MAC protocol for WSN is not a simple task, due to the challenging application environments and restrictions, such as energy constraints, latency, data delivery, self-configuration, self-organization and many other challenges in such networks [2]. The main aims of designing MAC protocols are reducing consumed energy, decreasing delay and increasing the reliability of such networks. A major motivation for this work is to design MAC protocols for WSN applications where energy saving, data delivery and latency from node to node in multi hops WSN networks need to be guaranteed. In a wireless sensor network, major energy waste can occur for several reasons, as described in [2], [7], [8]. The first and most important source of consuming energy in WSN is idle listening; this happens when a node is listening to an idle channel to share the medium, and it thinks there is a possibility of receiving or sending packets.

The second reason for the consumption of energy is collisions, due to a high number of sensor nodes deployed in a small area and a large number of control packets. The third reason for wasting energy is overhearing; overhearing occurs when a node listens or overhears a packet, thinking it may be the intended receiver, however, in fact the packet is not for that particular node. Some most important design factors for protocols in WSN that need to be considered while designing and deploying energy efficient MAC protocols for any applications are the following: network topology, type of antenna and clustering related issues [2].

In general, MAC protocols can be divided into two types, which are Time Division Multiple Access (TDMA) protocols and contention based protocols. Each of them has advantages and disadvantages. Schedule based protocols have no collision related problems and are energy efficient protocols, however, scalability in a very dynamic WSN is a big problem for such protocols. Contention based protocols have better performance in terms of scalability in distributed WSNs, however, collisions are a big problem for such protocols.

*1) Schedule Based MAC Protocols:* In WSNs, to allow sensors to gain access to the shared wireless medium in a cooperative manner, schedule-based MAC protocols have been proposed that regulate access to resources according to a schedule to avoid contention among nodes. Depending upon the medium access technique, the resources could be a time slot, a frequency band or a Code Division Multiple Access (CDMA) code. The main aim of schedule-base MAC protocols is to achieve a high degree of energy conservation to prolong the lifetime of the network. Most of the schedule-based MAC protocols for WSNs use a variant of a TDMA scheme whereby the time available is divided into slots. Using this scheme, a logical frame of N contiguous slots is formed and this logical frame repeats itself in cycles over time. Each sensor node is assigned a set of specific time slots per frame and this set constitutes the schedule according to which the sensor node gains access to the medium and has the right to transmit or receive. This schedule can be either fixed, or constructed on demand, on a per frame basis, by the base-station to reflect the current requirements of sensor nodes and traffic pattern. The nodes must also satisfy the interference constraint, which says that no nodes within two hops of each other may use the same slot [9].

This two hop constraint is needed to avoid the hidden node problem when there is chance this could happen. Energy conservation is achieved by using an on and off mechanism for the sensor radio transceiver [10]. According to the schedule of each sensor node, a sensor alternates between two modes of operation: active mode and sleep mode. A sensor is in active mode when it is its turn to use the assigned time slots within the logical frame to transmit and receive data frames. Outside these sensor assigned time slots, it moves into sleep mode by switching off its radio transceiver.

*2) Contention Based MAC Protocols:* Contention based MAC protocols are also known as Carrier Sense Multiple Access/Collision Avoidance based protocols (CSMA/CA). These protocols do not pre-allocate resources to individual sensors. Instead, they employ an on-demand channel access mechanism and in this way share a single radio channel among the contending nodes. Simultaneous attempts to access the communications medium, however, results in a collision. Effectively, these protocols try to minimize rather than completely avoid the occurrence of collisions. Traditional networks use Carrier Sense Multiple Access (CSMA) as a medium access mechanism. However, CSMA/CA mechanism gives poor performance in WSNs due to two unique problems: the hidden node problem and the exposed node problem. The hidden node problem is where node A is transmitting to node B and node C, which is out of coverage of A will sense the channel as idle and start packet transmission to node B as well. Consequently, the two packets will collide at node B. In this case CSMA/CA fails to foresee this collision [11]. In the proposed real time applications the main aim is to save energy and improve reliability so a schedule based MAC protocol has been chosen.

### B. Design Issues and Challenges for WSN

Due to the limitations and design restrictions of WSN, such as wireless communication and resource limitations, the design of protocols has many challenges, new proposed protocols need to consider these restrictions during their designing and deploying phases. To meet these restrictions, the following important factors and design issues need to be considered for new protocols [3] and [12].

**Data Delivery Models:** A WSN is an application specific network, so data delivery models need to be designed according to the given application. Some applications need to deliver data from sensor nodes directly toward the sink over a single hop away from the sink, while the others send data over multiple hops between source nodes and a sink. So data delivery models will impact the performance of the new proposed protocols.

**Operating Environment:** WSNs can be used for different kinds of applications and each of these applications will have a specific requirement. For instance, a WSN used for environment monitoring needs to have specific protocols that can deal with the specific challenges. Moreover, WSNs used in real-time related applications need to have efficient protocols in order to provide the required performance for these applications.

**Energy Saving:** Due to the limited power capacity associated with each node in a WSN, newly designed protocols must take power consumption related issues as their most important objective. Each node must consume as little power as possible in order to extend the lifetime of the whole network, therefore, the trade-off between energy consumption and data delivery in the WSN are hot topics in recent research studies. Energy can be saved by letting nodes go to sleep when there is no data to sent and received.

**Connectivity:** Pre-established connections between each pair of nodes in the WSN define the connectivity of the network. WSNs may be densely deployed in an interest area, and there will probably be cases where this connection will have failed and be disconnected. This can happen when some nodes leave the network or die and this means that the topology of the WSN may change very frequently. Therefore, mobility may need to be considered in new proposed protocols.

**Hardware Constraints:** Typically, nodes in WSN are equipped with small amounts of resources, such as memory, processing capability and power. However, in some applications protocols there is a need to store a large amount of data before forwarding it to the next hop. Because of the limited available memory at each node, that node may not be able to store all the data in its local memory. Hence some techniques need to be designed to reduce the overflow of the data at each node in the network.

**Low Node Cost:** As a WSN may consist of hundreds or even thousands of nodes, the cost of each individual node must be as low as possible as this will reduce the cost of the whole network.

**Scalability and Adaptation:** Since the number of nodes in the network may be large and the communication links are prone to fail, and nodes have the ability to join or leave the network, the new protocols need to be scalable and to be able to adapt to any size of network.

**Self-Configuring:** After nodes are deployed, they need to be able to organize themselves in order to be able to communicate, and when some nodes die and the topology has been changed, it should be possible for them to re-configure themselves without user interaction.

**Security and Privacy:** Due to the wireless communication between sensors in WSN, it is possible that data may be listened to by unauthorised nodes. Hence the requirements for security and privacy of data needs to be considered when designing applications using WSNs.

**Quality of Service (QoS) support:** Some applications in WSNs may need to deliver data with specific QoS requirements, for example, delivering data at a required time with bounded latency and reliability. In the proposed healthcare application, the reliability of the delivered data is the most important factor, which needs to be considered. In the following sections, most of the MAC protocols proposed in the literature will be debated when some of the above challenges are considered for the proposed application.

### C. Proposed MAC protocols for WSN

Some of the recently proposed MAC protocols such as [7], [2] are discussed in term of their suitability for real time applications, such as military, fire detection or health care related applications. A real time application deals with a hard deadline, so energy is not the only the consideration for the MAC protocol designs. Data delivery and reliability must also be taken into account before designing and deploying the proposed applications. Details of such MAC protocols, with their advantages and disadvantages in terms of energy saving, delay and reliability for data delivery over multi-hops WSNs are discussed in the following sections.

*1) Sensor-MAC (S-MAC):* This MAC protocol [7] has been designed mainly for WSNs, with energy efficiency as its primary goal. The traditional MAC protocols are not suitable to be used for WSN; they are designed for systems that power on most of the time, because nodes can be powered by recharges, so there is no power limitation. However, nodes in WSN need to be turned off as much as possible to enhance the lifetime of the entire network. S-MAC is based on the 802.15 IEEE standards; it uses the same techniques to share the medium. The S-MAC protocol reduces energy wasting from idle listening, collisions and overhead, using low duty cycle operations for all nodes in a multi hop WSN. It reduces the energy used by nodes in their idle listening time, by putting nodes in sleep mode when there is no need to be active and there is no data to sent and received at the current time.

S-MAC lets nodes periodically sleep, which decreases used energy, but increases end to end delay, because the sender needs to wait until the receiver wakes up to receive the data. In order to reduce this delay, S-MAC uses a new technique called *adaptive listen*, which lets nodes adaptively go to sleep in their listening time when no communications occur, and hence this will reduce long active idle times. In a WSN there may be cases where some nodes have more data than others to send or receive. In such cases, S-MAC uses a message passing technique to divide the long messages into small packets and transmits them in a burst, to avoid having to retransmit a long message again, in the case of failed delivery. Most of the proposed MAC protocols discussed in this paper are based on the S-MAC. Each of these protocols tries to solve problems associated with S-MAC.

*S-MAC Techniques for Energy saving and Reducing Delay:*

- Duty cycle scheme in multi-hop WSN that reduces energy consumption by nodes in their idle listening time.
- Adaptive listening technique, which greatly reduces the delay occurred during periodic sleeping.
- Using message passing to reduce the energy usage and delay caused by retransmitting after long message failed delivery

- Using Network Allocation Vector (NAV) with RTS and CTS to avoid collision and hidden terminal related problems, when several nodes at the same time need to communicate.
- S-MAC let nodes interfering with each other go to sleep to avoid overhearing, and this saves some energy as well.
- Schedule sleep synchronization, this technique is used by each node in the WSN to organize its schedule table with its neighbours.

*Choosing and Maintaining Sleep Scheduling Tables in S-MAC:* Each node in the WSN needs to organize and exchange its schedule time with its immediate neighbours before starting to communicate in its allowed time period. There is a schedule table stored at each node in the WSN, including the schedule of its own and for all of its neighbours. Each node in the WSN uses the following cases when obtaining its schedule tables from the network. More details can be found in [2] and [7].

- Each node waits for a fixed time before broadcasting its schedule table to its neighbours. If it does not receive any schedule from its neighbours, it will broadcast its own schedule table.
- If the node hears another schedule before announcing its own schedule, it uses the new one and simply discards its own.
- In the case where a node hears different schedule tables from different nodes, there are two possible ways to deal with this case. The first way is if the node does not have any neighbours, it simply discards its own schedule and follows the new one, while the second way is if the node has already received schedule adaptation from its neighbours, it updates its own table with the new received schedule tables and then broadcasts its own schedule table.

**Advantages:**

- Using the duty cycling concept, S-MAC saves energy for nodes in WSN.
- Using the adaptive listening concept, S-MAC reduces delays associated with unnecessary waiting times for sleep periods and hence reduces energy consumption.
- Good scalability and topology management.

**Disadvantages:**

- Fixed period sleeping and waking up is not suitable for real time applications as this may cause huge delays in multi hop networks.
- Does not provide reliability for end to end data delivery.
- S-MAC lets nodes that are interfering go to sleep, and this can cause problems when a path later on goes through one of these nodes, which shows that S-MAC does not support cross layer concepts.
- Due to the need to establish a sleep/wakeup schedule for each node in a WSN, there is an overhead, which will decrease the throughput for data delivery.
- The end to end delay is increased meaning that this protocol can not be applied for real time applications without improvement.

*2) Medium Access Control with a Dynamic Duty Cycle (DSMAC):* DSMAC [8] has been proposed with the aim of reducing energy wastage and decreasing the delay associated with S-MAC, using a dynamic duty cycle. It achieves a good trade off between energy saving and delay. DSMAC dynamically changes the state of the nodes, for instance, from active to sleep depending on the traffic conditions and level of consumed energy and current delay, without any predefined information. This will save energy and decrease delays associated with S-MAC in an efficient way.

DSMAC uses a synchronizing tables techniques to organize the scheduling time for nodes in the network, to let them know when they need to be asleep or to be active. Each node in the WSN maintains its own schedule table like S-MAC, from already received SYNC packets from its immediate neighbours, then follows and broadcasts its schedule table to its neighbours. In addition, DSMAC keeps a track of an average of energy consumption and latency delay, using scheduling operations related information. DSMAC estimates the current traffic load and then changes cycle dynamically if needed.

**Advantages:**

- Saving energy using dynamic multiple duty cycling improves S-MAC.
- Decreasing the delays the associated with S-MAC from node to node using wakeup and sleep, changing modes dynamically, depending on the current traffic load and level of the consumed energy.
- Increasing throughput when traffic is high compared with S-MAC.
- Good scalability.

**Disadvantages:**

- Does not provide reliability for end to end data delivery.
- DSMAC lets nodes that are interfering go to sleep, and this can cause problems when the path goes through one of these nodes. This shows that DSMAC does not support cross layer concepts.
- The need for the dynamic SYNC announcement for each node in the WSN and storing the average of consumed energy and delay, causes an overhead and this will decrease throughput.
- The end to end delay is increased, so DSMAC is not suitable to be used for the proposed application without improvement.

*3) An adaptivity Energy -Efficient and Low latency MAC for Data gathering (D-MAC):* In WSN most application traffic is represented as a directed tree related topology, which enables the applications to collect data from multiple source nodes, and send to a single sink. In this case, the sink node will be the root and the sensor nodes will be the children. This type of topology can control the traffic in the network compared with flat topologies. Nodes in the selected path can communicate with each other to solve the interfering problems in S-MAC. DMAC is designed to reduce energy and latency associated with S-MAC, more details can be found [2] and [13].

As mentioned before, S-MAC lets nodes that are interfering go to sleep, this will not allow nodes that are two hops away from the current node notify ongoing traffic, and this will introduce extra delay in the case where some of these nodes are selected later on in the path. Therefore, this will cause data forwarding interruption related problems. To solve this problem, D-MAC [13] has been proposed; DMAC utilises a sleep schedule of each node, which is dependent of its depth in the tree. D-MAC adaptively changes the cycle for the nodes according to the current traffic load in a similar way to DSMAC.

D-MAC uses data prediction techniques for data gathering from source nodes toward the sink, in case the traffic is low and the aggregated amount of data needed to be forwarded at intermediate nodes is high. This can be raised when the current duty cycle is unable to handle this transmission. Hence data prediction related approaches will let nodes be active as long as needed. Furthermore, D-MAC uses a More to Send (MTS) technique for the nodes in the multi paths to remain active when one node fails to send a packet to its parent.

**Advantages:**

- Energy saving using duty cycling technique
- Decreasing delay associated with S-MAC using data gathering and prediction techniques.
- Increasing throughput when traffic is high compared with S-MAC.
- Solving data forwarding interruption problems.
- Delay end to end decreased.

**Disadvantages:**

- Does not provide reliability for end to end data delivery.
- Suffers from overhead due to having extra SYNC announcement for each level of the traffic, to predict the nodes, which need to be active in WSN later on.
- Does not support cross layer.
- If data needs to be collected from arbitrary nodes, D-MAC may face problems.
- The end to end delay is not guaranteed.

*4) Routing Enhanced Duty Cycle MAC (RMAC):* RMAC [14] is a MAC protocol that supports a cross layer approach. This protocol has been designed to provide energy efficiency and to reduce delays associated with previous protocols such as S-MAC, DSMAC and D-MAC. RMAC lets nodes in the expected path from source nodes to the sink to go to sleep and intelligently wake up when they need to send or receive data in multi-hop networks. In addition, RMAC achieves significant improvement for the end to end data delivery in a single cycle in multi hops, as it reduces the contention period much more efficiently than S-MAC. Furthermore, RMAC sends a control frame along the path to inform the nodes in the selected path of traffic before the actual data packet is transmitted.

**Advantages:**

- RMAC saves energy using single duty cycling technique
- Increases throughput where traffic is high, compared to S-MAC.
- Supports a cross layer approach.
- End to end delay is decreased.

**Disadvantages:**

- Does not provide a guarantee for delay and reliability for end to end data delivery, which means that it is not suitable to be used for the proposed applications.

*5) Q-MAC:* Data collection for applications in WSN can be divided into three types; event-detection based applications, periodic-sensed-based applications and query-based applications. Each of these applications has its own techniques to deal with collecting data from one or more sensor nodes and sending to the sink. Various MAC protocols have been proposed for each type, with the aim of energy and delay efficiency for the indicated applications [15].

Query-based applications are types of applications where users put their request for data into a query and send this to the specific part of the area where sensor nodes are deployed. These types of applications can improve minimum end to end delay latency with efficient energy usage. When there are no queries in the network, all nodes will save energy by turning off their radios. However, when a query is initiated by a user and it has been sent to the network, scheduling and SYNCH related packets will be broadcast automatically to deal with data communication, depending on the locations of the specified nodes in the query. This will enhance the lifetime of the network, because only part of the network will deal with this data communication, and nodes in the rest of the network will be sleeping.

The main objectives of the Q-MAC [15] protocol are (1)reduce end to end delay by informing the intermediate nodes in advance about ongoing traffic using dynamic scheduling, (2) enhance the lifetime of the entire network by activating only the nodes that need to deal with data communication, which are predefined in the query. Simulation results in [15] concluded that Q-MAC improves latency $80\%$ over S-MAC.

**Advantages:**

- Q-MAC saves energy using query based techniques.
- Increases throughput when traffic is high, compared to S-MAC.
- End to end delay is decreased using queries based techniques.
- Supports multiple destinations.

**Disadvantages:**

- Does not provide reliability for end to end data delivery.
- Does not support cross layer.
- End to end delay not guaranteed, and so it is not the right protocol to be used for real time applications.

*6) PEDAMACS:* PEDAMACS [16] is a MAC protocol based on TDMA, the aim of this protocol is to save energy and to reduce end to end delay for multi hops in WSN. PEDAMACS provides the extension of single hop TDMA to be used in multi-hops TDMA. It uses a high power transmission Access Point (AP) to synchronize the scheduling information of the nodes using one hop away nodes. This means that this protocol needs to use different transmissions to collect data and organizes scheduling information among sensor nodes. It requires an AP which can reach any node in the network which has unlimited amounts of energy. It is the root of the deployed network.

PEDAMACS depends on topology discovery information to organize the nodes using different phases: topology learning, topology collection, scheduling and adjustment. PEDAMACS uses three different transmission ranges: largest transmission, lowest transmission and medium transmission ranges. The AP uses the largest transmission range to broadcast the topology and scheduling information to the network. Sensor nodes use lowest transmission to collect data in the network, and medium transmission is used to discover local topology related information.

**PEDAMACS phases** PEDAMAC uses the following phases to broadcast the required information to collect data between nodes in the network [16]:

**Topology Learning Phase:** The AP uses this phase to broadcast topology learning coordination packets to all sensor nodes or other nodes in the network, to organize the scheduling related issues. The topology learning packet contains two time slots, which represent the current, and next times. The current time is for sensor nodes to set their scheduling according to this time, and the next time is the time when nodes need to stop their transmission and wait for the AP to receive a new current and next times. After sensor nodes receive their current and next time, the AP needs to broadcast a tree construction packet. Nodes receive this packet according to their neighbours depth path to the AP. After the tree topology is constructed, nodes need to broadcast their updated scheduling information to the whole network.

**Topology Collection Phase:** After the AP broadcasts its topology learning phase, topology collection packets need to be broadcast in the next time slot and then each node organizes its local topology using the information in the topology collecting packet. Then they listen to their parents and transmit their local topology using lowest transmission range. In this phase, nodes use CSMA to listen to their parents and to receive next and current times from receiving topology packets.

**Scheduling Phase:** In order to organize the scheduling tables for all nodes in the network, the AP broadcasts the scheduling packets based on its knowledge of the complete network topology, to set the schedule tables for each node in the network. Each scheduling packet contains the current and next time as in the previous phases, to let nodes organize their times and later on to divide their times into slots depending on the data transmission requirements of each node in the network.

**Adjustment Phase:** PEDAMACS uses this phase at the end of scheduling phase to complete the topology of the network and to add any other required modifications, such as mobility of nodes and adding new nodes and so on, depending on the given application. The AP broadcasts an adjustment packet to spread the rest of the information using current and next times as done in the above phases using medium transmission range. Nodes need to access this packet to find how to organize their scheduling times with given current and next slot times. The adjustment packet also includes information to let nodes have access to the next adjustment packet, and to send it to the AP in the next time period. This will allow all nodes to be able to reach the AP.

**Advantages:**

- Energy saving for sending and receiving data in the network.
- Throughput increasing when traffic is high, compared to S-MAC.
- End to end delay guaranteed
- Supports cross layer, such as routing protocols.

**Disadvantages:**

- No reliability provided, this means that this protocol is not suitable to be used for the proposed application when reliability needs to be guaranteed.

*7) E2RMAC:* In general, Contention-based MAC protocols have been preferred for WSN over TDMA, because of the need for TDMA synchronization and the unsuitability of TDMA for distributed and dynamically changed topology of the WSN. Most of the proposed contention based MAC protocols for the WSN use adaptive duty cycling protocols and wake up on demand duty cycling techniques, in which different channels with different powers are used to deal with data transmission. E2RMAC [17] is a protocol based on Contention techniques, but which allows for CDMA operations. Its aim is to provide energy efficiency, reliability and bounded latency for data delivery from source nodes to the sink. E2RMAC performs wakeup duty cycling to achieve its goals.

**Basic Operations for E2RMAC**

- When nodes need to send or receive data, they need to send wakeup tones to the network to wake up the nodes that are expected to share the data communication, after waiting a random time.
- Secondly, all neighbours of the current sender that hear the wake up tone, put their radios into high power mode, to be ready for the data transmission.
- Thirdly, the sender sends a filter packet, which contains the address of the intended destination, and switches its radio to sleep mode, then the receiver receives the filter packet and keeps its radio in the high power mode and makes other neighbours put their radios into sleep mode.
- Finally, the sender sends the data packet to the destination and goes to sleep, then the receiver receives the data, sends back an ACK to the sender and goes to sleep.
- If packets are successfully received by intermediate nodes, they will forward these received packets to the next hop without waiting for back off time, which will reduce overall delay.

**Advantages:**

- Energy saving using duty cycling techniques.
- Throughput increasing when traffic is high, compared to S-MAC.

- Supports cross layer and solves the problem of data forwarding interruption using routing techniques.

**Disadvantages:**

- Overhearing may occur, when sender hears an ACK from some intermediate node and it thinks it is the intended receiver.
- E2RMAC uses wake up, filter packet and then data packet to transfer data from source to the sink, which may increase end to end delay in large networks.
- End to end reliability for data delivery is not guaranteed and hence this protocol can not be applied for real time applications when reliability and delay need to be guaranteed.

*8) QoSMAC protocol:* Quality of Services (QoS) in WSN is to guarantee some specific parameters, which need to be considered when designing for a given application. The QoSMAC [18] protocol is based on TDMA, which can handle routing with medium access. The topology that is used in this protocol is a tree, so in this protocol, nodes need to organize themselves as a tree, where the root is the sink and the leaves are nodes. Data collecting and processing are done among the sensor nodes and go up toward the sink. The services that this protocol aim to achieve are providing guarantees for node to node delay and reliability for the data delivery between source nodes to the base station (sink).

**Advantages:**

- Energy saving using duty cycling technique
- End to end delay decreases compared to S-MAC.
- Throughput increases when traffic is high, compared to S-MAC.
- Solves the problem of data forwarding interruption using routing techniques.
- Delay and reliability node to node guaranteed

**Disadvantages:**

- If data needs to be collected from arbitrary nodes, QoS-MAC may face problems.
- The maximum number of nodes is small, so it is not suitable for large WSN networks.
- Delay and reliability end to end are not guaranteed, so this protocol can not be applied for the proposed application where reliability is one of the most important parameters, which needs to be considered.

*9) GinMAC:* GinMAC [19] is the first MAC protocol that has been proposed to consider reliability for the data delivery in time critical related operations. GinMAC is a tree based MAC protocol and uses different techniques to achieve its goals, such as reliability and timely delivered data, by considering the topology of the environment, which must be known at the deployment phase before running the application. Examples of applications that GinMAC can support are real time applications in WSN, such as fire detection, military, health care related applications, with relatively small number of nodes.

GinMAC is a TDMA based MAC protocol, using low duty cycling to save energy for nodes when they have nothing to send and receive. We conclude that this MAC protocol is the best for energy consumption related issues over the pre discussed MAC protocols in this paper. In order to achieve this performance, GinMAC must be flexible in case the topology changes. In addition, GinMAC must be adaptable for adding or subtracting nodes from or into the network [20], [21].

GinMAC uses three features to deal with data delivery; Off-Line Dimensioning, Exclusive TDMA and Delay Confirm Reliability Control. Off-Line Dimensioning is used to divide the frames into three slots, which are basic, additional, and unused slots. The Basic slot is used for forwarding one message toward the sink within frame size F. The Additional slot is used to improve transmission reliability, and the unused slot is for improving low duty cycling to save energy. GinMAC uses these techniques and slots to improve energy consumption and reliability for data delivered from source nodes toward the sink.

**Advantages:**

- Energy saving for sending and receiving data in the WSN, using TDMA based techniques
- Throughput increases when traffic is high compared to S-MAC.
- Supports a cross layer approach.
- Supports real time communications.
- End to end timely data delivery and reliability guaranteed, so it is a good start point MAC protocol to be used for the proposed healthcare application with small number of nodes in the WSN.

**Disadvantages:**

- Supports small number of nodes; the maximum allowed number of nodes is 25.

## III. Motivations

Most of the recently proposed protocols for WSNs consider either energy saving or reliability for the target applications, none of them have considered both performance metrics at the same time [2]. However, some applications may need to guarantee both energy saving and reliability at the same time, otherwise the applications will not fulfil their purpose. Therefore, in order to provide this, new and very efficient Medium Access Control (MAC) protocols need to be designed. Previous works showed that GinMAC is the only protocol, which can be used for real-time applications to provide the required performances as shown in [4]. The motivations for this paper are the following:

- Design MAC protocols for the proposed healthcare application where the required energy saving, reliability and delay for data delivery need to be considered.
- Design mobility management modules for the proposed healthcare application.
- Adapt GinMAC to add new features to improve its applicability to real-time applications which require mobility, such as healthcare applications as described in [22].
- Simulate a GinMAC implementation including the proposed mobility management module given in [1] for the proposed healthcare application.

## IV. MAC PROTOCOLS FOR REAL-TIME APPLICATIONS

It was concluded in [4] that GinMAC is a possible MAC protocol for use in real-time applications, where reliability, energy saving and delay can be guaranteed. Challenges and requirements that need to be considered before designing any MAC protocols for such applications are also described in the same paper. The implementation of GinMAC including a mobility management module is described in this section.

### A. Implementation of GinMAC for Real-time Applications

GinMAC [23] is a TDMA based MAC protocol, so energy saving and reliability with bounded delay can be achieved. However, an efficient synchronization and slot allocation algorithm needs to be designed in order to allocate the required slot time for each node in the network and let the radio of the nodes be turned on only in the allocated time. In this case, each node needs enough slots of time to transmit data toward a sink, including control messages, such as messages for slots permission, mobility and topology control related messages. GinMAC has been modified to add new features to improve its applicability to applications, which require mobility, such as healthcare applications. The GinMAC implementation in [23] does not support mobility while this one does. Topology management and time synchronization for GinMAC in this implementation are described below.

*1) Slot allocations in GinMAC:* GinMAC is a TDMA based protocol and assumes that data is forwarded hop by hop toward a sink using a tree based topology, consisting of $n$ nodes. Time in GinMAC is divided into a fixed length called *Epoch E*, each E is subdivided by $n*k$ time slots so that each node allocates $k$ slots for transmitting data toward its parent until it reaches a sink. Each node is assigned $k$ exclusive slots with four different types; basic slots (*TX,RX*) for data transmitting and receiving, additional slots (*RTX,RRX*) for re transmitting, broadcast slots (*BROD*) for topology control between nodes in the network and unused slots (*U*) for saving energy (if any). More details about how these slots are used can be found in Figure 1.

Additional slots are used only for retransmission to achieve the required reliability of the target applications. These slots are used even in the case when no data is available for transmission, as described in [19]. Unused slots are used for saving energy when data cannot be delivered using basic and additional slots. This implementation for GinMAC does not contain unused slots, but they may be used in the future for increasing the lifetime of the network. Broadcasting slots are used for topology control. Slots for each node need to be allocated according to the defined topology so that the required performance can be achieved.

*2) GinMAC Topology Control Management:* GinMAC is a tree based WSN topology so that each node transmits its data toward a sink in its allocated slots and sleeps for the rest of the time. The current static topology that is proposed is a WSN with 13 nodes with static slot allocation, each node has enough slots of time to transmit all data from its children and its own, including control messages toward a sink. GinMAC supports mobility for leaf nodes and this will require the design of new topology control and management algorithms to provide connectivity between static and mobile nodes in the network. It is assumed that the BS has adequate power to reach all nodes in the network using down-link slots. However, the sensor nodes cannot always do this because of their limited power supply.

A node added to the network must determine in which slots it must become active before it can transmit or receive data. After a node is switched on, it must first ensure time synchronization with the rest of the nodes in the network. Both control and data messages transmitted in the network can be used to obtain time synchronization. The node continuously listens to overhear a packet from the sink. After overhearing one message, the node knows when the GinMAC frame starts as each message carries information about the slot in which it was transmitted.

As a next step, the node must find its position in the topology, which must stay within the defined topology envelope. For this purpose, the new node listens for packets in all slots. Transmitted data packets from a sink use a header field in which a node that is ready for transmission can find its information and then according to this information start and stop data transmission toward its parent. A node may be configured with a list of valid nodes or clusters that it is allowed to attach to when mobility is supported. This might be necessary to ensure that a node will only attempt to join the network using known good links, as determined by measurements before the deployment to provide the required performance.

*3) Synchronization Messages for GinMAC:* At the start of each frame, the sink needs to broadcast a synchronization packet which is denoted as *SYNCH* into the network. This packet holds the start time, end time and slot numbers for each node in the network. When nodes receive a SYNCH packet from the network, they will extract their information from the SYNCH packet and then discard it. In this case, CSMA is used by the sink to synchronize nodes in the network and nodes use TDMA to transmit their data to their parents. After nodes receive their slot information from the sink, they need to ask permission for data transmission from their parents. Then, after slots related information has been received by a node, it has to handshake with its parent and then can start to transmit data. After a node uses its allocated slots, it can go to sleep and wake up at the same time in the next frame. Each node in this case will access the channel using their unique start time, so this will avoid any chance of collision with transmissions from other nodes in the network.

GinMAC lets nodes and their parents be active at the same time so that data can be transmitted between them. This time synchronization algorithm is good enough to deliver packets with the required performances for the applications described in Section VI.

The core idea behind this GinMAC implementation is to let nodes sleep as much as possible without effecting data delivery and required maximum delay, and this can only be done using a TDMA based technique. The static topology is

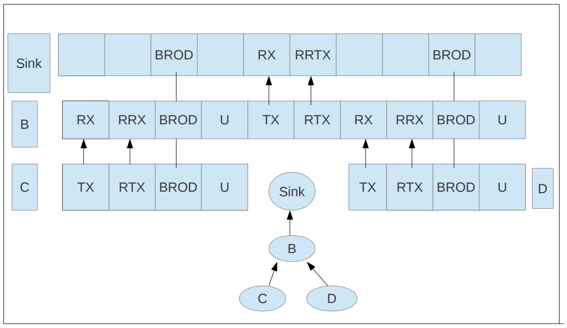


Fig. 1. Slot allocations and Synchronizations for nodes using GinMAC.

designed to let nodes have enough slots to transmit their data and in the rest of the frame go to sleep. The slot allocation and synchronization for GinMAC can be found in the Figure 1.

### B. Mobility for Real-time Applications Using GinMAC

A new challenge is posed when mobility needs to be considered in a WSN. In this case topology control, resource management and performance control need to be designed to provide good connectivity between static and mobile nodes in the network and provide the required performance. Mobility and topology control for critical applications using WSNs are described in [24], [25], [26]. The proposed mobility management module in this paper follows the same messages and concepts as in the above papers.

*1) Mobility Management Module for GinMAC:* There may be cases when moving from one location to another in the network effects the connectivity of the network and then reconfiguration algorithms are needed. In order to support mobility for real-time applications, control messages, which need to be transferred between static and mobile nodes to find a better attachment have been defined. Some of the possible control messages are Advertisement (*ADV*), join (*JOIN*), and join acknowledgement ( *JOIN ACK*) messages. Static nodes are formed into *Clusters*.

When nodes in a cluster switch on their radios, they need to send ADV to the network and then wait some time. When mobile nodes receive these ADV messages they will ask to join the network. When a static node receives JOIN messages from the mobile nodes they will send back a JOIN ACK message to let the mobile node know that request to join has been accepted. So using these control messages connectivity between mobile nodes and cluster nodes will be established. In the proposed application only leaf nodes are allowed to be mobile nodes and all other nodes are part of a fixed cluster. The mobility module lets nodes move across a line between mobile nodes and a sink.

Mobile nodes may have more than one cluster they could join, so they have to decide which cluster will be selected for transferring data toward their parents. In this GinMAC implementation, the cluster with maximum Receiver Signal Strength Indicator (RSSI) is considered the best one to be selected for the new attachment. Cluster nodes send ADV including available positions over time and when mobile nodes receive ADV, they compare the RSSI from their current parents to the received RSSI from the current ADV messages. In the case that a new cluster has a better RSSI, mobile nodes need to leave their current parents and attach to this new cluster, which is included in the currently received ADV message. When a new attachment is selected then a join request needs to be sent to that cluster. Upon receiving the JOIN request from a mobile node, JOIN ACK needs to be sent by the selected clusters.

Slots in the each frame need to be updated according to the new attachments. Mobile nodes need to release the first tree position after it is attached to the second tree address, so in this case slots allocated for the new clusters need to be increased and slots allocated for the old clusters need to be decreased. A new algorithm for updating slots is needed for GinMAC to balance allocated slots for nodes according to the different attachments. A new algorithm has been designed to update channel allocation according to new movements and changes in the topology of the network.

*2) Move Detection in GinMAC:* There are some cases when nodes can move without being detected. For instance, clusters may be unaware of leaving mobile nodes and then will keep space in the channel for that particular node. This will consume more energy and reduce the reliability of the network. There may be cases when clusters are not available for attachment any more without letting mobile nodes know. So an additional two control messages for this new mobility module for the proposed MAC protocol have been used, which are denoted by *KEEPALIVE* and *NODEALIVE*. The *KEEPALIVE* control message is used by clusters to let its currently attached mobile nodes know that this cluster is still available and *NODEALIVE* message is used by mobile nodes to let their attached clusters know that they are still available for attachment. Mobile nodes wait for a specific interval to receive messages from the attached clusters, if they do not receive anything during that interval, a *NODEALIVE* message needs to be sent, to let a cluster know that they still want to use that cluster. If no reply is received then mobile nodes need to search for a new address to make a new attachment.

## V. A Proposed Healthcare System

Because of the fast growing numbers of people aged over 80 years old, the cost of medical care is increasing day by day. Recent advances in technology have led to the development of small, intelligent, wearable sensors capable of remotely performing critical health monitoring tasks, and then transmitting the patient's data back to health care centres over the wireless medium. Such health monitoring platforms aim to continuously monitor mobile patients needing permanent surveillance. However, to set up such platforms several issues along the communication chain need to be resolved [27].

The healthcare field is always looking for more efficient ways to provide patients with the best and most comfortable care possible. Providing proper monitoring can be expensive for their family and may force them to move from their homes because living alone will be too much of a risk of their health. It has been assumed, such as in [22], that a WSN could be used to monitor and treat patients remotely, based on data collecting from the body of the patients.

One way to approach this task is to use an application to monitor the health of patients that allow caregiver or relatives to keep watch on the patients health status with much lower cost and without forcing them to move their patients into a unfamiliar environments such as hospitals. Furthermore, these applications can be helpful to the elderly people who suffer from poor memory problems by providing them with advanced features such as helping them to take medicine, locating important objects in their homes and so on [28].

In this paper, an application based on the prototype given in [22] has been used to monitor the healthcare of the patients remotely in their homes where mobility and reliability are the biggest issues. There is a large amount of data to be managed in the proposed application, therefore, an efficient MAC protocol needs to be designed in order to provide the required performance by the proposed application.

Based on the above criteria, the proposed MAC protocol and mobility module given in [1] is used to provide the required performance for this healthcare application. Some simulations have been performed to evaluate the performance of the proposed MAC protocol. Energy saving, delay, reliability and mobility are considered as the most important QoS parameters in this application.

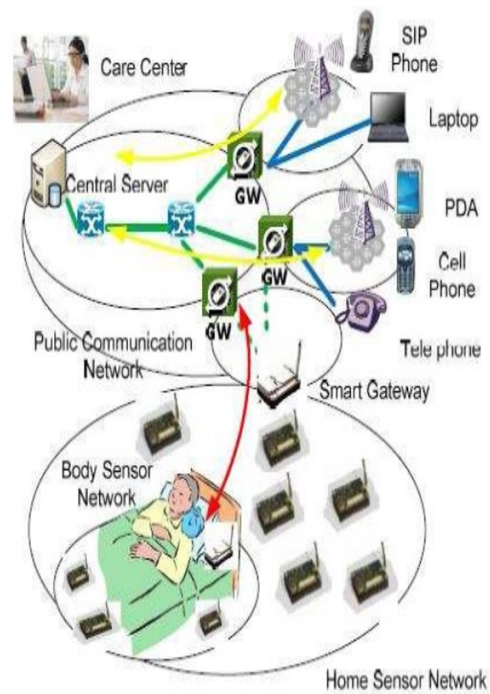


Fig. 2. Structure of the proposed Healthcare Application [22].

### A. Structure of the Proposed Application

The proposed healthcare system consists of four different parts as elaborated in [22] and shown in Figure 2. The first part is the home monitoring part where sensor nodes are probed to get multiple sets of data or behaviours, activities, health status using a Body Sensor Network (BSN), and living environment information via a Home Sensor Network (HSN). The HSN is distributed in living room, bedroom, kitchen, bathroom and corridor, to collect the required data. BSN and HSN sensors need to be attached to the body of the patients and to the environment that these patients are living in, without effecting their daily activities.

The second part is the decision part, which is the most important function in the proposed application, because the performance of the whole application depends of the decision made by this part. This part depends on the data received at the BS using both BSN and HSN. The required medical decisions need to be given depending on the data collecting from home, data from body of the patients and the previous status. Hence, the BS is responsible for collecting data from both the HSN and BSN and forwarding to the Health Centre (HC) or caregivers (doctors and relatives). Therefore, the BS needs to be smart enough to deal with data collecting from different parts of the network and to send to the medical centre, which will take the required decisions.

The third part involves care-givers, including doctors or nurses in the hospital and possibly relatives. These are responsible for dealing with the medical report messages (normal or alarm messages), that are sent to them. In the proposed application there should be the possibility for relatives to check the elder's current health status through online web pages using some sort of authentication techniques.

The fourth part is Public Communication Network (PCN) including Internet, GSM/GPRS, Ethernet, and WI-FI. PCN delivers generated messages from BS to care givers to do the required operations.

### B. WSN in the Healthcare System

The first part of the proposed healthcare system using WSNs is deployed in a home to monitor and collect data from the home and body of the patients. Each patient is monitored by a WSN divided into two sub networks, which are a BSN and a HSN. A Base Station receives data from both BSN and HSN and then gives commands to the corresponding network.

*1) Design of Body Sensor Networks (BSNs) for the proposed Healthcare Application:* Sensors for each BSN need to be deployed according to the physical diseases that the system is aimed at monitoring, for example heart rate sensors. More about physical processes and their issues can be found in Section V-D. In the proposed healthcare application only one physical medical parameter is considered for monitoring, which is body temperature. So, the BSN consists of one sensor attached to the body of the patient, data that represents temperature needs to be collected from this sensor and then combined with the sensors in the environment that these patients are living in, such as kitchen, living rooms and so on, and finally sent back to the BS, to take any required medical decisions.

If the proposed application needs to be used for more than one disease, then the BSN needs to be modified to sense data from all parts of the body and send back to a sink. In this Body Area Network (BAN), with several nodes, each node deals with one disease. The biggest challenges in this case is how to combine the BAN with the wider WSN and to combine this with data from the environments that these patients are living in.

In order to provide a comfortable system that in which does not effect the patients daily activities, there will be a lot of challenges, which need to be considered, such as size of sensors that need to be attached on the body of the patients. Each sensor needs to be as small as possible so that it can easily be attached to the body of the patients without affecting their daily activities, whilst still providing the required quality of service and performance.

*2) Design of Home Sensor Networks for the Proposed Healthcare Application:* HSNs in the WSNs for each patient needs to be designed to monitor the environment that a patient is living in. In this case, each room will have a number of sensors to measure the data needs to be collected and must cooperate with BSNs when the patient is in that room. The collected data then needs to be forwarded to the BS to take the required decisions. An efficient mobility module needs to be designed to provide the required connection between BSNs and HSNs when patients are moving from one room to another.

*3) Design of Base Station for the Proposed Healthcare Application:* As mentioned before, data from each patient needs to be collected and forwarded to the BS before transferring to the caregivers. Hence, in the proposed application, the BS becomes the core of the healthcare system. Thus, the proposed healthcare application needs a smart BS to deal with data collection from patients, for instance dealing with patient's activities, their behaviours, dealing with the required reports, such as normal and emergency alarms and so on.

In this application, each patient needs to be registered under at least one doctor in the medical centre so that all reports related to this patient can be forwarded to his or her caregivers. In addition, each patient needs to have at least one other contact in case there is an emergency. Therefore, a BS needs to include a data base to store information about all patients in the system including their close relatives and doctors such as names, addresses, phone numbers and so on.

Regular (not emergency) reports about the health status of patients need to be sent to their relatives over time. One way for providing reports for patients to their relatives is using personal web pages for each patient subject to some required authentication process. Two types of reports are provided in the proposed application; regular and healthcare reports. Regular reports record the health status for each patient over time during the application, while health reports show what medical operations and other necessary care needs to be carried out by relatives or doctors within a given time frame.

### *C. Data Communication in the Proposed Healthcare Application*

Based on the required criteria for the proposed healthcare application given in this paper, a GinMAC implementation given in [1] has been used to provide the required performance such as energy saving, delay, reliability and mobility. Some simulation results and conclusions will be given about GinMAC for the proposed healthcare system to demonstrate that GinMAC is a suitable MAC to be used for this application.

### *D. Designing Physical Process for the Proposed Healthcare Application*

Nodes in the simulated system can be fed by the physical process being monitored using three different cases, the first case is feeding nodes with static data. The second case is feeding nodes with different data based on the different sources, where each source can change in time and space. The third case is using a trace file, where nodes are assigned from the trace file. The simulation parameters used in Castalia determines the physical process at a certain time using the equation given in [29].

## VI. SIMULATING GINMAC FOR THE PROPOSED HEALTHCARE APPLICATION

The GinMAC protocol is compared with Time out MAC (TMAC) [30] in terms of performing the required performance for the proposed application. Reliability is considered to be the most important factor, which needs to be guaranteed for this application, but energy consumption, delay and mobility also are measured. A simple scenario, where the number of nodes is low, has been simulated using GinMAC, including the proposed mobility module with different parameters. More details about the simulation parameters and scenarios are given below.

### *A. Simulation Scenarios and Parameters*

Castalia has been used in this work, because of its capabilities for simulating protocols for WSNs based on the real data, as shown in [29]. Both MAC protocols were simulated according to the application requirements given in the following sections, using different sensing intervals. We define sensing interval by Ii = one packets per *i* second, so as it can be seen from the graphs in our simulation results that I1 means nodes sense environment and send data using one packet per second, I2 means nodes sense and send data using one packet per 2 seconds and so on. More details about the topology of the deployed WSN in the proposed healthcare application, MAC protocols and other parameters can be found in Table I.

### *B. Simulation Application and Measurements*

A simple scenario for the proposed healthcare application where all nodes send data towards a sink using different sensing intervals is used.

*1)* ***Reliability****:* Reliability is considered to be the percentage of packets successfully delivered from source nodes to the sink.

TABLE I
SIMULATION PARAMETERS.

| Paremeter | Value |
|---|---|
| MAC Protocols | GinMAC and TMAC |
| Network Dimensions(in meters) | 90 X 90 |
| Distance Between pair of nodes | 25 meters |
| Simulation Duration | 10 minutes |
| Measurement Metrics | Life time, delay and reliability |
| Number of Nodes | 13 |
| Sensing Intervals (packet per second(s)) | 1,2,5,10 |
| mobility speed(meters in seconds) | 5 |
| mobility interval(in minutes) | 1 |
| Advertisement interval (in seconds) | 15 |
| MaxLatency (in seconds) | 10 |
| MaxColumns | 6 |
| Initial Energy(in Joules) | 18720 |
| Real Radio | CC2420 |

2) ***Energy Saving and Lifetime**:* The lifetime of the network is the maximum days that a WSN can survive, whilst spending energy at a given rate. Let total consumed energy by each node be denoted by $C$ joules, initial energy by $E$ joules and current simulation time by $T$ seconds, then the lifetime of given MAC protocols for each node in the network has been calculated as follow:

$$LifeTime(n)(indays) = ((E/C) * T)/86400 \qquad (1)$$

where *86400* is number of seconds in each day and (E/T) is an average of consumed energy in a second by node n. In this way, the life time of the entire network is assumed to be an average of the lifetime for all nodes in the network. It has been assumed that nodes in the proposed healthcare application can be recharged every week.

3) ***Delay Calculation**:* Delay is defined as the difference between the time when each packet is sent from its source node to the time when the same packet is received by its final destination. Delay in real-time applications needs to be measured to ensure that all data is delivered within a bounded delay, i.e., each packet that is delivered after this delay is considered to be lost and will be ignored. All data needs to be collected from the source nodes and then delivered to the sink within a minimum delay.

### C. Simulation for Static and Mobility Scenarios

GinMAC and TMAC have been simulated with different sensing intervals as shown in each graph. The WSN topology and the results graphs from running simulation for both static and mobility scenarios are shown below.

## VII. SIMULATION RESULTS AND CONCLUSION

Simulation results and discussion for both static and mobility scenarios using GinMAC and TMAC including the proposed mobility module are described below.

*1) Packets Delivery and Reliability:* It is shown in Figure 4 that GinMAC can offer the applications requirements in term of reliability (as defined in Section VI) using various sensing intervals. GinMAC delivers more than 0.99 of packets

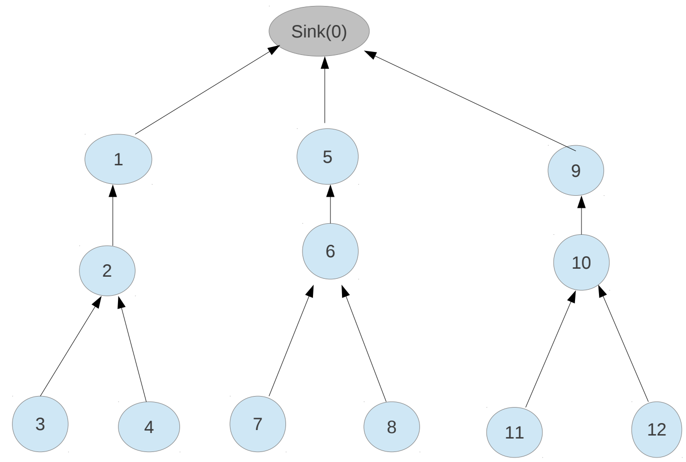


Fig. 3. Topology of the WSN in our simulation.

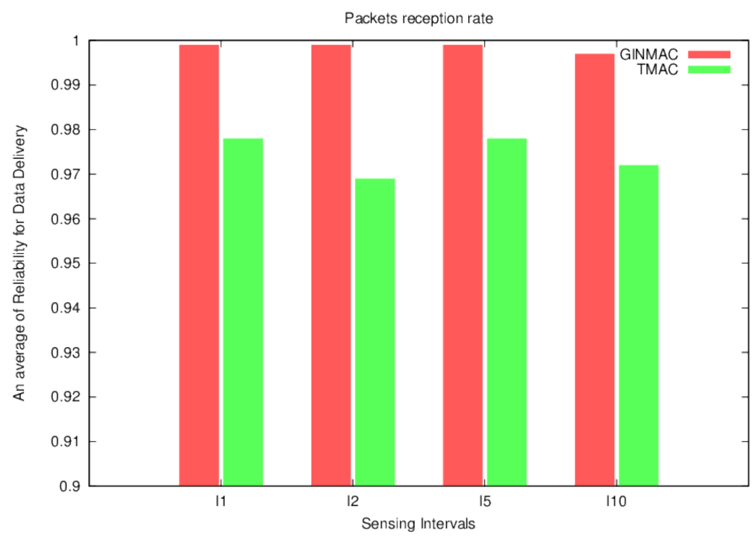


Fig. 4. Performances in term of Reliability using TMAC and GinMAC for Static scenario using different sensing intervals, see Section VI-A.

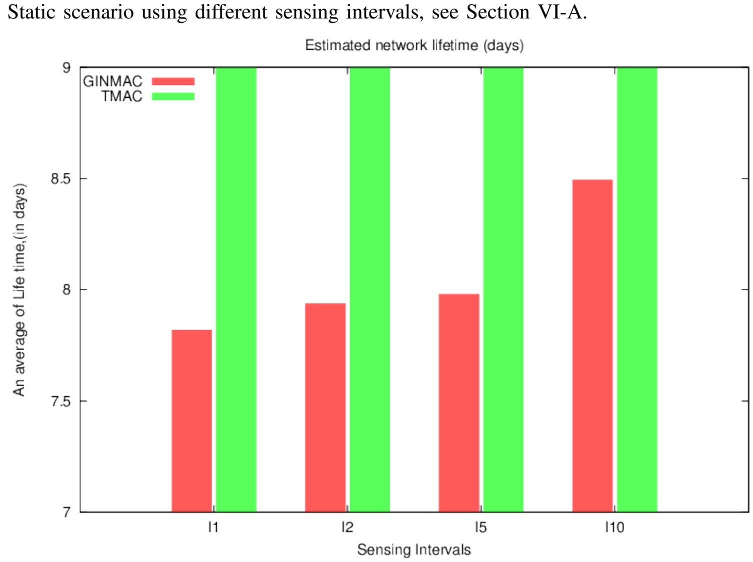


Fig. 5. Performances in term of life time of the nodes in networks using GinMAC and TMAC for Static scenario using different sensing intervals, see Section VI-A.

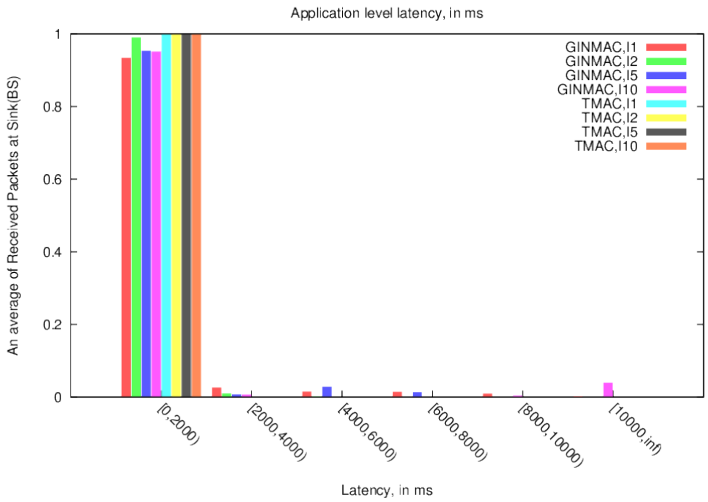


Fig. 6. Latency for delivered packets using TMAC and GinMAC for Static scenario using different sensing intervals, see Section VI-A.

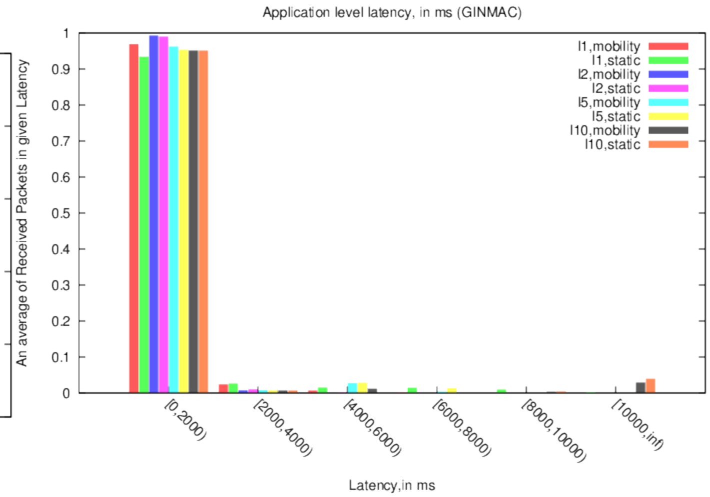


Fig. 9. Latency for delivered packets using both mobility and static scenarios for GinMAC using different sensing intervals, see Section VI-A.

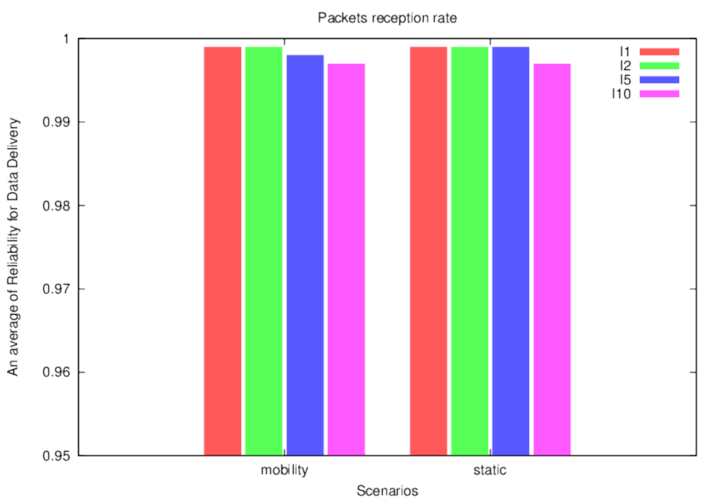


Fig. 7. Performances in term of Reliability using both mobility and static scenarios for GinMAC using different sensing intervals, see Section VI-A.

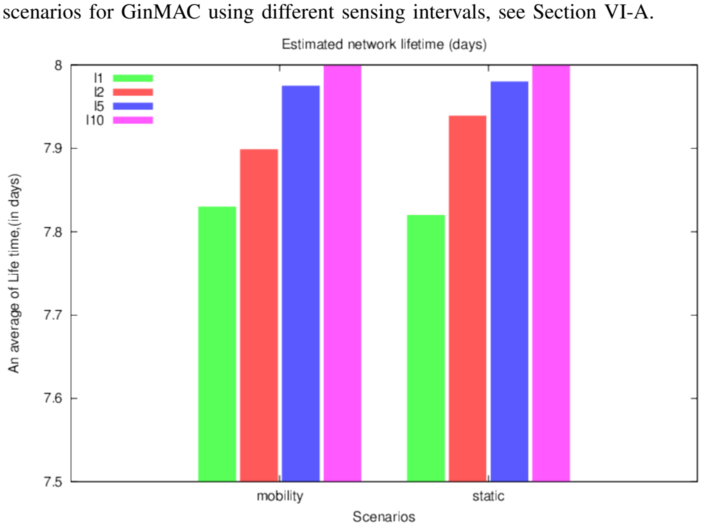


Fig. 8. Life time of the nodes in the network using both mobility and static scenarios for GinMAC using different sensing intervals, see Section VI-A.

from source nodes to a sink at given sensing intervals. This performance is due to the fact that GinMAC implements static TDMA schedules to allocate the required slots for nodes in the network and based on this, collision is reduced and reliability for delivered data is optimized. It can be said that GinMAC can be used for the proposed applications when the reliability is the biggest issue. However, TMAC cannot offer a reliability of more than 0.97 in both high and low sensing intervals using the same parameters.

GinMAC cannot offer reliability of more than 0.99 for sensing intervals more than 1 packets per second and if it is needed to increase this reliability for such sensing intervals, the number of slots for nodes in the static topology may be increased. But, GinMAC performs better than TMAC in both high and low sensing intervals as shown in the Figure 4.

2) *Energy Saving and Lifetime:* Figure 5 shows the average life time of the nodes in the network using GinMAC and TMAC using different sensing intervals. It can be seen that GinMAC cannot perform better than TMAC in terms of energy saving and life time of the entire network in all given sensing intervals, however, its performance is enough to be used in the proposed application. This is expected to be so, because of the adaptive related techniques for TMAC, which let nodes be active only when they have data to sent or received. GinMAC lets nodes be active even when they do not have data and hence consumes more energy. A WSN using GinMAC can survive more than 7 days at low sensing intervals and around 8 days at high sensing intervals as shown in Figure 5. This implies that GinMAC can be used for the proposed application when energy needs to be considered using a low number of nodes and high sensing intervals.

3) *Delay for Data Delivery:* Delay for delivered data using the proposed protocols in the proposed application is measured using *MaxLatency* and *MaxColumns* parameters. The *MaxLatency* parameter defines the bounded latency that all packets need to be delivered, which represents the threshold

for latency in the proposed applications. The *MaxColumns* parameter defines the number of columns to be used for measuring the latency for given MAC protocols. Initial values for these parameters are given in Table I, different values can be selected based on the requirement of the proposed application. Any delivered packets after the last column are considered to be lost and may be discarded. GinMAC does not perform better than TMAC in term of latency as shown in the Figure 6, however, this performance is good enough to be used for the proposed applications.

According to the results from Figure 6, most of the packets (which is about more than 0.98 of received packets) are received within the first 5 seconds at high sensing intervals, and the rest of packets are received within 10 seconds. Based on this and latency related parameters given in Table I, GinMAC delivers all packets within the required latency threshold value (*MaxLatency*). The reason behind this performance is that GinMAC implements static routes for delivering data based on static TDMA schedules between nodes and a sink and then delay for delivered data is reduced.

### A. Results from the Proposed Mobility Scenario

The Mobility module for GinMAC considers the RSSI, remaining energy and short distance to select a better attachment. Based on this and as shown in Figures 7 and 8 show that GinMAC offers nearly the same reliability and lifetime for both static and mobility scenarios. However, mobile nodes consume a bit more energy than the static nodes as shown in the same figures, this is due to an extra overhead from the control messages from mobile nodes used by the proposed mobility module. Figure 9 shows that latency is the same as in the static topology and the required delay performance is unaffected using the mobility module. This implies that the proposed mobility module provides the good connectivity between nodes compared to the static scenario

### B. Final Results

To conclude above results, reliability and energy saving are the most important performance criteria, which need to be guaranteed in the proposed healthcare application given in this paper, GinMAC achieves a very good performance in term of both reliability and energy saving using both mobile and static applications as shown above. This concludes that GinMAC can be used for the proposed application when the number of nodes is low.

## VIII. Conclusion

An implementation of GinMAC including a proposed mobility module for a healthcare application where data needs to be collected from the body of patients and sent to a medical centre has been described in this paper. It has been shown that GinMAC can be used for the target application where the number of nodes is low. A mobility module has been designed and simulated for GinMAC for the proposed application. The results from the mobility module have also shown that this GinMAC implementation will give the same performance in both mobile and static scenarios. GinMAC assumes that all non mobile nodes have static routes toward their parents in advance and these routes cannot be changed. Based on this, GinMAC cannot provide the required routing for the proposed application when number of nodes is high or some nodes have died. Therefore, efficient routing protocols will also need to be designed to cooperate with GinMAC in order to provide the required routing and extend the life time of the network for the proposed application.

## Acknowledgement

The authors would like to thank Mr James Brown from the University of Lancaster in UK, for his help for providing the basic ideas about the GinMAC and its specification. The authors would also like to thanks Dr Athanssions Boulis for information about Castalia simulator which helped a lot.

## References

[1] M. Atto and C. Guy, “Wireless sensor networks: MAC protocols and mobility management module for real-time applications,” in *The Ninth International Conference on Wireless and Mobile Communications (ICWMC 2013)*, Nice,France, July 2013, pp. 1 – 6.

[2] P. Suriyachai, U. Roedig, and A. Scott, “A survey of mac protocols for mission-critical applications in wireless sensor networks,” *Communications Surveys Tutorials, IEEE*, vol. 14, no. 2, pp. 240 – 264, 2012.

[3] X.-S. Yi, P.-J. Jiang, X.-W. Wang, and S.-C. Zhang, “Survey of energy-saving protocols in wireless sensor networks,” in *First International Conference on Robot, Vision and Signal Processing (RVSP), 2011*, Nov. 2011, pp. 208 –211.

[4] M. Atto and C. G. Guy, “Wireless sensor networks: MAC protocols and real time applications,” in *The 13th Annual Post Graduate Symposium on the Convergence of Telecommunications, Networking and Broadcasting (PGNet2012)*, Liverpool, UK, United Kingdom, June 2012, pp. 1 – 6.

[5] J. Lotf, M. Hosseinzadeh, and R. Alguliev, “Hierarchical routing in wireless sensor networks: a survey,” in *2nd International Conference on Computer Engineering and Technology (ICCET), 2010*, vol. 3, 2010, pp. V3–650–V3–654.

[6] J. Al-Karaki and A. Kamal, “Routing techniques in wireless sensor networks: a survey,” *Wireless Communications, IEEE*, vol. 11, no. 6, pp. 6 – 28, Dec. 2004.

[7] W. Ye, J. Heidemann, and D. Estrin, “Medium access control with coordinated adaptive sleeping for wireless sensor networks,” *IEEE/ACM Transactions on Networking*, vol. 12, no. 3, pp. 493 – 506, June 2004.

[8] P. Lin, C. Qiao, and X. Wang, “Medium access control with a dynamic duty cycle for sensor networks,” in *Wireless Communications and Networking Conference, 2004. WCNC. 2004 IEEE*, vol. 3, March 2004, pp. 1534 – 1539 Vol.3.

[9] X. Zhuang, Y. Yang, and W. Ding, “A tdma-based protocol and implementation for avoiding inter-cluster interference of wireless sensor network,” in *IEEE International Conference on Industrial Technology (ICIT)*, 2009, pp. 1–6.

[10] M. Thoppian, S. Venkatesan, and R. Prakash, “Csma-based mac protocol for cognitive radio networks,” in *IEEE International Symposium on a World of Wireless, Mobile and Multimedia Networks (WoWMoM)*, 2007, pp. 1–8.

[11] C. Antonopoulos, A. Prayati, F. Kerasiotis, and G. Papadopoulos, “Csma-mac performance evaluation for wsn applications,” in *Third International Conference on Sensor Technologies and Applications, 2009. SENSORCOMM ’09.*, 2009, pp. 13–18.

[12] S. Pal, D. Bhattacharyya, G. Tomar, and T. Kim, “Wireless sensor networks and its routing protocols: A comparative study,” in *International Conference on Computational Intelligence and Communication Networks (CICN)*, Nov. 2010, pp. 314 –319.

[13] G. Lu, B. Krishnamachari, and C. Raghavendra, “An adaptive energy-efficient and low-latency mac for data gathering in wireless sensor networks,” in *18th International in Parallel and Distributed Processing Symposium, 2004.*, 2004, pp. 224–232.

[14] S. Du, A. Saha, and D. Johnson, “Rmac: A routing-enhanced duty-cycle mac protocol for wireless sensor networks,” in *INFOCOM 2007. 26th IEEE International Conference on Computer Communications. IEEE*, 2007, pp. 1478 –1486.

[15] N. Vasanthi and S. Annadurai, “Energy efficient sleep schedule for achieving minimum latency in query based sensor networks,” in *IEEE International Conference on Sensor Networks, Ubiquitous, and Trustworthy Computing, 2006.*, vol. 2, June 2006, pp. 214 –219.

[16] S. Ergen and P. Varaiya, “Pedamacs: power efficient and delay aware medium access protocol for sensor networks,” *IEEE Transactions on Mobile Computing*, vol. 5, no. 7, July 2006.

[17] V. Jain, R. Biswas, and D. P. Agrawal, “Energy-efficient and reliable medium access in sensor networks,” in *IEEE International Symposium on a World of Wireless, Mobile and Multimedia Networks, 2007. WoWMoM 2007.*, June 2007, pp. 1 – 8.

[18] J. Lotf and S. Ghazani, “Overview on routing protocols in wireless sensor networks,” in *2nd International Conference on Computer Engineering and Technology (ICCET), 2010*, vol. 3, April 2010, pp. 610 – 614.

[19] P. Suriyachai, J. Brown, and U. Roedig, “Time-critical data delivery in wireless sensor networks,” in *6th IEEE International Conference on Distributed Computing in Sensor Systems (DCOSS 10)*. IEEE, June 2010, pp. 216–229.

[20] T. O’Donovan, J. Brown, U. Roedig, C. Sreenan, J. do O, A. Dunkels, A. Klein, J. Sa Silva, V. Vassiliou, and L. Wolf, “Ginseng: Performance control in wireless sensor networks,” in *7th Annual IEEE Communications Society Conference on Sensor Mesh and Ad Hoc Communications and Networks (SECON)*, June 2010, pp. 1 –3.

[21] W.-B. Pottner, H. Seidel, J. Brown, U. Roedig, and L. Wolf, “Constructing schedules for time-critical data delivery in wireless sensor networks,” *ACM Transactions on Sensor Networks (TOSN), due to August 2014*, vol. 10, no. 3, August 2014.

[22] H. Huo, Y. Xu, H. Yan, S. Mubeen, and H. Zhang, “An elderly health care system using wireless sensor networks at home,” in *Third International Conference on Sensor Technologies and Applications (SENSORCOMM)*, June 2009, pp. 158 –163.

[23] J. Brown and U. Roedig, “Demo abstract: Ginlite - a mac protocol for real-time sensor networks,” in *In Proceedings of 9th European Conference on Wireless Sensor Networks (EWSN’12)*, Feb 2012.

[24] Z. Zinonos, R. Silva, V. Vassiliou, and J. Silva, “Mobility solutions for wireless sensor and actuator networks with performance guarantees,” in *18th International Conference on Telecommunications (ICT)*, May 2011, pp. 406 –411.

[25] Z. Zinonos and V. Vassiliou, “Inter-mobility support in controlled 6lowpan networks,” in *IEEE Globecom 2010 Workshop on Ubiquitous Computing and Networks (UbiCoNet2010)*, Miami, Florida, USA, Dec 2010, pp. 1718–1723.

[26] R. Silva, Z. Zinonos, J. Sa Silva, and V. Vassiliou, “Mobility in wsns for critical applications,” in *IEEE Symposium on Computers and Communications (ISCC)*, July 2011, pp. 451 –456.

[27] Y. Zatout, “Using wireless technologies for healthcare monitoring at home: A survey,” in *IEEE 14th International Conference on e-Health Networking, Applications and Services (Healthcom)*, 2012, pp. 383–386.

[28] S. Khan, A. Khan, P. Nabil, and A. Alrajeh, *Wireless Sensor Networks: Current, Status and Future Trends*. France: CRC Press, Taylor and France Group, November 2012.

[29] A. Boulis, “Castalia simulator: A simulator for wireless sensor networks and body area networks,” in *http://castalia.npc.nicta.com.au, NICTA, [retrieved: May, 2014]*, March 2011, pp. 1 – 120.

[30] Y. Tselishchev, A. Boulis, and L. Libman, “Experiences and lessons from implementing a wireless sensor network mac protocol in the castalia simulator,” in *Wireless Communications and Networking Conference (WCNC), 2010 IEEE*, April 2010, pp. 1 –6.

# Triangle Routing in Wireless Sensor Networks with Unidirectional Links Revisited - a Look at Different Scenarios

Reinhardt Karnapke and Jörg Nolte
Distributed Systems/Operating Systems Group
Brandenburg University of Technology Cottbus - Senftenberg
Cottbus, Germany
Email: {Karnapke, Jon}@informatik.tu-cottbus.de

***Abstract*—Experiments with wireless sensor networks have shown that links are often asymmetric or unidirectional. This represents a serious problem for many routing protocols, which often depend on bidirectional links. Routing protocols that can use unidirectional links often induce a high overhead. To overcome this problem we introduced Unidirectional Link Triangle Routing, a routing protocol, which uses neighborhood information, gathered actively or passively, to route around unidirectional links. In this paper, we describe Unidirectional Link Triangle Routing in further detail and present additional evaluation results from different application scenarios.**

***Keywords - Wireless Sensor Networks, Routing, Unidirectional Links***

## I. Introduction

This paper is an extended presentation of Unidirectional Link Triangle Routing (ULTR) [1], a routing protocol designed specifically to enable the usage of unidirectional links, which was first published at Sensorcomm 2013.

A unidirectional link from a node A to a node B exists, when node B can receive messages from node A, but node A cannot receive messages from node B. Even though this definition seems straightforward, there are different definitions of asymmetric and unidirectional links in literature. This is partially due to the fact that links change over time. Definitions are often based on different packet reception rates, and a difference of, e.g., more than 90% signifies a unidirectional link. In the same definition, a difference of less than 10% signifies a bidirectional link while all other links are called asymmetric. However, this is just one of the many different definitions for unidirectional, asymmetric, and bidirectional links. In others, only two classes (bidirectional and asymmetric) exist or different percent values are used.

No matter, which definition is given, there is a large number of unidirectional links present in current sensor networks as many experiments have shown (e.g., [2], [3], [4], [5]).

Existing protocols for wireless sensor networks or Mobile Ad-Hoc Networks still lack the ability to handle unidirectional links in an efficient manner. Many of those protocols deal with unidirectional links by removing their negative impact on the routing tables, while some of them use unidirectional links explicitly. Making these unidirectional links usable introduces overhead, which has to be weighted against the gain.

TABLE I
Routing tables in ULTR

| Destination | Next Hop | Link Status | Forwarder |
|---|---|---|---|
| D | A | bidirectional | none |
| E | B | incoming | C |
| F | G | outgoing | none |

The authors of [6] have evaluated some of the existing protocols and concluded that the gain in connectivity is not worth the cost. While this might have been true for their scenario and the protocols they evaluated, it is possible to have scenarios where network separation occurs when unidirectional links are eliminated. It is also possible to have protocols that induce less overhead than the ones they considered.

Even though ULTR requires neighborhood information, the overhead induced can be kept small, either by gathering information passively, or by using information that is already provided from other communication layers. ULTR has already been published in, this paper takes a closer look at implementation details and offers additional insights into the usability of ULTR in different scenarios.

This paper is structured as follows: Section II describes ULTR in detail before a closer look at the cooperation between MAC and routing is taken in Section III. Section IV describes the general methodology of the evaluation, followed by Section V with details on the simulation setup and Section VI that describes hard- and software used in the real world experiments. The three application scenarios (sense-and-send, single pairing and multiple pairings) along with the evaluation results for simulations and real experiments are presented in Sections VII to IX. We finish with a conclusion in Section X.

## II. Unidirectional Link Triangle Routing

In ULTR, neighborhood information is needed. To make a neighborhood table entry on a node A usable for ULTR, it must at least contain the ID of the neighbor (e.g., B), the status of the link to that neighbor (bidirectional, unidirectional-incoming or unidirectional-outgoing) and, if the link is unidirectional-incoming, the identity of another neighboring node (e.g., C), which can be used to forward data to the node in question (node B). Table I shows an example for all three kinds of links.

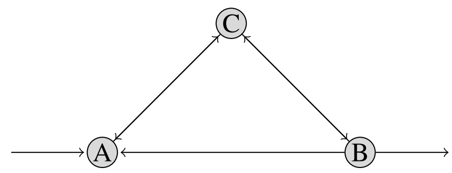


| ID, Status, Forwarder |
|---|
| B, incoming, C |
| C, bidirectional, none |

A

| ID, Status, Forwarder |
|---|
| A, outgoing, none |
| C, bidirectional, none |

B

| ID, Status, Forwarder |
|---|
| A, bidirectional, none |
| B, bidirectional, none |

C

Fig. 1. Neighbor table entries in ULTR

When a node wants to transmit a message to another node that is not included in its neighbor table or its routing table, it starts a route discovery by transmitting a route request (RREQ) message. This message is flooded through the network and creates routing entries for the source on all nodes it passes. The entries include only the next hop and the distance, resulting in a distance-vector protocol like, e.g., AODV [7].

However, the handling is different once the destination has been reached and transmits the route reply. When a node receives a message that is not flooded, i.e., a route reply (RREP) or DATA message, it checks its routing table to find out, which of its neighbors is the intended next hop just like in AODV. Unlike AODV, there is another step after that one. Once the node knows the neighbor that has been chosen to forward the message, it checks its neighbor table to see if the link to that node is *currently* a unidirectional-incoming one. If it is, and a detour of one hop is possible, the node forwards the packet first to the detour node, which, in turn, retransmits the message to the intended node. Otherwise, the message is silently discarded. Please note that broken links can be treated just like unidirectional-incoming ones.

Figure 1 shows a small part of a network and the corresponding neighborhood table entries used in this protocol: The nodes A, B and C from the example above are connected bidirectionally, with the exception of the link between nodes A and B, which is unidirectional, enabling only transmissions from B to A. The neighborhood table of node A consists of two entries, a bidirectional one for node C and a unidirectional-incoming one from node B, with node C denoted as designated forwarder. The neighborhood table of node B contains node A, which would not be possible without a two-hop neighborhood discovery protocol, as node B does not receive any messages from node A. The link is marked as unidirectional-outgoing, and thus does not need any forwarder. The second entry features node C with a bidirectional link, needing no forwarder either. Finally, the neighborhood table of node C contains nodes A and B, both marked as connected through bidirectional links and not needing any forwarders.

Due to the fact that the unidirectional link and the detour that is taken on the way back form a triangle, this protocol is called Unidirectional Link Triangle Routing.

ULTR is similar to the link layer tunneling mechanism proposed by the unidirectional link working group of the IETF [8], but does not require multiple interfaces on the nodes to communicate. Also, depending on the used neighborhood discovery protocol, it may even be able to work with triangles, which include more than one unidirectional link, which the link layer tunneling mechanism cannot handle. Moreover, ULTR works completely on the routing layer, the link layer is not involved. This is an advantage when timeouts are used, because the extra hop and thus longer delay are not hidden from the routing layer.

### A. Neighborhood Discovery

The neighborhood discovery protocol needed for ULTR can be quite simple and needs only be started on a node once it receives the first message from a neighbor, i.e., when the first route request message is flooded into the network. Once it has been started, the neighborhood discovery protocol regularly transmits a message containing the IDs of all nodes from, which this node has received messages recently and the status of its links to and from them. When a node receives such a hello message, it checks whether its ID is contained therein. If it is not, the receiving node knows that it is on the receiving side of a unidirectional link.

In other protocols, where unidirectional links are used, a lot of overhead would now be necessary to inform the upstream node (the sender of the hello message) of the unidirectional link. In this protocol, the upstream node does not need to know about its existence. The receiving node only marks the link as unidirectional-incoming in its neighbor table.

When a node A receives a hello message via the bidirectional link from node C in, which the upstream node of the unidirectional link is listed and the link to that node (from C to B) is marked as bidirectional, node A enters the sender of the hello message (node C) as a forwarding neighbor into the corresponding neighbor table entry (for node B). Please note that this would also be possible if there was a unidirectional link from C to B, but the proactive detection of this special case would probably introduce a large overhead and solve only one special case: If there is a unidirectional link from C to B and no other neighbor of A has a bidirectional link to B.

| Route Request | Route Reply | Data |
|---|---|---|
| Type = RREQ = 1 | Type = RREP = 2 | Type = DATA = 3 |
| Source Seq. Num. | Source Seq. Num. | Source Seq. Num. |
| Destination | Destination | Destination |
| Source | Source | Source |
| Hop Count | Hop Count | Next Hop |
| Current Hop | Next Hop | Forwarder |
| | Forwarder | DATA |

Fig. 2. Message types used in ULTR

When a message (RREP or DATA) is sent the reversed way, it needs to be forwarded along a one-hop-detour. This message can be used to inform the upstream node of the link, which is then entered into the upstream node's neighborhood table as unidirectional-outgoing. Please note that for the routing alone this information would not be necessary, indeed it would be easy to hide the fact that the message has taken a detour. But for the sake of timers that can be used for retries on MAC- or routing layer, it helps to know that the delay could be twice as high. In this case, the information about this special link can be acquired "for free" and could be used to solve the problem described above. The information about the unidirectional-outgoing link can also be used by the MAC layer not only for retries, but also to determine the right two-hop neighborhood of a node, which is a mandatory information for TDMA protocols.

### B. Message Types

ULTR uses the standard three message types used by most reactive routing protocols: Route Request, Route Reply and DATA. Figure 2 shows an example for each of them.

A RREQ message contains the identity and sequence number of the source that are used for duplicate detection, followed by the identity of the destination. The hop count is incremented by one on each hop as usual, and the identity of the last hop is used to build the backward route.

A Route Reply message contains sequence number and identity of the source for duplicate detection as well as the identity of the destination. For forwarding purposes the next hop and, if necessary, the forwarding node are included.

The DATA packet contains the sequence number and identity of its source as well as the identity of its destination and, of course, the application data. As the size of the data may vary, the identities of the next hop and, if suitable, the forwarding node needs to be inserted before the data for alignment reasons.

### C. Variations

ULTR relies on a neighborhood discovery protocol, which supplies information about incoming and outgoing unidirectional links. If neither the application nor the MAC protocol needs a neighborhood discovery protocol, a variation of ULTR with passive link detection may be used. But passive link detection means that sometimes a node does not know about links to its neighbors, even though they are available. Therefore, a second mode of operation is introduced: if a node does not have a link to the next hop in its neighbor table, it forwards the message nonetheless, with an additional flag telling its neighbors that any of them that do have an active link to the next-but-one hop (i.e., the siblings of the next hop) should also forward the message.

When this variation is used, some modifications of the message types are necessary (see Figure 3). Information about the last hop would have to be included in RREQ messages, in addition to the current hop. Both node IDs are stored in the routing table. A node decides, which entry to use depending on the overheard status of the link. If the next hop is assumed to be connected by a bidirectional link, the normal next hop is used. Otherwise, the message is set to alternate mode and the next-but-one hop is used. The last hop is also used for implicit link detection: If a node overhears the transmission of a message in, which it is denoted as last hop, it knows that the link between itself and the current hop denoted in the message is currently bidirectional.

A RREP message contains three node IDs instead of only two: The last hop ID and current hop ID are used to build the backward route for normal and for alternate mode just as they are used in the RREQ. The next hop ID is used for forwarding. However, the RREP also contains a flag denoting the mode of transmission, which can take on the values "normal" and "alternate". It is evaluated upon message reception to decide if a node shall forward the message or not. In normal mode it only forwards the message when it is denoted as next hop in the message, in alternate mode it also forwards the message if it has the next-but-one hop in its neighbor table.

The DATA message features the same three node IDs that are present in the RREP message. For routing purposes alone, the last hop ID would not be needed, but it is nevertheless included for link status detection. The mode flag is also present again, to enable the usage of alternate mode if the status of the next link is unknown or known to be unidirectional-incoming.

| Route Request | Route Reply | Data |
|---|---|---|
| Type = RREQ = 1 | Type = RREP = 2 | Type = DATA = 3 |
| Source Seq. Num. | Source Seq. Num. | Source Seq. Num. |
| Destination | Destination | Destination |
| Source | Source | Source |
| Hop Count | Hop Count | Last Hop |
| Last Hop | Last Hop | Current Hop |
| Current Hop | Current Hop | Next Hop |
| | Next Hop | Mode |
| | Mode | DATA |

Fig. 3. Message types in ULTR without neighborhood discovery

### D. Advantages and Disadvantages

ULTR is a complex protocol. The complexity is the price for the reduced number of data packet transmissions, as no flooding of DATA packets, not even a limited one, is used. Periodic updates of the neighborhood table ensure that the link status information it holds is always up to date, which also enables implicit local repair. Altogether this should lead to a higher delivery ratio. On the downside, the usage of hello messages also leads to more protocol overhead, as these messages can be quite large in dense networks. Therefore, the typical tradeoff between actuality and network load has to be made when setting the hello period, which makes configuring the protocol harder. On the other hand, a new option for cooperation between MAC and routing arises.

Like all routing protocols that use unidirectional links, ULTR also needs a MAC that can transmit over unidirectional links. The information about the existence of the unidirectional links probably needs to be collected to a certain extent anyway, depending on the MAC protocol used. So either this can be retrieved from the MAC without additional cost, or the MAC protocol can query the routing layer for it using an appropriate interface. More information about the cooperation options between MAC and routing is provided in Section III.

## III. Cooperation with the MAC-Layer

ULTR was designed specifically to utilize unidirectional links. This makes it imperative to use a MAC layer that can also transmit over unidirectional links. Any protocol that uses the standard "request to send" - "clear to send" mechanism is completely unsuitable, as no clear to send message will ever be received over an outgoing unidirectional link. Moreover, nodes with an outgoing unidirectional link will never know that they could be disturbing the communication between two other nodes.

There are some improvements that allow contention based protocols to work with unidirectional links, e.g., ECTS-MAC [9], [10]. Some of the MAC protocols that utilize unidirectional links route their link layer acknowledgments back to the upstream nodes. For this, the neighborhood table used by ULTR could be reused.

Plan based MAC protocols need to know the two-hop neighborhood of each node to identify the collision domain. Within this domain, the varying parameter (e.g., frequency (FDMA), code (CDMA) or slot (TDMA)) needs to be unique for each node. Therefore, a neighborhood discovery protocol is needed, which finds these two-hop neighbors. The protocol(s) used for ULTR could easily be enhanced to deliver this information. Otherwise, if the MAC protocol already has its own neighborhood discovery protocol, it only needs to make the gathered information available to the routing protocol.

The usage of such a neighborhood discovery protocol would also implicitly solve the "special case" of a unidirectional link triangle with more than one unidirectional link, enabling ULTR to make use of such links as well.

This usage of a single neighborhood discovery protocol for both MAC and routing reduces communication overhead and memory consumption by far. It also ensures that both layers work on the same data. If they would use different algorithms, different storage sizes or replacement strategies, lots of problems could result, as described, e.g., in Murphy Loves Potatoes [11].

## IV. Evaluation Methodology

For the evaluation, we chose a comparative approach: We evaluated the performance of ULTR and compared the results to those achieved by other typical routing protocols from the world of sensor networks or MANETs. The protocol most used in sensor network deployments was chosen as first competitor: A tree routing based approach with retransmissions, which is quite common in sense-and-send applications where all nodes transmit their data to the sink regularly (e.g., [4], [11], [12], [13]). As this may seem to be an unfair comparison, two protocols from the MANET area were also chosen as competitors: DSR in the version that uses unidirectional links [14] and AODVBR [15]. AODVBR does not use unidirectional links, but has an interesting way of detecting them and salvaging the data message that caused the detection. As fourth reference protocol, `Flooding` is included. While it is known that `Flooding` induces a lot of overhead, it can still deliver valuable insights. In the simulations, `Flooding` is used to determine the upper limit of messages that could reach the destination. In the real world experiments carried out for this work, the network load it generates is used to understand the performance of the MAC protocol supplied by the hardware in use.

The distance, measured in hops, is taken as weight function (minimum hop routing), but other weights, e.g., residual energy, could also be used with the same result, as all protocols would work on the same values. Routes with a lower weight replace older ones with a higher value in the routing tables.

The authors of [16] propose a combined evaluation method that uses experiments with real hardware, emulation and simulation techniques in order to speed up the deployment of new protocols. The combination of all three methods enables the developer to identify, which problems occur and shows him/her where further investigation is necessary. The routing protocols AODV, DSR and OLSR were used to evaluate the proposed approach to protocol monitoring. The authors found that latency and timing are crucial to the performance of reactive protocols like AODV and DSR, because of buffering times. The queue-ups that can result from this buffering were apparent in the experiments, but not in the emulations. In conclusion of this paper it can be said that all three methods of evaluation have their own gain for a protocol developer, if they are used correctly. For simulations, the choice of the underlying communication model is crucial. The emulation can be fed with real world connectivity data, and can be used to evaluate the implications of the network stack used on the real devices. Experiments are needed to generate this connectivity data. It is important that for all three methods exactly the same implementation of the protocol is used, and that this implementation is the one that can be used directly on the hardware, which is used in the real experiments.

Following this approach and the advice from Stojmenovic [17], the same implementation was used for both simulations and real world experiments in this evaluation.

In the next section, the methods used in the simulations are described. They enable the evaluation of the algorithms and their ability to handle unidirectional links under controlled circumstances (Section V). The general principle of the real world experiments, including the chosen locations, is described in Section VI.

The actual evaluation of the routing protocols is presented in Sections VII to IX, sorted by the application scenario in use.

## V. Simulations

All simulations were performed using the discrete event simulator OMNeT++ [18] with the MiXiM-extension [19]. We modified MiXiM to enable the simulation of unidirectional links [20]. The simulated networks consisted of four different sizes of grids: 100 nodes (10x10), 400 nodes (20x20), 900 nodes (30x30) and 1,600 nodes (40x40). A grid alignment was chosen to represent applications that need area coverage, where each node is equipped with sensors that have a range of one distance unit. But, as will be seen below, the exact placement of the nodes is not important, because connectivity is determined using a connectivity matrix (Section V-A). The different numbers of nodes represent network sizes ranging from small to huge networks, and thus increase the number of hops needed to communicate from one end of the network to the other. This determines the route length, which has a tremendous impact on the performance of all routing protocols.

All simulations are restricted to the usage of a "perfect behavior" MAC. While it is of course true that the choice of medium access control protocol can have a strong influence on the performance of the routing layer, the goal of the simulations is the evaluation of the ability of the routing protocols to work in the presence of unidirectional links, not of their interaction with the MAC layer. Also, many of the effects of a MAC layer, e.g., the available neighbors for each node, would be the same for all evaluated routing protocols. The effects could only differ between protocols, when they are depending on the generated network load, as different protocols transmit different types of messages with different sizes and in different frequencies. But all of these are highly dependent on the application, and it is not possible to evaluate all possible application scenarios.

As simulation results are never 100% accurate, real world experiments have been conducted, too. Details about the methods of evaluation used for the real world experiments are shown in Section VI. This section follows Stoijmenovic's advice [17], and uses a simple model in order to keep side influences small and results interpretable.

### A. Connectivity between Nodes

To simulate a certain connectivity between nodes, thousands of connectivity matrices were generated before running the simulations. The same generated matrices were used for all protocols. The large number of matrices is necessary to simulate the constantly changing nature of wireless links. As the largest networks, consisting of 1,600 nodes, needed to be simulated for the longest time, they also needed the highest number of connectivity matrices: For a single simulation 17,761 connectivity matrices were needed.

In each of these matrices, a (directed) link from node A to node B exists with a probability of $\alpha/d^6$ where $d$ is the distance between node A and node B. The inverse link, from node B to node A exists with the same probability. Therefore, the link is bidirectional with a probability of $(\alpha/d^6) \times (\alpha/d^6)$, unidirectional (in any one direction) with $\alpha/d^6 \times (1-(\alpha/d^6))$ and non existing with $(1-(\alpha/d^6))^2$. The quotient ($d^6$) reflects the dampening induced by the distance between nodes while $\alpha$ represents the probability that a link between geographically adjacent nodes exists.

Nodes were arranged on a regular grid to reflect application scenarios that need area coverage, e.g., vehicle tracking. As all nodes were arranged on a grid, nodes that are directly above, below, right or left of a node are called direct neighbors and their distance was defined as 1. $\alpha$ was varied between 0.9, 0.95 and 1, and for each value of $\alpha$ ten sets of matrices with different seeds for the random number generator were generated, leading to 30 sets of matrices per network size, and a total of 996,120 connectivity matrices containing between 10,000 and 2,560,000 entries.

Please note that due to the fact that the matrices were generated randomly, there is no guarantee that there always was a path from sender to destination. Therefore, no upper limit can be calculated, but `Flooding` is used as reference protocol: The number of application messages delivered by `Flooding` is taken as 100% and the delivery ratio of all other protocols calculated accordingly.

### B. Application Settings

In each simulation, each node wanted to transmit a total of 110 messages to one or more destinations, depending on the scenario. After the initialization phase of the network, one message was transmitted every 100 milliseconds. To ensure that route discovery was finished, the logging remained inactive until all nodes had started the transmission of their fifth message. The connectivity matrices were changed every second. Please note that the absolute values of the time units are not important for the simulation, only their relation (1:10). They could also have been set to 6 seconds and one minute yielding the same results.

### C. Protocol Performance

In the simulations, logging only began once each node had started the transmission of its fifth message. Therefore, the theoretical optimum of delivered messages could be calculated, if connectivity could be guaranteed. But the connectivity matrices were generated randomly, therefore network separation could be possible. `Flooding` delivered close to the theoretical optimum, and is used as maximum for the simulations. For all simulations, the delivery ratio of a protocol is defined as the number of messages delivered by the protocol divided by the number of messages delivered by `Flooding`.

## VI. Real World Experiments

To evaluate the influence of medium access control and the properties of real hardware, all protocols were evaluated on 36 eZ430-Chronos [21] sensor nodes.

All protocols use the same sensor nodes on the same locations, meaning that node 0 used to evaluate `Flooding` is the same piece of hardware on the same location as node 0 used in the experiments evaluating ULTR and so on. Depending on the application scenario, the experiments were conducted on some or all of the locations described below. Each protocol was evaluated using a freshly charged set of batteries.

### A. Application and Logging

In the real experiments, each node wanted to transmit a message every minute. The experiments ran for one hour each, therefore 60 messages were transmitted by the application on each node. In all experiments, 36 nodes were placed in a square of six times six. Each node recorded the number of application messages it received, and all nodes recorded the number, type and size of all messages they transmitted or forwarded.

Like in the simulations, it was once again possible that nodes were disconnected from the network and suffered from network separation. Also, sometimes nodes failed due to hardware problems. Therefore, the type of messages transmitted by a node was evaluated, too. When a node only transmitted route request messages and not a single data message, it did obviously not find any route to the sink.

### B. Protocol Performance

In the real world experiments, logging began at once. Therefore, the theoretical optimum of delivered messages could be calculated, if connectivity could be guaranteed, which is never the case in real world deployments. In contrast to the simulations, `Flooding` could not be used as reference protocol because it did not always deliver the highest number of application messages. Therefore, the delivery ratio is defined as the number of application messages delivered to their destination divided by the number of application messages transmitted.

### C. Program Size

The size of the programs deployed on the eZ430-Chronos is shown in Table II. Please note that the values were measured for scenario 1 (sense-and-send, Section VII), but differ only marginally for the other scenarios as the main components (system and routing protocol) are always the same. Only the application differs from scenario to scenario, but its influence on the program size is marginal.

TABLE II
Total size of the deployed systems for different routing protocols in Byte

| protocol | text | data | bss | dec |
|---|---|---|---|---|
| AODVBR | 14,590 | 0 | 2,260 | 16,850 |
| DSR | 17,760 | 0 | 3,586 | 21,346 |
| `Flooding` | 12,444 | 0 | 1,644 | 14,088 |
| `Tree Routing` | 13,234 | 0 | 1,990 | 15,224 |
| ULTR | 14,550 | 0 | 2,066 | 16,616 |
| System without routing | 11,918 | 0 | 1,418 | 13,336 |
| Basic System | 8612 | 0 | 994 | 9,606 |

It can be seen on the table that DSR has by far the largest memory footprint, concerning both flash (”text”) and RAM (”bss”). The lowest footprint can be seen on `Flooding`. It needs only about 500 Bytes flash and 200 Bytes RAM more compared to the system without routing, most of, which is needed for the duplicate suppression.

The basic system, including only the operating system REFLEX [22], [23] without any scenario specific parts (no routing protocol, no application) is also shown for comparison. It needs 8612 Bytes of flash and 994 Bytes of RAM. Most of the RAM consumption is due to the 10 network buffers with 64 Bytes each.

(a) affixed to poles (b) placed on the lawn (c) on a stone pavement

Fig. 4. A modified eZ430-Chronos sensor node

DSR did not fit on the micro controllers with the settings used in the simulations, therefore some of them (e.g., the number of messages that can be stored) had to be reduced to make it fit. As DSR has the largest memory footprint, all other protocols had no problem fitting on the micro controller when using the same settings.

### D. Experiment Locations

Four different locations were used for the real world experiments:

- On a Desk
- Affixed to Poles
- Placed directly onto a lawn
- Placed directly onto stones

*a) Desk Experiments:* This deployment is a single hop layout, where each node is able to receive messages from each other node. The nodes lay directly next to each other. An old set of batteries was used without re-charging them, because range did not really matter in these experiments. They were used to validate the correct operation of the protocols.

*b) Poles:* For the pole experiments, small poles were deployed on the lawn in front of the main building of our university, with about one meter distance between each of them. Then, the sensor nodes were affixed to them using cable straps, at a height of about 20 cm (Figure 4(a)). The pole placement was usually used at 8am.

*c) Lawn:* After the pole experiments were finished and evaluated, the nodes were reset and placed on the ground directly next to the poles as shown on Figure 4(b). The resets were done by disconnecting the batteries and reconnecting them directly afterwards. The same set of batteries as before was used on each node without charging. When using all four locations, the lawn experiments were started at about 10 AM.

*d) Stones:* After the lawn experiments, the nodes were disconnected, and poles as well as nodes and batteries collected. The experiments on the stones were always started at about 1 PM, using the same set of 72 AA batteries used in the morning without re-charging, but the pairing of batteries and nodes might have changed, i.e., the batteries that were connected to node 4 in the pole and lawn experiments might be connected, e.g., to node 27 in the stone experiments. These experiments were conducted on the stone pavement on our campus (Figure 4(c)).

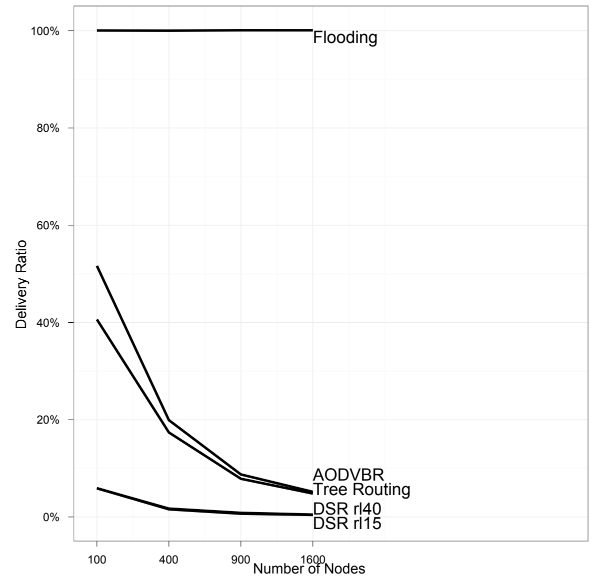


Fig. 5. Delivery ratio of AODVBR, `Tree Routing` and two DSR versions, first scenario

## VII. Application Scenario 1: Sense and Send

The application implemented for scenario 1 represents a sense-and-send behavior that is often found in sensor networks: All nodes within the network wanted to transmit all their messages to the same destination.

### A. Simulation Results

The destination (sink) was fixed within a single simulation, but multiple simulations with different destinations were evaluated. For the network containing 100 nodes, all nodes in the upper left quadrant were chosen (25 destinations), for the network with 400 nodes this quadrant contained 100 nodes. Evaluating only one quadrant was chosen because of the symmetry of the network, and because of run time limits (a single simulation of `Flooding` in a network consisting of 1,600 nodes took about 27 hours to complete). For the networks containing 900 and 1,600 nodes a whole quadrant would have meant too many simulations, therefore only the 20 most interesting nodes (the corners and the middle of each quadrant) were chosen (20 destinations).

As 30 different connectivity change lists were used for each destination in each network size, 4,950 simulations with run times between 5 minutes and more than a day were necessary for each protocol.

*1) Related Work Protocols:* The number of data messages received at the sink for the reference protocols is shown in Figure 5.

It can be seen that none of the other protocols gets anywhere near the performance of `Flooding`, with DSR performing worst. Even in the smallest network consisting of 10 times 10 nodes, both DSR versions (max route length 15 or 40) deliver only about 10% of the messages.

The other two protocols perform better in the small network, but show a steep decline in delivery ratio for the larger

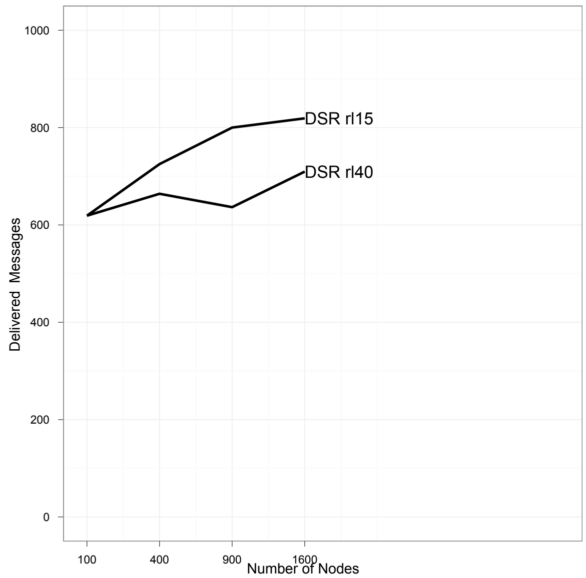


Fig. 6. Total number of Data messages at the sink, two DSR versions, first scenario

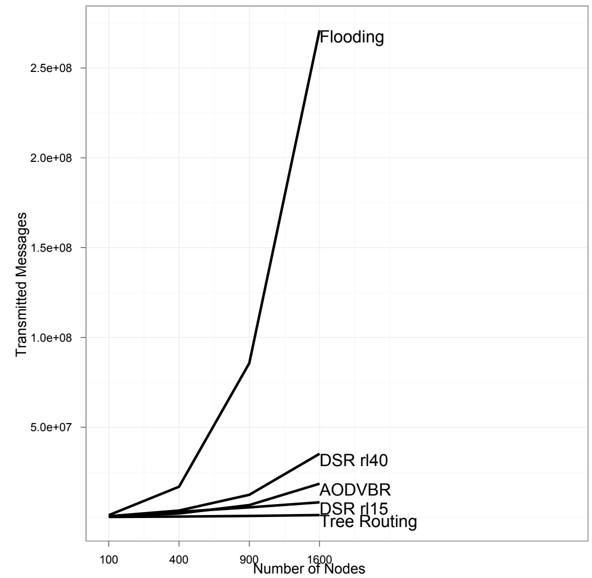


Fig. 7. Number of transmitted messages, `Flooding`, AODVBR, `Tree Routing` and two DSR versions, first scenario

networks. This decline is due to the fact that even though the number of nodes in the network and, therefore, the maximum possible number of delivered messages increases drastically, the total number of delivered messages increases only marginally.

The absolute number of messages received at the sink for the two versions of DSR is shown in Figure 6. It can be seen that DSR delivers a nearly constant number of messages, independent of the network size. While the number of nodes and thus the number of application messages handed to the routing protocol is multiplied by 16, the number of application messages that arrive at the sink increases only marginally. This is due to the fact that DSR suffers heavily from link changes and longer routes change more often. Another interesting fact about DSR is that the version with route length limited to 15 delivers more messages than the one, which allowed route lengths up to 40 hops for all larger networks. The reason for this seemingly strange behavior can be seen when investigating nodes that are about 15 to 17 hops from the sink. Please remember that the hop distance changes as links change. Therefore, nodes might have a distance of more than 15 during their first route discovery, and less during a later one. When only short routes are allowed and no route is found, the messages are stored until a later route discovery finds a route containing 15 hops at max. Then, all stored messages are transmitted at once. These messages have a higher chance of being delivered, as the route information is current and the path is shorter. When using the 40 hop limit, these nodes choose the first, long path that is found. But longer paths have a higher probability of message loss, leading to fewer messages being delivered in total.

The total number of messages transmitted by each of the protocols chosen for comparison is shown in Figure 7. `Flooding` naturally transmitted the most messages by far.

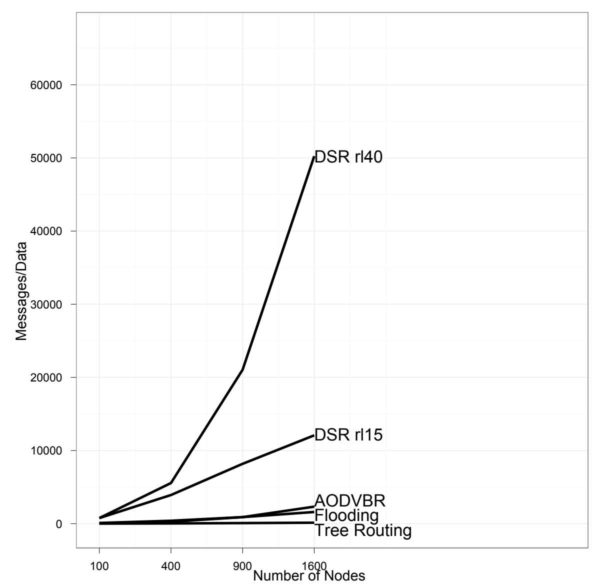


Fig. 8. Number of messages transmitted to deliver a single application message, `Flooding`, AODVBR, `Tree Routing` and two DSR versions, first scenario

Also, it can be seen that `Tree Routing` transmitted very few messages, and DSR with route length 40 transmitted much more messages than the version with route length 15.

The number of messages transmitted in order to bring a single application message to the sink is shown in Figure 8. Even though DSR with route length 40 delivered nearly the same amount of data as DSR with route length 15, the high number of transmitted messages makes it the most costly related work protocol by far. Interestingly, even though it transmits a large number of messages, the high number of delivered messages make `Flooding` the second best. Only

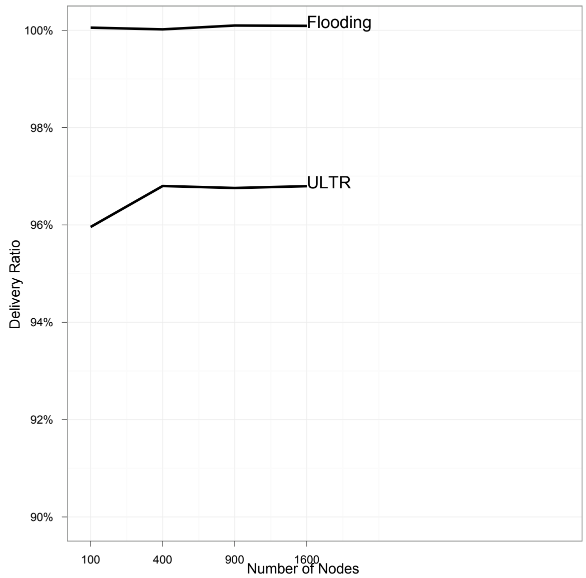


Fig. 9. Delivery ratio of ULTR and `Flooding`, scale starts at 90%, first scenario

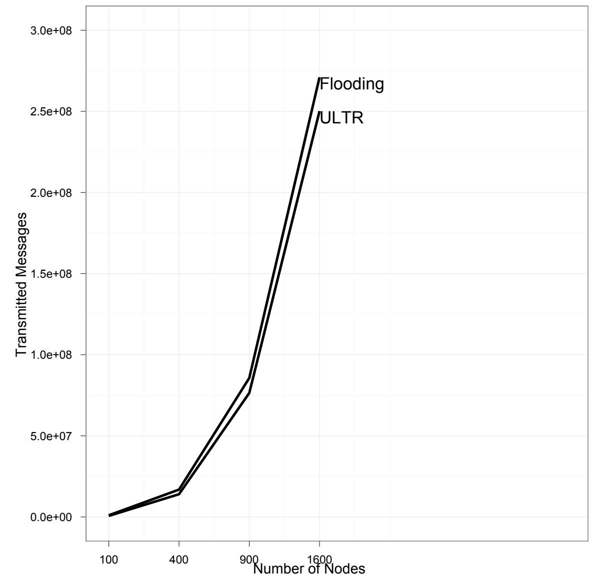


Fig. 10. Number of messages transmitted by ULTR and `Flooding`, first scenario

`Tree Routing` performs better. This is due to the fact that `Tree Routing` has very low costs for delivery failures. Nodes close to the sink are often able to deliver their messages. Nodes that are farther away transmit their messages, and try two retransmissions if the message is not forwarded by the next hop. But, contrary to the other protocols, no route error messages are generated and no new route discovery is initiated when the retransmissions are unsuccessful.

*2) ULTR:* The delivery ratio of ULTR is compared to `Flooding` in Figure 9. Note that the scale starts at 90%.

What catches the eye right away on the figure is that the delivery ratio is very high and increases with network size. ULTR seems to have reached its maximum at 97% already in networks consisting of 20 times 20 nodes, but to be sure more simulations with larger networks would be necessary. These were not done for this paper for two reasons: First, the simulation run time would be very high. A single simulation of `Flooding` in the 40 times 40 network took more than a day, and 600 of them were necessary. In 50 times 50 networks the value would be much higher. Second, the largest network that was simulated, 40 times 40, already contains 1,600 nodes and it is unlikely that such large sensor networks will be deployed for a real application in the near future. If larger networks are deployed, it is likely that a logical partitioning of the network would be realized on application level, and multiple sinks would be used.

The number of messages transmitted by ULTR and `Flooding` is compared in Figure 10. The figure shows that ULTR needs a lot of message transmissions to compensate for the missing neighborhood discovery protocols: As the protocol was designed with the assumption that either a neighborhood discovery protocol or the used MAC layer would supply link information, it suffered from the absence of accurate information. The passive overhearing that was implemented instead

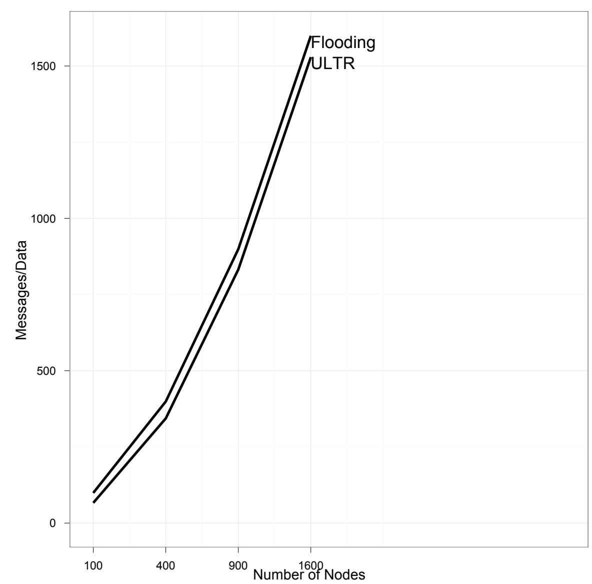


Fig. 11. Number of messages transmitted to deliver a single application message, ULTR and `Flooding, first scenario`

can only detect bidirectional and unidirectional incoming links, which makes the explicit usage of unidirectional links all but impossible. Therefore, ULTR tries to find bidirectional links, or, if these are not available, switches to alternate mode for one hop, which increases the network load very much when it is initiated too often. Another problem is timing: Passive detection of links only works when messages are transmitted, but links change more often than messages are transmitted. Therefore, ULTR often worked on outdated information.

The costs that the delivery of a single data message caused on average are shown in Figure 11. ULTR produces almost

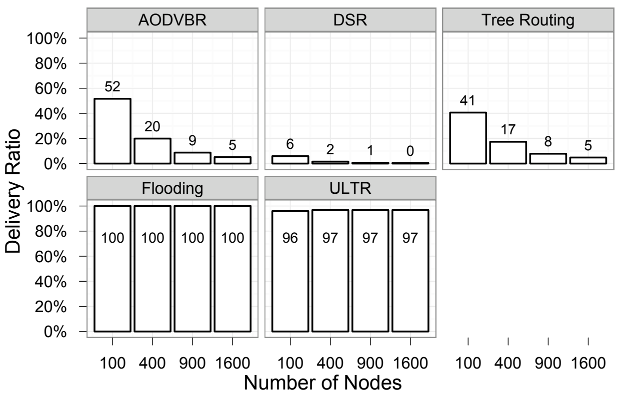


Fig. 12. Delivery ratio of all protocols for different network sizes, first scenario

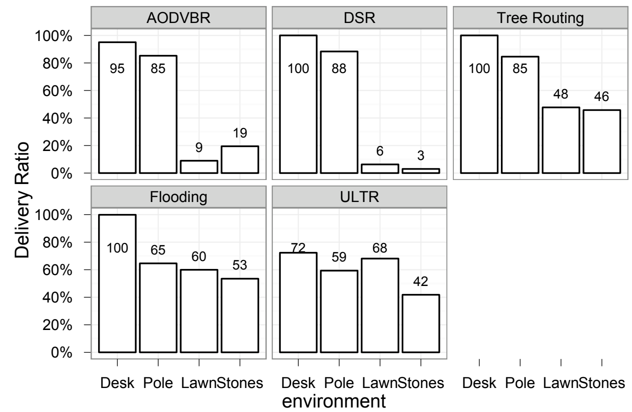


Fig. 13. Delivery ratio of each protocol achieved in the real experiments, first scenario

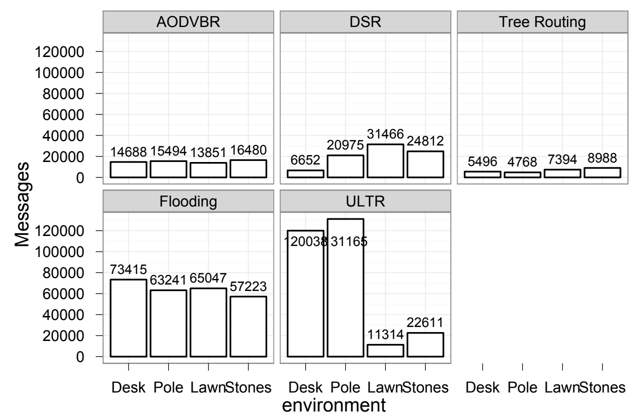


Fig. 14. Total number of messages transmitted by each protocol, real experiments, first scenario

the same costs as `Flooding` with more than 1,500 messages in the network consisting of 1,600 nodes.

*3) Comparison between all Protocols:* Concluding the evaluation of these simulations it can be said that ULTR has achieved a much better delivery ratio in application scenario 1 than the protocols used for comparison. Only `Flooding` delivered more messages, which is why it was used as reference, and the delivery ratio of a protocol defined as the number of messages delivered by that protocol divided by the number of messages delivered by `Flooding` (Figure 12).

Even though the simulations did not feature MAC layer elements, it can already be seen that the protocols chosen from related work are not able to work in an environment with many unidirectional links and often changing links in general. On the other hand, the results clearly show that the developed protocol, ULTR, has achieved its design goals, namely resistance against often changing links and usage of unidirectional links. Only `Flooding` delivered better results in the simulations, and it is known that `Flooding` runs into huge MAC layer problems when it is used on real hardware.

### B. Real World Experiment Results

For the real world experiments of scenario 1, all four different locations described in Section VI-D were used. Each protocol was evaluated on each location, with node 0 in the lower left corner as destination (sink).

The delivery ratio of each protocol is shown in Figure 13, sorted by protocol and location. For most protocols, the number of delivered messages for the desk and pole locations is roughly the same, as these two locations differed only marginally. The desk location is one hop, while the pole location contained between one and two hops on average. The figure also shows that `Flooding` delivers a nearly constant number of messages for the pole, lawn and stone environments.

The other three reference protocols, AODVBR, DSR and `Tree Routing` show a steep decline in delivered messages for the lawn and stone pavement placements. ULTR always delivered more messages to their destination, except for the stones placement. The reason for the bad results from ULTR lies in its dependency on accurate link information. As described in Section II, ULTR tries to route messages around unidirectional links explicitly. But in order to build this triangle, neighborhood information is needed. The current implementation of ULTR tries to obtain this information passively, by overhearing forwarded messages. For a rapidly changing environment this approach is bound to fail. It would be interesting to see, how a protocol implementation that uses a neighborhood discovery protocol or neighborhood information provided by the MAC-layer would perform.

The number of protocol and data messages transmitted by each protocol can be seen in Figure 14. Once again, `Flooding` remains fairly stable throughout the locations. While all other protocols transmitted more messages in the last two locations (lawn, stone pavement), the number of messages transmitted by ULTR declines. This is once more due to the absence of accurate link information. ULTR was designed with the assumption that link information would be available either from a neighborhood discovery protocol or from the MAC layer. Using only overheard messages instead does not work

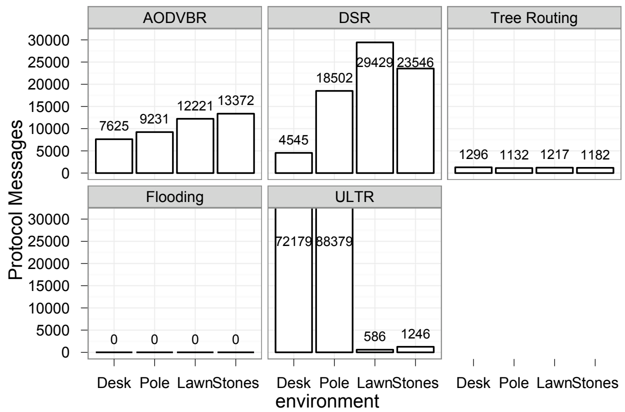


Fig. 15. Number of protocol messages transmitted by each protocol, first scenario

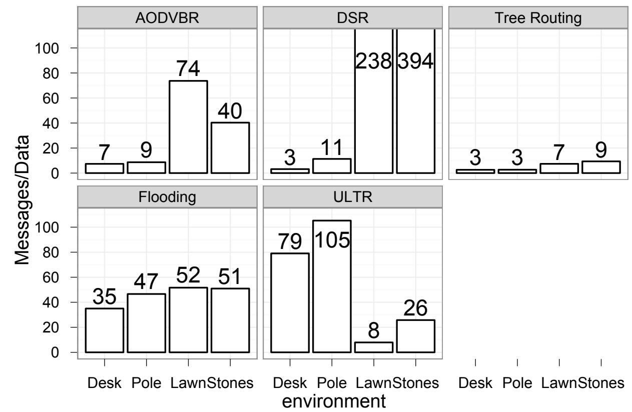


Fig. 16. Total number of messages transmitted by each protocol divided by the number of delivered data messages, first scenario

in the first two locations: When all nodes can transmit directly to the sink and the sink never answers, all links are assumed to be unidirectional and alternate mode is induced for every message. Therefore, every message is flooded. As ULTR uses a route request - route reply mechanism to find routes, the number of transmitted messages in a single hop scenario is even higher than that of `Flooding`, which only transmits data messages.

An even more interesting fact that can be seen in the figure is that the passive neighborhood discovery mechanism starts to work in the multihop environments. When paths are more than 1-2 hops in length, forwarded messages are received more often and the nature of the links can be observed. Therefore, even though it might seem strange, ULTR needs to transmit fewer messages in networks with a larger diameter.

The number of protocol messages, i.e., non-data messages, transmitted by each protocol can be seen in Figure 15. As already seen above, ULTR suffered badly from the missing neighborhood discovery protocol. ULTR nearly always switched to alternate mode. The huge number of protocol messages transmitted by ULTR consisted mainly of route request messages. In fact, a route discovery took place for nearly each data message generated by the application in ULTR.

Another measurement of the cost paid to deliver an application message is shown in Figure 16. The figure shows the total number of transmitted messages divided by the number of application messages that reached the sink. Unsurprisingly, `Flooding` once more shows a relatively constant performance and DSR and AODVBR show too high values. Interestingly, `Tree Routing` seems to have performed quite well. If only this figure was taken into account when choosing a protocol, `Tree Routing` would be preferred. However, the numbers presented here have to be put into perspective. The result of `Tree Routing` is achieved because it uses nearly no protocol messages, and two retransmissions are its only reaction to message loss. No route error messages are generated and no new route discovery is started. Therefore, the cost of a lost application message is much lower than in the other protocols. DSR represents the other end of the spectrum: When a message loss is detected there, a route error message is created and transmitted to the originator. When the route error is received, the route is deleted and a new route discovery is initiated, which leads to a flooding of the whole network. If conditions are really bad, it may even lead to flooding the network twice. Except for the problems experienced by ULTR in the 1-2 hop locations, it performs fairly well. But the results also show that the number of nodes used in the real world experiments was actually a little low - as the simulations have shown (see Section VII-A), the big differences between protocols can be seen better in larger networks. However, using a few hundred nodes in the real world experiments was not possible as there were not that many nodes available.

### C. Comparison between Simulations and Experiments

The real world experiments were conducted with 36 nodes, while the simulations featured either 100, 400, 900 or 1,600 nodes. To show that the tendencies seen in the simulations represent those that would be achieved with a large scale sensor network, a network consisting of 36 nodes was also simulated.

Figure 17 shows the median of the delivery ratio of all evaluated protocols for the two multihop experiments (lawn, stones) and the 36 nodes simulation. Naturally, the results of `Flooding` in the simulation are much better than those achieved in the real world experiments, as `Flooding` suffers heavily from the broadcast storm problem in the real experiments. The used CSMA MAC layer simply cannot handle the huge number of messages. The simulation results and those of the two experiment settings are quite similar for the protocols surveyed in this paper. From the protocols used for comparison, only AODVBR shows a large difference between simulation and real world results.

When looking at the results, which those two protocols, AODVBR and ULTR, achieved in the real world experiments, it can be seen that they have a strong variation in delivery ratio between the lawn and stone experiments. This high variation seems to imply that both protocols are especially vulnerable

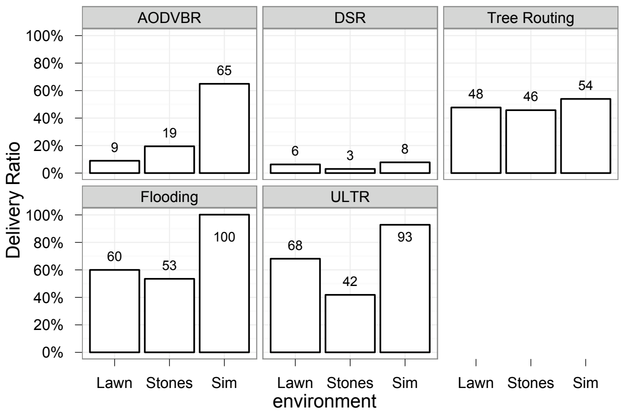


Fig. 17. Delivery ratio of each protocol; experiments vs. simulations

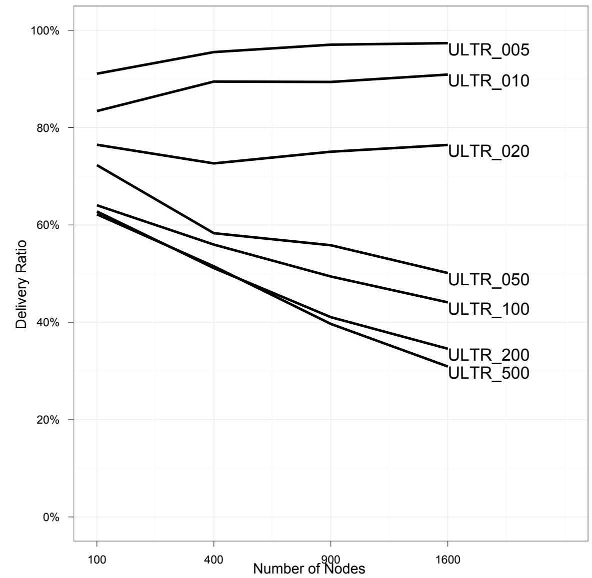


Fig. 18. Delivery ratio achieved in the simulations for different timeouts

to one or more properties of the real experiments, which do not have so much influence on the other protocols.

Both AODVBR and ULTR try to use an explicit detour around unidirectional links, using link information detected during route reply transmission (AODVBR) or during transmission of DATA messages (ULTR). As the connectivity measurements we conducted [2] have shown, link changes occurred even more often than expected, making conditions for AODVBR and ULTR harder in the real world than in the simulations. None of the other protocols suffered as much as these two. For DSR, an additional increase in frequency of changes made no difference, as it could not even tolerate the one simulated. For `Tree Routing`, the small network diameter and the 2 retransmissions on each hop were enough to deliver about 50% of application messages. The link changes would not have influenced `Flooding`, but `Flooding` produced a very high network load, which the MAC layer could not handle. Still, it can also be seen that the deployed sensor network was not large enough for them to show their full potential.

In summary it can be said that the used simulation approach has some limitations, as it does not include the medium access control protocol used in the real experiments. However, the results show that the usage of connectivity matrices and the way they were generated is close to reality, and can be used to evaluate the influence of unidirectional links and frequent link changes on the routing protocols. This is exactly what the simulations were intended for as the used MAC layer and other side effects of the used hardware might (and hopefully will) change for future deployments. When the exact properties of the hardware that will be used in a deployment are known beforehand, these could be included in the simulations. Some of the less favorable communication properties of the eZ430-Chronos (e.g., the inability of the CCA to receive messages during backoff) were only discovered during the connectivity measurements [2].

Another advantage of the simulation model is the fact that the connectivity data gathered during the connectivity measurement experiments can easily be included. The data that could be gathered this way was not presented in this work, because the number of data sets from the connectivity experiments currently available is too small.

### D. Importance of Timeouts

The implemented version of ULTR with passive link detection is heavily dependent on the timeouts that are used for the links. If it is set too low, the links are deleted before they may be used, even though they might still exist, resulting in a local broadcast on every hop. If it is set too high, links are assumed to exist, but have broken a long time ago.

The implementation of ULTR uses a timer that fires every 100 ms, and has a parameter called `linkTimeout` that defines how many times that timer must fire before a link is removed from the neighbor table. The results presented above were achieved with a `linkTimeout` of 5, and resulted in a lot of message transmissions but also fairly high delivery ratio. To quantify the impact of the `linkTimeout`, the performance of ULTR was measured with different values of `linkTimeout`: 5, 10, 20, 50, 100, 200 and 500.

Figure 18 shows the delivery ratio achieved by ULTR with the seven different timeouts. It seems that the delivery ratio is constantly decreasing with increasing timeout lengths. This is not surprising, since a link that has been removed from the neighbor table results in a local broadcast. All nodes that receive this message and know the intended next-but-one hop retransmit the message, adding a lot of redundancy. Therefore, removing a link too early does not result in message loss, but in unnecessary network load. However, if the link is deleted too late, i.e., a link is assumed to exist where it has already broken, the message gets lost. Therefore, when considering only the delivery ratio, using a small timeout seems favorable.

However, when the network load is considered, the choice seems to be quite the opposite. Figure 19 shows the cost of delivering a single application message measured in transmitted messages. When using the smallest timeout of 5, about

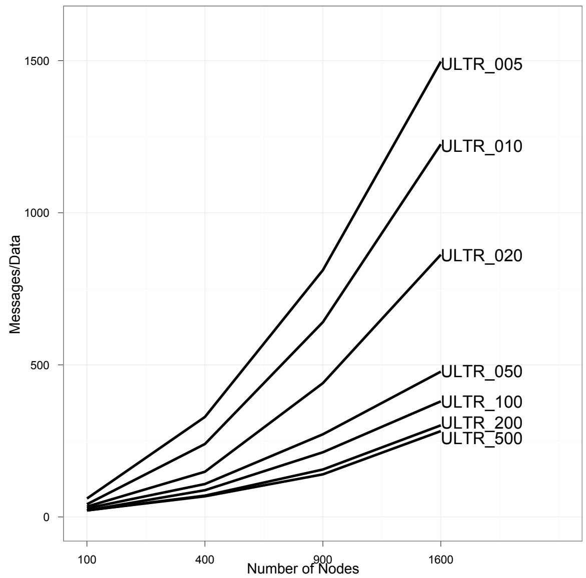


Fig. 19. Number of messages transmitted to deliver a single application message in the simulations for different timeouts

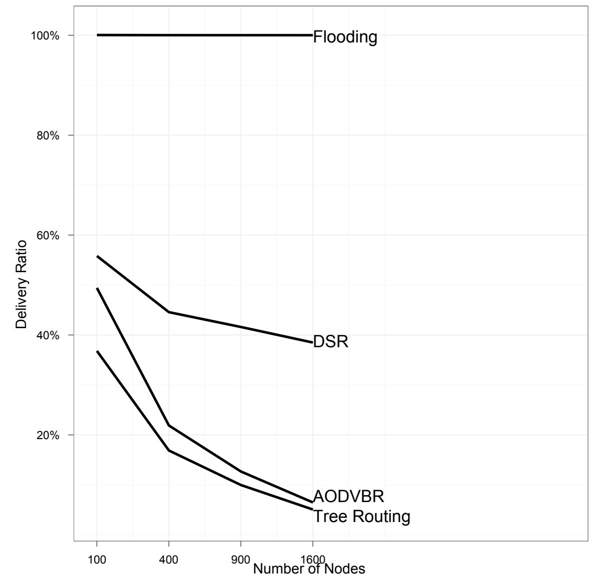


Fig. 20. Delivery ratio of AODVBR, DSR, `Flooding` and `Tree Routing`, second scenario

1,500 messages are transmitted for each application message delivered in the network consisting of 1,600 nodes, which is quite close to the cost of flooding the message. Therefore, the decision, which timeout should be used is a tradeoff between delivery ratio and network load. However, there are limits to the choice: Increasing the timeout above 200 does not change delivery ratio or efficiency much. Also, as the delivery ratio is most often more important than the network load, it is unlikely that a timeout of more than 50 would be used, because higher timeout values lead to a delivery ratio of less than 50%. Still, even this is much more than what the related work protocols achieved, making ULTR a fine choice for the evaluated network types.

## VIII. Application Scenario 2: Single Pairing

In this scenario, all settings, including the number of messages a node wants to transmit, are the same as in the sense-and-send scenario. However, instead of a single sink as destination for all messages from all nodes, each node has a randomly chosen partner node it wants to communicate with. This pairing of nodes was generated before the simulations and experiments, and differs only between different network sizes: If, e.g., node 15 is the partner of node 21 for the network consisting of 36 nodes, this pairing remains fixed for all protocols as well as for simulations and real world experiments.

This pairing of nodes represents a communication pattern for MANETs and was chosen because two of the protocols used for comparison (AODVBR and DSR) are MANET protocols.

### *A. Simulation results*

In the simulations for the single pairing scenario, the same connectivity change lists were used that have already been used in the sense-and-send scenario. However, as the destination was not a single fixed one for all nodes, the simulations were not varied according to the destination. Instead, the generated pairings were used as stated above.

Flooding was once again used to measure the upper limit for delivered messages and the delivery ratio was defined as the number of messages delivered by a protocol divided by the number of message delivered by `Flooding`.

*1) Related Work Protocols:* The delivery ratio of AODVBR, DSR, `Flooding` and `Tree Routing` is shown in Figure 20. For all protocols except `Flooding` the delivery ratio declines with increasing number of nodes. It can be seen that AODVBR and `Tree Routing` suffer the most from the increased route length in the larger networks, as the decline of their delivery ratio is steep. For AODVBR, building the initial route is the crucial part. When a route has been successfully established, the fish bone structure can be used to salvage data packets. But since building the initial route requires a bidirectional path and the probability of a complete path being bidirectional decreases with route length, AODVBR only works in small networks. For `Tree Routing`, building the initial route is no problem. However, due to the dynamic nature of links between nodes, the initial path is obsolete soon and the two retransmissions used as reaction to message loss are not sufficient in larger networks.

The delivery ratio of DSR also declines due to its source routing nature. However, finding the initial route is not a problem, as DSR uses one flooding for each direction. The main problem of DSR is its route maintenance mechanism. When DSR detects a route break it tries to inform the originator of the message that caused the detection of the break. Following this, a new route discovery with all its costs takes place.

The number of transmitted messages for each protocol is shown in Figure 21. Here, the impact of the route maintenance

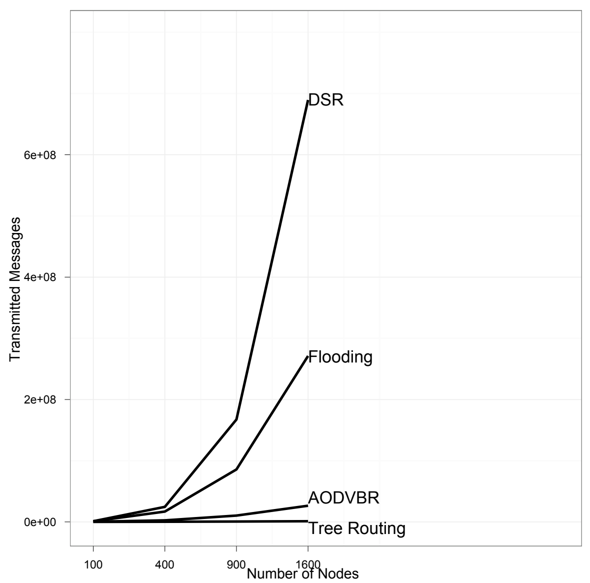


Fig. 21. Number of transmitted messages, AODVBR, DSR, `Flooding` and `Tree Routing`, second scenario

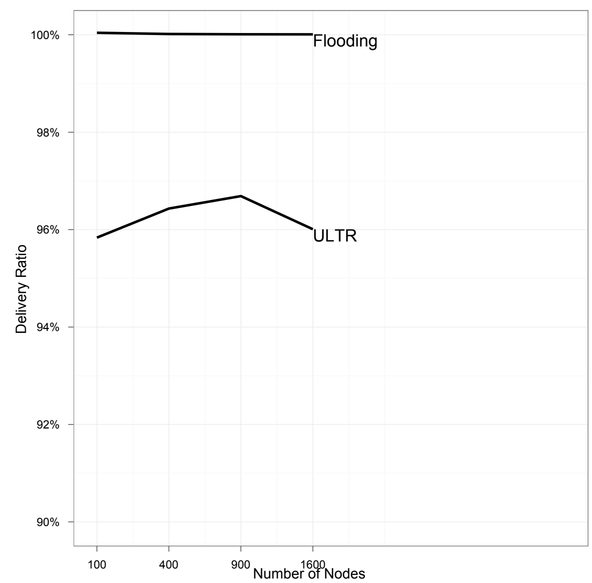


Fig. 23. Delivery ratio of `Flooding` and ULTR, scale starts at 90%, second scenario

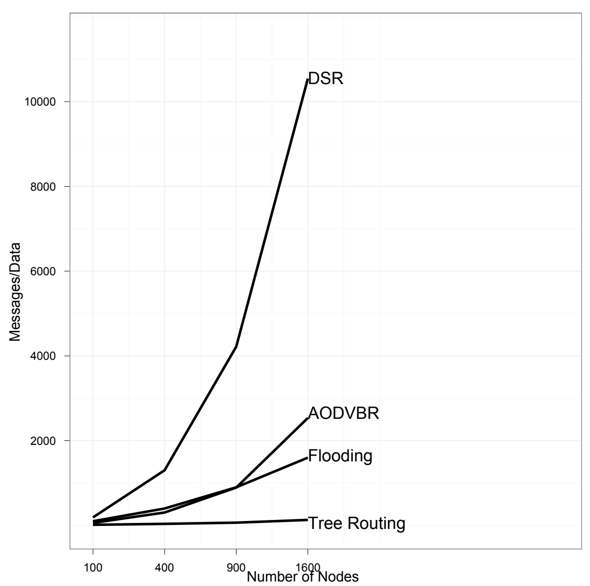


Fig. 22. Number of messages transmitted to deliver a single application message, AODVBR, DSR, `Flooding` and `Tree Routing`, second scenario

mechanism of DSR can be seen: It transmits more than twice as many messages as `Flooding` as it tries to repair broken routes. `Tree Routing` presents the other extreme, it transmits nearly no messages at all, while AODVBR needs slightly more messages.

When the network load is considered (Figure 22), the impact of the low number of messages transmitted by `Tree Routing` can be seen even better: The number of messages transmitted to deliver a single application message would suggest that `Tree Routing` is an excellent choice. However, this fact needs to be correlated with the delivery ratio in most cases, and the delivery ratio of `Tree Routing` is the lowest of all protocols. This is once again due to the length of routes. `Tree Routing` delivers a nearly constant number of data messages to the destination (roundabout 8,000) for the networks with 400, 900, and 1,600 nodes, even though the total number of application messages that is handed to the routing protocol increases proportionally to the number of nodes in the network.

*2) ULTR:* The delivery ratios of `Flooding` and ULTR are compared in Figure 23. Note that the scale starts at 90%. ULTR delivers well above 95% of application messages for all network sizes. In fact, the performance of ULTR seems largely independent of the network size with a slight increase from 96% to 97% for the network with 900 nodes.

Figure 24 shows the total number of messages transmitted by `Flooding` and ULTR. When these results are compared to those of the sense-and-send scenario (Figure 10), it can be seen that the number of messages transmitted by ULTR has decreased.

Figure 25 shows the number of messages transmitted by `Flooding` and ULTR in order to deliver a single application message. As the delivery ratio of both protocols is nearly equal but ULTR needs much less transmitted messages, the ratio of ULTR is much better than that of `Flooding`.

*3) Comparison between all Protocols:* The delivery ratio achieved by each of the simulated protocols in the single pairing scenario is shown in Figure 26. It can be seen that ULTR performs better than those chosen from related work. Moreover, the delivery ratio stays roughly the same with increasing network size. For AODVBR, DSR and `Tree Routing` the delivery ratio decreased with network size. But most interestingly, the delivery ratio of DSR improved drastically when compared to the sense-and-send scenario (see Figure 12). Also, the decline in delivery ratio with increasing

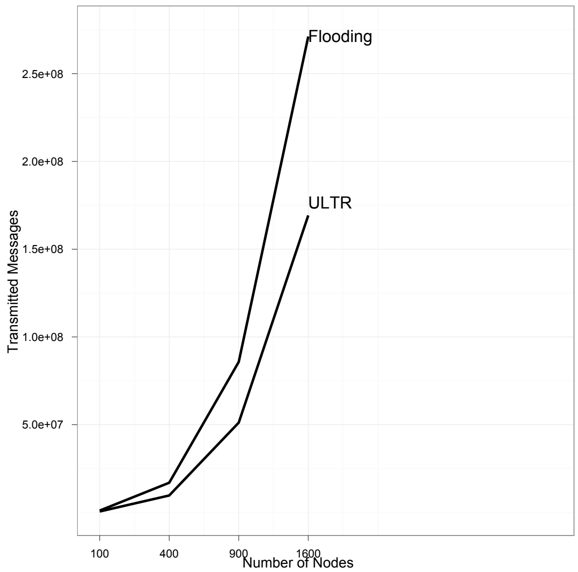


Fig. 24. Number of transmitted messages, `Flooding` and ULTR, second scenario

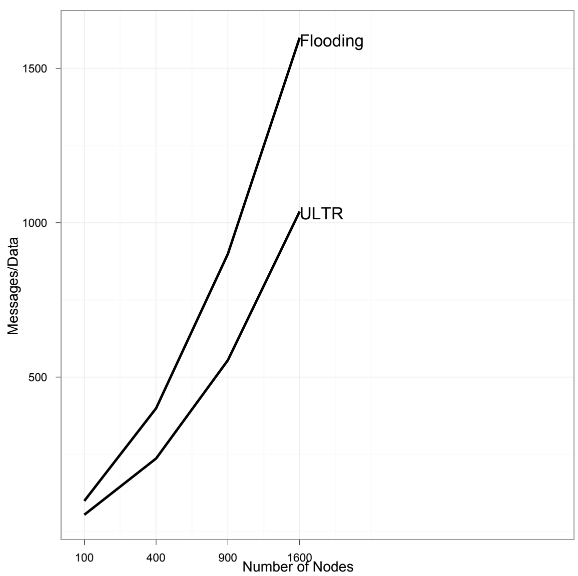


Fig. 25. Number of messages transmitted to deliver a single application message, `Flooding` and ULTR, second scenario

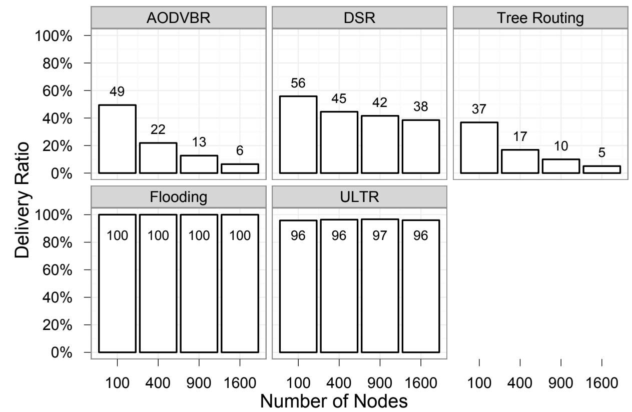


Fig. 26. Delivery ratio of all protocols for different network sizes, second scenario

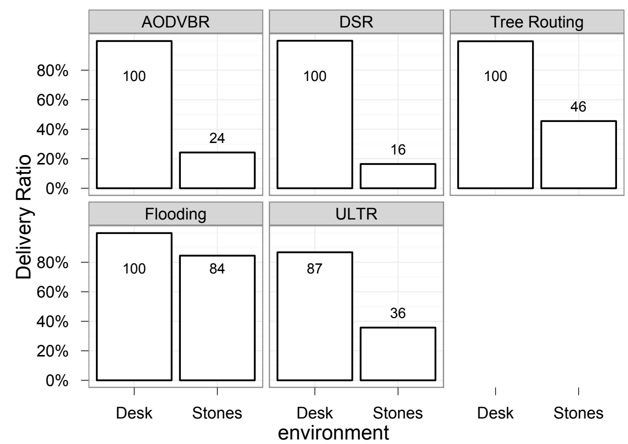


Fig. 27. Delivery ratio of each protocol achieved in the real experiments, second scenario

number of nodes is visible, but it is not as steep as for AODVBR and `Tree Routing`.

Concluding the evaluation of these simulations it can be said that DSR gained most from the change of application scenario. This was expected, as DSR was designed for MANET scenarios, not for sense-and-send scenarios in wireless sensor networks. However, the delivery ratio of ULTR is still higher than that of the related work protocols, for all network sizes.

### *B. Real World Experiment results*

In the experiments for the single paring scenario, only two locations were used: The desk and the stone pavement. No experiments were made on the poles, because of the similarity between pole and desk scenario. On the desk, all nodes can communicate directly while on the poles the logical distance between nodes was only 1-2 hops even in the sense-and-send scenario where the destination was on the corner of the deployed grid. The pairings used in this scenario reduce the average route length and would result in even more single hop routes for the pole scenario, making the experiments redundant. The lawn placement has been neglected due to its similarity with the stone pavement placement.

Figure 27 shows the delivery ratios of all protocols that were achieved in the real world experiments on the desk and stone pavement. With the exception of ULTR, all protocols delivered 100% of messages in the desk scenario. This behavior has also been seen in the sense-and-send scenario (see Figure 13) and can be explained by the absence of up-to-date link information. ULTR normally depends on the MAC layer or the application to deliver neighborhood information. As none was available, neither from MAC nor from the application, the current implementation relies on passive gathering of neighborhood

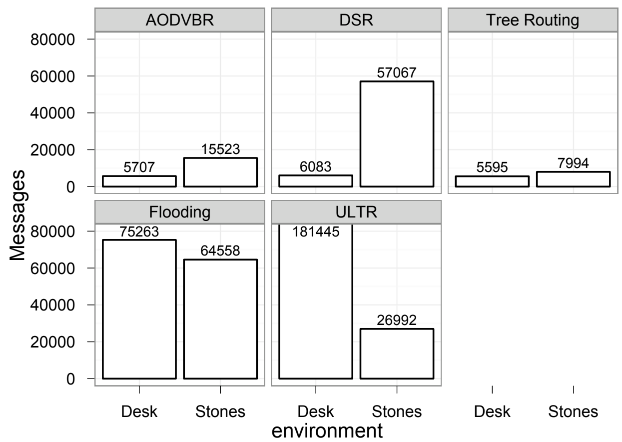


Fig. 28. Total number of messages transmitted by each protocol, second scenario

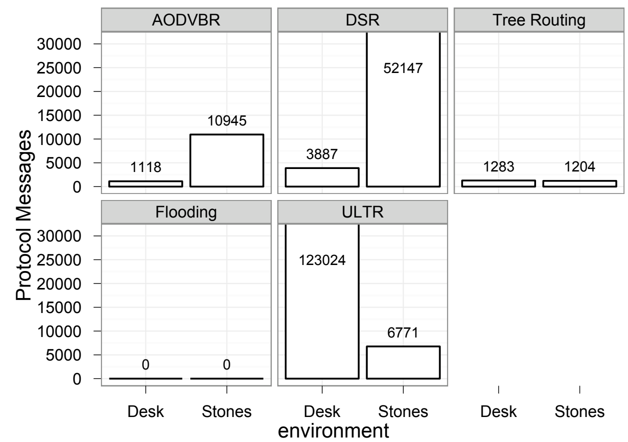


Fig. 29. Number of protocol messages transmitted by each protocol, second scenario

information by overhearing the forwarding of messages. But in a single hop environment not enough forwarded messages are overheard.

In the stone pavement experiments, even `Flooding` did not deliver all messages, which gives an insight into the MAC-layer problematic experienced more or less by all protocols. `Tree Routing` has a good delivery ratio in this scenario as it does not produce too much network load and the average path length was fairly small, making its two retransmissions a good reaction to message loss. ULTR suffers from inaccurate information in its neighbor tables, and often uses its fallback mechanism. DSR is continuously trying to repair routes, and thereby increases the network load very much, which can be seen in the next figure.

The total number of messages transmitted by each protocol is shown in Figure 28. For the experiments on the desk it can be noted that ULTR transmits more messages than `Flooding`, which can also be explained by the fallback mechanism in use: When ULTR starts route discovery, the network is flooded with a route request message. The destination receives this message and answers with a route reply but does not know if the link to the previous hop is unidirectional or bidirectional. Therefore, it uses the fallback mechanism, meaning that each node that knows the next hop forwards the message, which results in a second flooding of the network. Now that the route has been built, the data message can be transmitted. This process is repeated every time that the link timeout removes a link to the destination from a nodes neighbor table. In the stone pavement placement, the passive neighborhood discovery works much better, leading to fewer messages transmitted by ULTR. Here, DSR transmits more than 57,000 messages and thus nearly as many as `Flooding`. ULTR transmits roundabout 27,000 messages while AODVBR and `Tree Routing` transmit about 15,000 and 8,000 messages respectively. These numbers already hint at the fact that `Tree Routing` profits quite a lot from the application setting and the small network diameter.

A more detailed look at the number of messages transmitted by each protocol is given in Figure 29, where only the protocol packets are counted. Naturally, `Flooding` has the least number of protocol messages as it does not use any, and all transmitted packets are data messages. On the desk, AODVBR and `Tree Routing` transmit 1,118 and 1,283 messages respectively. As 36 nodes were present in the network, a flooding of one route request or tree building message by each node would result in 1,296 ($36 \times 36$) transmissions. Therefore, these three protocols transmitted the expected number of messages. DSR and ULTR flood the network multiple times for each route discovery, resulting in an awfully high number of route request and route reply messages. For DSR this is due to the specification for the operation in the presence of unidirectional links. For ULTR it is once more due to the absence of accurate neighborhood information.

On the stone pavement, the number of protocol messages rises enormously for DSR, as a lot of link breaks lead to the creation of route error messages and subsequent new floodings of the network in order to find a new route. The lowest number of protocol messages (apart from `Flooding`) is transmitted by `Tree Routing`, which only transmits its tree building messages at the start of the experiment. When this figure is compared to the previous one, it can be seen that `Tree Routing` transmitted about 6,800 data messages (7,994 total messages - 1,204 protocol messages), meaning that most of the time the two retransmissions took place.

The number of messages transmitted to deliver a single application message is shown in Figure 30. As there were 36 nodes in the network, `Flooding` transmitted 36 messages for each data message delivered to the destination. AODVBR, DSR and `Tree Routing` transmitted exactly 3 messages for each data message received. The high number of data messages transmitted due to the inaccurate neighborhood information leads to a performance even worse than `Flooding` for ULTR.

On the stone pavement, `Tree Routing` performed best. When the delivery ratio (Figure 27) is also taken into account it can be said that for this application scenario, network size

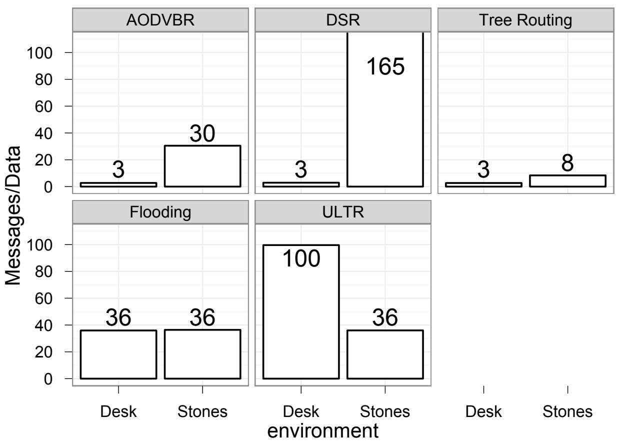


Fig. 30. Total number of messages transmitted by each protocol divided by the number of delivered data messages, second scenario

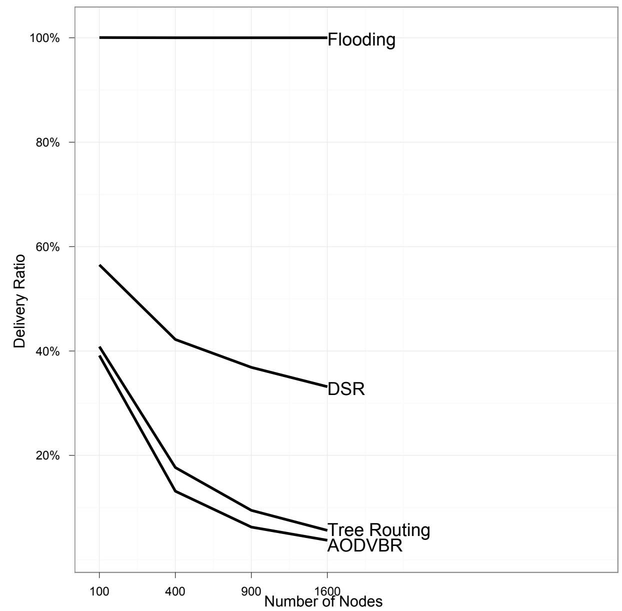


Fig. 31. Delivery ratio of AODVBR, DSR, `Flooding` and `Tree Routing`, third scenario

and placement, the choice of routing protocol should be made between `Tree Routing`, `Flooding` and ULTR. `Tree Routing` produced the least network load per application message delivered and should be chosen if some message losses could be tolerated but the network load is the most important factor. If number of delivered messages is most important, `Flooding` should be used. ULTR represents a good choice in between.

## IX. Application Scenario 3: Multiple Pairings

The third application scenario, multiple pairings, once again uses the same settings as the two previous ones, only the application was changed. Instead of all nodes transmitting to a single sink or one communication partner for each node, there are multiple partners now. Each node has one communication partner at the start of the simulations/experiments and transmits the first five messages to this node. Once five messages have been transmitted, the communication partner is changed. This is repeated every time five messages have been transmitted, until the total number of messages specified (110 for simulations, 60 for experiments) has been reached. The pairings of nodes were once again generated randomly before the start, and the same pairings were used for all protocols.

This represents a MANET scenario where all nodes only want to exchange a few messages with a chosen partner before communicating with a different node. The fact that each pairing is only used for five messages results in a reduction of the importance of route maintenance. It is much more likely that a route is stable for five minutes than for a whole simulation/experiment, resulting in less route errors. Instead, route discovery rises in importance, as it is carried out after every five application messages.

### A. Simulation results

The simulations once again used the connectivity change lists that were generated before the start, to keep network connectivity equal for all protocols. As in the single pairing scenario, the pairings define a different destination for each node, making the additional simulation parameter `destination` used in the sense-and-send scenario unnecessary.

The delivery ratio remains defined as the number of application messages delivered by a protocol divided by the number of messages delivered by `Flooding` in the simulations.

*1) Related Work Protocols:* The delivery ratio of the related work protocols is shown in Figure 31. For AODVBR and `Tree Routing`, the number of nodes and, therefore, the route length is much more important than the communication pattern of the application: The changes between single pairing and multiple pairings are marginal (compare Figure 20). The performance of `Tree Routing` increased by one percent for the largest network while that of AODVBR decreased by two percent. A bigger difference can be seen for the smaller networks, where AODVBR has lost 10% of its performance compared to the single pairing scenario in the network consisting of 100 nodes. This decrease in delivery ratio is due to the fact that building the initial route is one of the weaknesses in AODVBR. When searching for a route, the path has to be bidirectional to enable the route reply to use the same path as the route request. Once this path has been established, the fish bone structure that has been built with the route replies can be used to salvage data messages when links break. In the multiple pairings scenario, each node needs to search routes to 22 different nodes instead of only one.

The number of messages transmitted by the related work protocols is shown in Figure 32. With twice the number of transmitted messages as `Flooding`, DSR once more transmitted the most messages by far. AODVBR and `Tree Routing` transmitted far less messages, with `Tree Routing` producing the least number. When the results are compared to those of the single pairing scenario, no substantial differences can be discerned (compare Figure 21).

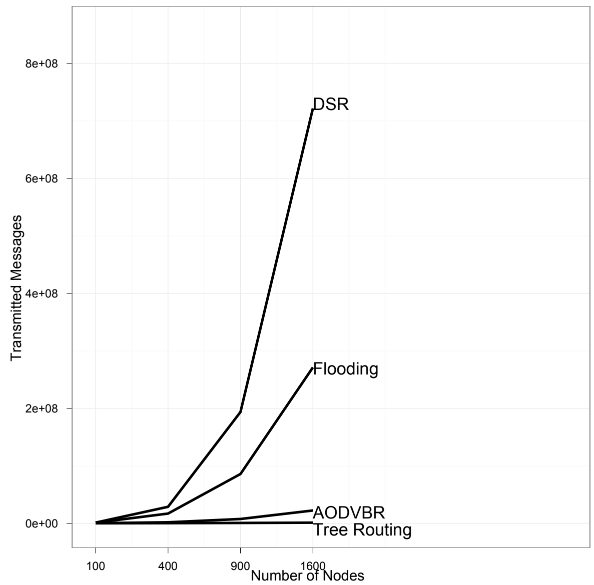


Fig. 32. Number of transmitted messages, AODVBR, DSR, `Flooding` and `Tree Routing`, third scenario

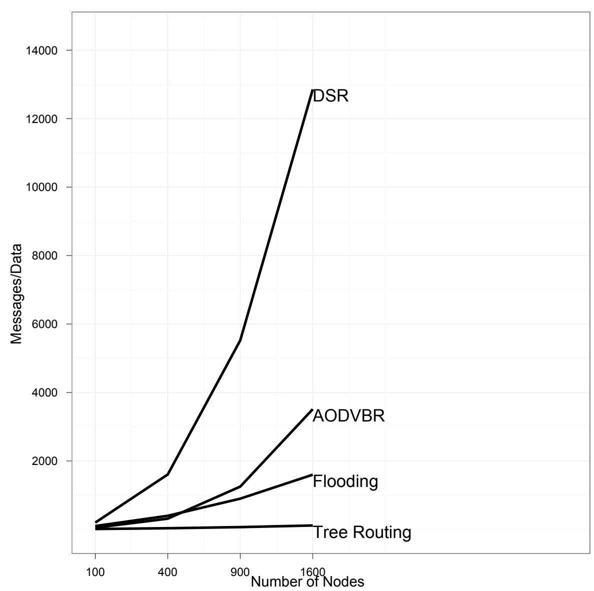


Fig. 33. Number of messages transmitted to deliver a single application message, AODVBR, DSR, `Flooding` and `Tree Routing`, third scenario

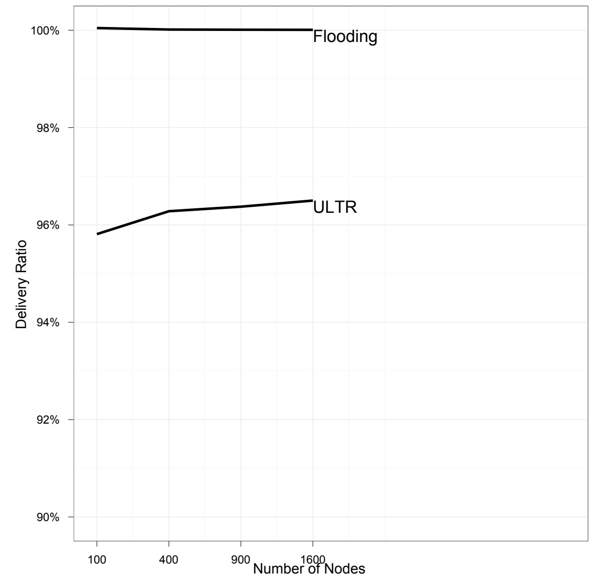


Fig. 34. Delivery ratio of `Flooding` and ULTR, scale starts at 90%, third scenario

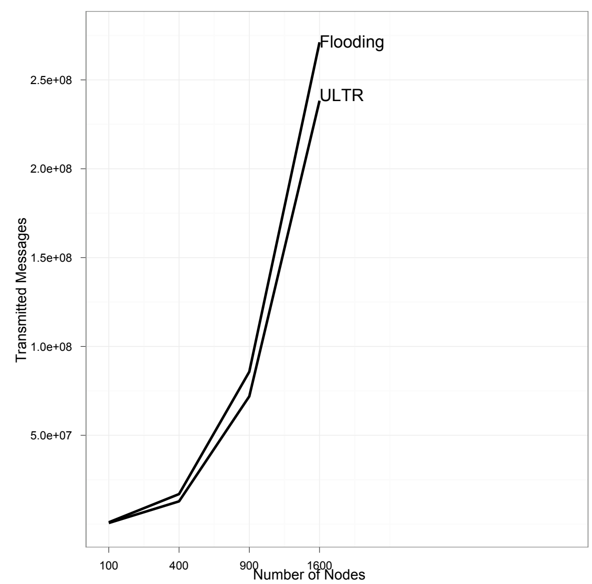


Fig. 35. Number of transmitted messages, `Flooding` and ULTR, third scenario

The cost of delivering a single data message measured in transmitted messages is shown in Figure 33. Only `Tree Routing` transmitted less messages per application message delivered than `Flooding`. This is once more due to the fact that the cost of delivery failure is small in `Tree Routing`. However, when the delivery ratio is also taken into account, `Tree Routing` looses parts of its advantage over AODVBR.

*2) ULTR:* The delivery ratio achieved by ULTR is compared to that of `Flooding` in Figure 34, note that the scale starts at 90%. It can be seen that ULTR delivers more than 95% of application messages, regardless of network size. It delivers between 95% and 97%, with only a low variation between network sizes.

The high number of delivered messages comes at the price of an increased number of transmitted messages, as Figure 35 confirms. Here, it can be seen that the number of messages transmitted by ULTR has risen when compared to the single pairing scenario (Figure 24). While the number is still lower than that of `Flooding`, it has gotten closer.

This high number of transmitted messages is the reason why the performance of ULTR decreases in the multiple pairings scenario. Figure 36 shows the performance of ULTR and `Flooding`, measured in messages transmitted per application

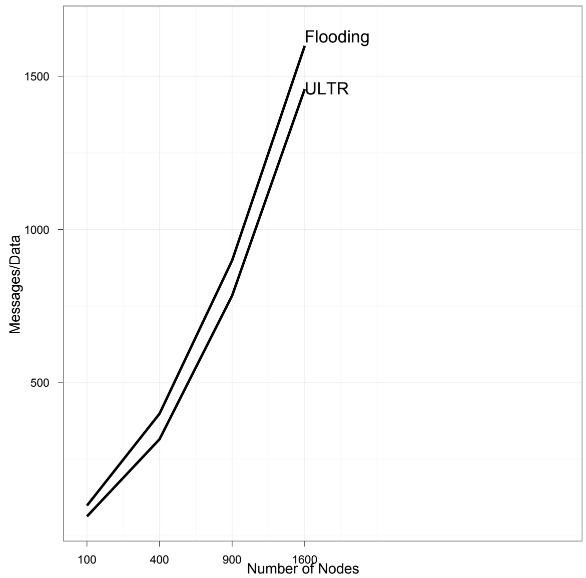


Fig. 36. Number of messages transmitted to deliver a single application message, `Flooding` and ULTR, third scenario

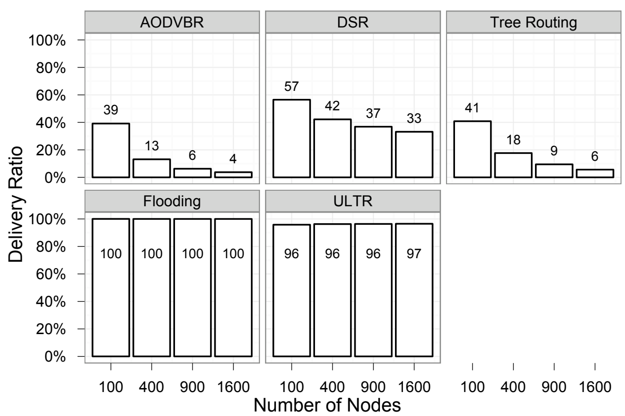


Fig. 37. Delivery ratio of all protocols for different network sizes, third scenario

message delivered. The figure shows that the performance of ULTR not much better that of `Flooding` in this scenario.

*3) Comparison between all Protocols:* The delivery ratio of all protocols is compared in Figure 37. The related work protocols, AODVBR, DSR and `Tree Routing` all show a steep decline in delivery ratio. Interestingly, the decline of delivery ratio is not as steep for DSR as it is for AODVBR and `Tree Routing`. This is due to the fact that DSR has a better route discovery mechanism. While flooding the whole network twice in order to establish a route produces a lot of network load, it also means that a route will be found in most cases. Only if network separation occurred, no route would be found. How long a route found this way can be used depends on link stability, however. But since it only needs to be used for five messages before a different destination is selected, there is a good chance some of the five messages can

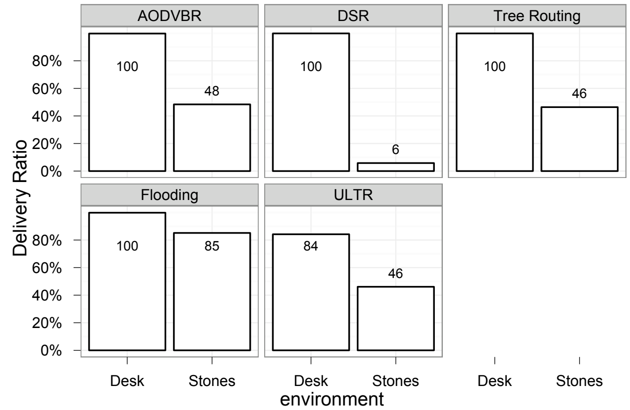


Fig. 38. Delivery ratio of each protocol achieved in the real experiments, third scenario

be transmitted successfully. This can be seen in the network with 1,600 nodes, where DSR was able to deliver one third of application messages, meaning that between one and two messages were delivered to each destination on average. ULTR increases its performance with increased number of nodes.

### *B. Real World Experiment results*

The experiments for the multiple pairings scenario featured the same settings and locations as the experiments for the single pairing scenario (Section VIII-B): The desk placement was used as single hop, and the stone pavement as multihop environment. The pole placement would have been redundant to the desk placement while the lawn placement would have been similar to the stone pavement environment.

The delivery ratio achieved by all protocols in the multiple pairing scenario is shown in Figure 38. In the desk experiments, all protocols reached 100% delivery ratio except for ULTR. This is due to the passive neighborhood discovery: Only when the forwarding of a message is overheard by a node that has already forwarded that message and is listed as last hop, the neighborhood discovery assumes bidirectional links. Otherwise, links are assumed to be unidirectional. This leads to a lot of mistakes, as nodes do not need to forward messages in a single hop environment, meaning that all links in the network are assumed to be unidirectional. Therefore, the backup mechanism is always used unnecessarily, resulting in a high network load, which in turn leads to more collisions and message losses.

On the stone pavement, `Flooding` delivers most application messages, followed by AODVBR, ULTR and `Tree Routing`, which deliver about half of the messages transmitted. Only DSR is far worse, with a delivery ratio of only 6%.

The total number of transmitted messages is shown for all protocols in Figure 39. ULTR once more has the highest number of transmitted messages for the single hop environment due to the problems with the neighborhood detection. On the stone pavement, the passive neighborhood detection works better, and the number of transmitted messages is

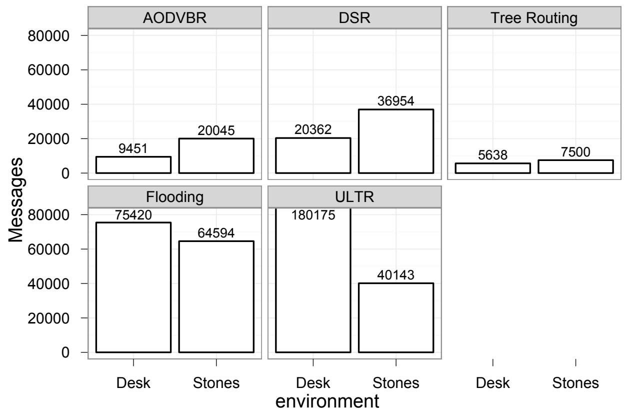


Fig. 39. Total number of messages transmitted by each protocol, third scenario

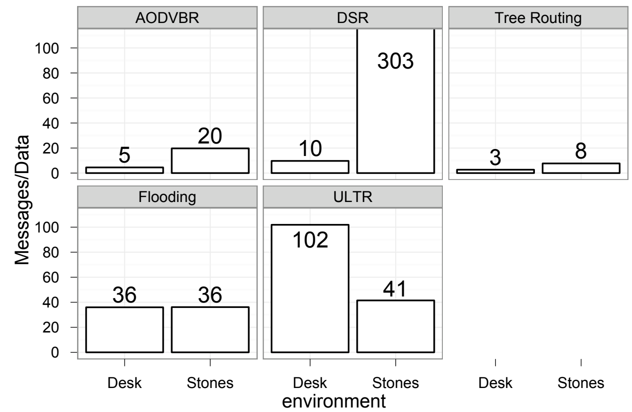


Fig. 41. Total number of messages transmitted by each protocol divided by the number of delivered data messages, third scenario

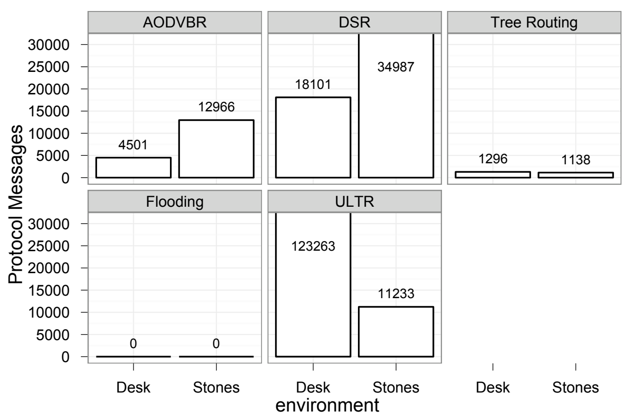


Fig. 40. Number of protocol messages transmitted by each protocol, third scenario

reduced. There, `Flooding` transmits the greatest number of messages while `Tree Routing` transmits the smallest. Still, when considering that only 2,160 application messages were generated it can be seen that `Tree Routing` often used its two retransmissions.

The number of protocol messages transmitted by each protocol can be seen in Figure 40. `Flooding` naturally did not transmit any protocol messages, while ULTR transmitted the most protocol messages in the desk scenario.

On the stone pavement, `Tree Routing` needed the least number of protocol messages, apart from `Flooding`. DSR transmitted the most protocol messages, followed by AODVBR and ULTR.

The number of transmitted messages divided by the number of delivered application messages is used to measure the performance of all protocols in Figure 41. For the desk placement, `Tree Routing` shows the best performance, directly followed by AODVBR.

When the sensor nodes were placed on the stone pavement, `Tree Routing` needed the least number of transmissions to deliver a single application message, which is once again due to the low cost of delivery failure. When only the cost of an application message delivery is considered, `Tree Routing` performs best. However, `Flooding` delivered nearly twice as many messages but needs to transmit three times more messages per delivered application message to reach this increase in delivery ratio. If the delivery ratio is most important, `Flooding` would be chosen for such small networks and this application scenario. If the network load is more important, `Tree Routing` should be chosen.

## X. Conclusion

Unidirectional links present a challenge for routing protocols and there are a number different ways of dealing with them.

In this paper we presented ULTR, a routing protocol that uses unidirectional links explicitly, meaning that it needs to know about their existence. This knowledge can either be achieved through a neighborhood discovery protocol, or implicitly by overhearing transmissions.

The version of ULTR described and evaluated in this paper follows the second approach. We compared the delivery ratio and the cost associated with it for ULTR in the version with passive neighborhood discovery and four protocols from related work in three scenarios and showed their advantages and limitations. The evaluation featured simulations as well as experiments with real sensor nodes.

## References

[1] R. Karnapke and J. Nolte, “Unidirectional link triangle routing for wireless sensor networks,” in *Proceedings of the seventh International Conference on Sensor Technologies and Applications*, 2013, pp. 7–14.

[2] S. Lohs, R. Karnapke, and J. Nolte, “Link stability in a wireless sensor network - an experimental study,” in *3rd International Conference on Sensor Systems and Software*, 2012, pp. 146 – 161.

[3] L. Sang, A. Arora, and H. Zhang, “On exploiting asymmetric wireless links via one-way estimation,” in *MobiHoc ’07: Proceedings of the 8th ACM international symposium on Mobile ad hoc networking and computing*. New York, NY, USA: ACM Press, 2007, pp. 11–21.

[4] V. Turau, C. Renner, M. Venzke, S. Waschik, C. Weyer, and M. Witt, “The heathland experiment: Results and experiences,” in *Proceedings of the REALWSN’05 Workshop on Real-World Wireless Sensor Networks.*, Jun 2005. [Online]. Available: citeseer.ist.psu.edu/732032.html

[5] J. Zhao and R. Govindan, “Understanding packet delivery performance in dense wireless sensor networks,” in *SenSys ’03: Proceedings of the 1st international conference on Embedded networked sensor systems*. New York, NY, USA: ACM Press, 2003, pp. 1–13.

[6] M. K. Marina and S. R. Das, “Routing performance in the presence of unidirectional links in multihop wireless networks,” in *Proceedings of the 3rd ACM international symposium on Mobile ad hoc networking & computing*, ser. MobiHoc ’02. New York, NY, USA: ACM, 2002, pp. 12–23. [Online]. Available: http://doi.acm.org/10.1145/513800.513803

[7] C. E. Perkins and E. M. Royer, “”ad hoc on-demand distance vector routing.”,” in *Proceedings of the 2nd IEEE Workshop on Mobile Computing Systems and Applications, New Orleans, LA*, FEB 1999, pp. 90–100.

[8] IETF, “Unidirectional link routing (udlr).” [Online]. Available: http://datatracker.ietf.org/wg/udlr/charter/ last acessed May 2014

[9] S. Mank, R. Karnapke, and J. Nolte, “Mac protocols for wireless sensor networks: Tackling the problem of unidirectional links,” in *International Journal on Advances in Networks and Services, vol 2 no 4*, 2009, pp. 218 – 229.

[10] ——, “Mlmac-ul and ects-mac - two mac protocols for wireless sensor networks with unidirectional links,” in *Third International Conference on Sensor Technologies and Applications*, Athens, Greece, 2009.

[11] K. Langendoen, A. Baggio, and O. Visser, “Murphy loves potatoes: Experiences from a pilot sensor network deployment in precision agriculture,” in *Proc. 14th Intl. Workshop on Parallel and Distributed Real-Time Systems (WPDRTS)*, Apr. 2006.

[12] T. L. Dinh, W. Hu, P. Sikka, P. Corke, L. Overs, and S. Brosnan, “Design and deployment of a remote robust sensor network: Experiences from an outdoor water quality monitoring network,” in *LCN ’07: Proceedings of the 32nd IEEE Conference on Local Computer Networks*. Washington, DC, USA: IEEE Computer Society, 2007, pp. 799–806.

[13] T. He, S. Krishnamurthy, L. Luo, T. Yan, L. Gu, R. Stoleru, G. Zhou, Q. Cao, P. Vicaire, J. A. Stankovic, T. F. Abdelzaher, J. Hui, and B. Krogh, “Vigilnet: An integrated sensor network system for energy-efficient surveillance,” *ACM Trans. Sen. Netw.*, vol. 2, no. 1, pp. 1–38, 2006.

[14] D. Johnson, D. Maltz, and J. Broch, *DSR The Dynamic Source Routing Protocol for Multihop Wireless Ad Hoc Networks*. Addison-Wesley, 2001, ch. 5, pp. 139–172.

[15] S.-J. Lee and M. Gerla, “AODV-BR: Backup routing in ad hoc networks,” in *Proceedings of the IEEE Wireless Communications and Networking Conference (WCNC 2000)*, Chicago, IL, Sepember 2000. [Online]. Available: citeseer.ist.psu.edu/lee00aodvbr.html

[16] E. Nordström, P. Gunningberg, C. Rohner, and O. Wibling, “Evaluating wireless multi-hop networks using a combination of simulation, emulation, and real world experiments,” in *MobiEval ’07: Proceedings of the 1st international workshop on System evaluation for mobile platforms*. New York, NY, USA: ACM, 2007, pp. 29–34.

[17] I. Stojmenovic, “Simulations in wireless sensor and ad hoc networks: matching and advancing models, metrics, and solutions [topics in ad hoc and sensor networks],” *IEEE Communications Magazine*, vol. 46, no. 12, pp. 102–107, 2008.

[18] A. Varga, “The omnet++ discrete event simulation system,” in *Proceedings of the European Simulation Multiconference (ESM’2001)*, Prague, Czech Republic, Jun. 2001.

[19] A. Koepke, M. Swigulski, K. Wessel, D. Willkomm, P. Klein Haneveld, T. Parker, O. Visser, H. Lichte, and S. Valentin, “Simulating wireless and mobile networks in OMNeT++: The MiXiM vision,” in *1st Int. Workshop on OMNeT++*, mar 2008. [Online]. Available: http://www.st.ewi.tudelft.nl/ koen/papers/mixim.pdf

[20] R. Karnapke, S. Lohs, A. Lagemann, and J. Nolte, “Simulation of unidirectional links in wireless sensor networks,” in *7th International ICST Conference on Simulation Tools and Techniques, Lisbon, Portugal*, 2014.

[21] “Texas instruments ez430-chronos.” [Online]. Available: http://focus.ti.com/docs/toolsw/folders/print/ez430-chronos.html?DCMP=Chronos&HQS=Other+OT+chronos last acessed May 2014

[22] K. Walther, “Ein ereignisbasiertes betriebssystemkonzept für tief eingebettete steuersysteme,” Ph.D. dissertation, BTU Cottbus, 2009. [Online]. Available: http://opus.kobv.de/btu/volltexte/2009/772/

[23] A. Lagemann and J. Nolte, “Integration of event-driven embedded operating systems into omnet++ – a case study with reflex,” in *2nd International Workshop on OMNeT++*, Rome, Italy, March 2009.

# 3D Network Structures using Circuit Switches and Packet Switches for on-chip Data Centers

Takahide Ikeda, Yuichi Ohsita, and Masayuki Murata
Graduate School of Information Science and Technology, Osaka University
Osaka, Japan
{t-ikeda, y-ohsita, murata}@ist.osaka-u.ac.jp

***Abstract*—The energy consumption of the data center becomes a great problem. One approach to reducing the energy consumption of the data center is to use *on-chip data centers*, which are integrated circuit chips that perform the tasks in a data center. On-chip data centers are constructed of cores and the network between cores. Because the tasks are performed by the cooperation between cores in the on-chip data center, the network between cores in the on-chip data center may have a large impact on the performance and the energy consumption of the chip. In this paper, we investigate the network structures for the on-chip data centers. We focus on the 3D network structure using both circuit and packet switches, and compare the energy consumption of the candidate network structures. The results show that (1) the packet switches connected to cores should be placed in the same layer, (2) the packet switches should connect to the circuit switches in all layers, and (3) each layer should include only the minimum number of switches regardless of the traffic pattern, the size of the chip, and the ratio of the energy consumption of the packet and circuit switches.**

***Keywords*—network on-chip; data center; energy consumption; topology; 3D on-chip network**

## I. Introduction

One approach to reducing the energy consumption is to use the *on-chip data centers*, which are integrated circuit chips that performs the tasks in a data center. Because the network between cores in the on-chip data center may have a large impact on the performance and the energy consumption of the chip, we investigated the network structures suitable for the on-chip data center [1]. In this paper, in addition to the above results discussed on the previous version of this paper [1], we also investigate the impact of the traffic pattern, the size of the chip, and the ratio of the energy consumption of the packet and circuit switches on the suitable network structure.

In recent years, online services such as cloud computing have become popular, and the amount of data, required to be processed by such online services, is increasing. Such a large amount of data is handed by data centers, and many data centers have been built [2],[3]. As the services provided by data centers become popular, the energy consumption of the data centers becomes an important problem; the energy consumed by data centers occupies 1.5 % of the total energy consumption consumed in the world [3].

One approach to reduction of the energy consumption caused by the data centers is an integrated circuit chip that can perform the tasks in a data center. This kind of chip is called an *on-chip data center* [4],[5]. An on-chip data center is made of a large number of CPU cores and the network between the cores on a single chip. An on-chip data center works with a significantly small energy because of its small wiring length of the network within a chip [4].

Most of existing work on on-chip data centers focus on the usage of many cores on the chip. However, because tasks in a data center require communication between servers, the network structures between cores may have a large impact on the performance and/or the energy consumption of the on-chip data center.

The network within a chip is often called a *Network on-chip (NoC)*, and constructed of switches [6],[7]. Two types of switches are used in a NoC, packet switches and circuit switches.

A packet switch relays packets, based on their destination addresses. On the other hand, a circuit switch connects its input port with one of its output ports based on the configuration. A circuit switch consumes a small energy compared with a packet switch because it does not require any processing to relay traffic, though multiple flows from different input ports cannot share the same output port.

Several NoC architectures that use both packet and circuit switches have been proposed [6],[8],[9]. In these architectures, the circuit path between packet switches is established by configuring the circuit switches along the route of the circuit path. The set of the packet switches and the established circuit paths constructs the logical network topology. In these architectures, the logical network topology can be changed by the configuration of the circuit switches. Stensgaard et al. [9] proposed a method to configure the circuit switches suitable to the application before starting the application.

The network architectures using both of packet and circuit switches are also effective in an on-chip data center. In a data center, though the traffic pattern changes significantly and frequently, each server communicate with only a small number of servers at once [10]. Considering such traffic, the logical topology where the communicating server pairs are connected closely is preferable. This network topology can be set by setting the circuit switches in the network using both of the packet and circuit switches. Even if the traffic pattern changes, we change the network topology so as to suit the current traffic pattern by reconfiguring the circuit switches.

In recent years, another new NoC architecture called *3D NoC* has been proposed s7,ron2,ron3,ron4. The 3D NoC is constructed by stacking multiple 2D chip layers vertically. The vertically stacked layers decrease the number of hops between switches. Moreover, the vertical links of the 3D NoC are significantly shorter than the horizontal links. As a result, the 3D NoC reduces both of the energy consumption and latency.

In addition, the 3D NoC improves the effectiveness of using packet and circuit switches. Because the 3D NoC increases the number of candidate routes of the circuit paths, more circuit paths are established, which reduce the energy consumption.

However, the 3D NoC using both packet and circuit switches has not been discussed sufficiently.

We investigated the network structures suitable for the on-chip data center [1]. In this investigation, a server in an on-chip data center is constructed by multiple directly connected cores. Then, the network connects the servers.

We focused on the network constructed as a 3D network using circuit and packet switches. We investigated the network structures, focusing on the following three points; (1) connection between layers in the 3D network, (2) connection between servers and switches, and (3) placement of switches within each layer. The results show that (1) all servers should be connected to the packet switches in the same layer, (2) all packet switches should be connected to all layers, and (3) each layer should include minimum number of switches.

In addition to the above results discussed on the previous version of this paper [1], the network structures are compared, changing the traffic pattern, the size of the chip, and the ratio of the energy consumption of the packet and circuit switches. Through this evaluation, we show that our discussion on the suitable network structure is applicable regardless of the traffic pattern, the size of the chip, and the ratio of the energy consumption of the packet and circuit switches.

The rest of this paper is organized as follows. Section II explains the overview of the on-chip data center used in this paper. In Section III, we investigate the network structures suitable to the on-chip data center. Section IV presents the conclusion.

## II. On-Chip Data Center Network

### A. The Outline Of On-Chip Data Center

The on-chip data center is a chip that plays the roles of the servers and network between servers in a data center. The on-chip data center is constructed of cores and the network between cores. Similar to the traditional data center, where a task handling a large amount of data is performed by the cooperation of the servers [11],[12] , the tasks in an on-chip data center are performed by cores cooperating with each other; each task is split into subtasks, and the subtasks are assigned to the cores. Each core performs the assigned subtask, and it obtains the data or the results of the other subtasks from the other cores via the network, if the data or the results are required.

The network between cores is important in the on-chip data center, because the cores cooperate with each other via the network to complete the task. The network should provide the bandwidth between communicating cores with small energy consumption. The network within the on-chip data center consumes less energy than the traditional data center network, because of its small wiring length of the network within a chip [4]. However, the energy consumption of the on-chip network depends on the network structures. Therefore, we investigate the network structures for the on-chip data center.

### B. Components of On-Chip Data Center

The on-chip data center is constructed of multiple cores and a network between cores. The details of the components in the on-chip data center are described below.

*1) Core:* In the on-chip data center, there are two kinds of the cores. One is the computing core that performs the process of the assigned task. The other is the memory core that stores the data.

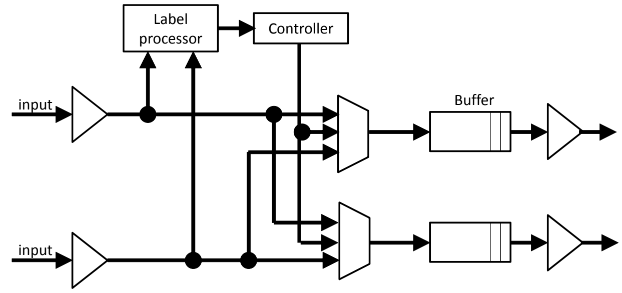


Figure. 1. Packet switch

In an on-chip data center, each task is split into multiple subtasks, and the subtasks are assigned to the computing cores. The computing core performs the assigned subtask, cooperating with multiple memory cores; the computing core reads the required data from the memory cores, and writes the results of the process to the memory cores.

As described above, the cores cooperating with each other; the results of the other computing cores may be required to complete the assigned subtask. In this case, the core obtains the required data generated by the other cores via the network between cores.

*2) Network:* The network within an on-chip data center is constructed of two kinds of switches described below.

*a) Packet Switch:* A packet switch is a switch that relays the packet based on the destination written in the header of the packet. An example of the architecture of the packet switch is shown in Figure 1. When a packet arrives, the destination written in the header of the packet are processed by the label processor. Based on the destination, the output port, to which the packet is relayed, is determined. Then, the controller configure the switch to relay the packet to the buffer deployed at the output port. Finally, the packet is sent to the next switch or core from the buffer.

The energy consumption of the packet switch increases as the number of arriving packets increases, because the processes of the label processors and the controller are performed each time a packet arrives. Moreover, writing a packet to a buffer or reading a packet from a buffer also consumes energy. Therefore, the number of packet passing the packet switches should be reduced to save the energy consumption.

*b) Circuit Switch:* A circuit switch is a switch that connects its input and output ports based on the configuration. After the configuration of the ports, all packets arriving the input port is relayed to the output port connected to the input port. An example of the architecture of the circuit switch is shown in Figure 2.

The circuit switch consumes less energy than the packet switch, because the circuit switch does not require complicated processing such as label processing and decision of the output ports. However, the circuit switch cannot relay flows from different input ports to the same output port, because each output port can be connected at most one input port in the circuit switch.

### C. The Architecture of On-Chip Data Center Used in This Paper

Figure 3 shows the on-chip data center used in this paper.

In this architecture, one computing core and multiple memory cores are vertically stacked and directly connected.

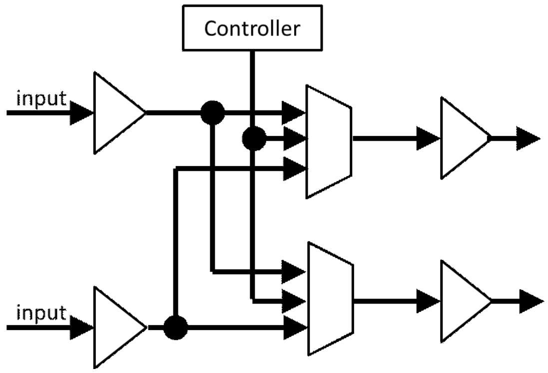


Figure. 2. Circuit switch

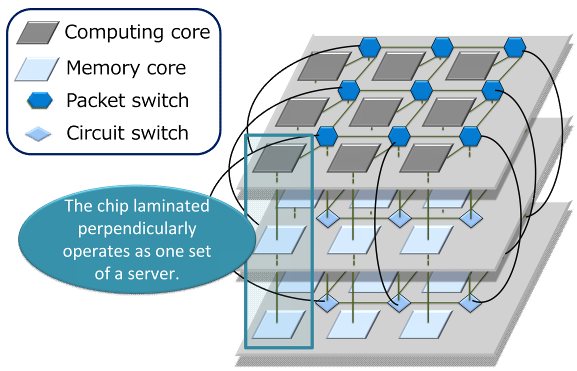


Figure. 3. On-chip data center used in this paper

The connected cores act as a single server in a data center. Hereafter, the connected cores are simply called *server*.

In this architecture, the servers are placed in a lattice, and the network between servers is constructed of switches placed in a 3D lattice, because the lattice network can be easily constructed on a chip.

In this architecture, both kinds of switches, packet switches and circuit switches are used. The packet switches are deployed where there is a link from/to a server, so that each server communicates with multiple servers at once. In this paper, the same number of packet switches as the servers are deployed, and each server is connected to the network by connecting one of its cores to one of the packet switches.

Though we do not allow each packet switch to be connected to multiple servers in this paper, the discussion of the suitable network structure is applicable to the case that each packet switch can be connected to multiple servers, because connection to multiple servers has no impact except for the increase of the candidates of the first packet switch and the last packet switch on the route between the servers. The switches not connected to servers are circuit switches because the circuit switches consumes less energy.

In this network, the traffic is sent after constructing the logical network topology by setting the circuit paths between packet switches. The circuit paths are established by configuring the circuit switches along the paths. Then, the traffic is sent over the logical network topology of the packet switches constructed by the circuit paths.

This network structure has the following parameters; (1) the connection between layers, (2) the layers where switches connected to servers are deployed, and (3) the types of switches deployed in each layer, which are discussed in Section III.

## III. Comparison of Network Structures for On-Chip Data Centers

### A. Compared Network Structures

In this section, we investigate the network structures suitable to on-chip data centers by comparing the network structures constructed with various parameters. In our comparison, all network structures are constructed of packet switches with 9 ports and circuit switches with 10 ports. The number of vertical layers are set to 5.

The rest of this subsection describes how to set the parameters of the network structures in this comparison.

*1) Inter-Layer Connection:* The first parameter is the inter-layer connection. There are two types of the inter-layer connection. The first one is shown in Figure 4(a) In this type of the connection, switches in all layers are connected to the same packet switch. We call this type of connection the *packet switch centric connection (PCC)*.

The other type is shown in Figure 4(b) In this types of connection, all vertical links are constructed only between nearest layers. For example, a switch placed at the $i$th layer is connected only with the switches placed at the $i-1$th layer and the $i+1$th layer. This type is called of connection the *nearest layer connection (NLC)*. In the NLC, we construct the close connection between the nearest layers. All vertical links from the switches are connected to the switches at the nearest layer.

In our comparison, the PCC and the NLC use 1 of 9 port of a packet switch to connect to the server, 4 of 9 ports of each packet switch to connect the switches within the same layer, and the other ports to connect the switches at the different layers.

*2) Connection between Servers and Switches:* In the on-chip data center investigated in this paper, each server is connected to one of the packet switches nearest to the server. As shown in Figure 5, there are two types of connections between servers and switches. In the first type of the connection, all servers are connected to the switches in the same layer. We call this type of connection the *same layer connection (SLC)*. In the other type of connection, the servers neighboring with each other are connected to the switches in the different layers. We call this type of connection the *different layer connection (DLC)*.

In the SLC, the number of hops between servers is small because all servers are connected in the same layer. However, the connections of packet switches at the first layer are static. On the other hand, the connections between packet switches can be changed in any layers in the DLC.

*3) Placement of Switches within a Layer:* There are two kinds of placement of the switches in the same layer. The first one is shown in Figure 6(a). In this type of the placement, we deploy the same number of switches as the number of servers in each layer. We call this type of placement *minimum placement (MP)*. In the other type of placement, we add the circuit switches around the packet switches. We call this type of placement the *additional circuit switch placement (ACP)*.

The ACP has more candidates of routes of circuit paths between the packet switches than the MP. Thus, the energy efficient routes may be found, even when the number of circuit

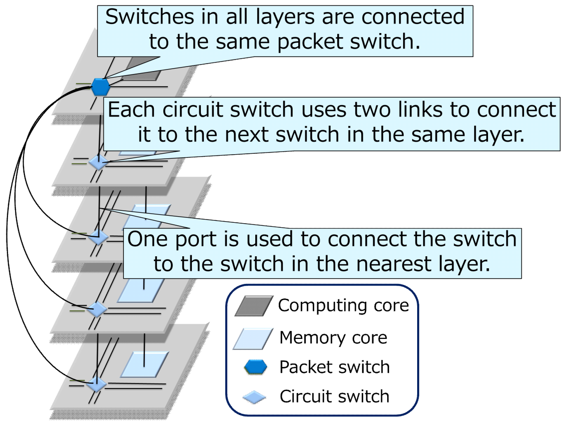


(a) Packet switch centric connection

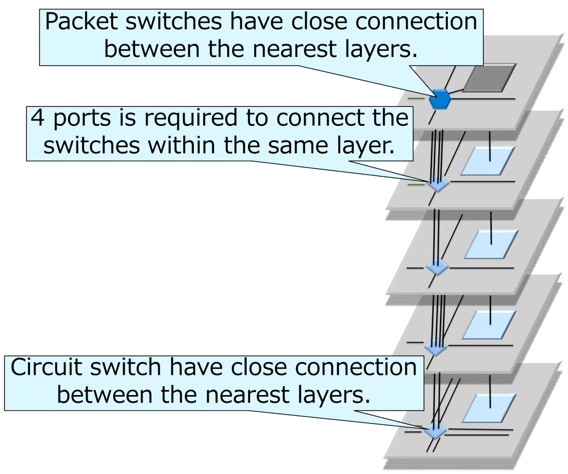


(b) Nearest layer connection

Figure. 4. Inter layer connection

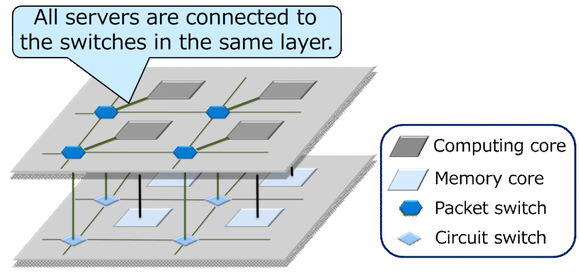


(a) Same layer connection

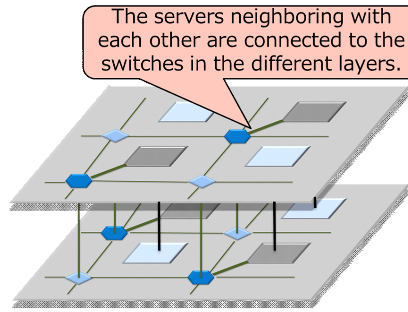


(b) Different layer connection

Figure. 5. Connection from servers

path to be established is large. However, the number of circuit switches passed by each circuit path in the ACP is larger than that in the MP.

### B. Models Used in Our Comparison

*1) Energy consumption model:* The energy consumed by the network on-chip depends on (1) network structure, (2) the traffic amount on the network, and (3) the bit flips of the traffic.

Wolkotte et al. [13] model the energy consumed by a circuit switch, a packet switch and a link in the NoC. In this model, the circuit switch consumes $E^{\text{packet}}$ $\mu$W, the packet switch consumes $E^{\text{circuit}}$ $\mu$W, and the link consumes $(E^{\text{stlink}} + E^{\text{prlink}}L)$ $\mu$W : where $L$ is a length of link (mm) to relay 1 bit of traffic. In this paper, this model is used to evaluate the energy consumption. In our comparison, we first set $E^{\text{packet}}$ to 0.98, $E^{\text{circuit}}$ to 0.37, $E^{\text{stlink}}$ to 0.39, and $E^{\text{prlink}}$ to 0.12, according to results by Wolkotte et al. [13]. Then, we also investigate the impact of the ratio of the energy consumption of the packet and circuit switches by changing $E^{\text{circuit}}$.

In this paper, we focus only on the energy consumed by the network, and exclude the energy consumed by the cores, because the energy consumed by the cores is independent from the network structures.

*2) Traffic Model:* According to Benson et al. [10], each server communicates with only a small number of servers at once, though all server pairs can communicate with each other and communicating server pairs change in time. In this paper, we focus on the energy consumption to relay all traffic generated at a certain time period. Thus, we generate traffic between the server pairs selected by using the uniform random values, and set the traffic rates between the server pair to 10,000 bits. In our evaluation, we vary the number of communicating server pairs from 500 to 2,000, and generate 10 patterns of traffic for each of the cases of the number of communicating server pairs by using the different random seeds.

*3) Latency Model:* In this paper, we also compare the latency to relay the generated traffic. We define the latency as the time required to receive all traffic by the destination servers after generating the traffic demands.

In this paper, we assume that each packet can be relayed by a packet switch to the next packet switch in 1 clock cycle. Though the clock cycle required to relay a packet depends on the switch architectures and may be different from this model. The suitable network structures discussed in this paper are independent of switch architectures because the order of latencies is the same as the results in this paper even if multiple clock cycles are required to relay a packet.

In the on-chip data center, we also use the circuit switches. The circuit switch is configured to connect the input and output ports in advance. The packet switches can be connected by configuring the circuit switches. The packet switch pairs, connected by the circuit paths, relay the packets by the same way as the packet switches that are directly connected to each other. The relay of the packets by the circuit switch takes no clock cycles. Thus, the latency depends only on the number of packet switches passed by the flow.

*4) Path Computation Model:* We calculate the routes of traffic so as to make the energy consumed by the traffic small. In this paper, the route of each traffic demand is calculated by the Dijkstra algorithm setting the weights of the links to the

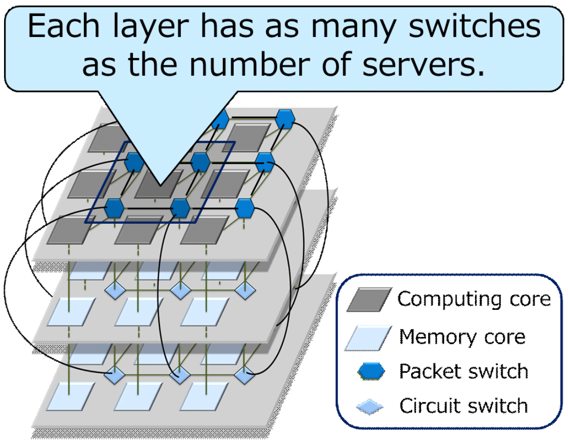


(a) Minimum placement

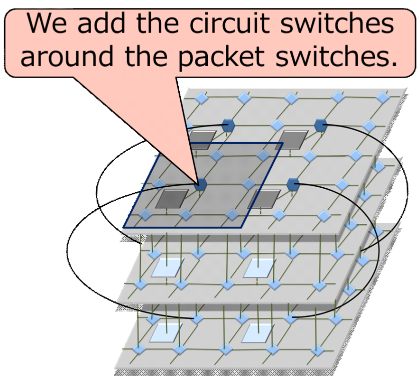


(b) Additional circuit switch placement

Figure. 6. Placement of switches within each layer

energy consumed to relay the traffic. If the calculated route uses the circuit switch, we connect both ends of the input and the output ports, and remove the ports of the circuit switch before the calculation of the routes of the next traffic demands, so as to avoid the output ports of the circuit switch used by the other traffic from the different input ports.

In this path computation, we assume that the traffic demands are known before calculating the routes. By using this model, we discuss the suitable network structure when the routes are calculated optimally. However, the actual traffic demands may be unknown when calculating routes, and we require a method to calculate the routes without traffic demand information, which is one of our future work.

### *C. Network Structure Suitable to On-Chip Data Centers*

In this subsection, we discuss the network structure suitable to on-chip data centers, which accommodates traffic between servers with low energy consumption. We compare the network structures constructed by various parameters of the network structures. The network structure has three kinds of parameters as described in Section III-A. For each kind of parameter, we have two types of settings. Therefore, $2 \times 2 \times 2 = 8$ network structures are constructed by setting the parameters of the network structure. In this subsection, we compare all of them.

To evaluate the energy consumption, we use the energy model based on the results by Wolkotte et al. [13]. That is,

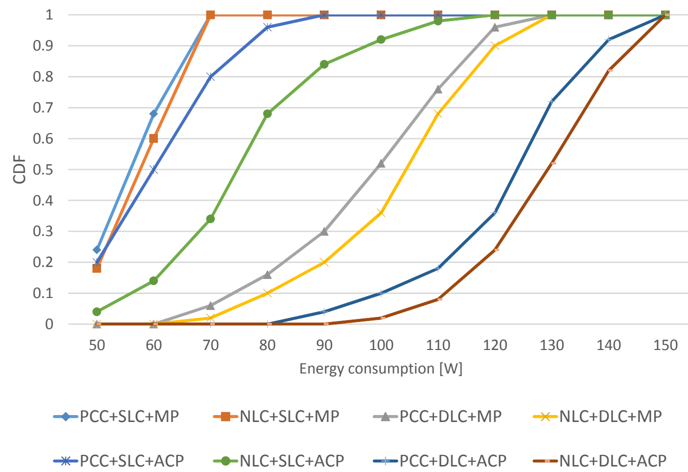


Figure. 7. CDF of the energy consumption (Chip size=10 $\times$ 10, Number of communicating server pairs=1000, Energy model by Wolkotte et al. [13])

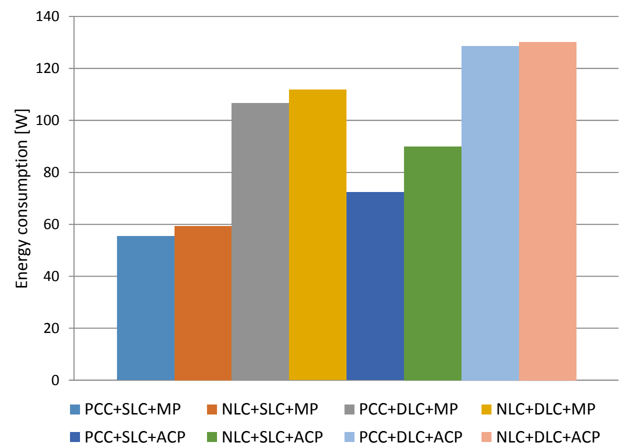


Figure. 8. Comparison of the worst-case energy consumption (Chip size=10$\times$10, Number of communicating server pairs=1000, Energy model by Wolkotte et al. [13])

we set $E^{\text{packet}}$ to 0.98, $E^{\text{circuit}}$ to 0.37, $E^{\text{stlink}}$ to 0.39, and $E^{\text{prlink}}$ to 0.12. We set the number of servers in the chip to 100, and the servers are placed in $10 \times 10$ lattice. We set the length of the intra-layer link to 2 mm, and the length of the inter-layer link to 1 $\mu$m. We select 1000 communicating server pairs randomly and generate traffic between the selected server pairs.

Figure 7 shows the comparison of the cumulative distribution function of the energy consumption. The vertical axis is the cumulative distributed function, and the horizontal axis is the energy consumption. We also compare the worst-case energy consumption, and the average of the energy consumption in Figures 8 and 9. In these figures, the vertical axis is the energy consumption.

Figure 10 shows the comparison of the cumulative distribution function of the latency. The vertical axis is the cumulative distribution function, and the horizontal axis is the latency. We also compare the worst-case of the latency in Figure 11.

The rest of this subsection discusses the impact of each parameter of the network structure.

*1) Comparison of Inter-layer connections:* We first discuss the impact of the inter-layer connections by comparing the

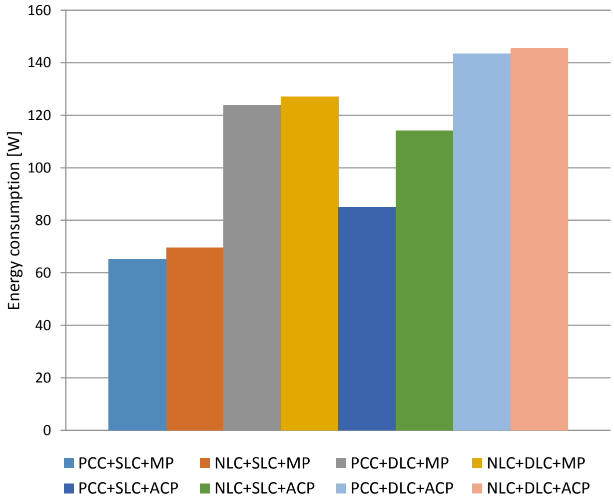


Figure. 9. Comparison of the average of the energy consumption (Chip size=10 × 10, Number of communicating server pairs=1000, Energy model by Wolkotte et al. [13])

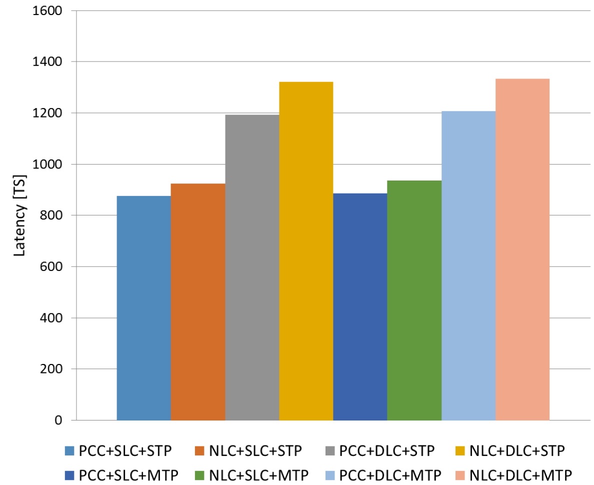


Figure. 11. Comparison of the worst-case of the latency (Chip size=10 × 10, Number of communicating server pairs=1000, Energy model by Wolkotte et al. [13])

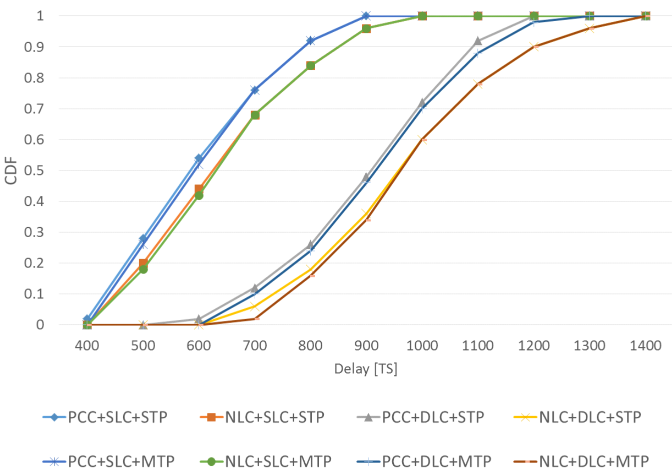


Figure. 10. CDF of the latency (Chip size=10 × 10, Number of communicating server pairs=1000, Energy model by Wolkotte et al. [13])

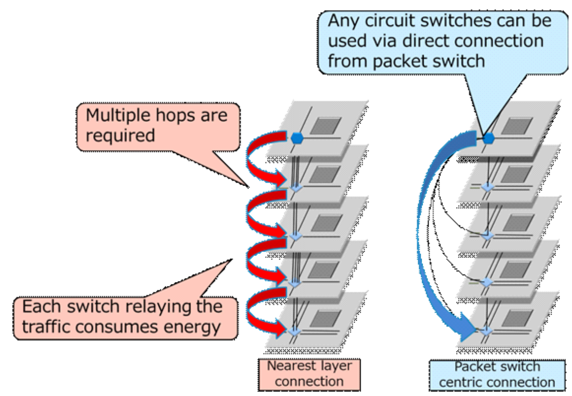


Figure. 12. The cause of the difference between the PCC and the NLC

network structures with the PCC and those with the NLC. That is, we perform the following comparisons.

- Network structure with PCC, SLC and MP vs. Network structure with NLC, SLC and MP
- Network structure with PCC, DLC and MP vs. Network structure with NLC, DLC and MP
- Network structure with PCC, SLC and MP vs. Network structure with NLC, SLC and ACP
- Network structure with PCC, DLC and MP vs. Network structure with NLC, DLC and ACP

Figures 7, 8, and 9 show that the energy consumption of the network structures with the PCC is always smaller than those with the NLC. This is because a circuit path using the circuit switch whose layer is far from the packet switch is required to pass multiple layers in the NLC as shown in Figure 12. Because each circuit switch relaying the traffic consumes energy, the large number of circuit switches passed by the circuit paths causes a large energy consumption. On the other hand, the packet switches are directly connected to the circuit switches in all layers in the PCC, and the number of switches passed by traffic is smaller than the NLC.

Figures 10 and 11 show that the PCC also achieves smaller latency than the NLC. This is because the PCC establishes more circuit paths since circuit paths consumes less energy in the network structures with the PCC than the NLC. The circuit paths reduce not only the energy consumption but also the latency, because the packet switch relays the packet to the switch connected via the circuit path within one clock cycle.

*2) Comparison of the Connection between Servers and Switches:* We investigate the impact of the connection between servers and switches by comparing the network structures with the SLC and those with the DLC. That is, we perform the following comparisons.

- Network structure with PCC, SLC and MP vs. Network structure with PCC, DLC and MP
- Network structure with NLC, SLC and MP vs. Network structure with NLC, DLC and MP
- Network structure with PCC, SLC and MP vs. Network structure with PCC, DLC and ACP
- Network structure with NLC, SLC and MP vs. Net-

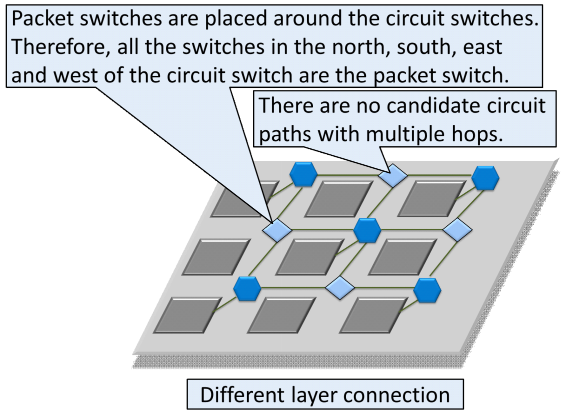


Figure. 13. Circuit path establishment within a layer in the DLC

work structure with NLC, DLC and ACP

Figures 7, 8, and 9 show that the energy consumption of the network structures with the SLC is smaller than those with the DLC. There are two reasons for this. The first reason is that the packet switches prevent establishment of long circuit paths in the DLC. As shown in Figure 13, the packet switches are placed around the circuit switches in some layers in the DLC, and the circuit paths with multiple hops should be established via the different layers, while such long circuit paths are established via any layers including the circuit switches in the network structure with the SLC.

The other reason is that there are no packet switches directly connected to each other in the DLC. Therefore, even the flow between the servers neighboring with each other requires the circuit paths, which consumes more energy than the directly connected link between packet switches.

Figures 10 and 11 show that the SLC achieves the smaller latency than the DLC, because the SLC can establish more circuit paths than the DLC.

*3) Comparison of Placement of Switches within a Layer:* Finally, we discuss the impact of the placement of switches within a layer. The ACP increases the number of candidate routes for the circuit paths. However, the number of hops becomes larger than the MP. Comparing the network structures with the ACP and those with the MP, we clarify whether the larger number of candidate circuit paths is preferable or the smaller number of hops between servers is preferable.

We compare the network structures with the MP and those with the ACP. That is, we perform the following comparisons.

- Network structure with PCC, SLC and MP vs. Network structure with PCC, SLC and ACP
- Network structure with NLC, SLC and MP vs. Network structure with NLC, SLC and ACP
- Network structure with PCC, DLC and MP vs. Network structure with PCC, DLC and ACP
- Network structure with NLC, DLC and MP vs. Network structure with NLC, DLC and ACP

Figures 7, 8, and 9 show that the network structures with the MP always achieve a smaller energy consumption than those with the ACP. That is, in despite of the large number of candidate circuit paths, the ACP does not reduce the energy consumption.

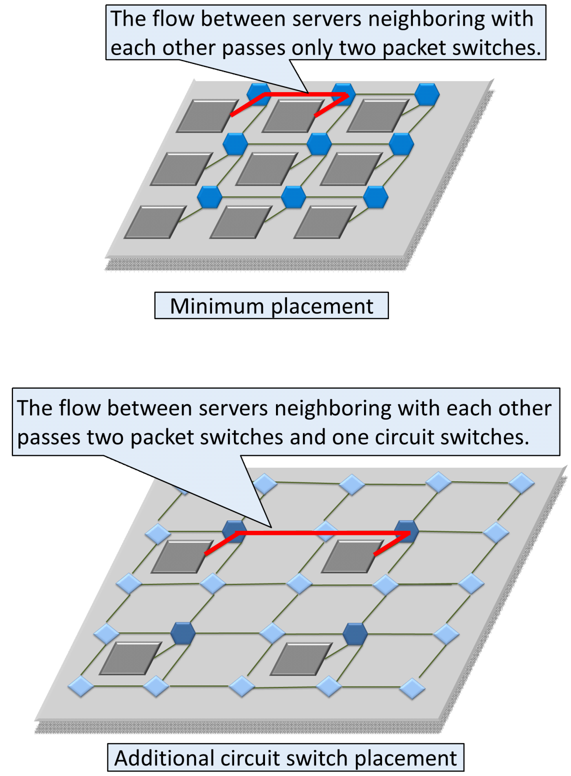


Figure. 14. Routes of the flow between the servers neighboring with each other

This is because a sufficient number of circuit paths are established even in the network structures with the MP. In addition, circuit paths pass more circuit switches in the network structures with the ACP than those with the MP. Especially, the flow between servers neighboring with each other passes only two packet switches in the network with the MP, but it passes two packet switches and one circuit switches in the network with the ACP as shown in Figure 14. Such additional switches passed by the flows increases the energy consumption.

Figures 10 and 11 show that the MP and ACP achieve the similar latency. This is because the similar number of circuit paths are established in the MP and the ACP as discussed above.

*4) Summary of the Results:* As discussed above, to save the energy consumption and reduce the latency, (1) the suitable inter-layer connection is the PCC, (2) the suitable connection between servers and switches is the SLC, and (3) the suitable placement of switches within a layer is the MP.

### *D. Impact of the number of communicating server pairs*

In Section III-C, we investigated only the case that the number of communicating server pairs is 1000. However, the number of communicating server pair has an impact on the energy consumption or the latency of the network; as the number of communicating server pair increases, the energy consumption becomes large. This may have an impact on the suitable network structures.

In this subsection, we discuss the impact of the number of communicating server pairs on the suitable network structures. In this subsection, we compare the network structures, changing the number of communicating server pairs from 500

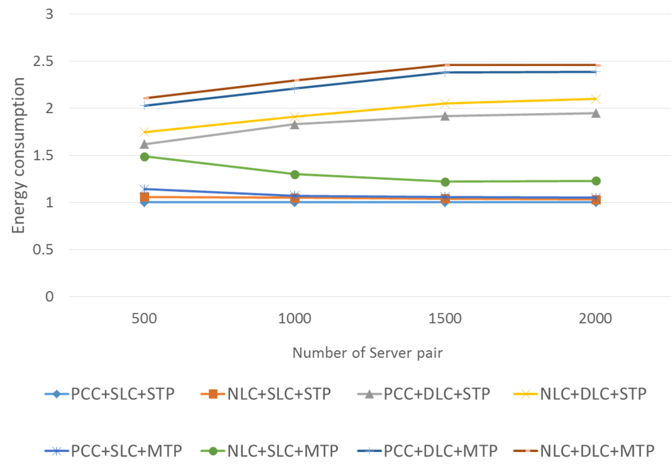


(a) Average

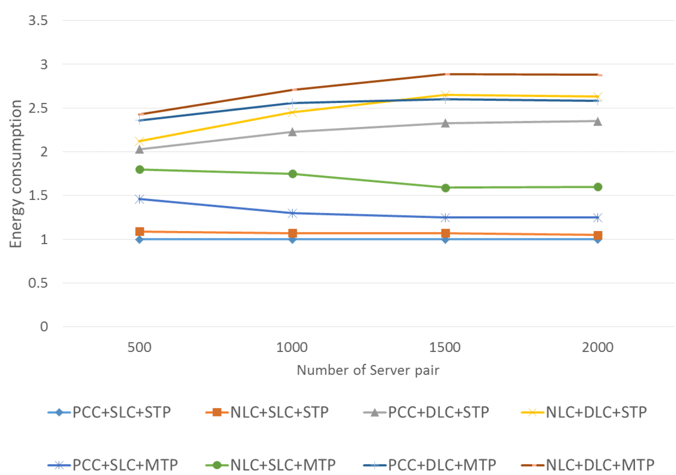


(b) Worst-case

Figure. 15. The impact of the number of communicating server pairs on the energy consumption

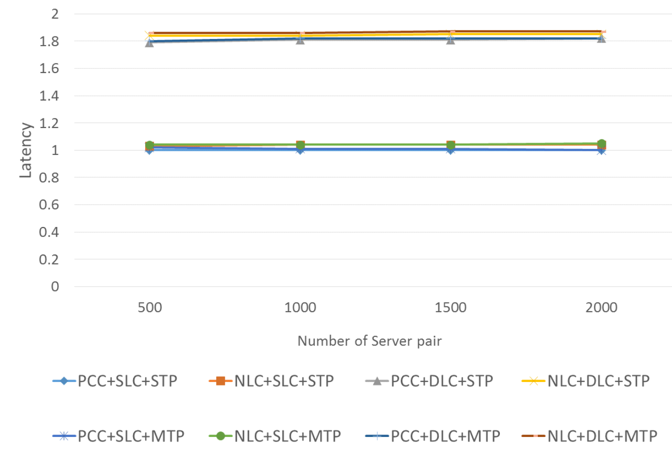


(a) Average

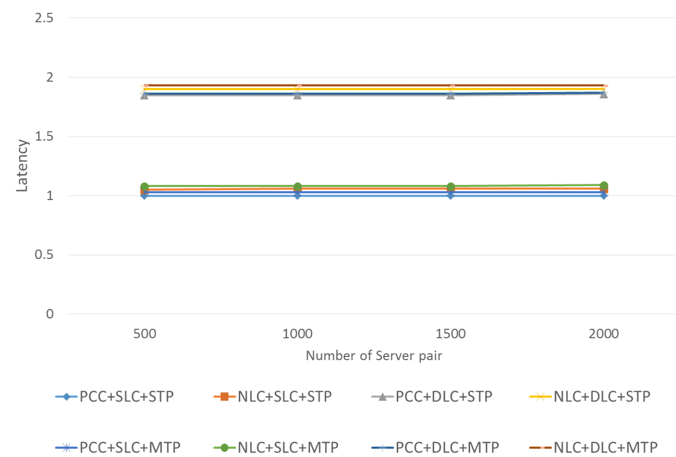


(b) Worst-case

Figure. 16. The impact of the number of communicating server pairs on the latency

to 2,000. We set the other parameters to the same values as Section III-C. We generated 10 patterns of traffic for each case.

Figures 15 and 16 show the results. In these figures, the horizontal axis is the number of communicating server pairs, and the vertical axis is the energy consumption or latency normalized by that of the network structure with the PCC, the SLC and the MP, that achieves the smallest energy consumption in the results.

As shown in Figure 16, the number of communicating server pairs has no impact on the ratio of the latency of the network structures. The latency depends on the number of packet switches passed by each packet. The number of packet switches passed by each packet depends on whether the circuit paths to bypass packet switches can be established, and is independent from the number of communicating server pairs. As a result, the number of communicating server pairs has no impact on the ratio of the latency. Therefore, the rest of this subsection discusses the impact of the number of communicating server pairs on the energy consumption.

*1) Impact on Suitable Inter-layer Connections:* First, we investigate the impact of the number of communicating server pairs on the suitable inter-layer connections.

Figure 15 shows that the network structures with the PCC consume the smaller energy than those with the NLC regardless of the number of communicating server pairs. As discussed in Section III-C1, the difference of the energy consumption between the PCC and the NLC is caused by the difference of the number of switches passed by the circuit paths. Regardless of the number of communicating server pairs, the number of switches passed by the circuit paths in the NLC is larger than those in the PCC, because the circuit paths pass multiple layers to use the circuit switches in the layer far from the packet switch in the NLC while each packet switch has direct connection to any layers in the PCC. As a result, even if the communicating server pair changes, the network structures with the PCC achieves the small energy consumption.

*2) Impact on Suitable Connection between Servers and Switches:* We investigate the impact of the number of communicating server pairs on the suitable connection between servers and switches.

Figure 15 shows that the energy consumption of the network structures with the DLC is larger than those with the SLC, and the difference of the energy consumption increases as the number of communicating server pair increases. As discussed in Section III-C2, one of the reasons of the difference of the energy consumption between the SLC and the DLC is the difference of the number of candidate circuit paths. When the number of communicating server pairs is large, a large number of circuit paths are established to accommodate the flows between server pairs with a small energy consumption in the network structures with the SLC. However, due to the small number of candidate circuit paths, in the network structures with the DLC, we cannot establish as many circuit paths as the SLC. As a result, the difference of the number of established circuit paths causes the difference of the amount of traffic passing the packet switches; more traffic passes the packet switches and consumes more energy in the network structures with the DLC than those with the SLC.

*3) Impact on Suitable Placement of Switches within a Layer:* Finally, we investigate the impact of the number of communicating server pairs on the suitable placement of switches within a layer.

Figure 15 shows that the energy consumption of the network structures with the ACP is larger than those with the MP, but the difference of the energy consumption decreases as the number of communicating server pair increases.

The difference of the energy consumption between the network structures with the MP and those with the ACP is caused by the difference in the number of candidate circuit paths and the length of the circuit paths; the network structures with the ACP provides more candidate circuit paths than the network structures with the MP, though the number of circuit switches passed by the circuit paths is large. When the number of communicating server pairs is small, both of the MP and the ACP can establish the sufficient number of circuit paths. Thus, the difference of the energy consumption is caused only by the difference of the number of switches passed by the circuit paths, and the network structures with the MP achieve the smaller energy consumption than the ACP. On the other hand, when the number of communicating server pairs is large, more circuit paths are required. In this case, the MP cannot establish the sufficient number of circuit paths, and the flows passes multiple packet switches. In the ACP, we add more circuit paths, though the number of circuit switches passed by the circuit paths is large. This causes the decrease of the difference of the energy consumption between the MP and the ACP.

Figure 15 shows that even when the number of communicating server pairs is 2,000, the network structures with the MP achieve the smaller energy consumption than those with the ACP. When the number of communicating server pairs is 2,000, each server communicates with 20 % of the servers at once. Because each server communicates with only a small number of servers at once in the typical data centers [10], the case that each server communicates with more than 20 % of the servers seldom occurs. Therefore, the MP is suitable for the on-chip data centers regardless of the number of communicating server pairs.

## E. Impact of the size of the chip

In the above discussions, we investigate only the case that the chip includes 100 servers. However, the size of the chip has an impact on the energy consumption of the network; as the size of the chip increases, the energy consumption becomes large. This may have an impact on the suitable network structure.

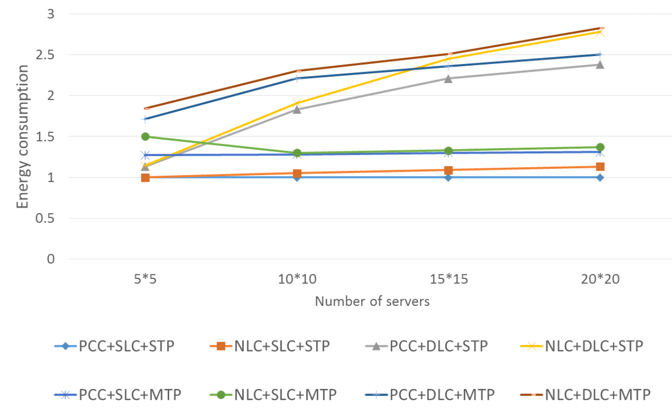


(a) Average

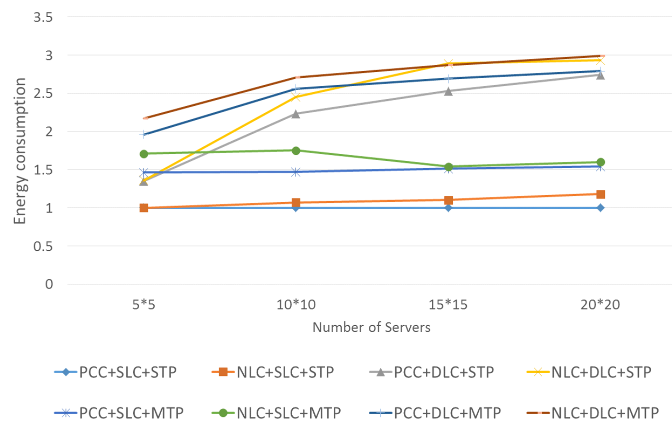


(b) Worst-case

Figure. 17. Impact of the size of the chip on the energy consumption

In this subsection, we discuss the impact of the size of the chip on the suitable network structures. In this subsection, we compare the network structures, changing the number of servers within a chip from 25 to 400. We set the other parameters to the same values as Section III-C.

Figures 17 and 18 show the results. In these figures, the horizontal axis is the size of the chip, and the vertical axis is the energy consumption or latency normalized by that of the network structure with the PCC, the SLC and the MP, that achieves the smallest energy consumption in results.

Based on these figures, the rest of this subsection discusses the impact of the size of the chip on suitable parameters of the network structures.

*1) Impact on Suitable Inter-layer connections:* We discuss the impact of the size of the chip on the suitable inter-layer connections.

Figure 17 shows that the energy consumption of the network structures with the PCC is smaller than those with the NLC regardless of the size of the chip, though there are the cases that the difference is significantly small.

As discussed in Section III-C1, the difference of the energy consumption between the PCC and the NLC is caused by the difference of the number of switches passed by the circuit paths. If we can establish the sufficient number of circuit paths without using the layers far from the packet switches, the

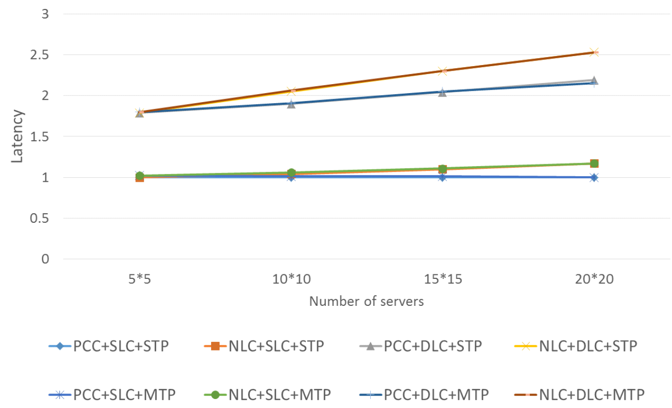


(a) Average

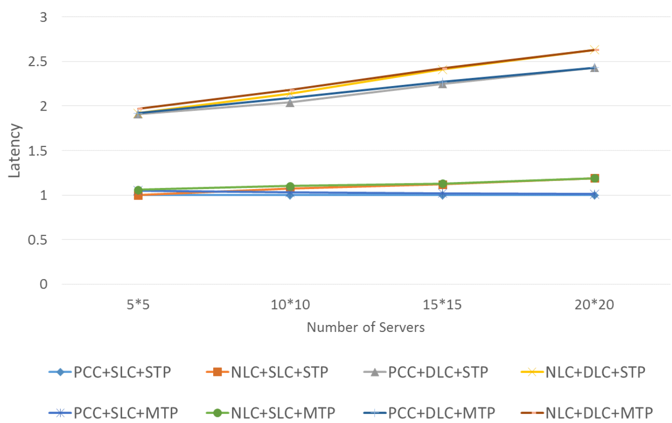


(b) Worst-case

Figure. 18. Impact of the size of the chip on the latency

network structures with the NLC achieves the similar energy consumption to those with the PCC. However, the number of circuit switches passed by the circuit paths in the network structures with the NLC is always larger than those with the PCC, because the circuit paths passes multiple layers to use the circuit switches in the layer far from the packet switch in the NLC while each packet switch has direct connection to any layers in the PCC. As a result, the energy consumption of the network structures with the PCC is smaller than those with the NLC regardless of the size of the chip.

Figure 18 shows that the latency of the network structure with the PCC is smaller than those with the NLC, and the difference becomes large as the size of the chip increases. This is because the PCC tends to establish more circuit paths than the NLC, because establishing the circuit paths in the PCC consumes less energy than the NLC. As the size of the chip increases, the number of hops of the established circuit paths becomes large, and the latency reduced by establishing the circuit path becomes large. As a result, the difference of the latency caused by the difference of the number of the established circuit paths becomes large as the size of the chip increases.

*2) Impact on Suitable Connection between Servers and Switches:* We investigate the impact of the size of the chip on the suitable connection between servers and switches.

Figure 17 shows that the energy consumption of the network structures with the SLC is smaller than those with the DLC, and the difference becomes large as the size of the chip increases. As the size of the chip becomes large, the difference of the energy consumption between the circuit paths and the routes without using the circuit paths becomes large, due to the increase of the switches passed by the flow. Thus, more circuit paths are required to be established. However, the number of candidate circuit paths in the network structures with the DLC is smaller than that in the network structures with the SLC. Thus, we cannot establish the sufficient number of circuit paths in the DLC because of the lack of the candidate paths, while sufficient number of circuit paths are established in the SLC. This causes the increase of the difference of the energy consumption.

Figure 18 shows that the latency of the network strucures with the SLC is smaller than those with the DLC and the difference becomes large as the size of the chip increases. This is because we cannot establish the sufficient number of circuit paths in the DLC, while the SLC establishes more circuit paths. As discussed in the section III-E1, the difference of the latency caused by the number of established circuit paths becomes large as the size of the chip. As a result, the difference of the latency between the SLC and the DLC becomes large as the size of the chip increases.

*3) Impact of Suitable Placement of Switches within a Layer:* We discuss the impact of the size of the chip on the suitable placement of switches within a layer.

Figure 17 shows that the energy consumption of the network structures with the MP is smaller than those with the ACP regardless of the size of the chip. This is because even the network structures with the MP have a sufficient number of candidate circuit paths regardless of the size of the chip, though the network structures with the ACP provides more candidate circuit paths than the network structures with the MP. As a result, the ACP consume more energy since the circuit paths pass more circuit switches.

Figure 18 shows that the MP and the ACP achieve the similar latency. This is because the MP and the ACP establishes the similar number of circuit paths regardless of the size of the chip.

### *F. Impact of the energy consumption of the switches*

In the above discussions, we investigate only the case that the energy consumption of the circuit switch $0.37\mu$W/bit. However, the energy consumption of the circuit switch depends on the architecture of the switches. Therefore, in this subsection, we investigate the impact of the energy consumption of the switches on the energy consumption of the network structures. We change the energy consumption of the circuit switch from 1/2 to 1/10 of the model used in the previous subsections. We set the other parameters to the same values as Section III-C.

Figure 19 shows the result. In this figure, the horizontal axis is the ratio of the energy consumption of the circuit switch compared with the model by Wolkotte et al. [13], and the vertical axis is the energy consumption normalized by that of the network structure with the PCC, the SLC, and the MP, that achieves the smallest energy consumption in the results.

*1) Impact on Suitable Inter-layer connections:* We investigate the impact of the energy consumption of the circuit switches on the suitable inter-layer connection.

Figure 19 shows that the energy consumption of the network structures with PCC is smaller than those with the NLC,

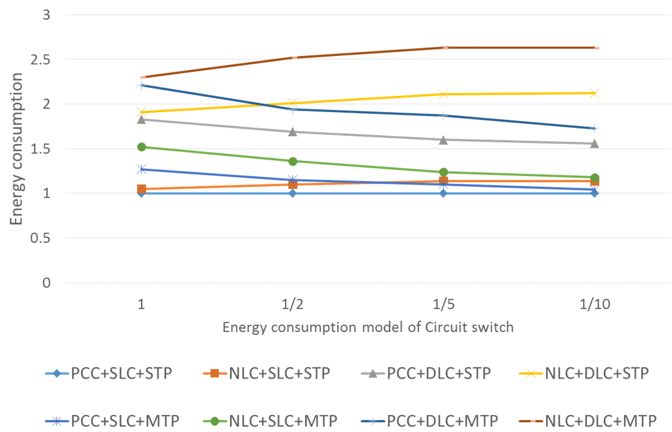


(a) Average

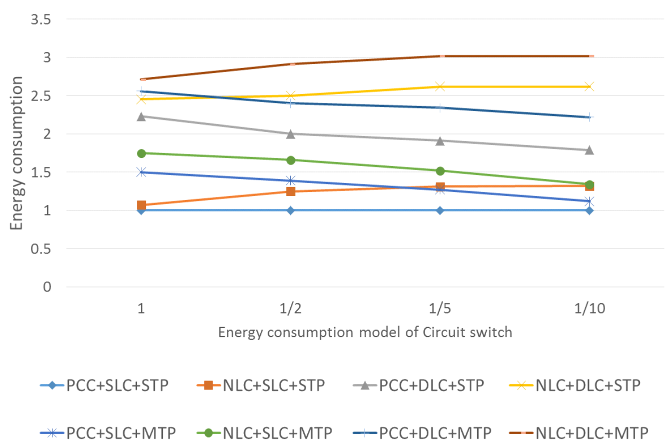


(b) Worst-case

Figure. 19. Impact of the energy consumption of circuit switches on the energy consumption

but the difference becomes small as the energy consumption of the circuit swich decreases. As discussed in Section III-C1, in the NLC, the circuit path passes multiple circuit switches to use the circuit switches in the layer far from the packet switches. Thus, the energy consumption in the case of using the circuit paths is large in the network structure with the NLC, compared with the PCC. When the energy consumption of the circuit switches becomes small, more circuit paths are established because the energy reduction by using the circuit path increases. Thus, the difference caused by the number of circuit switches passed by the circuit paths becomes large.

*2) Impact on Suitable Connection between Servers and Switches:* In this subsection, we compare the network structures of the different types of the connections between servers and switches.

Figure 19 shows that the energy consumption of the network structures with the SLC is smaller than those with the DLC, and the difference becomes small as the energy consumption of the circuit switch becomes small except the comparison between the network structure with the NLC, the SLC and the ACP, and that with the NLC, the DLC and the ACP, where the number of the circuit switches passed by the circuit paths is the largest among the compared network structures. As discussed in Section III-C2, the circuit paths is required even for the flow between the servers neighboring with each other in the DLC, which is one of the reasons why the DLC consumes more energy than the SLC. As the energy consumption of the circuit switches becomes small, the energy consumed by the circuit paths established for the flows between the servers neighboring with each other decreases. As a result, the difference of the energy consumption between the SLC and the DLC becomes small.

However, as shown in Figure 19, even if the energy consumption of the circuit switch becomes 1/10 of the model by Wolkotte et al. [13], the energy consumption of the network structures with the DLC is much larger than those with the SLC. That is, even if the energy consumption of the circuit switches is reduced, the SLC is suitable to the on-chip data centers.

*3) Impact on Suitable Placement of Switches within a Layer:* Finally, we compare the impact of the energy consumption of circuit switches on the suitable placement of switches within a layer.

Figure 19 shows that the energy consumption of the MP is smaller than the ACP, but the difference becomes small as the energy consumption of the circuit switch becomes small. This is because the network structures with the ACP has more candidate circuit paths between packet switches, though the number of circuit switches passed by the circuit paths is large. As the energy consumption of the circuit switch becomes small, the additional energy caused by the number of circuit switches passed by the circuit paths becomes small, and the impact of the number of candidate circuit paths becomes large.

However, even when the energy consumption of the circuit switches becomes 1/10 of the model by Wolkotte et al. [13], the ACP consumes more energy than the MP. That is, even if the energy consumption of the circuit switches is reduced, the MP is suitable to the on-chip data centers.

### *G. The number of the required layers*

In the network structure with the PCC, SLC, and STP, the circuit switch nearest to the packet switch among the available circuit switches is used to establish a circuit path, because using the circuit paths far from the packet switch consumes more energy. Thus, even if we construct an on-chip data center with many layers, the layers far from the packet switches may not be used at all.

In this subsection, we investigate the number of layers used to establish a circuit switches. Figure 20 shows the results. In

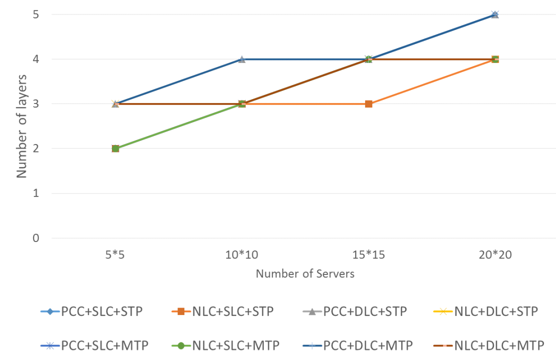


Figure. 20. The cause of the difference between the PCC and the NLC

this figure, the horizontal axis is the size of the chip, and the vertical axis is the maximum number of layers used to establish circuit paths in our method.

As shown in Figure 20, as the number of servers increases, the number of used layers becomes large. However, Figure 20 indicates that the circuit switches at the 5-th layer are never used even in case of 15*15 servers. That is, a small number of layers is sufficient in the on-chip data center.

## IV. Conclusion and Future Work

In this paper, we evaluated the 3D on-chip network structures for the on-chip data centers, which uses both of the circuit and packet switches. According to the results, to reduce the energy consumption, (1) the servers should connect to the packet switches in the same layer, (2) the packet switches should connect to the circuit switches in all layers, and (3) each layer should include minimum number of switches, regardless of the size of the chip, and the ratio of the energy consumption of the packet and circuit switches.

Our future work includes the method to calculate the routes suitable to the on-chip networks.

## Acknowledgments

This work was partially supported by JSPS Grant-in-Aid for Young Scientists (B)23700077.

## References

[1] T. Ikeda, Y. Ohsita and M. Murata, “3D on-chip data center networks using circuit switches and packet switches,” in *Proceedings of The Eighth International Conference on Systems and Networks Communications*, Oct. 2013, pp. 125–130.

[2] D. Abts and B. Felderman, “A guided tour of data-center networking,” in *Communications of the ACM*, vol. 10, Jun. 2012, pp. 44–51.

[3] J. G. Koomey and P. D, “Growth in data center electricity use 2005 to 2010,” *The New York Times*, Aug. 2011.

[4] R. Iyer, R. Illikkal, L. Zhao, S. Makineni, D. Newell, J. Moses, and P. Apparao, “Datacenter-on-chip architectures: Tera-scale opportunities and challenges in Intel’s manufacturing environment,” in *Intel Technology Journal*, vol. 11, Aug. 2007, pp. 227–237.

[5] M. Kas, “Toward on-chip datacenters: a perspective on general trends and on-chip particulars,” in *The Journal of Supercomputing*, vol. 62, Oct. 2012, pp. 214–226.

[6] T. Bjerregaard and S. Mahadevan, “A survey of research and practice of network-on-chip,” vol. 1-51, Mar. 2006.

[7] A. Ankur, C. Iskander, and R. Shankar, “Survey of network on chip architectures & contributions,” *Journal of Engineering, Computing and Architecture*, pp. 21–27, 2009.

[8] M. B. Stensgaard and J. Sparso, “ReNoC: A network-on-chip architecture with reconfigurable topology,” in *Proceedings of the Second ACM/IEEE International Symposium on Networks-on-Chip*, Apr. 2008, pp. 55–64.

[9] M. Modarressi, H. Sarbazi-Azad, and M. Arjomand, “A hybrid packet-circuit switched on-chip network based on sdm,” in *Proceedings of the Design, Automation & Test in Europe Conference & Exhibition, 2009. DATE ’09*, Apr. 2009, pp. 566–569.

[10] T. Benson, A. Anand, A. Akella, and M. Zhang, “MicroTE : Fine grained traffic engineering for data centers,” in *Proceedings of the Seventh COnference on emerging Networking EXperiments and Technologies*, Dec. 2011, pp. 1–12.

[11] J. Dean and S. Ghemawat, “MapReduce: simplied data processing on large clusters,” in *Communications of the ACM*, vol. 51, Jan. 2008, pp. 107–114.

[12] J. Leibiusky, G. Eisbruch, and D. Simonassi, “Getting Started with Storm,” in *O’Reilly*, 2012.

[13] P. T. Wolkotte, G. J. M. Smit, N. Kavaldjiev, J. E. Becker, and J. Becker, “Energy model of networks-on-chip and a bus,” in *Proceedings of IEEE International Symposium on System-on-Chip*, Nov. 2005, pp. 82–85.

# An Energy-Efficient Multichannel Packet Transmission Scheduling for Ad Hoc Networks

Thiago Fernandes Neves, Felipe de Moraes Modesto, and Jacir Luiz Bordim
Department of Computer Science
University of Brasilia, UnB
Brasilia, Brazil.
Email: {tfn.thiago, felipe, bordim}@cic.unb.br

***Abstract*—The popularization of wireless network technologies has driven the quest for efficient solutions in the use of the available resources. In particular, there is an increasing demand for solutions to reduce energy consumption and improve channel use. This work addresses the problems of multi-channel assignment and communication scheduling in wireless networks. Considering that channel allocation is a NP-complete problem, this paper presents a time and energy-efficient heuristic to tackle the multi-channel assignment problem. Once channel assignment is performed, an energy-efficient protocol allows the stations to complete their data transfers using minimum resources. The protocol divides its operation in management and transmission stages. The main contribution of this work is to present a multi-channel communication protocol that efficiently reduces communication time by exploring multiple channels even for control messages. Empirical results show that the management stage takes, in average, less than $9\%$ from the protocol total time while the transmission stage, in average, takes only $5\%$ more time than the optimum time.**

***Keywords–energy efficient protocols, multi-channel assignment, scheduling, wireless networks.***

## I. Introduction

The quest for uninterrupted wireless connectivity has been highly influenced by the popularization of mobile devices and social networks. This trend in mobile applications has motivated the proposal of Medium Access Control (MAC) protocols capable of coping with a varying number of application demands and devices characteristics. Despite of these advances, one of the major concern regarding the design of such protocols is the need to reduce energy consuption [1]. As wireless devices usually operate on battery power, and recharging them may not be an option while on the move, means to preserve and extend nodal lifespan is of interest.

Among existing energy-saving strategies, *topology control* and *duty-cycle* have been widely employed in the context of wireless networks [2]. Topology control techniques typically allow wireless devices to adjust their transmission power in order to conserve energy without affecting network connectivity [3]. Duty-cycle schemes, on the other hand, allow wireless devices to alternate between inactive and active mode. When in active mode, devices are able to send or receive data; while in doze mode devices remain in energy conservation mode and are not able to send or receive data. This last strategy is particularly challenging as devices in doze mode are not able to receive data packets. There are research opportunities regarding the development of techniques that ensure communicating devices are only active when they have data to send or receive [4]. In [5], the authors show that energy consumption can be reduced by increasing the time needed to complete a given task and vice-versa. The authors have shown that these parameters are usually conflicting and finding a compromise between them is not trivial.

Regardless the fact that most wireless devices are capable to tune to different frequencies to send and/or receive data packets, existing MAC protocols are usually designed to operate on a single-channel, where all the nodes are confined [6]. Channel assignment in wireless networks is usually performed during the deployment phase. The reason behind this is that channel assignment is a complex and time consuming task that may not produce the desirable results when naive approaches are employed. Indeed, the Channel Assignment Problem (CAP) satisfies the interference constraints by maximizing throughput. In its general form, the CAP problem is equivalent to the Generalized Graph-coloring Problem (GCP), which has been proved to be an NP-complete problem [7]. This work explores duty-cycle techniques and propose a multi-channel assignment heuristic that enables the transmission scheduling of data items to be carried out in an energy-efficient manner.

The remainder of this paper is organized as follows. Section II describes related works. Section III describes the communication model considered in this work. Section IV presents the channel assignment problem along with an energy-efficient heuristic to tackle it. The EEMC-MAC protocol details is described in Section V. The simulation environment and results are presented in Section VI. The building blocks to adapt the proposed EEMC-MAC to multi-hop environment is presented is Section VII. Finally, Section VIII concludes the work and presents future direction.

## II. State of the Art

To reduce packet collision, protocols such as the IEEE 802.11 are available and can reduce interference in ongoing communications. The control mechanism applied in IEEE 802.11 is the well-known CSMA/CA protocol [8]. By listening before transmitting data, nodes can determine whether a channel is busy or available. However, this mechanism does not avoid the overexploitation of spectrum resources. Indeed, scenarios with excessive competition may drastically reduce network throughput. The CSMA/CA protocol relies on random *backoff* and cannot prevent communications from starting simultaneously. Channel assignment in wireless network environments is typically static. This means that, while channel selection can be based on spectrum conditions during network initialization, channel degradation does not cause the data channel to be changed. Thus, MAC protocols that are tailored for single-channel settings have difficulties copping with heavy network loads and fail to provide means for networks to switch channels depending on spectrum occupancy.

Access to multiple communication channels is an alternative to increase throughput in wireless networks [9]. For example, by employing opportunistic spectrum access techniques, users can temporary access unused licensed frequencies [10]. With access to multiple channels, Frequency Division Multiple Access (FDMA) based techniques allows the selection of several communication channels with non-overlapping and non-interfering frequencies. Therefore, multiple pairs of nodes can communicate at the same time without interference given they have been allocated to different channels. Indeed, a number of works consider the use of multiple channels in wireless networks [11], [12], [13], [14], [15], [16]. Hamdaoui *et al.* [11] proposed a protocol where the channels are assigned to groups based on "transmission intentions". In this scheme, each group elects a leader to study channel conditions and select the best channel for itself. All data channels operate independently and intergroup coordination is performed by channel leaders using a dedicated control channel. Alternatively, Hsu *et al.* [12] propose a contention model based on channel aggregation. The protocol considers that multiple data channels can be used simultaneously for data transfers. Transmission pairs select the channels used for transmission based on average occupancy and *backoff* necessary to access these channels. These protocols focus in increasing network throughput and do not consider the energy costs involved with their communication cycles. An example of an early energy efficient protocol is defined in [5], where a randomized time- and energy-optimal routing protocol is proposed. To achieve this goal, users learn their roles in packet routing and wait for their turn by deferring spectrum access to either receive or send data packets, thus reducing energy costs. The protocol, however, requires that users know information about the network during initialization and is applied to a single-channel network context.

The use of multi-channel MAC protocols with duty-cycle schemes to increase network throughput and decrease energy consumption is proposed in [14], [17]. These works focused on multi-channel energy-efficient protocol tailored for wireless sensor networks. Incel *et al.* [14] proposed a scheme that works in a distributed fashion and schedules communications based on Time Division Multiple Access (TDMA) algorithms. This approach has been shown to reduce packet collision by informing the nodes what periods of time they need to be active. The proposed scheme, however, focuses on maximizing throughout while energy consumption is a secondary goal. Tang *et al.* [17] proposed a protocol that allows transmitting nodes to estimate the receiving nodes' activation time without the use of a control channel. Zhang *et al.* [15] proposed a multi-channel MAC protocol for ad hoc networks. The proposed scheme works by dividing its operation in management and transmission stages. At the beginning of the management stage, all the nodes wishing to communicate turn to the control channel. The management stage dynamically adjusts its duration based on the traffic and it is used to allow the nodes to reserve data channels using a dedicated, common, control channel. During the transmission window, nodes communicate using several channels, while non-communicating nodes stay in doze mode.

In previous work, we proposed an energy efficient protocol for multi-channel allocation and transmission scheduling in wireless networks, termed ECOA-BP [18]. As in [15], the ECOA-BP protocol divides its operation in management and transmission stages and uses a control channel during the management stage. The technique proposed uses efficient transmission assignment and duty-cycle strategy to alternate the nodes between active and inactive modes, thus reducing the power drainage rate. Previous works show that is possible to reduce energy consumption at the cost of higher communication time [5]. Both Zhang *et al.* [15] and Neves *et al.* [18] focus on balancing these parameters. Additionally, both works consider that network coordination is performed in a single control channel. Independently of the number of available channels, the use of a single control channel to manage channel access can be a bottleneck, as it increases the communication time [19]. Concerned with coordination costs, Cordeiro *et al.* [20] propose that the management stage, known as Beacon Period (BP), takes place in the data channels. The authors suggest that channel access is structured into recurring super-frames synchronized globally so that users can migrate between channels to communicate with different nodes. While the model proposed achieved promising results, it does not consider the energy costs required to implement and maintain global coordination.

### A. Our Contribution

The aforementioned works focused on exploiting the availability of multiple channels to improve communication time. However, they neglect to analyze energy conservation and the overhead introduced by the proposed coordination schemes. This paper addresses the problems of multi-channel allocation, transmission scheduling and energy consumption in wireless networks. As in related works, it assumes that the devices work on batteries and have a single transceiver, capable of tuning to one of the several available channels and to switch between active (regular energy consumption) and inactive (reduced energy consumption) operation modes. As customary, time is assumed to be slotted with slot durations long enough to ensure that a single data packet can be transmitted or received by any user in the network within a single slot [5], [14]. In this context, this paper proposes a time and energy-efficient protocol capable of performing multi-channel allocation and transmission scheduling in a wireless setting. This paper is an extended version of work published in [1]. The proposed scheme, termed *Energy-Efficient Multi-Channel MAC protocol* (EEMC-MAC) divides its operation into management and transmission stages. Unlike most similar proposals, the proposed protocol uses all the available channels in both management and transmission stages. Experimental results show that the management stage, in average, takes less than $5\%$ from the total protocol execution time, while the transmission stage is optimum in terms of energy consumption.

## III. Communication Model

Consider an Ad Hoc network consisting of a group of $n$ nodes each with a single transceiver and unique identifier

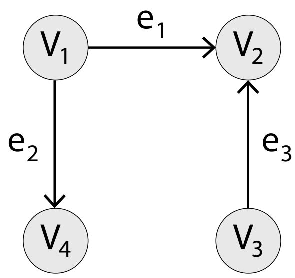


Figure 1: Communication graph example with 4 nodes.

(UID), connected as a single-hop network represented by the complete graph $\mathcal{G}_n$. The communication scenario of this network is represented by a directional graph $G = (V, E)$, where $V = \{v_1, v_2, ..., v_n\}$ is a set of nodes (vertices) and $E$ is a set of communications (edges), $E \subseteq V^2$. Consider $E = \{e_1, e_2, ..., e_p\}$, where $e_h = \{(v_s, v_d) | \{v_s, v_d\} \subseteq V, s \neq d\}$, $1 \leq h \leq p$, as a set of edges representing the communication graph of the network $\mathcal{G}_n$. Each edge $e_h = (v_s, v_d) \in E$ represents a communication between a source node $v_s$ and a destination node $v_d$. Each node is assumed to have at most one packet per destination in the communication graph. Let $s_i$ be the transmission set of a node $v_i$ ($v_i \in V$). That is, $s_i$ represents all the nodes that $v_i$ has data packets to send to. Furthermore, let $d_i$ be the reception set of a node $v_i$. Hence, $d_i$ represents all the nodes that have data packets to send to $v_i$. Thus, for a given communication graph $\mathcal{G}_n$, each node $v_i$ has $\tau_i = |s_i| + |d_i|$ data packets to send and receive. In other words, $\tau$ represents the amount of time a node needs to be awake to ($i$) transmit the data packets to its neighbours; and ($ii$) receive the items destined to it.

As an example, Figure 1 represents a possible communication graph for a network topology $\mathcal{G}_n$. In this figure, $V = \{v_1, v_2, v_3, v_4\}$ and $E = \{e_1, e_2, e_3\}$, where $e_1 = (v_1, v_2)$, $e_2 = (v_1, v_4)$ and $e_3 = (v_3, v_2)$. In this communication graph, node $v_1$ has data to send to nodes $v_2$ and $v_4$ and no data to receive, thus, $s_1 = \{v_2, v_4\}$ and $d_1 = \emptyset$. Similarly, $s_2 = \emptyset$, $d_2 = \{v_1, v_3\}$, $s_3 = \{v_2\}$, $d_3 = \emptyset$, $s_4 = \emptyset$ and $d_4 = \{v_1\}$.

As presented in [15], this paper assumes that data transmission/reception occur in time slots, with each transmission/reception taking exactly one time slot. In each time slot $t_j$, $j \geq 0$, where $t_j$ is equal to the time interval $[t_j, t_{j+1})$, a node can be in active or inactive operation mode. When active, a node can send or receive data. In case a node is not transmitting or receiving data, the node goes into idle mode so as to save power. That is, energy consumption is associated with the amount of time that the node remains in active mode. Consider $C = \{c_1, c_2, ..., c_k\}$ as the set of available channels for communication. When a channel $c_i, 1 \leq i \leq k$, is used by a pair of nodes in the time slot $t_j$, it will be unavailable for other nodes in this time slot. In the case that two or more transmitting nodes use the channel $c_i$ during time slot $t_j$, a collision occurs and the data packets are lost. Hence, the challenge is to find a scheduling that: ($i$) allows the transmitting nodes to send and receive data without collision; and ($ii$) minimizes the communication time. Table I summarizes the notations used throughout this work.

## IV. The Channel Assignment Problem (CAP)

In a network environment where many data channels are available, the task of channel assignment that satisfies interference constraints and maximizes throughput is known as the Channel Assignment Problem (CAP). To prevent interference between communications, a same channel cannot be allocated for two pairs of neighbouring nodes simultaneously. In its general form, the CAP problem is equivalent to the Generalized Graph-coloring Problem (GCP), which is known as a NP-complete problem [7]. Given the communication graph $G$ and $k$ channels in the presented communication model, the CAP consists in performing the communications using the minimum amount of time and communication channels. Note that if $k = 1$ this problem is simplified, once all the communications must be serialized. However, in the general case scenario, optimum solutions are complex to obtain.

Because the CAP is NP-complete, many researchers have proposed heuristics and approximation algorithms with lower computational costs. These solutions, however, can not guarantee optimum results. The proposed alternatives vary from neural networks, to genetic and graph theory based heuristics [7]. Next, an heuristic based on graph theory to solve the CAP problem is presented.

### A. ECOH: An Edge Coloring Heuristic

The proposed heuristic, termed *Edge COloring Heuristic* (ECOH), takes as input a communication graph $G = (V, E)$ and a number $k$ of available channels and produces as output a list of “communication sets”, called $CS$. The list of communication sets is defined by $CS = \{CS_1, CS_2, ..., CS_r\}$, with $CS_i \subseteq E$ and the elements in $CS_i$ are disjoint, $1 \leq i \leq r \leq |E|$. The details of the ECOH is presented in Figure 2. The basic idea behind the proposed heuristic is the distribution of edges belonging to $E$ into $r$ communication sets, so that the edges contained in a set $CS_i$ have no dependencies with each other. In this context, dependencies occur between two or more communication sets that involve a same node $v_i$. The selection criterion is the choice of an edge belonging to a greater degree vertex in $E$. This edge will be part of the initial transmission set $CS_i$ and it will be a comparison base for the other edges belonging to $E$. Only the edges without dependences with other elements in $CS_i$ will be removed from $E$ and incorporated into this set. An edge is considered not dependent on a set of edges when it does not share any vertex with the edges on this set. The procedure is repeated until the $r$ transmission sets are formed and the set $E$ is empty.

To better understand the operations of the ECOH, consider as input the communication graph represented in Figure 1 and the number of available channels to be equal to 2 ($k = 2$). Thus, $E = \{e_1, e_2, e_3\}$, where $e_1 = (v_1, v_2)$, $e_2 = (v_1, v_4)$ and $e_3 = (v_3, v_2)$. Suppose that the edge $e_2$ is inserted into the first set of edges in $CS_1$, line 5 (Figure 2). Going through all edges of $E$, line 6, the algorithm checks that the edge $e_3$ has no dependence on the set $CS_1$ and decides to insert it, line 8. As there are no more edges in $E$ without dependencies with the elements of the set $CS_1$, the algorithm terminates the loop. A new loop is then started, line 2, and the variable $r$ is incremented to 2. In the new loop, the algorithm inserts the edge $e_1$ in the set $CS_2$, ending the algorithm, since

TABLE I: TABLE OF NOTATIONS.

| Symbol | Definition |
|---|---|
| $\mathcal{G}_n$ | Graph modelling the wireless network topology; |
| $G = (V, E)$ | Graph representing the communication scenario; |
| $V = \{v_1, v_2, ..., v_n\}$ | Set of nodes (or devices); |
| $E = \{e_1, e_2, ..., e_p\}$ | Set od edges (or transmissions); |
| $n$ | Number of nodes ($n = \|V\|$); |
| $p$ | Number of edges, ($p = \|E\|$); |
| $\Delta(G)$ | Maximum graph degree; |
| $s_i$ | Number of items $v_i$ has to send (i.e., $v_i$'s transmission set); |
| $d_i$ | Number of items destined to $v_i$ (i.e., $v_i$'s reception set); |
| $\tau_i$ | Total number of items $v_i$ sends and receives ($\tau_i = \|s_i\| + \|d_i\|$); |
| $C = \{c_1, c_2, ..., c_k\}$ | Set of channels; |
| $k$ | Number of available channels ($k = \|C\|$); |
| $g_i$ | Subset of $V$ ($g_i \subseteq V$); |
| $l$ | Number of nodes in $\|g_i\|$; |
| $T_m$ | EEMC-MAC management stage time (in time slots); |
| $T_t$ | EEMC-MAC transmission stage time (in time slots); |
| $T$ | Management and transmission stage time ($T = T_m + T_t$); |
| $T_{t'}$ | EEMC-MAC transmission state optimum time (in time slots); |

**Algorithm** ECOH($G$,$k$)

```
1: G = (V, E), r ← 0;
2: while (E ≠ ∅) do
3:     r ← r + 1;
4:     Select an edge e of the vertex with higher degree in E;
5:     CS_r ← e, E ← E − e;
6:     for (each e_h ∈ E) do
7:         if (no vertex in e_h ∈ CS_r) and (|CS_r| ≤ k) then
8:             CS_r ← CS_r ⋃ e_h;
9:             E ← E − e_h;
10:        end if
11:    end for
12: end while
13: CS ← {CS_1, CS_2, ..., CS_r};
```

Figure 2: The details of the proposed Edge COloring Heuristic (ECOH).

the condition $E = \emptyset$ is reached, line 2. In this example, the algorithm output would be $CS = \{CS_1, CS_2\}$, where $CS_1 = \{e_2, e_3\}$ and $CS_2 = \{e_1\}$. Note that, according to the algorithm, $|CS_i| \leq k$. That means each communication set has at most $k = 2$ disjoint elements. This construction allows the nodes in each communication set $CS_i$ to communicate concurrently using the $k$ channels in the same time slot.

From the above, it is clear that the ECOH processes all edges of the graph (while-loop), selecting, at each iteration, a set of at most $k$ independent edges (i.e., no two edges share a common vertex). As the set operations can be performed in $O(1)$ time, the ECOH takes $O(p{\cdot}k) \leq O(p^2)$ time to complete its execution. For latter reference, we state the above results in the following Lemma:

*Lemma 1:* The task of computing $r$ disjoint communication sets $CS_i$, $(1 \leq i \leq r)$, where each $CS_i$ comprises of at most $k$ independent edges, can be computed in $O(p^2)$ time, where $p = |E|$.

## V. Proposed Protocol

This section presents the details of the proposed protocol, named *Energy Efficient Multi-Channel MAC Protocol* (EEMC-MAC Protocol). This protocol aims to perform multi-channel allocation and scheduling to enable data communication. The protocol performs these tasks in order to minimize both energy consumption and the time required to transmit data. Thus, the goodness of the protocol, in terms of energy consumption, is assessed by evaluating the number of transmitting time slots a node is awake during the protocol execution. This evaluation does not consider the processing time of a given task, which is assumed to be lower than the cost of tramissing or receving a data packet [5]. First, the overall routines performed by the protocol are presented. Then, the protocol is described in detail, followed the analysis of its complexity.

### A. Transmission Set Grouping Routines

Recall that each node $v_j \in V$ contains a set $s_j$ identifying the destination nodes that $v_j$ has data to send. In this subsection, the objective is to combine such sets for a given node. The $CombineGroup$ routine, presented in Figure 3, aims to achieve this goal using a single communication channel. The routine takes as input a set of nodes $g_i$, $g_i \subseteq V$, and a communication channel $c_i$. In the first step of the algorithm, each node in $g_i$ computes a consecutive local ID in the range $[1, .., l]$, in line 2. That is, $|g_i| = l$. This task can be accomplish by employing fast, energy-efficient, leader election algorithms such as those presented in [21], [22]. Clearly, after this step, node $v_l$ representes the node with the highest ID in $g_i$. The loop in lines $3 - 8$ combines the transmission sets $s_j$, $1 \leq j \leq l$ so that node $v_l$ knows $s_l \cup s_{l-1} \cup ... \cup s_1$ at the end of the algorithm. Note that the routine above is very efficient in terms of energy consumption given that each node stays in active mode for 2 time slots: one to receive the transmission set and another to sent the combined transmission set. For latter reference, we state the following result:

*Lemma 2:* The task of combining $l$ transmissions sets $s_l \cup s_{l-1} \cup ... \cup s_1$ can be performed on a single channel in $l - 1$ time slots with each node $v_j$, $(1 \leq j \leq l)$, awake for at most 2 time slots.

Consider a set of channels $C = \{c_1, c_2, ..., c_k\}$ where $|C| = k$, $k > 1$ are available. In this example, the $CombineGroup$ routine can be improved to take advantage of several channels. The routine $CombineTS$, as depicted

**Algorithm** CombineGroup($g_i$,$c_i$)

1: Let $|g_i| = l$;
2: Each node computes its local ID within the range $[1, ..., l]$ such that $g_i = \{v_1, v_2, ..., v_l\}$;
3: **for** $j \leftarrow 1$ **to** $l - 1$ **do**
4: Nodes $v_j$ and $v_{j+1}$ enter in active mode;
5: $v_j$ sends its transmission set $s_j$ to $v_{j+1}$ using channel $c_i$;
6: Node $v_{j+1}$ attaches $s_j$ to $s_{j+1}$;
7: Node $v_j$ enters in inactive mode;
8: **end for**

Figure 3: Algorithm that combines the transmission sets in a group.

**Algorithm** CombineTS($g_i$,$C$)

1: Let $|g_i| = l$ e $|C| = k$;
2: **if** ($k \geq \lfloor \frac{l}{2} \rfloor$) **then**
3: Let $C = \{c_1, c_2, ..., c_k\}$;
4: Each node computes its local ID within the range $[1, ..., l]$ such that $g_i = \{v_1, v_2, ..., v_l\}$;
5: **while** ($l > 1$) **do**
6: **for** ($i \leftarrow 0$ **to** $(\frac{l}{2} - 1)$) in parallel **do**
7: Assign channel $c_{i+1}$ to pair ($v_{i+1}$,$v_{l-i}$);
8: $v_{l-i}$ sends its transmission set $s_{l-i}$ to $v_{i+1}$;
9: $v_{i+1}$ makes $s_{i+1} = s_{i+1} \bigcup s_{l-i}$;
10: $v_{l-i}$ goes into inactive mode;
11: **end for**
12: $l \leftarrow l/2$;
13: **end while**
14: **end if**

Figure 4: Algorithm that combines the transmission on all groups.

**Algorithm** ManagementStage($n, k$)

1: All the nodes in $V = \{v_1, v_2, ..., v_n\}$ start in inactive mode;
2: **if** ( $k < \lfloor \frac{n}{2} \rfloor$) **then**
3: Divide the nodes in $V$ into $k$ groups: $g_1, g_2, ..., g_k$;
4: **for** $i \leftarrow 1$ **to** $k$ in parallel **do**
5: Execute *CombineGroup*($g_i$,$c_i$);
6: **end for**
7: **end if**
8: Let $g_l$ denote de set of active stations;
9: The active stations execute *CombineTS*($g_l$,$C$);
10: Let $v_m$ be the last active station from the previous step;
11: Node $v_m$ uses the transmission sets information to build the communication graph $G$;

Figure 5: Building the communication graph from the obtained transmission sets.

in Figure 4, shows how transmission sets can be combined, using multiple channels simultaneously. Similarly to the $CombineGroup$ routine, $CombineTS$ takes two parameters as input: a group of nodes $g_l$, $g_l \subseteq V$, and a set of channels $C$, where $|g_l| = l$ and $|C| = k$. The routine is only executed if $k \geq \lfloor \frac{l}{2} \rfloor$, this way, all the transmissions in $g_l$ can be parallelized in the $k$ channels. At the beginning of the algorithm, all the active nodes compute their local ID in the range $[1, ..., l]$, line 4. The procedure grows a binary tree, combining the leaf nodes and working its way to the root using the $k$ available channels, lines 5-13. At the end of the algorithm, the local node $v_1$ will have all the transmission sets $s_l \cup s_{l-1} \cup ... \cup s_1$.

The $CombineTS$ routing algorithm consists of two nested loops (line 5 and 6). The inner loop is executed in parallel for all available channels, taking a single time slot for each $l/2$ channels while the outer loop is executed for $\log l{+}1$ iterations. As $k \geq \lfloor \frac{l}{2} \rfloor$, the $CombineTS$ takes at most $\log k{+}1$ time slots to combine the transmitting sets of a group of $l$ nodes. The above discussion is summarized into the following Lemma:

*Lemma 3:* The task of combining $l$ transmissions sets $s_l \cup s_{l-1} \cup ... \cup s_1$ on a $k$-channel setting can be accomplished in $\log k + 1$ time slots with each node $v_i$, $(1 \leq i \leq l)$, being awake for at most $\log k + 1$ time slots.

### B. EEMC-MAC Details

This subsection presents the details of the EEMC-MAC protocol, which aims to explore the availability of multiple channels to allow nodes to send and receive data packets using as few time slots as possible. As it will be shown latter, the EEMC-MAC performs this task in an energy-efficient manner. The proposed protocol consists of a management and a transmission stages. The first stage builds the communication graph using the $CombineGroup$ and $CombineTS$ routines. Then, the communication graph is used to compute the communication sets during the transmission stage with the help of the ECOH heuristic. With this information at hand, each node learns when it must be awake to transmit and to receive its share of items. The details of the management and transmission states are presented next.

*1) EEMC-MAC: Management Stage:* The management stage main idea is to ensure that a leader node gets all the $s_i$ transmission sets from all the nodes $v_i \in V$. This process must occur in a energy efficient way and use the maximum number of available channels. Then, the leader node can join all the communication sets and create the communication graph $G = (V, E)$. Figure 5 shows the management stage steps. At the beginning of the algorithm all the nodes are in inactive mode. If $k < \frac{n}{2}$, the $n$ nodes in the set $V = \{v_1, v_2, ..., v_n\}$ are divided in $k$ groups of nodes $g_1$, $g_2$, ..., $g_k$, lines 2-3. Once each node knows the values of $k$, $n$ and its local ID, it has the condition to identify the group it belongs to. The goal is to reduce the number of active stations down to $k$. In the next step, $k$ calls of the routine $CombineGroup$ are performed, line 5. As described above, the routine $CombineGroup$ will combine the transmission sets in each group $g_i$ to just one node per group and the other nodes involved are set to inactive mode. The routine $CombineTS$ is called for all the active nodes. This routine will guarantee that all the transmission sets

**Algorithm** TransmissionStage

1: Let $v_m$ be the network node leader (from the previous stage) with the communication graph $G$;
2: Node $v_m$ executes $ECOH(G, k)$ and gets the communication sets $CS = \{CS_1, CS_2, ..., CS_r\}$;
3: All the nodes in $V$ enter in active mode and tunes into channel $c_1$. Node $v_m$ broadcasts $CS$ in channel $c_1$. All the nodes in $V$ receives the $CS$ broadcast and enters in inactive mode;
4: **for** $i \leftarrow 1$ **to** $r$ **do**
5:   **for** $j \leftarrow 1$ **to** $|CS_i|$ in parallel **do**
6:     Select an unused edge $e_h = \{v_s, v_d\}$ from $CS_i$;
7:     Nodes $v_s$ and $v_d$ enter in active mode;
8:     Node $v_s$ sends a packet to $v_d$ using channel $c_j$;
9:     Nodes $v_s$ and $v_d$ enter in inactive mode;
10:     Mark the edge $e_h$ from $CS_i$ as used;
11:   **end for**
12: **end for**

Figure 6: Each node proceeds to the assigned channel to transmit and receive data packets.

will be combined and forwarded to a single node $v_m \in V$, lines 9-10. Node $v_m$ will hold all the network transmission sets. At the end, node $v_m$ uses the transmission sets information to build the communication graph $G = (V, E)$ (line 11).

In the worst case scenario, when $k < \lfloor \frac{n}{2} \rfloor$ (line 2), the Algorithm $ManagementStage$ makes $k$ parallel calls to the $CombineGroup$ routine. As each group has $n/k$ stations, the routine $CombineGroup$ takes $\lceil \frac{n}{k} \rceil - 1$ time slots according to Lemma 2 with each node awake for at most 2 time slots. Next, the $CombineTS$ (line 9) is executed for all $k$ active stations. According to Lemma 4, $\log k + 1$ time slots are required to combine the transmission sets of $k$ nodes with each node being awake for at most $\log k + 1$ time slots. Thus, overall, the $ManagementStage$ takes $O(\lceil \frac{n}{k} \rceil + \log k)$ time slots to compute the communication sets of all nodes in $G$ with no station begin awake for more than $O(\log k)$ time slots. For latter reference, we state the following result:

*Lemma 4:* The $ManagementStage$ routine takes at most $O(\lceil \frac{n}{k} \rceil + \log k)$ time slots to combine the transmission sets of $n$ stations using $k$ channels with no station being awake for more than $\log k + 3$ time slots.

Clearly, this stage works based on the capability of the nodes to compute locals IDs in a given range. As mentioned in Section V-A, this task can be accomplished by employing fast and energy-efficient leader election algorithms, such as those proposed in [21], [22], [23]. As the number of nodes increases, it may be necessary to restrict the number of transmission sets in a given round of the management phase. This would prevent the combined transmission set to grow without bound. Again, a leader election algorithm could be employed to select a reasonable number of nodes to a particular round, thus limiting the number of data transfers in a given management phase. Another alternative is to allow the nodes to only combine sets up to a certain threshold, after that, the nodes would only relay the data sets. These nodes would, however, be able to receive data, but not transmit date in this particular round. Nodes that participated in the management phase, without completing their transmissions, could be given higher priority in the subsequente rounds. The aforementioned strategies would suffice to guarantee that the combined transmission set would be transferred within a single slot of time. Hence, in this work, we assume that the transmission set is such that is can be transferred within a single slot time.

*2) EEMC-MAC: Transmission Stage:* The transmission stage of the EEMC-MAC protocol begins immediately after the management stage. At the beginning of this stage, the leader node $v_m$ has already computed the communication graph $G$. Figure 6 presents the $TransmissionStage$ details. To solve the communication dependences, the leader node $v_m$ executes the ECOH heuristic and generates the list of communication sets $CS = \{CS_1, CS_2, ..., CS_r\}$, lines 1-2. The ECOH ensures that $|CS_i| \leq k$, that is, each set has at most the number of available channels and all the elements in each set $CS_i$ are disjoint. In the following step, all the nodes enter in active mode and tune to channel $c_1$ to receive the $CS$ broadcast from the leader node $v_m$ and then return into inactive mode (line 3). The first loop, line 4-12, iterates from 1 to $r$ (the number of communication sets) while the second loop iterates from 1 to the number of elements in the communication set indicated by the previous loop (lines 5-11). The inner loop begins by selecting an unused edge from the set $CS_i$. The nodes in this set enter in active mode (line 7), tune to the indicated channel and perform the data transmission (line 8). After transmitting their packets, these nodes return to inactive mode (line 9). This process continues until all the nodes in each communication set exchange their data sets.

It should be clear that the duration of the transmission stage depends on dependencies of the communication sets computed by the $ECOH$ heuristic. We consider that the execution of the $ECOH$ and the broadcast of the $CS$ (lines 2-3) can be completed in a single time slot. As each communication set $CS_i$ has at most $k$ elements, the $TransmissionStage$ allows the concurrent transmission of all the elements in a given communication set $CS_i$ in a single iteration of the outer loop. As there are $r$ communications sets, $r$ iterations of the outer loop are required. Clearly, in the worst case, none of the $p$ transmissions can be performed in parallel. In this case, $p$ transmissions are required. On the other hand, when all transmissions can be performed in parallel, $TransmissionStage$ takes $n/k$ time slots. Thus, the amount of time that the $TransmissionStage$ needs to complete all data transfers is between $\Omega(\lceil \frac{p}{k} \rceil)$ and $O(p)$. The following Lemma summarizes the discussion above:

*Lemma 5:* The task of transferring $p$ data items in a $k$-channel setting, where each node $v_i$, $1 \leq i \leq n$, has $\tau_i$ items to send and receive, can be completed by the $TransmissionStage$ algorithm in $\Omega(\lceil \frac{p}{k} \rceil)$ and $O(p)$ in the best and worst case scenarios, respectively, with no station being awake for more than $\tau_i + 1$ time slots.

### C. EEMC-MAC: Main Procedure and Complexities

The main procedure of the EEMC-MAC protocol consists in the sequential execution of the management and transmis-

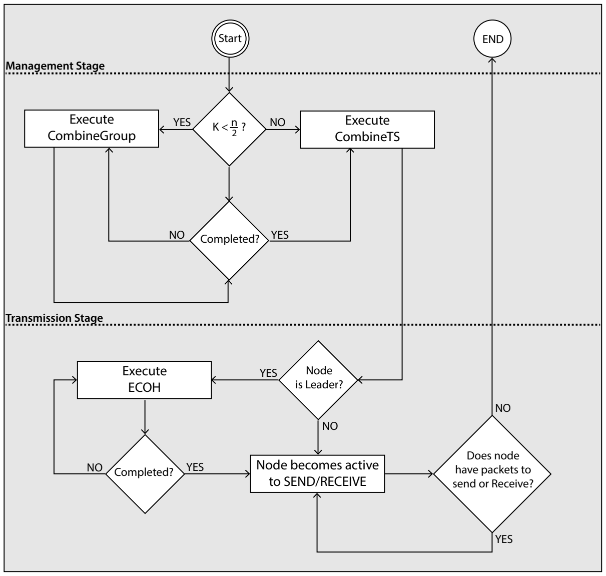


Figure 7: The EEMC-MAC protocol main tasks.

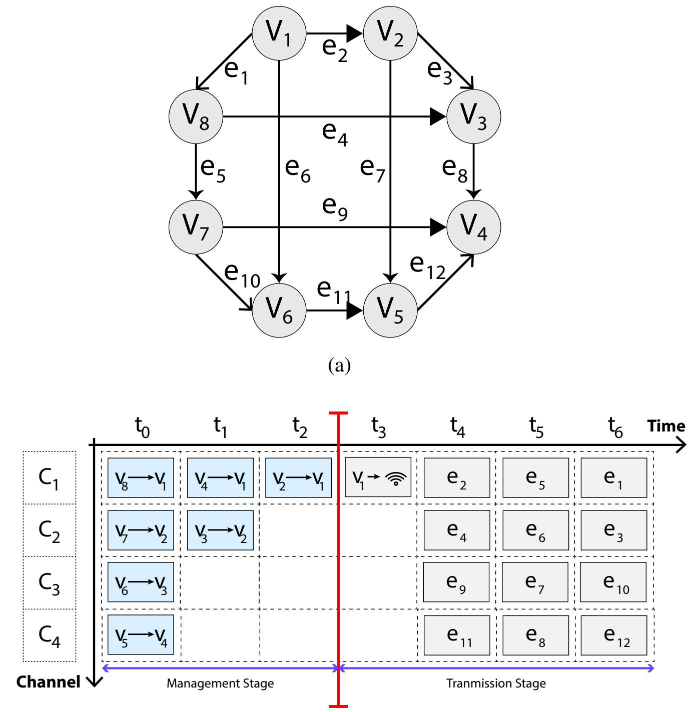


(a)

(b)

Figure 8: (a) Communication graph example with 8 nodes. (b) Channel representation for the EEMC-MAC protocol.

sion stages. The sequence of steps executed by the EEMC-MAC protocol is depicted in Figure 7. The protocol initiates in the management stage, where all communication sets are computed and combined with the aid of the $CombineGroup$ and $CombineTS$ routines. Once the communication sets are computed, the $TransmissionStage$ calls the $ECOH$ heuristic to compose the independent edges set. According to the arrangement of the independent edges set, the available channels are explored to reduce the overall communication time. Based on its ID, which is know to each node, they area able to determine the exact time to awake to send or receive their data items. Hence, each node stays in doze mode as long as possible so as to preserve battery power.

The time complexity and number of awake time slots for each station running the EEMC-MAC protocol can be obtained by combining the results in the Lemma 4 and Lemma 5.

*Theorem 1:* The tasks of channel assignment and transmission scheduling in a $k$-channel, single hop, wireless network represented by a communication graph $G = (V, E)$, can be solved by the EEMC-MAC protocol in $O(\lceil \frac{n}{k} \rceil + \log k + p)$ time slots with each node $v_i \in V$ being awake for at most $O(\log k + \tau_i)$ time slots, where $|V| = n$, $|E| = p$, $|C| = k$ and $\tau_i$ is the total number of items a node $v_i$ has to send or receive.

### D. EEMC-MAC: A working example

To exemplify the protocol application, consider the communication graph represented by Figure 8a. This graph has 8 vertices, $V = \{v_1, v_2, ..., v_8\}$, and 12 edges, $E = \{e_1, e_2, ..., e_{12}\}$. Consider the presence of $k = 4$ communication channels.

Figure 8b represents a possible data transmissions using $4$ channels, the proposed communication graph and the EEMC-MAC protocol. The protocol main procedure begins with the execution of the management stage (shown in Figure 5). Once the number of channels is large enough ($k \geq \lfloor \frac{n}{2} \rfloor$), the routine $CombineTS$ is called. This routine will group all the transmission sets $s_i$ of nodes in $V$, using the $k = 4$ channels, until the leader node $v_1$ gets all the communication sets, represented in time slots $t_0$ to $t_2$ in Figure 8b. This procedure of grouping transmission sets ends the management stage. The transmission stage (shown in Figure 6) starts immediately after the management stage ends. In this stage, the leader node $v_1$ uses the ECOH heuristic (Figure 2) to solve the graph communication dependencies and to obtain the list of communication sets $CS$. This list allows to perform the transmission scheduling, containing the channel and time slot each node must tune to send or receive data. Note that the ECOH heuristic ensures that parallel transmission does not share vertices in common. The leader node, then, broadcasts $CS$ to all the other nodes in time slot $t_3$. Time slots $t_4$ to $t_6$ represent the scheduled packet transmissions.

## VI. Simulation

The evaluation of the proposed protocol has been performed through simulation. To this end, the communication model presented in Section III was implemented in Matlab environment [24]. The simulator incorporates the characteristics of the EEMC-MAC protocol, described in Section V. To verify the goodness of the proposed solution, the simulation results are compared with the theoretical optimum solutions. This section begins by describing the simulation parameters and evaluation metrics followed by the simulation results and analysis.

### A. Simulation Parameters and Evaluation Metrics

To analyze the EEMC-MAC, simulations have been conduced for a varying number of nodes, data packets per node and data channels. The number of nodes assume the following values: $n = 16, 32, 48, 64, 80$. Recall, from the communication model, that each node can have a maximum a degree of at most $n - 1$ edges, that is, a node can send 0 or 1 packet to any destination in the communication graph per EEMC-MAC execution cycle. Thus, for a given set of nodes, the data items range from a few data items to send up to $n - 1$ data items. The number of data packets per node assume values in one of the five different ranges: $R_1 = 10\%$ to $20\%$, $R_2 = 30\%$ to $40\%$, $R_3 = 50\%$ to $60\%$, $R_4 = 70\%$ to $80\%$ and $R_5 = 90\%$ to $100\%$. Each range represents a percentage of the maximum number of transmissions per node. For example, in a setting with 16 nodes using the first range ($R_1$), each node would have from $10\% * (16 - 1) = 1.5$ (say 1) to $20\% * (16 - 1) = 3$ data packets to send. The number of channels assume the following values $k = 1, 2, ..., \lfloor \frac{n}{2} \rfloor$. The simulation results are drawn from the average of 200 simulation runs for each setting.

The following metrics are used to assess the goodness of the EEMC-MAC protocol:

- **Total execution time (M1)**: The amount of time (in the slots) that EEMC-MAC protocol needed to complete its operation for a given scenario;
- **Effective channel use (M2)**: The percentage of communication channel throughput that was used for effective data transmission (goodput) during the EEMC-MAC operation;
- **Protocol time in transmission stage (M3)**: The percentage of time that EEMC-MAC protocol spend at the transmission stage during its operation;
- **Ratio between EEMC-MAC transmission stage and and the optimum transmission stage time (M4)**;
- **Energy consumption estimation (M5)**.

Metric M1 aims to evaluate the reduction of the protocol operation time with the increase in the number of communication channels. As the number of available channels increases, more parallel transmissions can share the same time slot, reducing the overall completing time. Obviously, this limit dependes on the ECOH arrangement. Hence, M1 is an indicator of both, the impact of the communication channels and the goodness of the ECOH heuristic. Metric M2 evaluates the effective channel use, that is, the ratio between the number of packets that were transmitted by the number of packets that could have been transmitted. For example, consider that EEMC-MAC transmitted $|E|$ packets in $T$ time slots using $k$ channels. Once it is assumed that one packet is transmitted in one time slot, the maximum number of packets would be $T \cdot k$ and the effective channel use is the ratio $\frac{|E|}{T \cdot k}$. Metric M3 evaluates the percentage of time the EEMC-MAC remained in the transmission stage. This metric gives a direct indication of the EEMC-MAC overhead for transmitting data packets. For example, consider that the EEMC-MAC needed $T_m$ time slots for the management stage and $T_t$ time slots for the transmission stage. This metric calculates the percentage of time spent in the transmission stage, that is, the ratio $\frac{T_t}{T}$, where $T = T_m + T_t$. Metric M4 evaluates how far the EEMC-MAC schedule scheme is from the optimum one. It consists on the ratio between the EEMC-MAC transmission stage time and what would be the optimum time. For example, consider the EEMC-MAC needed $T_t$ time slots for the transmission stage and the optimum time would be $T'_t$ time slots. This metric calculates the ratio $\frac{T_t}{T'_t}$. Clearly, when $\frac{T_t}{T'_t} = 1$, the EEMC-MAC protocol achieved the minimum time to complete the transmission stage. Note that, in every case, $\frac{T_t}{T'_t} \geq 1$. Finally, Metric M5 shows energy cost of the proposed scheme considering current devices.

### B. Simulation Results

The simulation results for metric M1 are presented in Figures 9a to 9d, where the number of nodes are fixed in 16, 32, 64 and 80 nodes, respectively. These figures present the results for all defined ranges ($R_1$, $R_2$, ..., $R_5$). The $x$-axis shows the variation in the number of channels while the $y$-axis presents the number of time slots required to complete the protocol execution. Two main characteristics can be observed in these graphics: ($i$) when the number os channels increases, the time required to complete the transmissions decrease, and; ($ii$) this reduction in time tends to stabilize. Table II, line 1, summarizes the average reduction in communication time for each range when compared with the serialized solution ($k = 1$). The average reduction for range $R_1$ is equal to $13.5922$ times, for range $R_2$ is equal to $16.6856$ times. When all the simulations are considered, we have that EEMC-MAC is able to reduce the average communication time in over than 17 times.

Figures 10a and 10d present the simulation results for metric M2 using the same parameters as in M1. As before, the $x$-axis shows the variation in the number of channels while in the $y$-axis presents the values for effective channel use. It can be observed that the effective channel use is higher when fewer channels are available. This occurs because with fewer channels the execution time takes longer and the time required for management tends to impact less in the total transmission time. As the number of channels increases, the total time tends to decrease, as can be seen in the results for metric M1, and the impact of the management increases. However, after a certain point, the management tends to become more efficient once lesser groups are created in the management stage. Table II, line 2, summarizes the average values for metric M2 for each range. The average ratio for range $R_1$ is equal to $68.4786\%$, for range $R_2$ is equal to $79.5270\%$. When the average of all the communication settings is computed, EEMC-MAC achieved a effective channel use of more than $80\%$.

Figures 11a and 11d present the simulation results for metric M3 using the same parameters as in the previous metrics. The $x$-axis shows the variation in the number of channels while in the $y$-axis presents the values for the percentage of protocol time in the transmission stage. Note that the percentage of protocol time in transmission stage tends to decrease once the protocol transmission stage time decrease with an increase in the number of channels. There is a small increase when the number of channels is close to the maximum once the management stage becomes more efficient. These results are in agreement with those in metric M2. Table II line 3 summarizes the average values for metric M2 for each range. The average

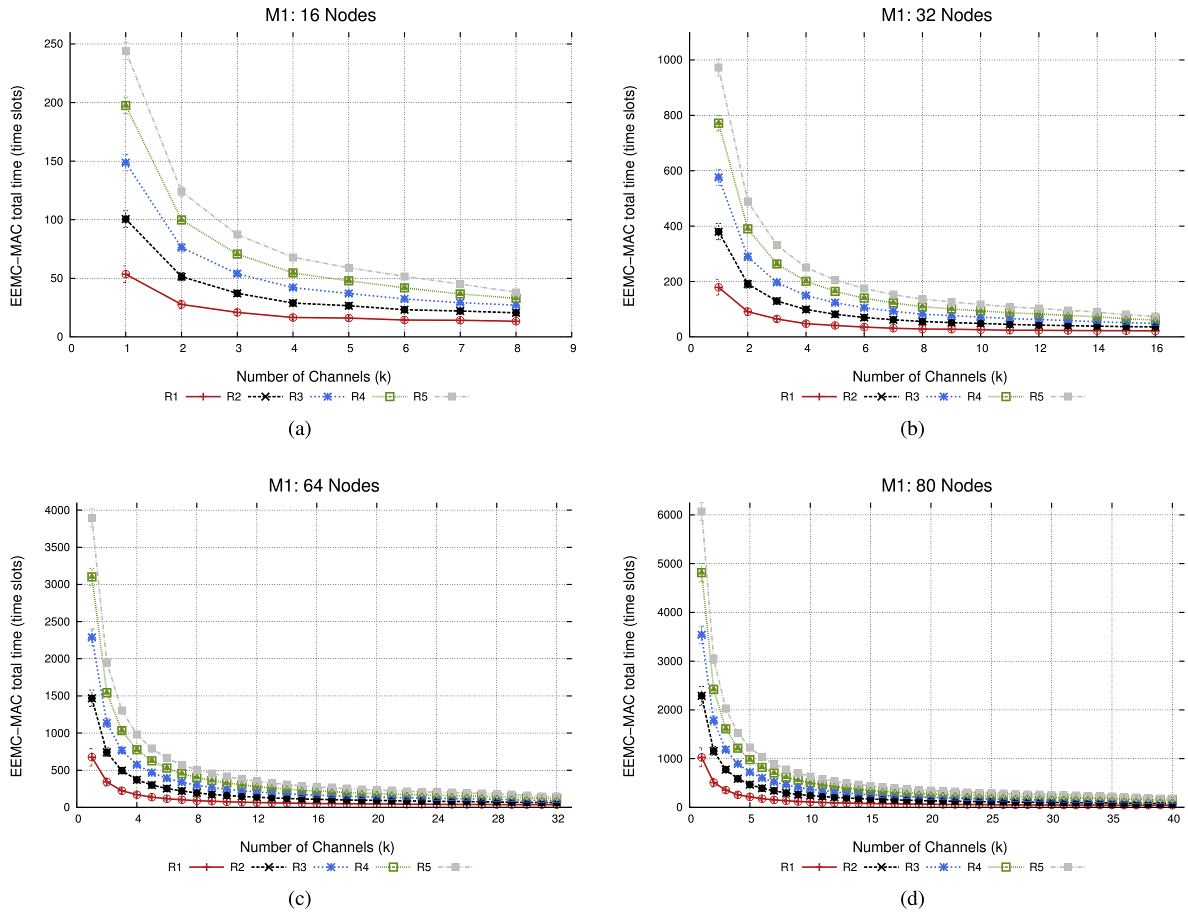


Figure 9: Simulation results for metric M1.

ratio for range $R_1$ is equal to $82.6813\%$, for range $R_2$ is equal to $91.1936\%$ and so on. As can be observed, the percentage of time the protocol needs for management is minimal when compared with the total protocol execution time. In fact, this time is, on average, less than $9\%$ from the total protocol execution time. In should be noted that for dense graphs, as in range $R_5$, the average time for management was less than $4\%$ from the total protocol execution time.

Figure 12 presents the simulation results for the metric M4. From the *Vizing Theorem* [25], it is a valid lower bound to assume that the optimum channel assignment execution time, when there is no channel restriction, is equal to $\Delta(G)$, where $\Delta(G)$ is the graph maximum degree. Thus, for comparison purposes, it is assumed that $T_{t'} = \Delta(G)$ and that $k = \lfloor \frac{n}{2} \rfloor$. This channel restriction is necessary so that the EEMC can be compared to the optimum values. In the $x$-axis, in Figure 12, shows the number of nodes in the communication graph while the $y$-axis presents the values for the $T_t/T'_t$ ratio. The number of data packets per node follows the previously defined ranges.

It can be observed in Figure 12 that $T_t/T'_t \approx 1$ when lower packet loads are presented ($R1$ and $R2$). The values obtained for $T_t/T'_t$ increase with the number the of nodes and transmissions per communication graph. However, even in such cases, the EEMC-MAC transmission stage execution time was always less than $14\%$ higher when compared with the optimum transmission stage time. Clearly, a larger communication graph increases the number of similar choices in the selection criterion of the protocol transmission scheduling. This, in turn, increases the chance of producing an unfavourable scheduling, thus increasing the communication time. Note that the choice of an inappropriate transmission scheduling at a given step $W$ impacts in the choice of other transmissions at step $W + 1$. Table II, line 4, summarizes the average values for metric M4 for each range. The average ratio for range $R_1$ is equal to $1.0184$, for range $R_2$ is equal to $1.0211$. From the results for metric M4 it is concluded that the EEMC-MAC achieved performance close to the optimum in many cases. When the average of all the communication settings are taken into consideration, the EEMC-MAC is less than $5\%$ from the optimum time.

Table III shows the amount of power for different operation modes of three popular devices [26]. To assess the energy consumption of the proposed scheme, metric M5, the Cisco Aironet is considered. Recall that, according to Lemma (4) and (5), a node $v_i$ is awake for at most $\log k + \tau_i + 4$ time slots during the Management and Transmission stages. In what follows, $k = 4$ and 1Mbps channels are assumed. Each node $v_i$ is supposed to hold $s_i$ data packets of 512 bytes that must be transferred to the corresponding destination.

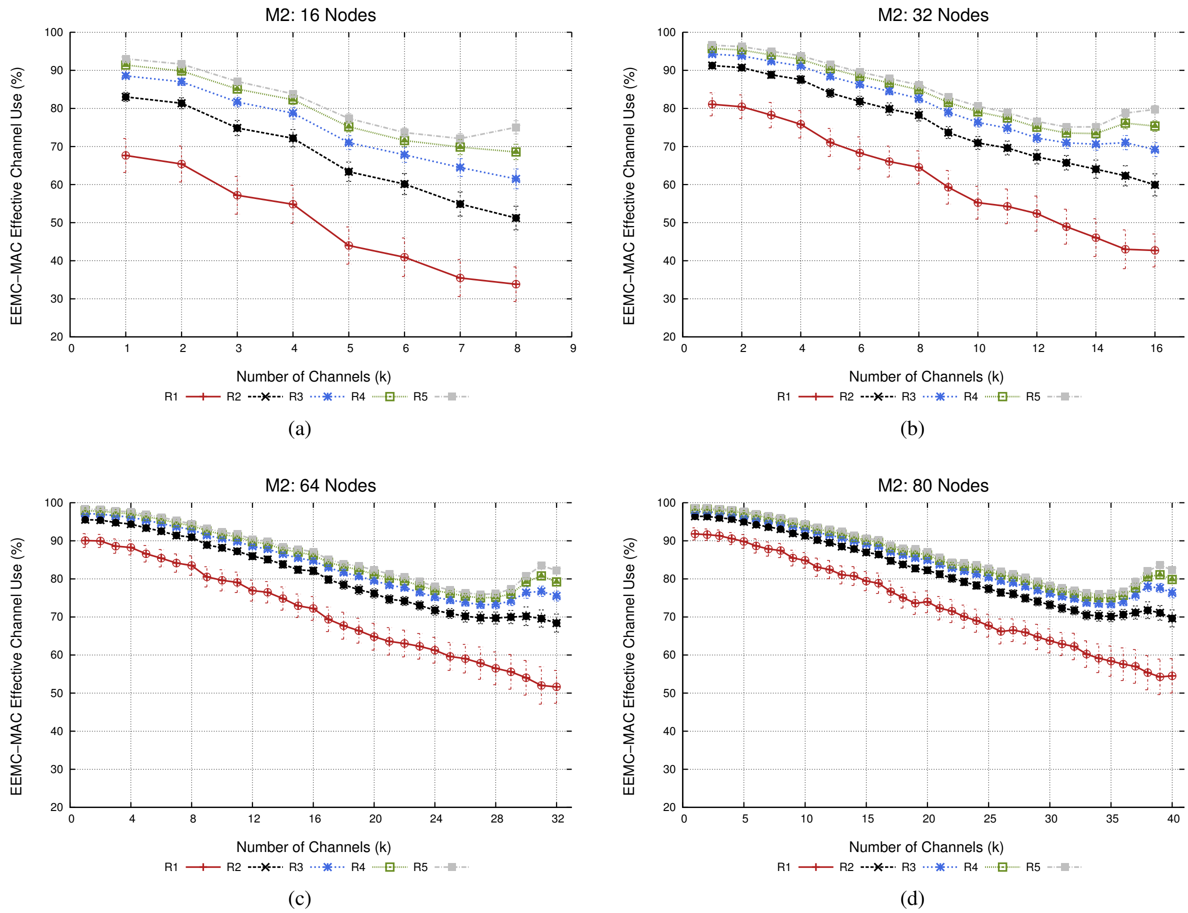


Figure 10: Simulation results for metric M2.

TABLE II: SUMMARY OF RESULTS.

| Metric | $R_1$ | $R_2$ | $R_3$ | $R_4$ | $R_5$ | Total |
|---|---|---|---|---|---|---|
| M1 | 13.5922 | 16.6856 | 18.3645 | 19.1940 | 19.9054 | **17.5483** |
| M2 | 68.4786 | 79.5270 | 83.2576 | 85.1464 | 86.2663 | **80.5352** |
| M3 | 82.6813 | 91.1936 | 94.0510 | 95.5074 | 96.3886 | **91.9644** |
| M4 | 1.0184 | 1.0211 | 1.0348 | 1.0602 | 1.1102 | **1.0489** |

Similarly, $d_i$ packets are expected to be received by node $v_i$. The amount of packets, $\tau_i$, is computed based on the higher values of each range ($R_1$ to $R_5$). The energy consumption of a node $v_i$ considers only the worse case scenario for both management and transmission stages. For comparison purpose, a single channel (SC), slotted time, protocol is considered. This latter protocol, hereafter referred to as SC, works in a similar fashion as the slotted Aloha protocol [27]. Note that, without a suitable scheduling algorithm, nodes must compete for channel resources. Thus, in order to make a fair comparison, the SC energy consumption is computed based on the amount of time a node $v_i$, in the worst case, expends to send and receive, respectively, $s_i$ and $d_i$, data items. In other words, contention time to access the common channel and idle time is not considered. Table IV shows the energy consumption ($E_j$), in Joules, for both protocols. As can be seen in the table, with an increase in the number of packets each node has to exchange, the proposed scheme provides higher energy savings. Note that, in the SC protocol, each node has to constantly monitor the channel to verify whether a packet is destined to itself or not. Hence, in the worst case, a node must wait for all transmissions (that is, receive all transmitted packets) to correctly obtain its share of items. In the EEMC, on the other hand, each nodes awakes only to send and receive data.

TABLE III: POWER CONSUMPTION TO TRANSMIT AND RECEIVE FOR DIFERENTE DEVICES [26]

| Device | Transmit | Receive | Idle | Sleep |
|---|---|---|---|---|
| Cisco Aironet | 1.48W | 1.0W | 830mW | 75mW |
| ORiNOCO 11b | 1.43W | 925mW | 925mW | 45mW |
| Mica mote | 36mW | 13.5mW | 13.5mW | < 1 $\mu$A |

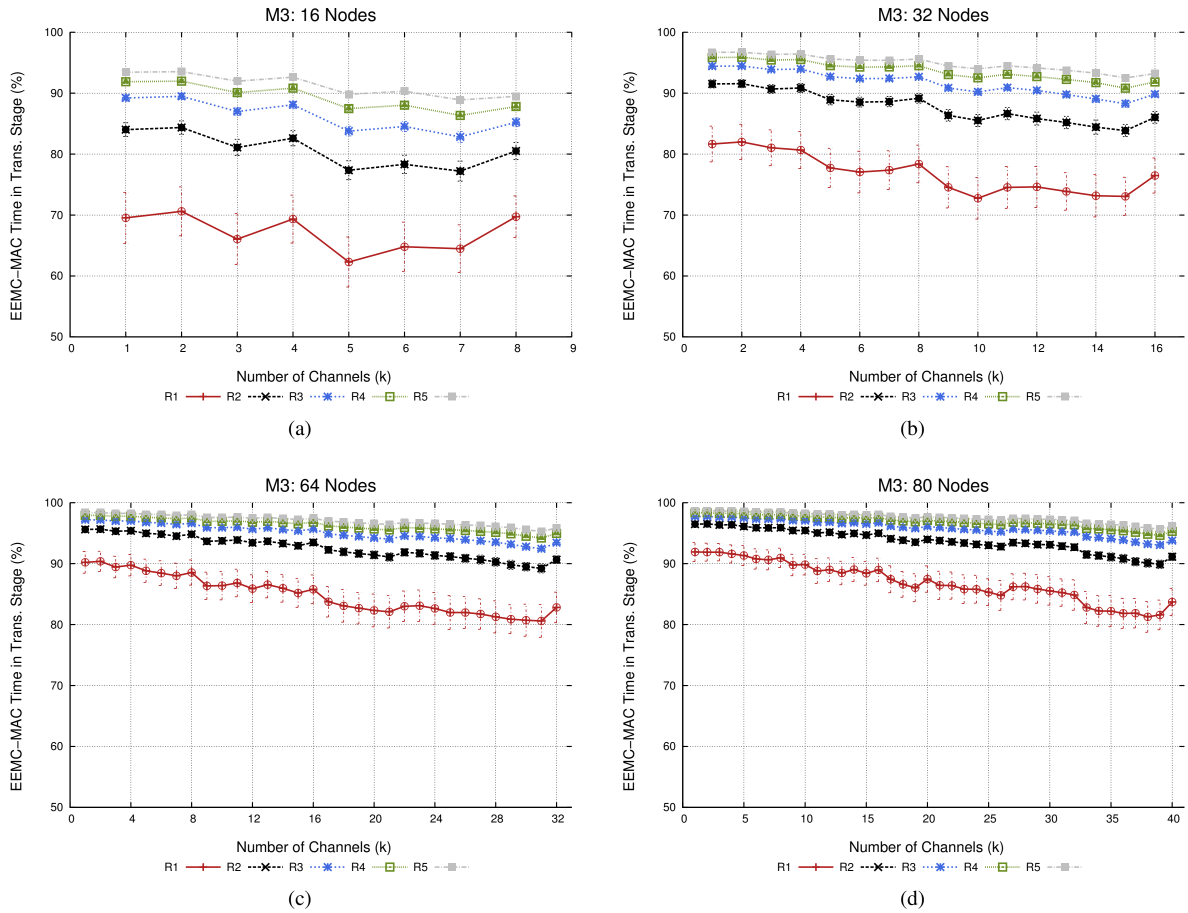


Figure 11: Simulation results for metric M3.

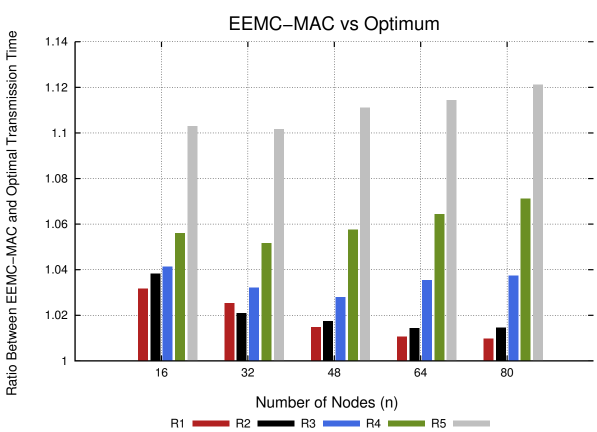


Figure 12: Simulation results for metric M4.

## VII. EEMC-MAC for Multiple Hops

In this section, it is proposed a possible extension of the EEMC-MAC for multiple hops using a cluster scheme. Younis *et al.* [28] proposes HEED, an energy efficient clustering approach for distributed ad hoc networks. This approach fits with the deterministic nature of the EEMC-MAC as the clustering process is completed within a constant number of iterations (regardless the network diameter) and the control overhead is linear in the number of nodes. Every node uses just local information in the clustering process. For this purpose, at the beginning of the EEMC-MAC for multiple hops, all the networks nodes are organized into clusters, following the HEED scheme. Each cluster has the following features: synchronous time; single hop communication; a list of communication channels; and a Cluster Head (CH). The CH has the following roles: to act like the leader node of the EEMC-MAC protocol, being the responsible for grouping all the transmission sets, create and deliver the data scheduling to the other cluster nodes; to create and maintain an inter-cluster routing table; and

TABLE IV: ENERGY EXPENDITURE OF THE PROPOSED PROTOCOL FOR DIFFERENT NODE DENSITY AND $\tau$ VALUES.

| | EEMC | | | | |
|---|---|---|---|---|---|
| | 16 | 32 | 48 | 64 | 80 |
| R1 | 0.0319 | 0.0666 | 0.1040 | 0.1443 | 0.1976 |
| R2 | 0.0624 | 0.1275 | 0.2056 | 0.2764 | 0.3265 |
| R3 | 0.0928 | 0.1986 | 0.2971 | 0.4085 | 0.4890 |
| R4 | 0.1233 | 0.2596 | 0.3986 | 0.5405 | 0.6515 |
| R5 | 0.1538 | 0.3205 | 0.4901 | 0.6624 | 0.8039 |
| | SC | | | | |
| R1 | 0.2148 | 0.8228 | 1.8240 | 3.2185 | 5.3399 |
| R2 | 0.4296 | 1.6456 | 3.8507 | 6.7052 | 10.6797 |
| R3 | 0.6444 | 2.6055 | 5.6748 | 10.1918 | 16.0196 |
| R4 | 0.8592 | 3.4284 | 7.7015 | 13.6785 | 21.3595 |
| R5 | 1.0740 | 4.2512 | 9.5255 | 16.8970 | 26.3656 |

to perform the inter-cluster communication. Nodes in different clusters are not necessarily synchronized. There is a common channel for inter-cluster communication.

The EEMC-MAC can be executed within each cluster with just a few modifications in the original algorithm. If a node $v_s$ in cluster $A$ wants to send a packet to node $v_d$ in cluster $B$, it sends the packet to the CH of cluster $A$, which stores the packet in its local buffer. Observe that, from the EEMC-MAC protocol, the CH knows exactly the time slots in both management and transmission stages it has no data to send or receive. This way, the CH uses these available time slots to perform the inter-cluster communication in the common channel. When the CH of cluster $B$ receives the relayed packet from the CH of cluster $A$, it will add this packet to its transmission set, delivering the packet to $v_d$ in the next EEMC-MAC cycle.

## VIII. Conclusion

The increasing popularization of mobile devices and the emergence of high content applications, increased the need for high throughput and energy efficient protocols for wireless networks. In this context, this work proposes an energy efficient protocol, named EEMC-MAC, for multi-channel allocation and transmission scheduling in wireless networks. The EEMC-MAC protocol divides its operation in management and transmission stages. The energy expenditure in the management stage is reduced and empirical results shows that this stage represents less than $9\%$ of the total protocol operation time. The transmission stage is optimum in energy consumption and, when compared with the optimum transmission stage time, the protocol needs, in average, $5\%$ more time. It is also proposed a possible extension of the protocol for multiple hops. In future works, it is intended to address fault tolerance and to improve the communication model.

## References

[1] T. F. Neves and J. L. Bordim, "EEMC-MAC: An energy efficient protocol for multi-channel wireless networks," in The Eighth International Conference on Systems and Networks Communications (ICSNC2013), 2013, pp. 6–12.

[2] P. Mohapatra and S. V. Krishnamurthy, Ad Hoc Networks - Technologies and Protocols. Springer Sciente + Business Media, Inc. chapters 1, 3, 6, 2005.

[3] Y. Zhu, M. Huang, S. Chen, and Y. Wang, "Energy-efficient topology control in cooperative ad hoc networks," IEEE Transactions on Parallel and Distributed Systems, vol. 23, no. 8, 2012, pp. 1480–1491.

[4] K. Chowdhury, N. Nandiraju, D. Cavalcanti, and D. Agrawal, "CMAC - A multi-channel energy efficient MAC for wireless sensor networks," in Wireless Communications and Networking Conference, vol. 2. IEEE, 2006, pp. 1172–1177.

[5] J. L. Bordim, J. Cui, and K. Nakano, "Randomized time-and energy-optimal routing in single-hop, single-channel radio networks," IEICE Transactions on Fundamentals of Electronics, Communications and Computer Sciences, vol. 86, no. 5, May 2003, pp. 1103–1112.

[6] S. Tsao and C. Huang, "A survey of energy efficient mac protocols for IEEE 802.11 wlan," Computer Communications, vol. 34, no. 1, 2011, pp. 54–67.

[7] G. Audhya, K. Sinha, S. Ghosh, and B. Sinha, "A survey on the channel assignment problem in wireless networks," Wireless Communications and Mobile Computing, vol. 11, no. 5, 2011, pp. 583–609.

[8] I. C. Society, "802.11-2012 - IEEE standard for information technology-telecommunications and information exchange between systems local and metropolitan area networks–specific requirements part 11: Wireless LAN medium access control (MAC) and physical layer (PHY) specifications," IEEE, Tech. Rep., July 2011.

[9] Q. Zhao and B. M. Sadler, "A survey of dynamic spectrum access," Signal Processing Magazine, vol. 24, no. 3, 2007, pp. 79–89.

[10] C. Stevenson, G. Chouinard, Z. Lei, W. Hu, S. Shellhammer, and W. Caldwell, "Ieee 802.22: The first cognitive radio wireless regional area network standard," Communications Magazine, vol. 47, no. 1, January 2009, pp. 130–138.

[11] B. Hamdaoui and K. Shin, "OS-MAC: An efficient MAC protocol for spectrum-agile wireless networks," IEEE Transactions on Mobile Computing, vol. 7, no. 8, August 2008, pp. 915–930.

[12] A. Hsu., D. Wei, and C. Kuo, "A cognitive MAC protocol using statistical channel allocation for wireless ad-hoc networks," in Wireless Communications and Networking Conference, March 2007, pp. 105–110.

[13] J. Jia, Q. Zhang, and X. Shen, "HC-MAC: A hardware-constrained cognitive MAC for efficient spectrum management," IEEE Journal on Selected Areas in Communications, vol. 26, no. 1, January 2008, pp. 106–117.

[14] O. Incel, L. Van Hoesel, P. Jansen, and P. Havinga, "MC-LMAC: A multi-channel mac protocol for wireless sensor networks," Ad Hoc Networks, vol. 9, no. 1, 2011, pp. 73–94.

[15] J. Zhang, G. Zhou, C. Huang, S. Son, and J. Stankovic, "Tmmac: An energy efficient multi-channel mac protocol for ad hoc networks," in IEEE International Conference on Communications, 2007, pp. 3554–3561.

[16] A. Raniwala, K. Gopalan, and T. Chiueh, "Centralized channel assignment and routing algorithms for multi-channel wireless mesh networks," ACM SIGMOBILE Mobile Computing and Communications Review, vol. 8, no. 2, 2004, pp. 50–65.

[17] L. Tang, Y. Sun, O. Gurewitz, and D. Johnson, "Em-mac: a dynamic multichannel energy-efficient mac protocol for wireless sensor networks," in Proceedings of the Twelfth ACM International Symposium on Mobile Ad Hoc Networking and Computing. ACM, 2011, p. 23.

[18] T. F. Neves, M. F. Caetano, and J. L. Bordim, "An energy-optimum and communication-time efficient protocol for allocation, scheduling and routing in wireless networks," in 26th International Parallel and Distributed Processing Symposium Workshops & PhD Forum, 2012, pp. 848–854.

[19] M. F. Caetano, B. F. Lourenço, and J. L. Bordim, "On the performance of the IEEE 802.11 in a multi-channel environment," in 22nd International Conference on Computer Communications and Networks, July 2013, pp. 1–7.

[20] C. Cordeiro and K. Challapali, "C-MAC: A cognitive MAC protocol for multi-channel wireless networks," in IEEE Symposium on New Frontiers in Dynamic Spectrum Access Networks, April 2007, pp. 147–157.

[21] C. Lavault, J.-F. Marckert, and V. Ravelomanana, "Quasi-optimal leader election algorithms in radio networks with log-logarithmic awake time-slots," in Telecommunications, 2003. ICT 2003. 10th International Conference on, vol. 2, Feb 2003, pp. 1113–1119 vol.2.

[22] M. Kardas, M. Klonowski, and D. Pajak, "Energy-efficient leader election protocols for single-hop radio networks," in Parallel Processing (ICPP), 2013 42nd International Conference on, Oct 2013, pp. 399–408.

[23] Energy-Efficient Initialization Protocols for Ad-Hoc Radio Networks, vol. Vol.E83-A, 2000.

[24] M. Grant and S. Boyd, "Cvx: Matlab software for disciplined convex programming," http://cvxr.com/cvx, March 2014.

[25] V. G. Vizing, "On an estimate of the chromatic class of a p-graph," Diskret. Analiz, vol. 3, no. 7, 1964, pp. 25–30.

[26] J. C. Zheng, Rong Hou and N. Li, Power management and power control in wireless networks, Y. Pan and X. Yang, Eds. Nova Science Publishers, 2004, vol. 2.

[27] A. S. Tanenbaum, Redes de Computadores. Campus, chapter 4, 2003.

[28] O. Younis and S. Fahmy, "Heed: a hybrid, energy-efficient, distributed clustering approach for ad hoc sensor networks," IEEE Transactions on Mobile Computing, vol. 3, no. 4, 2004, pp. 366–379.

# Simulation of Hardware and Software in Heterogeneous Wireless Sensor Network

David Navarro, Fabien Mieyeville, Mihai Galos, and Laurent Carrel
Université de Lyon, Institut des Nanotechnologies de Lyon (INL)
UMR5270 - CNRS, Ecole Centrale de Lyon, Ecully, F-69134, France
David.Navarro@ec-lyon.fr, Fabien.Mieyeville@ec-lyon.fr, Mihai.Galos@ec-lyon.fr, Laurent.Carrel@ec-lyon.fr

*Abstract* – **This paper presents a new feature of the IDEA1 Wireless Sensor Network (WSN) simulation platform: its ability to run simulations on heterogeneous sensor nodes that compose a network. This platform allows system-level simulations with hardware accurate models, with graphical inputs and outputs to easily simulate such distributed systems. When comparing IDEA1 simulation results to physical measurements, difference is 6 percent. IDEA1 is more than three times faster simulation compared to another simulator (NS2). In the testbed we consider, the well-known IEEE 802.15.4 standard is considered and different microcontroller units (MCU) and radiofrequency units (transceivers) compose the heterogeneous nodes. Output curves, packet delivery rate (PDR), packet latency can be evaluated. Moreover, energy consumption of sensor nodes is detailed with a very fine granularity, at hardware and software level. Indeed, energy consumption of each internal block of each device on each node can be monitored with IDEA1. Therefore, it is possible to simulate quickly and accurately heterogeneous (hardware different) nodes. Indeed, multitude of hardware platforms and communication standards lead to inter-communicating heterogeneous networks. This simulation platform can be used to explore design space in order to find the hardware devices and IEEE 802.15.4 algorithm that best fit a given application with a constrained energy budget.**

***Keywords – Wireless Sensor Network; WSN; heterogeneous; simulation; model; SystemC.***

## I. INTRODUCTION

Wireless Sensor Networks (WSN) are widespread sensor systems. This paper presents IDEA1, a Wireless Sensor Networks simulator, as briefly presented in The Sixth International Conference on Sensor Technologies and Applications (SENSORCOMM) [1]. Wireless Sensor Networks are used in a large variety of applications, such as environmental data collection, security monitoring, logistics or health [2]. Wireless Sensor Networks are composed of resource-constrained sensor nodes that are deployed at different locations. The sensor nodes cooperatively monitor physical or environmental conditions, such as temperature, sound, vibration or pressure. Because of autonomy requirements, they have a specific architecture; they are typically composed of one or more sensors, an 8-bit or 16-bit microcontroller, sometimes an external non-volatile memory, a radiofrequency unit (transceiver) and an energy supply. Limited resources are energy, memory and processing capabilities. As mentioned in [3], many different platforms exist, and hardware heterogeneity is now a reality. Indeed, standards like IEEE 802.15.4 permit heterogeneous nodes to communicate. Meanwhile, such networks have to be simulated in order to estimate performances of the network.

The typical hardware architecture of a sensor node is detailed in Fig. 1. As introduced previously, it is composed of a sensor, a microcontroller, a radiofrequency unit (transceiver) and a battery. The sensor converts physical data into electrical signal. Microcontroller is the central element in the node as it executes user software. It embeds an analog to digital converter that is connected to sensor, a synchronous serial communication block that is connected to radiofrequency unit, power aware functions (like sleep or power-down modes). Radiofrequency unit give the possibility of remote connections to other nodes and gives the wireless functionality in the network. A battery supplies all the circuits; its characteristics give node autonomy.

Manufacturers of WSN hardware include ATMEL, Texas Instruments or Microchip microcontrollers and Texas Instruments, ATMEL, Freescale, or ST-Micro-electronics radiofrequency units. Many manufacturers supply sensors and battery modules. WSN applications are mainly low data rate.

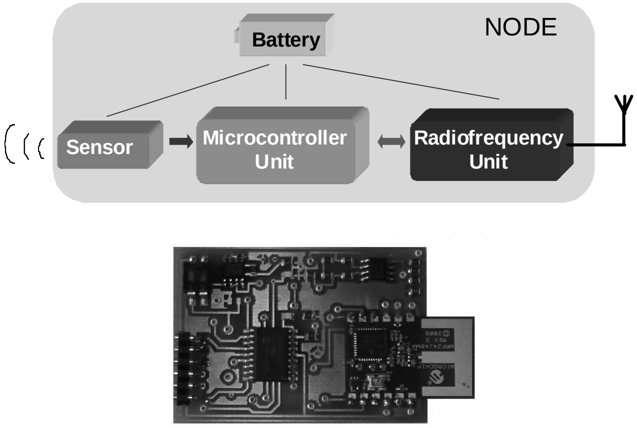


Figure 1. Typical wireless sensor node architecture, block diagram and hardware example N@L

For high data rate applications and intensive computations, Linux systems composed of 32-bit RISC processors are preferred but energy consumption is still prohibitive and autonomy is largely affected. Examples are the well-known Crossbow's Stargate platform [4] (Intel X-Scale processor at 400 MHz), or the TI CC2538 [5]. Even if these architectures will be probably more and more used in the future even though these systems shall be low-powered, they are for the moment relegated to the border of the WSN field. As stated in [3], 8-bit and 16-bit architectures represent 75% of microcontrollers in WSN applications. We also do not consider high data rate systems for the moment, and we focus on several months of battery life systems. Meanwhile, our platform is able to support these circuits if new models are included in the framework.

Wireless Sensor Networks design is a difficult task because designers have to develop a network at system level, with low-level (at sensor node: hardware and software) constraints. Therefore, CAD tools are required to make system-level simulations, considering low-level parameters. Our simulator IDEA1 permits that. Thus, we detail in this paper a new feature of our simulation platform: heterogeneous sensor nodes support.

Structure of the paper is as follows. Section II gives state of art on WSN simulators and basis of our work. Section III details our work: models and IDEA1 simulator. Section IV presents classical simulation results and related work. Section V shows latest results on heterogeneous simulation results.

## II. WIRELESS SENSOR NETWORKS SIMULATORS

Many simulators were developed over the last few years. Most of them are restricted to specific hardware or focus on either network level or node level. Research on sensor network evaluation can be broadly divided in two categories: network simulators enhanced with node models, and node simulators enhanced with network models. A more detailed description is available in [6]. A summary and the heterogeneity support are detailed in Table I.

Typical network simulators are general-purpose network simulators, such as Network Simulator 2 (NS2) [7] and OMNeT++ [8] (and their declinations).

NS2 [7], an event-driven object-oriented network simulator belonging to NSNM, is by far the most used simulator [9] in the Mobile Ad hoc NETworks (MANETs) domain. Simulations are implemented in the C++ language and Object-oriented Tcl (OTcl). Protocols and extension libraries are written in C++; creation, control and management of simulations in OTcl. The extension policy of NS2 library has greatly contributed to its popularity, many protocols being implemented by the scientific community. WSN-specific protocols were implemented in NS2 among which a version of the IEEE802.15.4 standard. Large-size networks are difficult to implement because of their memory requirements and their simulation time [10]. Furthermore, detailed energy models for the different hardware and software elements of the node are lacking, resulting in poor precision at high abstraction level. Among the extensions of NS2 dedicated to WSN, SensorSim was developed too. Criticisms often made to NS2 are about the interdependences between modules resulting from its object-oriented structure. Hence, developing protocols for the NS2 library is complex and requires from developers a thorough knowledge of the software architecture of NS2. In the network community where standard protocols are clearly identified, such a limitation can be tolerated, but in WSN field, where no real standard was adopted and where research in protocols domain remains dominant, these mixing-up of modules become a hindrance to WSN-specific library development. Indeed, even if IEEE 802.15.4 or Zigbee are widespread, the increasing need for always-lower power consumption keeps the protocols domain in the most active research field in WSN.

The third generation of NS simulator started in July 2006. If NS3 is, as its predecessor, based on C++, OTcl is neglected in favor of C++ (network models) and the Python language (optional). In addition, it incorporates GTNetS [11], a simulator that is known for its support of scalability. These choices were made at the expense of backward compatibility that involves the manual and complete rewriting of any model developed under NS2. This incompatibility explains the sustained use of NS2 for which many protocols exist. [12] details more differences between these two generations.

Second well-known simulator in this category (while technically it is an all-around simulation environment based on discrete events), OMNeT++ [8] is a simulator adopting a modular approach developed in a graphical Integrated Development Environment (IDE) based on Eclipse for development, creation, configuration, execution and analysis results. OMNeT++ is composed of modules that communicate through messages. OMNeT++ provides the infrastructure to assemble the simulations of models and manage their configuration through a specific language named NED (NEtwork Description). OMNeT++ was designed to overcome the development problems in NS2 [13] [14] and is becoming even more popular. Often compared, they are the two most widely used simulators in the world of WSN [14]. Many WSN simulators are based on OMNeT++, like Mixim [15] (formerly Mobility Framework) -dedicated to the simulation of wireless network and mobile- or Pawis [16].

The problem is these interesting network simulators are not sensor platform-oriented and they are thus too high-level for hardware considerations. Moreover, there is no separation between computation and communication models. That modeling is not suitable for hardware analysis and explorations. Then, such simulators do not have accurate energy models [17], whereas it is the main constraint in WSN.

Node simulators refer to precise hardware descriptions, with a synchronization strategy among the nodes, such as Avrora [18], TOSSIM [19], powerTOSSIM [20], Sycyphos [21] or SCNSL [22]. These simulators are well suited for embedded system designs analysis, requiring precise low-level models.

TABLE I. SIMULATION PLATFORMS AND HARDWARE HETEROGENITY SUPPORT

| Simulator | Language | Hardware modeling | Heterogeneity support |
|---|---|---|---|
| NS2 | C++, OTcl | No | Yes |
| OMNeT ++ | C++ | No | Yes |
| Avrora | Java | Yes (limited to ATMEL) | No |
| TOSSIM | C | Power TOSSIM: limited to ATMEL | Yes |
| Sycyphos | SystemC | Yes | No |
| SCNSL | SystemC | No | No |

Avrora [18] is a sensor network instruction set simulator (written in Java). It combines the precision of ATEMU [23] (cycle accurate) to the scalability of TOSSIM (up to 10,000 nodes). Avrora is furthermore language independent and of the embedded operating systems. The disadvantage of such a tool is its hardware support limited to ATMEGA128 architecture from ATMEL (node MICA and MICAZ). Moreover, using a high-level language, Avrora cannot be easily integrated into a conventional hardware design flow.

TOSSIM [19] and PowerTOSSIM [20] can emulate the execution of TinyOS. The application code of TinyOS is compiled and taken into account in the simulation framework. TOSSIM can consider thousands of TinyOS nodes with a very fine granularity. PowerTOSSIM is an extension of TOSSIM that gives power consumption evaluation. The main problem of these frameworks is that the user is constrained to a specific platform (typically MICA motes) and a single programming language (typically TinyOS/NesC) [24].

Sycyphos [21] objective is to enable design at system level down to circuit-level, with the help from multilevel simulation. Sycyphos is dedicated to power consumption evaluation and reliability study. It is based on Transaction Level Modeling (TLM), and uses multi-master bus architecture for radiofrequency network modeling. Nodes models are based on a multi-threaded instruction set simulator.

SCNSL (SystemC Network Simulation Library) [22] is an event-driven simulator of networked embedded systems, written in SystemC and C++. As SystemC is a C++ class library, it has the advantage to model both hardware and software. SystemC is a classical and widely used modeling language in micro-electronic systems design and particularly in System-On-Chip design.

Table I gives an overview of the most known simulators, it details their modeling language, if hardware is modeled, and if simulators support heterogeneous nodes (different hardware) simulation. The analysis of Table I leads to the conclusion that there is no simulation platform taking hardware into account (electronics designer level) and at the same time supporting heterogeneous (hardware different) nodes in the same network. Based on this conclusion, we planned to answer this problem.

Even with no support on hardware details and heterogeneity, SCNSL demonstrates a great perspective for accurate system-level simulation of WSN systems, and its architecture and language are well suited. Indeed, SCNSL models include nodes and network separately. That permits a low level modeling, with hardware support, and an easily scalable and tunable architecture. By our opinion, it also could answer fine granularity modeling, fine and accurate power consumption analysis and heterogeneous support.

Meanwhile, limitations of that library are numerous. We detail some of them. The "node" block models at once the hardware node (microcontroller and radiofrequency unit); therefore, its behavior does not reflect real hardware. Moreover, only a subset of the IEEE 802.15.4 standard is implemented in this alpha version: unslotted CSMA-CA policy with acknowledgments. Then, simulation result is a CPU time; important node-level and network-level results are not calculated. SCNSL includes three modules: node (SystemC), node_proxy (SystemC) and network (C++), as shown in Fig. 2.

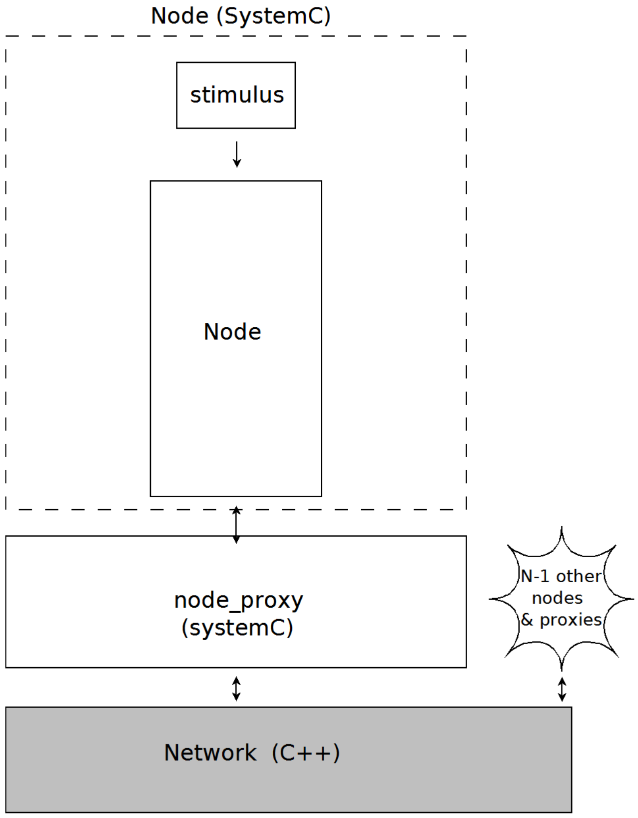


Figure 2. SCNSL model architecture

During the initialization of the simulation, each node registers its information (e.g., location, TX power and RX sensitivity) to a network class, which maintains the network topology and transmits packets to other nodes. The node_proxy is an interface between the network and nodes. By using node_proxy, nodes can be designed as pure SystemC modules so as to exploit all advantages of SystemC in hardware/software co-design and verification.

Our simulation platform is based on SystemC and C++, and SCNSL architecture was the starting point of our work.

## III. IDEA1 SIMULATOR

### A. Model architecture

The architecture of our model is close to real node hardware architecture, as Fig. 3 (compared to Fig. 2) shows. It includes sensor, microcontroller and radiofrequency unit blocks. Hardware, software and the whole IEEE 802.15.4 standard with many configurations are modeled. The SystemC blocks connected through a C++ network model was kept. The network model was modified to consider free space propagation. This simple propagation model could be extended to indoor context for example. Complex components, such as microcontroller or radiofrequency unit, are modeled as a Finite State Machine (FSM). Computing a Finite State Machine model in TLM with the efficient event-driven kernel simulator of SystemC is an interesting approach to reach fast simulation. It is the reason why IDEA1 is faster when compared to others simulators, like NS2.

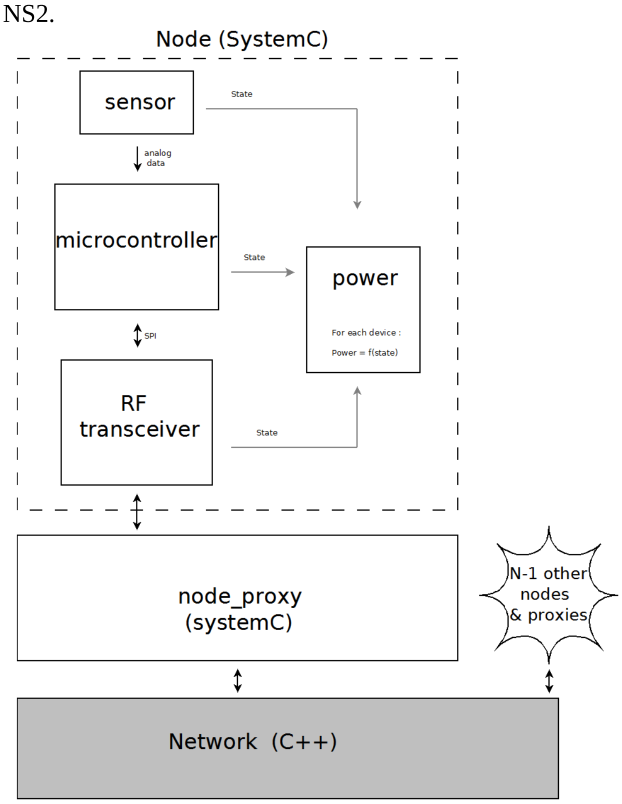


Figure 3. IDEA1 model architecture

### B. Hardware and Software models

The sensor block receives physical data from a file, and sends its output voltage to the microcontroller. The sensor, microcontroller and radiofrequency unit are modeled separately, so that designers can easily switch these inter-changeable devices. These two parts communicate through SPI (Serial Peripheral Interface) interfaces.

The microcontroller is the central unit for processing and controlling purposes. In our typical case, the microcontroller initializes the radiofrequency transceiver, it reads (converts) analog data from the sensor, and communicates (digital) data with radiofrequency transceiver. As SystemC is event-driven, it is possible to configure events in the sensor, and make the node react to the sensor with hardware interrupts available in the microcontroller.

Switching between architectures is done by changing some parameters in the configuration files. The microcontroller model can for example switch from ATMEL to Microchip or Texas Instruments' ones. Radiofrequency unit can be Microchip or Texas Instruments devices. Figs. 4 and 5 show Finite State Machine examples for microcontroller. Parameters depend on the microcontroller itself and on the radiofrequency unit (for example if hardware support of IEEE 802.15.4 is present or not).

In the first case (Fig. 4), the microcontroller has to perform few tasks, as the radiofrequency unit is a relatively autonomous circuit: once configured, it is able to manage packet sending, packet reception or acknowledgments alone. The microcontroller has therefore to read the analog to digital converter, and send the data to the radio frequency circuit. In the second case (Fig. 5), the microcontroller is connected to a simple radiofrequency unit that just modulates ready-to-send data.

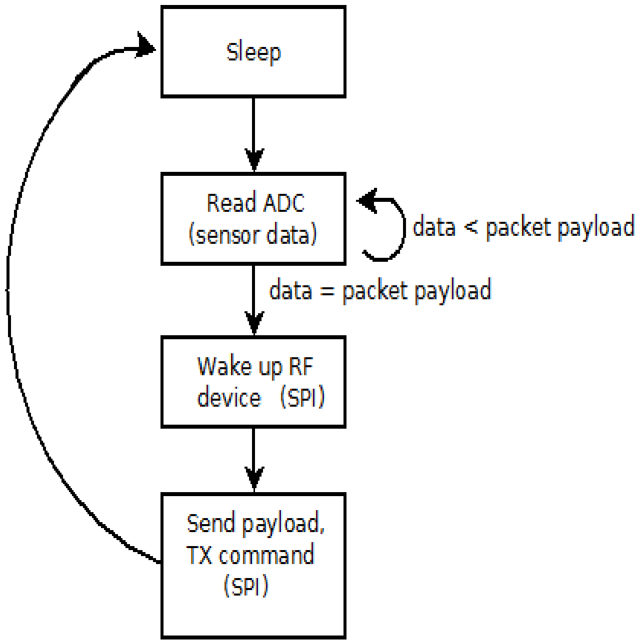


Figure 4. FSM of a microcontroller connected to a smart RF unit

The microcontroller must ensure all tasks, such as the composition of the packet (encapsulation of the data), or the waiting time for access to the channel (CSMA-CA mechanism) that depends on the channel load. Choice of the devices thus largely affects timing, communications and power consumptions.

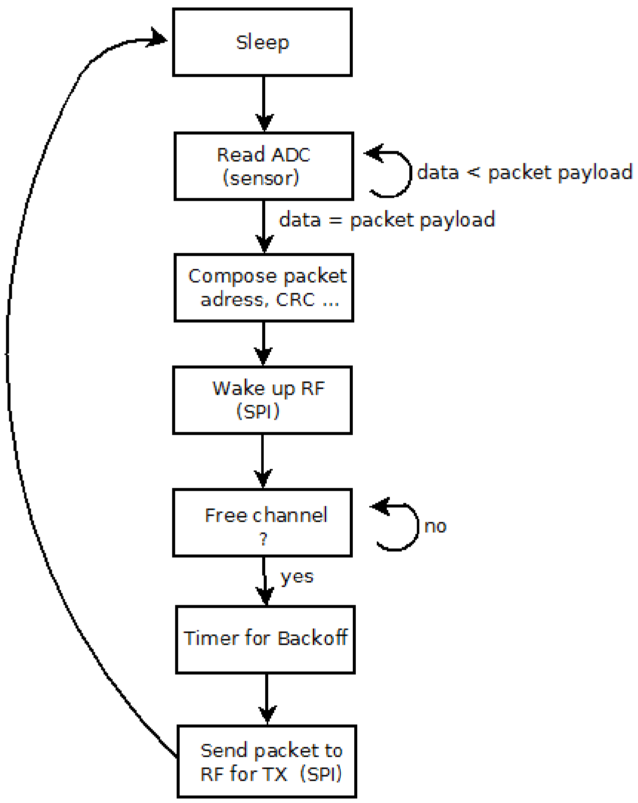


Figure 5. FSM of a microcontroller connected to a basic RF unit

In Finite State Machine, states are annotated by their duration and their power consumption. These values come from devices datasheets, and are all validated by measurements in our model implementation methodology. In order to have more accuracy, the CPU activity is considered. Fig. 6 shows the classical model that reflects the hardware part: sensor, microcontroller and radiofrequency units. The power module receives the current state of devices, and records all the state changes and timing in order to calculate and to log the power consumption. Energy can thus be evaluated with this power module. Table II details part of the lookup table that is implemented in power module (for ATMEL ATMega 128 and Texas Instruments CC2420 devices). All the devices in the library are modeled in this way.

The sensor and radiofrequency units are passive (basic) parts or active hard-coded, and their timing are well known. Meanwhile, the microcontroller has a more detailed finite state machine because of the (user) software that is running.

TABLE II. POWER INFORMATION OF ATMEGA128 AND TI CC2420

| ATMega128 microcontroller | | CC2420 RF transceiver | |
|---|---|---|---|
| Mode | Consumption | Mode | Consumption |
| Active | 27 mW | Sleep | 60 µW |
| Power Save | 26.7 µW | Idle | 1.28 mW |
| Power Down | 0.9 µW | RX | 56.4 mW |
| | | TX (0 dBm) | 52.2 mW |
| | | TX (-1 dBm) | 49.5 mW |
| | | TX (-3 dBm) | 45.6 mW |
| | | TX (-5 dBm) | 41.7 mW |
| | | TX (-7 dBm) | 37.5 mW |
| | | TX (-10 dBm) | 33.6 mW |
| | | TX (-15 dBm) | 29.7 mW |
| | | TX (-25 dBm) | 25.5 mW |

Indeed, this software -often written in assembly or C language- can change, and thus behavior and timing of microcontroller. This software is analyzed with an Instruction Set Simulator (ISS) we have developed for a better integration in our platform. Our ISS calculates durations of all the functions. Whatever the function that is called, even by a hardware interrupt, it is taken into account in terms of timing and power consumption. Processing states in the finite state machine are thus accurate. This ISS was developed for several hardware architectures: ATMEL AVR ATMega and Texas Instruments MSP430 for the moment.

Owing to the fact that ISS are time-consuming simulators, we did not choose a co-simulation method; hence, the ISS does not run in parallel with the SystemC kernel. Indeed, the ISS runs once at the beginning of the simulation, and code is analyzed in order to calculate tasks timing. These timings are then associated with the finite state machine, as Fig. 6 shows.

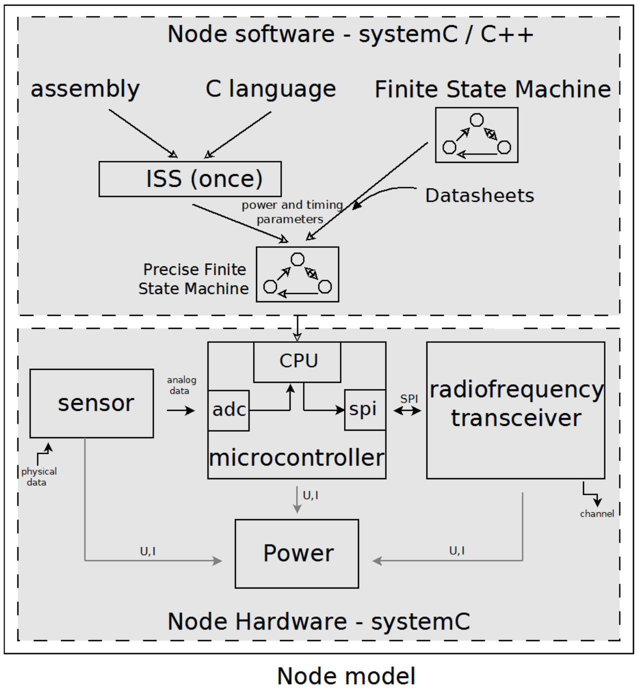


Figure 6. Node model including software for more accuracy

In detail, the ISS we have coded is an instruction set simulator that targets multiple hardware architectures. The whole instruction set of each targeted microcontroller is taken into account. It is written in C++ to offer compatibility support with our SustemC / C++ simulator. The ISS takes as input the ELF file produced by a compiler, often a C compiler. Next, it decodes the ELF file, looks which instruction is currently in scope and starts executing the functionality. At the end, the ISS produces an output file consisting of a lookup table pair: function name - number of corresponding clock cycles. ISS is also ran only once before SystemC simulation. More details on this ISS can be read in [25]. It is the main difference with classical ISS, that classically run in parallel with the main simulation kernel. Classical ISS thus slow down drastically the simulation speed. Using this lookup table and knowing the clock frequency of the microcontroller, these cycles are translated into timings. Once inserted in the SystemC simulation, software states in the finite state machine are timed, so a precise finite state machine is set.

Radiofrequency units are modeled individually because of their complexity and wide differences (that would make difficult a generic FSM). In Fig. 7 and Fig. 8 below, two FSM examples are drawn, of two well-known IEEE 802.15.4 compliant radiofrequency units: T.I CC2420 and Microchip MRF24J40.

As a whole, several sensors, microcontrollers and several radiofrequency units can be selected; the current library is detailed in Table III. Each sensor, microcontroller and radiofrequency unit can be mapped to each other. Each compliant radiofrequency transceiver includes the whole IEEE 802.15.4 standard.

Due to its architecture and file organization, the models library is easy to extend: new files, containing new models, are added in the folders, the main file includes them. C language #define statements permit to change the modeled hardware. Signals between modules are connected in the SystemC model, as it would be in real hardware.

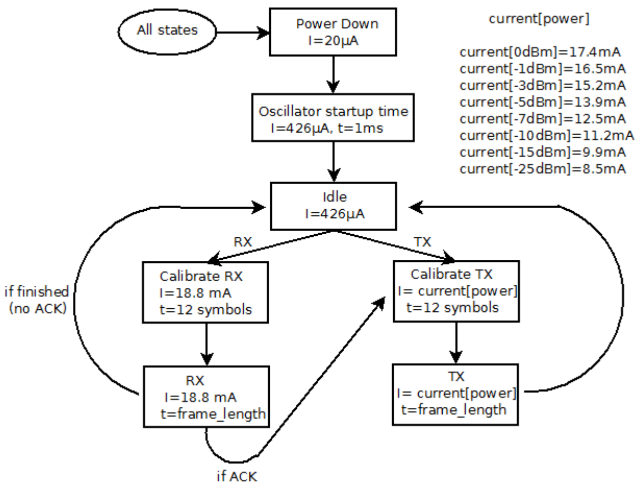


Figure 7. TI CC2420 simplified Finite State Machine

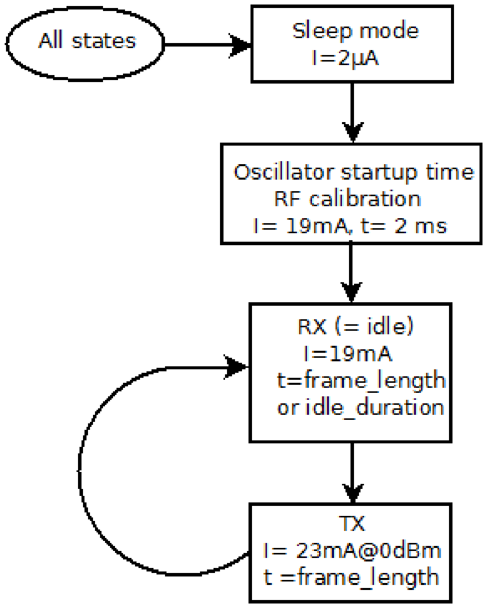


Figure 8. MRF24J40 simplified Finite State Machine

As it was previously published, all of these models were validated with experimental measurements on many test-beds [26], as detailed in Section IV.

TABLE III. MODELED HARDWARE DEVICES IN SIMULATOR LIBRARY

| Sensor units | Microcontroller units | Radiofrequency units |
|---|---|---|
| N.S. LM35DZ<br>Clairex CL9P4L | ATMEL ATMega128<br>Microchip 16LF88<br>T.I. MSP 430 | T.I. CC2420<br>T.I. CC1000<br>Microchip MRJ24J40 |

## C. *The simulator user interface*

The presented models can be used to simulate wireless sensor network communications at system level. To help SystemC / C++ non-specialists to use easily the simulation tool, we developed a graphical interface that is shown in Fig. 9.

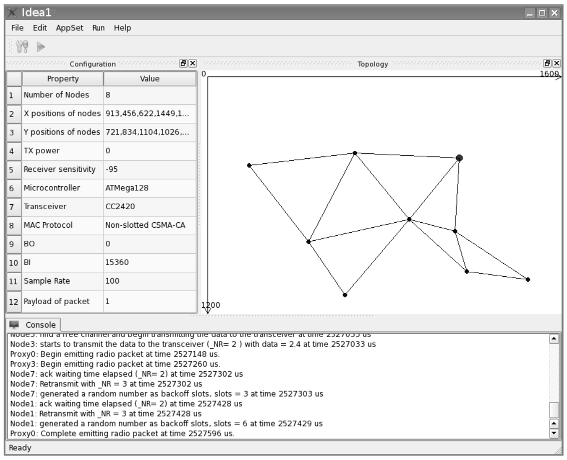


Figure 9. Simulator graphical user interface

The user interface is composed of different sub-windows. A graphical viewer shows spatial position of nodes and the lines between nodes represent the possible communications according to locations, power of the transmission and sensitivity of the receiver. Hardware parameters are some of selectable microcontrollers and radiofrequency units. One of the many IEEE 802.15.4 configurations (in slotted or unslotted modes) and superframe parameters (SO, BO, BI etc.) can be selected. Sampling rate and payload of packets can thus be configured. User enters all parameters though a configuration window, called from menus. A click on the launch button in the graphical interface launches a SystemC simulation in background. Simulation log is displayed in the bottom window of the graphical interface, and a timing trace (Value Change Dump format: VCD) is created and can be opened. Output log files are thus generated for deeper analysis.

## IV. CLASSICAL RESULTS AND RELATED WORK

From these log files, we can explore design space for the best solution (often the lower latency, best packet delivery rate, and the lower energy consumption). Many output curves are accessible: packet delivery rate (PDR), packet latency, node power consumption and energy per packet. All these results were validated with measurements on a 9 nodes network [27] with a TDMA-based GTS algorithm. These nodes, called N@L, are composed of Microchip devices: PIC16LF88 microcontroller and MRF24J40 radiofrequency unit. Each of the 8 nodes senses periodically a data and tries to send it to the coordinator. This period (sample rate) is the parameter for this study. Non-periodical scenario can be configured as well, timing is simply defined sequentially in the testbench file.

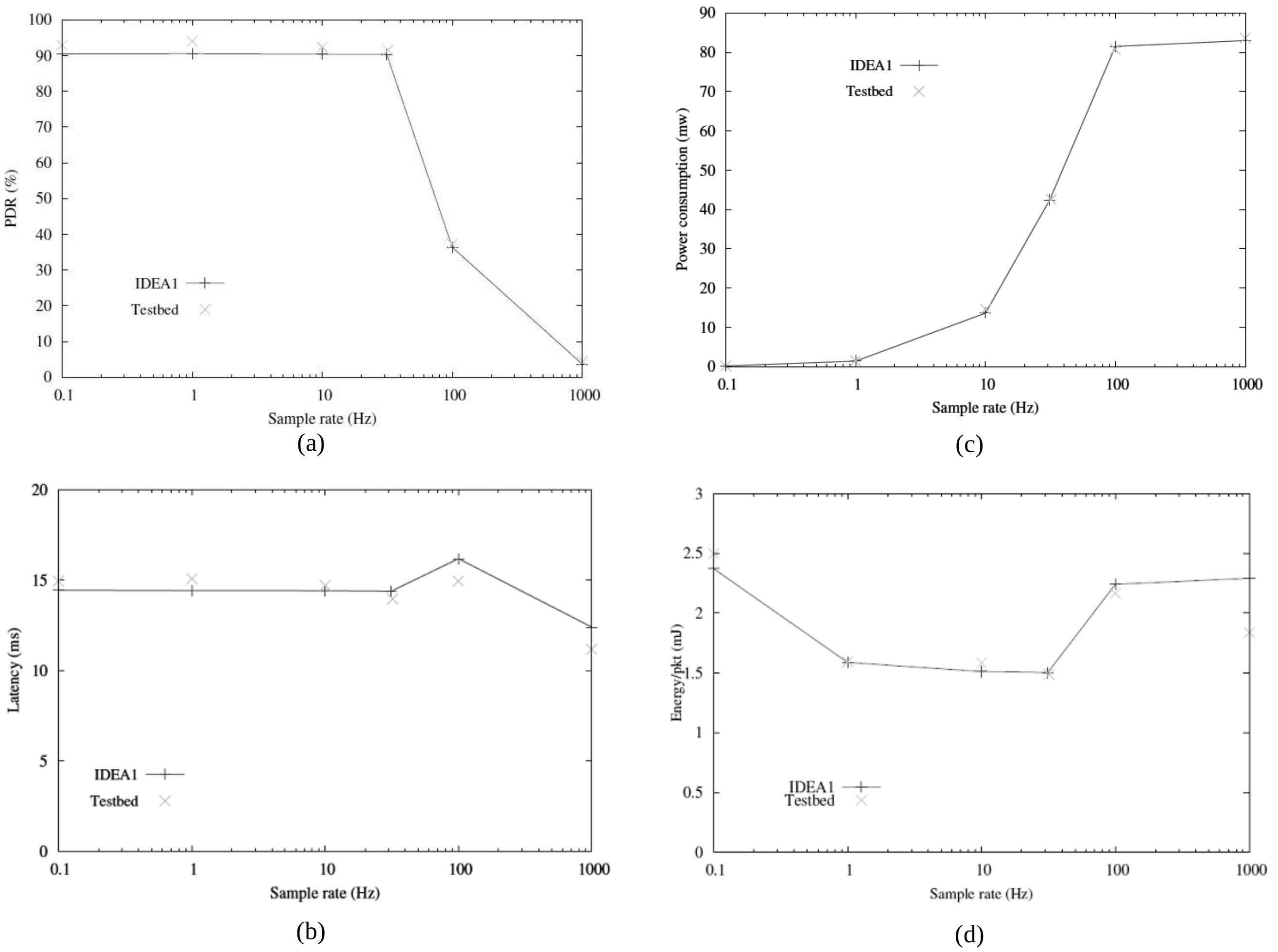


Figure 10. IDEA1 simulation and testbed measurements. Typical output curves: packet delivery rate PDR (a), packet latency (b), node power consumption (c), energy per packet (d).

IDEA1 simulation results are within 6% of the actual value obtained from real measurements. This good accuracy is not surprising since models are based on devices datasheets. Simulations and measurement simply validate datasheets.

Moreover, these results were compared to NS2 that we considered as a reference for this study. As our results are measurement-validated, we could explore accuracy of NS2 as well. NS2 is accurate for network-level results, such as packet delivery rate or latency. Indeed, hardware components have a small impact on these delays according to framing spacing and packet length compared to electronics components delays (software were taken into account at the same level in both simulators for this comparison). Meanwhile, the simulators have different results for energy per packet consumption, as Fig. 11 shows. This difference is especially important for low data-rate applications. Power consumption between IDEA1 and NS2 ranges from 9% to 16% in a non-beacon CSMA-CA algorithm. A simulation time analysis is shown in Fig. 12 where scalability is detailed. Fig. 12 presents relative simulation time: simulation time over simulated time. Even if both simulators are event-driven, Fig. 12 shows that IDEA1 kernel with FSM-based modeling takes a better advantage than NS2 on the application discrete behavior: IDEA1 curve is much more constant than NS2' one. Scalability is also better. Indeed, in low data rate scenario (typical WSN case), few events appear; simulator also simulates idle or sleep states. IDEA1 is 3.3 times faster than NS2. NS2 is more interesting in high data rate scenario (typical networked-computers case) because the ratio decreases. Anyway, ratio of IDEA1 decreases too, and it is still 3.1 times faster at 1000 Hz sampling rate.

Moreover, we showed that IDEA1 is able to provide a fine and precise power consumption analysis over many solutions: [27] detailed –for all IEEE 802.15.4 configurations- active and sleep consumptions of radiofrequency unit and microcontroller.

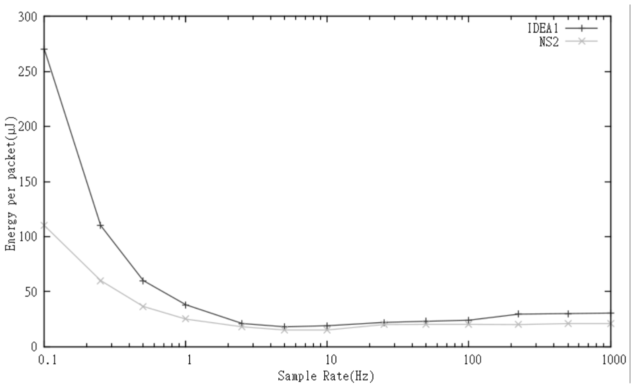


Figure 11. Node energy per packet. IDEA1 and NS2 simulations in non-beacon CSMA-CA.

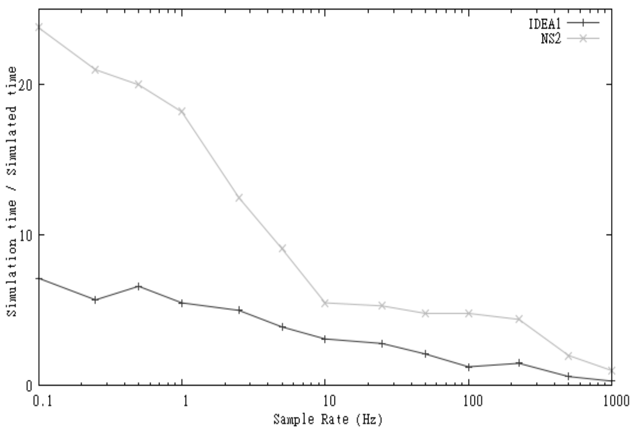


Figure 12. Relative simulation time (simulation time / simulated time). IDEA1 and NS2 simulations.

Fig. 13 shows this result. For two separate nodes, energy of radiofrequency unit in active mode (EnergyTransActive) and sleep mode (EnergyTransSleep) is detailed. In microcontroller, energy of internal hardware blocks (CPU, EnergyCPUPerNode, SPI communication block EnergySPIPerNode, analog to digital SAR converter EnergyADCPerNode) are monitored.

All these above results were obtained for homogeneous networks, so a single node hardware architecture.

The section below presents new simulation results in a heterogeneous network context.

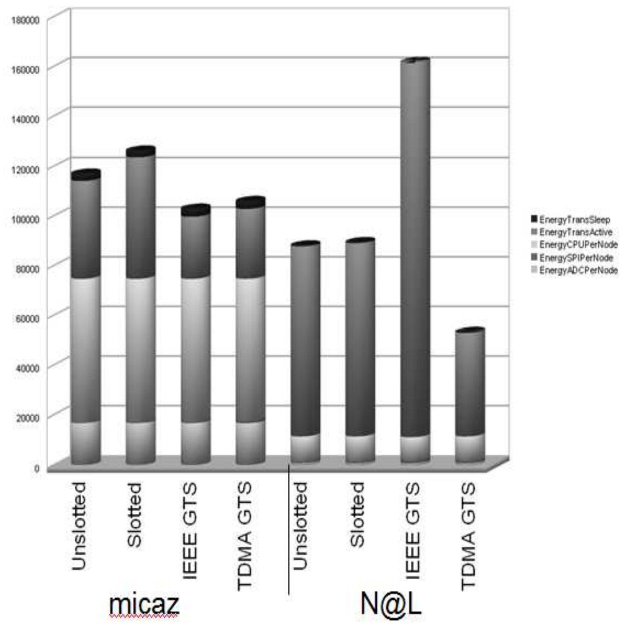


Figure 13. Energy consumption of radiofrequency transceiver and microcontroller internal blocks for two different platforms (µJ)

## V. HETEROGENEOUS SIMULATION RESULTS

Heterogeneous support in simulators with fine and accurate hardware and software models is necessary, but few simulators support this feature, like [28]. One reason is the need of a complex instantiation of models.

Typical heterogeneous nodes are detailed in Fig. 14: node A and node B have different hardware devices. In our simulation, microcontrollers, and radiofrequency units are different (brand and model).

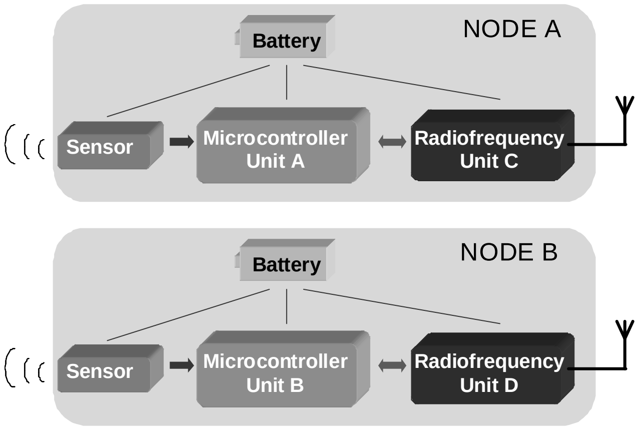


Figure 14. Typical node architectures in a Wireless Sensor Network (heterogeneous network)

As a test example, we simulated a 9 nodes network: one coordinator and eight nodes composed of Microchip PIC16LF88 and ATMEL ATMega128L microcontrollers and Microchip MRF24J40 and Texas Instruments CC2420 radiofrequency units, as specified in Table IV.

TABLE IV. NODES DEVICES FOR TESTBED AND SIMULATION

| WSN device | Microcontroller unit | Radiofrequency unit |
|---|---|---|
| Coordinator | ATMega128 | CC2420 |
| Nodes 0..3 | PIC16LF88 | MRF24J40 |
| Nodes 4..7 | ATMega128 | CC2420 |

Nodes sense the environment periodically every second, and transmit data over the network. Each transmission (packet) includes two data bytes (payload). Sensor nodes enter sleep mode as long as they can; the coordinator is always awake. The IEEE 802.15.4 non-beacon CSMA-CA communication scheme with no acknowledge is used, but all of the IEEE 802.15.4 can be configured for wider exploration. Simulation of this testbed gives a VCD trace, an extract is shown in Fig. 15. We can observe the coordinator's and nodes' microcontroller and radiofrequency unit states (R: Receive, T: Transmit, A: Active, S: Sleep CooMCUState stand for coordinator microcontroller state, Cooradiostate is the coordinator radiofrequency state. For classical nodes, states of microcontroller and radiofrequency unit are also detailed with mcustate0 and radiostate0 for node 0 and mcustate7 and radiostate7 for node 7. In this example, coordinator microcontroller is always active (A). At time 1065ms, coordinator radiofrequency unit sends a packet (T), node0 radiofrequency unit is in receive mode (R), node7 is in power down mode (0). Then, radiostate0 sends an acknowledgement (T), and then enters sleep mode. As no more processing is required, microcontroller of node 0 enters sleep mode. Node 7 wakes up at 1066ms. After a calibrating phase, microcontroller is active; radiofrequency unit is in receive mode. At 1066.5ms, microcontroller samples a data, sends it over SPI. After CCA, radiofrequency unit sends the data (T), and enters power down at 1069.3ms. Microcontroller enters sleep mode too, node 7 is totally in sleep mode too. ….). It is possible to monitor more signals in order to see for example the wireless channel usage, or the data transfer from the sensor to the radiofrequency unit through the microcontroller on each node, and data from the radiofrequency unit to the microcontroller on the coordinator.

Information in the log file gives a lot of output data, as packet delivery rate (PDR), and latency. Moreover, log file includes energy of each block of each circuit in each node. It is also possible to draw graphs such as the following ones. Fig. 16. presents the overall energy consumptions of the nodes.

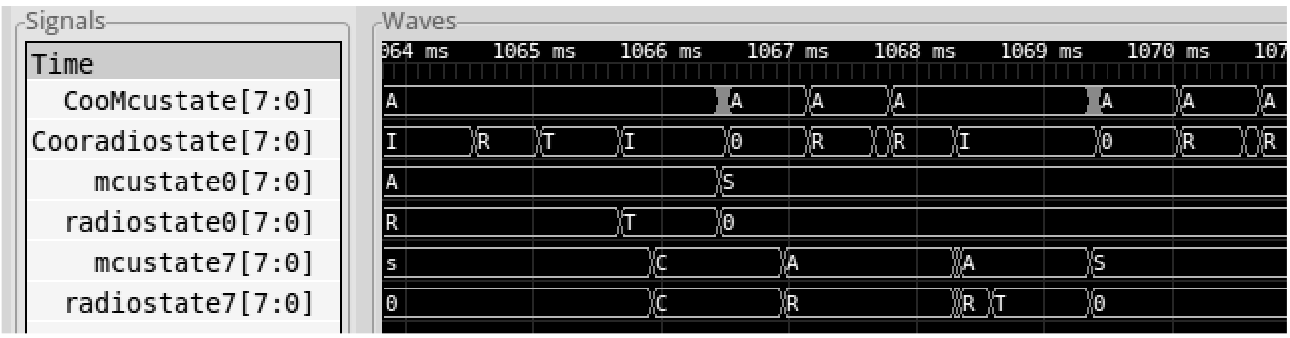


Figure 15. Extract of the output VCD file, focus on coordinator and nodes 0 and 5 (microcontrollers and radiofrequency units states)

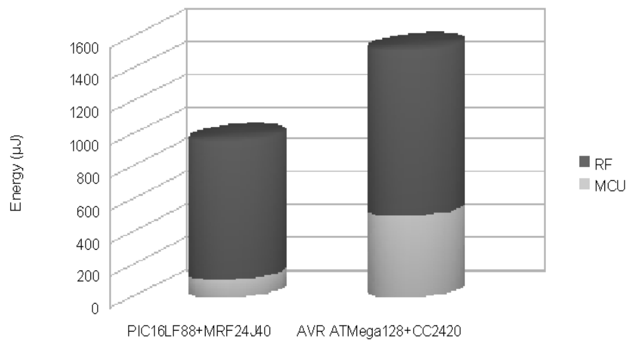


Figure 16. Heterogeneous nodes energy consumption

Energy partitioning between the microcontroller and the radiofrequency unit for two heterogeneous nodes (node 0: Microchip PIC16LF88 and MRF24J40 and node 5: ATMEL AVR ATMega128 and T.I. CC2420) are shown. We can see the energy consumed by microcontroller (MCU energy in grey) compared to the radiofrequency unit one (RF energy in dark). In detail, PIC16LF88 consumes a total energy of 109µJ, AVR ATMega128 consumes 498µJ, so a 4.5 ratio. MRF24J40 consumes 848µJ, whereas CC2420 consumes 1016µJ, so a 1.2 ratio. This testbed shows an interesting combination of circuits that composes node 0, because it embeds the two most energy-aware circuits. Meanwhile, it is interesting to detail this big difference.

It is possible to have finer granularity and to detail the energy consumption of each block within hardware devices. Fig. 17 shows the microcontroller energy spent during (from top to bottom in bars) sleep, idle and SPI communications states. It is to note that CC24220 radiofrequency unit (with no IEEE 802.15.4 hardware support) has an impact on the active state duration of the microcontroller. Indeed, in that example, the CC2420 transceiver just modulates the packet; microcontroller implements the IEEE 802.15.4 standard by software. For example, it has to check for free channel, to respect delays (backoffs), to generate IEEE 802.15.4 compliant packets, to acknowledge if it is activated, etc. More SPI communications are thus required. This fact is visible on Fig. 17: active and SPI communication energy consumptions are important on AVR ATMega128.

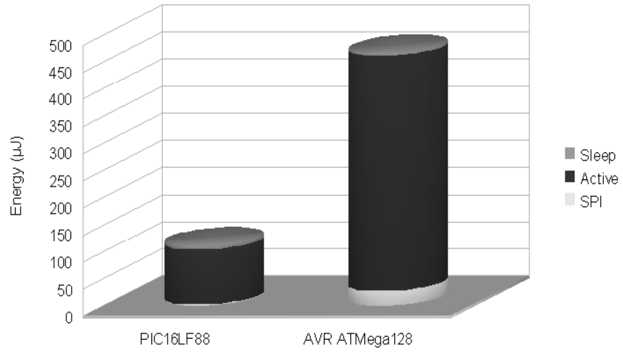


Figure 17. Microcontroller energy consumption comparison

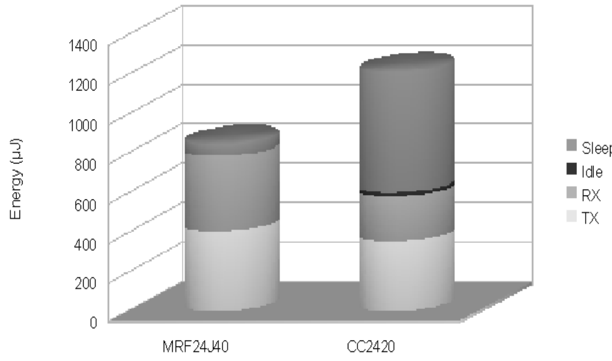


Figure 18. Radiofrequency units energy consumption comparison

On the other hand, the MRF24J40 transceiver is a more autonomous circuit, as it supports all the aforementioned aspects of IEEE 802.15.4 by hardware, the microcontroller is thus less active.

With the same fine granularity, it is possible to detail states of radiofrequency units, as shown in Fig. 18.

This figure shows it is possible to monitor energy consumed during states (from top to bottom on bars) of each radiofrequency unit: sleep, idle, receive (RX) and transmit (TX). Although sleep mode is the less power consuming, it is the longest state. Testbed is typical in WSN: duty cycle (wake-up duration / application period) is low. CC2420 has important energy consumption in sleep mode (compared to MRF24J40) because its power consumption is 8.5 times bigger. Sleep mode durations depend on activity of nodes, node 5 (AVR ATMEga128 + CC2420) needs more processing because of the basic radiofrequency unit, as discussed above. It is also meaningful to obtain a 10 ratio on energy consumption compared to node0. We can remark that MRF24J40 has no idle state; default state is RX (Fig. 8). While communicating or processing a packet, MRF24J40 is in RX state, it is why RX state is so energy consuming. As CC2420 has a lower power consumption in TX mode (52.2mW at 0dBm) compared to MRF24J40 (69mW at 0dBm), CC2420 has a lower energy consumption to transmit the same amount of packets.

We can see it is possible to optimize total energy with such a deep exploration.

## VI. CONCLUSION

In this paper, heterogeneous support of IDEA1, our system-level simulator for Wireless Sensor Networks, was presented. This simulator is written in SystemC and C++. SystemC combines advantages of being a widely-used language in micro-electronic systems design flow, and permitting hardware and software co-modeling. Moreover, its kernel is efficient, and as our models are based on Finite State Machines, less events appear and simulation speed is fast compared to other simulators. The simulator graphical user interface permits configure easily a network and set the sensor nodes characteristics Simulation gives easy-to-read waveforms and easy-to-process output logs. IDEA1 library contains many hardware devices and the whole IEEE 802.15.4 standard. We demonstrated that it is possible to run quick and accurate simulations with different hardware devices on the nodes. Classical network simulators outputs (packet delivery rate (PDR), packet latency) are supported; as well as accurate timing, and detailed energy consumption of hardware devices that are measurement validated. It is also possible to simulate and compare many scenarios and configurations in order to run design-space exploration for the best-suited and lower power solution. Current release of IDEA1 is publicly available at http://www.idea1.fr.

## REFERENCES

[1] D. Navarro, M. Galos, F. Mieyeville, and W. Du, "Heterogeneous Wireless Sensor Network Simulation," Proc. Sixth International Conference on Sensor Technologies and Applications, SENSORCOMM, pp. 292-295, Rome, Italy, August 2012.

[2] M. Horton and J. Suh, "A vision for wireless sensor networks," Proc. IEEE Microwave Symposium Digest, 2005.

[3] C. Fortuna, "Why is sensor data hard to get ?," Proc. COIN-ACTIVE Summer School on Advanced Technologies for Knowledge Intensive Networked Organizations in Aachen, 2010.

[4] Crossbow technologies inc, Document Part Number: 6020-0049-01-Rev-A, "Stargate X-Scale processor platform;" http://www.eol.ucar.edu/isf/facilities/isa/internal/CrossBow/DataSheets/stargate.pdf. Last accessed: May 16th, 2014.

[5] Texas Instruments, "A Powerful System-On-Chip for 2.4-GHz IEEE 802.15.4, 6LoWPAN and ZigBee Applications," SWRS096A –December 2012 – Revised April 2013, http://www.ti.com/cc2538-pr-ds1. Last accessed: May 16th, 2014.

[6] W. Du, D. Navarro, and F. Gaffiot, "Towards a Taxonomy of Simulation Tools for Wireless Sensor Network," Proc. International Conference on Simulation Tools and Techniques, 2010.

[7] S. McCanne and S. Floyd, "Network Simulator NS-2," http://www.isi.edu/nsnam/ns, 2010. Last accessed: May 16th, 2014.

[8] A. Varga, "The OMNeT++ discrete event simulation system," Proc. European Simulation Multiconference, 2001.

[9] J. Yick, B. Mukherjee, and D. Ghosal, "Wireless sensor network survey," Computer Network journal, vol 52, pp. 2292-2330, August 2008.

[10] V. Naoumov and T. Gross, "Simulation of large ad hoc networks," Proc. 6th ACM international workshop on modeling analysis and simulation of wireless and mobile systems, New York, USA, 2003.

[11] G. F. Riley, "Large-scale network simulations with GTNetS," Proc. Winter simulation conference, pp. 676-684, 2003.

[12] J. L. Font, P. Inigo, M. Domínguez, J. L. Sevillano, and C. Amaya, "Analysis of source code metrics from ns-2 and ns-3 network simulators," Simulation Modelling Practice and Theory, Elsevier, Vol 19, issue 5, pp. 1330-1346, 2011.

[13] E. Weingartner, H. vom Lehn, and K. Wehrle, "A performance comparison of recent network simulators," Proc. IEEE international conference on communications, Dresden, Germany, 2009.

[14] C. Mallanda et al., "Simulating wireless sensor networks with OMNeT++," http://citeseerx.ist.psu.edu/viewdoc/download?doi=10.1.1.331.6889&rep=rep1&type=pdf. Last accessed: May 16th, 2014.

[15] A. Kopke et al., "Simulating Wireless and Mobile Networks in OMNeT++, The MiXiM vision," Proc 1st international conference on simulation tools and techniques for communications, networks and systems & workshops, Simutools '08, Brussels, Belgium, 2008.

[16] J. Glaser, D. Weber, S. A. Madani, and S. Mahlknecht, "Power aware simulation framework for wireless sensor networks and nodes," EURASIP Journal on Embedded Systems 2008.

[17] F. Chen, I. Dietrich, R. German, and F. Dressler, "An Energy Model for Simulation Studies of Wireless Sensor Networks using OMNeT++," PIK - Praxis der Informationsverarbeitung und Kommunikation, vol. 32, issue 2, pp. 133–138, 2009.

[18] B. Titzer, D. Lee, and J. Palsberg, "Avrora: Scalable sensor network simulation with precise timing," Proc. Symposium on Information Processing in Sensor Networks, pp. 477-482, USA, 2005.

[19] P. Levis, N. Lee, M. Welsh, and D. Culler, "Tossim: accurate and scalable simulation of entire tinyos applications," Proc. of the 1st int. conf. on Embedded networked sensor systems, ser. SenSys '03, pp. 126-137, New York, USA, ACM, 2003.

[20] V. Shnayder, M. Hempstead, B. Chen, G. W. Allen, and M. Welsh, "Simulating the power consumption of large-scale sensor network applications," Proc. of the 2nd int. conf. on Embedded networked sensor systems, SenSys '04, pp. 188-200, New York, USA, ACM, 2004.

[21] J. Wenninger, J. Moreno, J. Haase, and C. Grimm, "Designing lowpower wireless sensor networks," Proc. Forum on Specification & Design Languages, Oldenburg, Germany, September 2011.

[22] F. Fummi, D. Quaglia, and F. Stefanni, "A SystemC-based Framework for Modeling and Simulation of Networked Embedded Systems," Proc. Forum on Specification and Design Languages, 2008.

[23] J. Polley, D. Blazakis, J. McGee, D. Rusk, and J. S. Baras, "ATEMU: a fine-grained sensor network simulator," First Annual IEEE Communications Society Conference on Sensor and Ad Hoc Communications and Networks, pp. 145-152, Oct. 2004.

[24] D. Weber, J. Glaser, and S. Mahlknecht, "Discrete event simulation framework for power aware wireless sensor networks," in Proc. of the 5th Int. Conf. on Industrial Informatics, pp. 335-340, 2007.

[25] M. Galos, D. Navarro, F. Mieyeville, and I. O Connor, "A Cycle-Accurate Transaction-Level Modelled Energy Simulation Approach for Heterogeneous Wireless Sensor Networks," 10th IEEE International NEWCAS Conference, Montréal, Canada, June 2012.

[26] F. Mieyeville, W. Du, I. Daikh, and D. Navarro, "Wireless Sensor Networks for active control noise reduction in automotive domain," Proc. 14th International Symposium on Wireless Personal Multimedia Communications, 2011.

[27] F. Mieyeville, D. Navarro, W. Du, and M. Galos, "Energy-centric simulation and design space exploration for Wireless Sensor Networks," Wireless Sensor Networks: Current Status and Future Trends, CRC Press, Taylor & Francis Group, November 2012.

[28] L. Girod, T. Stathopoulos, N. Ramanathan, J. Elson, D. Estrin, E. Osterweil, and T. Schoellhammer, "A system for simulation, emulation, and deployment of heterogeneous sensor networks," Proc. Int. Conf. on Embedded Networked Sensor Systems, 2004.

# Provisioning, Resource Allocation, and DVFS in Green Clouds

Guilherme Arthur Geronimo, Jorge Werner, Rafael Weingartner, Carlos Becker Westphall, and Carla Merkle Westphall
Networks and Management Laboratory
Federal University of Santa Catarina
Florianópolis, Brazil
E-Mail:{arthur,jorge,weingartner,westphal,carla}@lrg.ufsc.br

*Abstract*—**The aim of Green Cloud Computing is to achieve a balance between resource consumption and quality of service. In order to achieve this objective and to maintain the flexibility of the Cloud, dynamic provisioning and allocation strategies are needed to manage the internal settings of the Cloud, addressing oscillatory peaks of workload. In this context, we propose strategies to optimize the use of the Cloud resources while maintaining the service availability. This work introduces two hybrid strategies based on a distributed system management model; it describes the base strategies, operation principles, it validates and analyzes them, and it presents the results. In order to validate our proposed strategies, we extended CloudSim to simulate our strategies. We achieved a consumption reduction up to 87% comparing Standard Clouds with Green Clouds, up to 52% comparing the proposed strategy with other Green Cloud Strategy, and 13% less consumption using Dynamic Voltage and Frequency Scaling (DVFS) in hybrid provisioning strategy.**

***Keywords—Green Clouds; Provisioning; Resource Allocation; DVFS.***

## I. Introduction

This paper extends our previous work [1] proposing two strategies for allocation and provisioning of physical machines **(PMs)** and virtual machines **(VMs)** using DVFS as an improvement of private Clouds sustainability, transforming the Cloud into Green Cloud [2]. Green Clouds crave for efficiency of its components, so, we adopted positive characteristics of multiple existing strategies [3], developing hybrid strategies that, in our scope, aim to address:

- A sustainable solution to mitigate peaks in unpredictable workload environments with rapid changes;
- An optimization of the data center infrastructure without compromising the availability of services during the workload peaks;
- Balance between the sustainability of the infrastructure and the services availability defined on Services Level Agreements (SLAs).

This work was based on actual data collected by the university data center, that has multiple services suffering often with unexpected workload peaks, whether from attacks on servers or overuse of services in short periods of time. First, we propose an allocation model for private Clouds that aims to reduce the costs (energy and SLA fines) while improving the resource optimization. Second, we propose a provisioning model for private Clouds, turning them into Green Clouds, allowing the reduction of energy consumption and resource optimization while maintaining the Service Level Agreements (SLAs) with the integration of public Cloud resources. Third, after we validate our hybrid provisioning strategy, we have the opportunity to apply the hybrid provisioning strategy in a Cloud environment that uses Dynamic Voltage and Frequency Scaling (DVFS) in its physical machines. This way we achieve an improvement in energy consumption and resource optimization with no impacts on the Cloud SLAs.

### A. Motivation

The motivation for this work can be summarized in the following points:

- **Energy saving**: Murugesan [5] says "Energy saving is just one of the motivational topics within green IT environments." We highlight the following points: (1) the reduction of monthly data center operating expenses (OPEX), (2) the reduction of carbon emissions into the atmosphere (depending on the country), and (3) the extension of the lifespan of Uninterruptible Power Supply (UPS) [6].
- **Availability of Services**: Given the wave of products, components, and computing elements being delivered as services by the Cloud (*aaS), a series of pre-defined agreements or governing the behavior of the service that will be supplied / provided is needed [7]. According to Cloud Administrators, agreements that provide availability rates, usually 99.9% of the time (or more) are a concerning factor. Thus, the question is how to provide this availability rate while consuming little power.
- **Variation Workload**: In environments with multiple services, the workload prediction is complex work. Historical data is mostly used to predict future needs and behaviors. However, abrupt changes are unpredictable causing temporary unavailability of provided services. The need to find new ways to deal with these sudden changes in the workload is evident.
- **Delayed Activation**: Activation and deactivation of resources are a common technique for reducing power

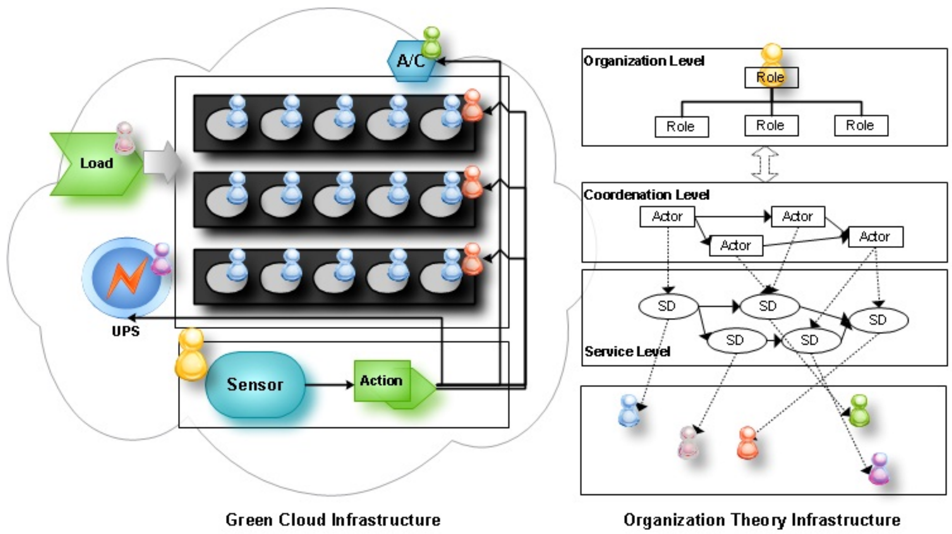


Fig. 1. Model Based in Organization Theory [4]

consumption, but the time required to complete this process can cause some unavailability of provided services, generating contractual fines.

- **Public Clouds**: Given the growing amount of public Clouds and the development of communication methods among Clouds, like Open Cloud Consortium [8], and Open Cloud Computing Interface [9], it became possible, for small or big companies, to easily use multiple public Clouds as extensions of a single private Cloud. We considered this as an alternative resource to implement new Green Cloud strategies. This is beneficial to those who need to expand their Cloud, and to the new clients of Cloud providers.

In a broad sense, this proposed model is for the Cloud provider that seeks the balance between energy saving and service providing (defined by the SLA).

### B. Objective

We aim to propose an allocation strategy for private Clouds and a provisioning strategy for Green Clouds, which suits the oscillatory workload and unexpected peaks. We will focus on finding a solution that consumes low power and generates acceptable request losses, in comparison to other base strategies.

### C. Paper Organization

This paper is organized as follows:

- Section II explains the bases of Organization Theory Model.
- Section III explains how DVFS works; this is one of the strategies used to compare our Green Cloud provisioning Hybrid Strategy.
- Section IV brings the state of the art, which includes a selection of works that were considered in our research.
- Section V presents the proposal, the idea behind each strategy, their pros and cons and where each one should be applied or not, tests, and results.
- In Section VI, we conclude this paper making some observations and analysis about the results and address some future works.

## II. MODEL

The concept of combining Organization Theory and complex distributed computing environments is not new. Foster [10] already proposed the idea of virtual organizations (VOs) as a set of individuals and / or institutions defined by such sharing rules in grid computing environments. This work concludes that VOs have the potential to radically change the way we use computers to solve problems the same way as the Web has changed the way we consume and create information.

Following this analogy, we have a similar view: Management Systems based on the Organization Theory would provide means to describe why / how elements of the Cloud should behave to achieve global system objectives, which are (among others): optimum performance, reduced operating costs, appointment of dependence, service level agreements, and energy efficiency.

These organizational structures, proposed in [11], allow network managers to understand the interactions between the Cloud elements, how their behavior is influenced in the organization, the impact of actions on macro and micro structures, as the macro level processes allowing and restricting activities at the micro level. This way, it provides computational models to classify, predict, and understand the elements interactions and their influence on the whole environment.

Managing Cloud through the principles of the Organization Theory provides the possibility for an automatic configuration management system, since adding a new element (e.g., Virtual Machines, Physical Machines, Uninterrupted Power Supply, Air Conditioning) is just a matter of adding a new service on the Management Group.

The proposed strategies are based on a pro-active management of Clouds, which is based on the distribution of responsibilities in holes. The management responsibility of the Cloud elements is distributed among several agents; each agent controls individually a Cloud element that suits him, as seen in Fig. 1.

### A. Case Study

In [3], Werner et al. proposed a model based on the Organization Theory to manage a Cloud environment using decentralized management services. They proposed agents to manage the Cloud elements, each agent managing the elements that are in its area. These agents would individually monitor and manage the elements they are responsible for, orchestrating them to fulfill the norms that are imposed to the system.

Norms are the rules or agreements used as input into the system such as SLAs, energy consumption, resource optimization, air conditioning (data center temperature), etc. They are a primitive knowledge collected from experienced administrators and are used at times when decisions need to be made. In complement to Norms, Werner et al. [3] defined believes that are empirical knowledge used to improve the decisions at management. It is the junction of the practical knowledge from the norms and empirical knowledge from historical data, derived by the system, analyzing historical data traces and correlating them with the norms that have or have not been fulfilled.

Werner et al. [3] also defined roles that the agents would assume while monitoring/managing the Cloud environments or services. The roles defined for agents that act at Cloud environment level are: VM management, server management, network management and environment management. The roles defined for agents that act at service level are: monitor element, service scheduler and service analyzer.

Based on [3], we conclude that the Organization Theory model would be applicable for managing the entities of a Cloud computing environment in a decentralized way. So far, our models apply the Organization Theory ideas as describe by Werner et al. [3], using decentralized agents to monitor and manage the Cloud entities.

## III. DVFS - Dynamic Voltage and Frequency Scaling

The DVFS was presented by Magklis et al. in [12]. It provides an alternative solution to decrease power consumption by giving the possibility to the PMs to independently decrease their power dissipation, by lowering the processor clock speed and supply voltage during the idle periods of time of the processor as seen on the left side of Fig. 2.

DVFS pros:

- Adaptive Consumption: lower energy consumption by adapting the processor frequency to the workload.
- Out-of-the-box: There is no need to adapt applications or services to use it.
- Management: The user (or application) is allowed to determine when to use (or not) the solution, giving the possibility to control the CPU temperature.

DVFS cons:

- Low Performance: decreasing the CPU frequency will reduce the system performance, which is expected [14].
- Inertia of Changes: The frequency takes some time to adapt to the system's needs. So, in scenarios with high load variations, DVFS could become a problem.
- Over Changes: The rapid and constant act of 'overvolting' and 'undervolting' the processor, trying to fulfill immediately the system needs, could decrease the equipment lifetime [15].

DVFS enhancements, as seen on the right side of Fig. 2, also shows a deeper level of DVFS. The idea is to apply it at the core level, not at the processor level as a global unit. Another work is trying to decrease the gap between voltage and frequency changes. The idea is to optimize the processor and build a fast DVFS that adapts quickly to system needs, as shown in Fig. 3. Kim et al. [16] use both strategies at the same time, achieving a mark of 21 % of energy saved.

## IV. State Of The Art

### A. Hardware Level

According to Von Laszewski et al. [17], energy consumption is a major challenge. They use a DVFS strategy to decrease the energy consumption in PMs used as virtualization hosts. It adapts the clock frequency of the CPUs to the real usage of the PMs, decreasing the frequency in idle nodes and increasing when is needed. However, the major energy consumption is not in the CPU, but in other parts of the PM, so to really decrease the energy consumption you need to turn them off.

Gunaratne et al. [18] stated that on USA just the network interface controllers (NICs) consume hundreds of millions of US dollars in electricity every year. That amount of energy used by the NICs is growing rapidly as the default 100Mbps controllers are being replace by brand new 1Gbps controllers, which consume about 4 W more than a 100Mbps controllers. They also found out that idle and fully loaded Ethernet links consume about the same amount of power while the amount of power used by an Ethernet link is actually dependent on

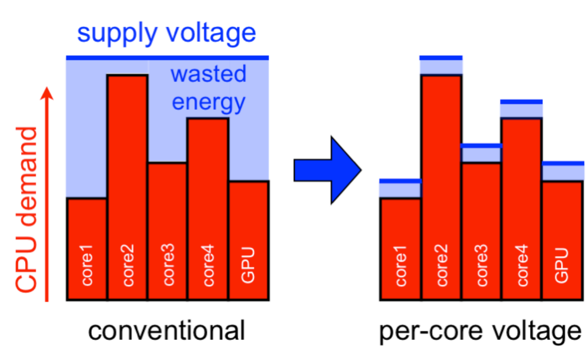


Fig. 2. DVFS - Main Idea [13]

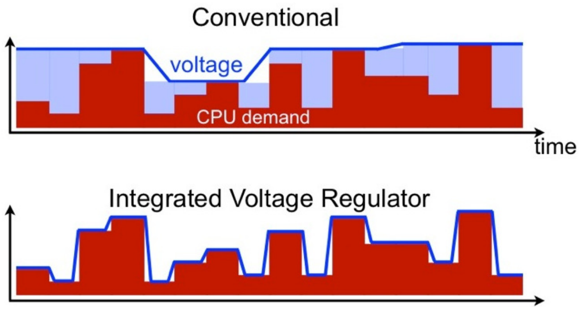


Fig. 3. Fast DVFS - Main Idea [13]

the link speed. Given the fact that measurements shown that the usage rate of Ethernets links are about 1% to 5% of the capacity, that brought attentions to the "Network Layer" as a new field to lower the energy consumption in the datacenter.

Gunaratne et al. [18] proposed a system design for adaptive link rate (ALR) [19] to be applied not just on edge links but rather on the whole network. With this approach was possible to operate Ethernet links 80% of the time on lower frequency, lowering the power consumption of the datacenter without affecting services and users. Given the fact that the network management is out of this paper scope, it was decided to not include the network infrastructure consumption in the final calculations.

### B. Datacenter Level

The workload balance strategy for clusters in [20] tries to achieve a lower energy consumption unbalancing the cluster workload, generating idle nodes and turning them off. In Cloud Computing, this strategy will not work in the case of Denial-of-Service attacks. Because in that scenario all nodes will be on, and there will be none node to turn off. This way, we foresee the need for VM migration between Clouds as mandatory function, to avoid cases where the unbalance of the load cannot be done.

Urgaonkar [21] proposed an overbooking strategy to consolidate virtual machines in physical machines and this way a lower resource consumption would be achieved. But, this work did not care that much for service degradation generated by resource contention that happens when you consolidate workloads.

Anh Vu [22] proposed a model that instead of taking just historic data of workload resource consumption and behavior for resource allocation and provisioning also takes in the interference generated by applications that compete for resource. It applies a canonical correlation analysis technique to find the resources that influence the most the application behavior; this way they could consolidate workloads with less impact on provided services. Their model presents a better result than [21], but, it has high computational costs and still does not have a good performance while predicting workload needs.

Gong [23] proposed PRESS (PRedictive Elastic ReSource Scaling for Cloud systems), a lightweight model to predict workload resource needs, based mainly on historical data. It uses a Fast Fourier Transform (FFT) to spot dominant frequencies and identify workload behaviors of resource usage. When there are no dominant frequencies found it applies a Markov Chain technique to predict the workload resource need for a short period of time. It is an early work that does not have the overhead problems found in [22], but it still does not have a great performance, since there are much more variables to take in, such as background workload, VMs migration need, application design, etc.

Shen et al. [24] improved the work done in [23]. They propose a smart model for provisioning resource that aims at reducing the SLAs breaches The PRESS prediction was extended to round data values. This way, it would achieve a better result since PRESS has not been so accurate to predict workload need. In order to improve the management of resources by the predictive model PRESS, they added SLAs breaches measurement as a new variable into the prediction model. It was also proposed a predictive migration model since the migration is one of the most expensive processes when dealing with virtualized resources. It is best to start a migration before the resource contention happens, avoiding this way a long period of service degradation. They keep track of all VMs needs in a physical machine of the Cloud. This way, when the resource prediction of VMs in that physical machine uses up the amount of resources the machine has, the model triggers a migration process before the resource contention happens.

### C. Cloud Level

Franke [25] tries to decrease the hosting costs in public and/or federated Clouds using costs and fines in contracts as constraints to better allocate resources. But, it limits itself in migrating VMs between Clouds, in a pool of pre-hired Clouds. This way, we foresaw that the resource consumption should also be considered as a metric to allocate the VMs.

Dawoud [26] highlights that the use of "historical resource usage traces" by themselves are not enough for a predictive model. That could lead to wrong actions at management level, especially when dealing with Web applications that usually are deployed in a multi-tier way (front end, application layer and database). So, he proposed a model to manage Web applications (in public Cloud environments) that correlates three factors, (1) historical traces of resource usage, (2) workload and (3) request types. Given the fact that the Web Applications are, in most cases, developed in a multi-tier way, the work raises the attention to the fact that each tier load does not interfere with the other tiers equally. That means, if we give more resource to a tier, we should proportionally increase the resource of every single tier of the application, since they all are tied together.

Hulkury et al. [27] proposed an integrated Green Cloud Computing Architecture that addresses the workload placement problem, determining the better place to deploy the users jobs based on their theoretical energy consumption. It requires a manager (cloud client side) to provide the jobs SLAs, job descriptions, network and server specifications, to calculate the energy consumption of the job in each cloud scenario (local, private or public Cloud). Just like [11], it touches the point of

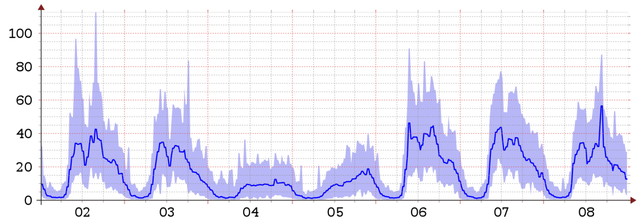


Fig. 4. Week Workload Distribution (Reqs/s)

using public clouds as an extension, and routing jobs between the clouds when it can be profitable. Sadly, it depends on some information that, in most cases, the Cloud client does not have access to, like the energy consumption of the public Cloud elements. It also mentions the idea of using XML to store SLAs and QoSs constraints in the Cloud Manager; however, it does not define any standard for that.

## V. PROPOSAL

For the conscious resource provisioning in Green Cloud environments, we propose a hybrid strategy that uses public Cloud as an external resource used to mitigate SLA breaches due to unexpected workload peaks. In parallel, for the optimal use of local resources, we propose a strategy of dynamic reconfiguration of the VMs attributes, allocated in the data center. Given the distributed model presented in the previous section, we used the Cloud simulation tool CloudSim [28] to simulate the university data center environment and workload.

In order to simulate a distribution faithful to reality and also stressful to the infrastructure, we (1) chose as a workload pattern the distribution of requests from the university's main websites (as shown in Fig. 4), and then (2) multiplied the request load by factors between 2 and 20, in order to apply stress to the system. We defined this strategy with the goal of obtaining results that reflect the reality and, at the same time pushing the request rate, striving for correlating the workload behavior trends with the load.

### A. Allocation

The resource allocation strategy is a proposal that introduces a composition of two other approaches: (1) the migration of VMs, which aims to consolidate VMs and optimize resource utilization, and (2) the Dynamic Reconfiguration of VMs, which aims to reconfigure dynamically the resources used by the VMs, increasing the consolidation factor.

*1) VMs Migration Strategy:* This strategy aims to reduce power consumption by disabling the idle PMs of the Cloud. To induce idleness in the PMs, the VMs are migrated and concentrated in few PMs. This way, the Cloud manager can disable the idle PMs, reducing the consumption of the data center. However, for optimal results, this strategy must be used with a reconfiguration strategy that enables hosting more VMs in less PMs, increasing the idle PMs.

TABLE I. RESULTS OF ALLOCATION'S SCENARIOS

| Scenario | Reconf. Strategy | Mig. Strategy | Consumption |
|---|---|---|---|
| 1 | No | No | - |
| 2 | No | Yes | 84.3% |
| 3 | Yes | No | 0.4% |
| 4 | Yes | Yes | 87.2% % |

*2) VMs Dynamic Reconfiguration Strategy:* Seeking the improvement of the previous strategy, this strategy is an alternative optimization that dynamically shrinks the VM. It adjusts the parameters of the VM [29], without migrating it or turning it off. For example, we can increase or decrease the parameters of CPU and memory allocated. Thus, the VMs would adapt its configurations according to the demand.

*3) Tests & Results:* To simulate the strategies we used a Cloud simulator tool developed in Melbourne, CloudSim [28]. But, in order to achieve the simulations needed, we made some changes in the code [4], allowing to simulate the distributions patterns and scenario defined before. Four scenarios were simulated in order to seek the comparative analysis between ordinary Cloud (Scenario 1), the existing methods (Scenarios: 2 and 3), and the proposed approach (Scenario 4). Those were:

1) No strategies;
2) Migrating VMs Strategy;
3) Reconfiguring the VMs Strategy;
4) Reconfiguring and migrating VMs Strategy.

At the simulations, we gathered behavior, sustainability, and availability metrics, such as the number of idle PMs, total energy consumption, and number of SLA breaches. Table I presents the percentage of energy consumption in each scenario with 100 PMs. Analyzing it we see that without any strategy implemented, the power consumption is stable during the whole period, since all the VMs and PMs were activated, which happens if we implement just the reconfiguration strategy by itself. The migration scenario shows a significant reduction in power consumption, since it consolidate VMs in PMs and latter disabling the idle ones. And last, the mix of migration and reconfiguration approach shows a steady noticeable reduction in power consumption since it consolidates more VMs in fewer PMs.

### B. Provisioning

The Green Cloud provisioning hybrid strategy is based on two other strategies, which are the On Demand strategy (OD) and the Spare Resources strategy (SR). It tries to be the middle ground between the two, enjoying the strengths of both sides, and aiming to present power consumption lower like the OD strategy while maintaining the availability as the SR strategy.

*1) On Demand Strategy:* The principle of OD strategy is to activate the resources when they are needed. In our case, when a service reaches a saturation threshold, new VMs would be instantiated. And, when there is no more space to instantiate new VMs, new PMs would be activated to host the new VMs. The opposite also applies; when a threshold of idleness is reached, the idle VMs and PMs are disabled. Fig. 5 shows an OD Strategy scenario, where only the needed VMs (green circles) and PMs (white slim rectangles) are turned on. The other units (red crosses and lined rectangles) are off.

- Pros: energetically efficient since it maintains just a minimum amount of active resources.
- Cons: ineffective in scenarios that have sudden spikes in demand because the process to activate resource takes time, and some requests end up being lost.

*2) Spare Resource Strategy:* To mitigate the problem of requests timeouts originated by a long activation time of resources, we adopted the strategy SR, whose principle is to reserve idle resources ready to be used. In our case, there was always one idle VM ready to process the incoming requests and one idle PM ready to instantiate new VMs. If these resources were used, they were no longer considered idle, and new idle resources were activated. As soon as the resources were no longer being used they were disabled. Figure 6 shows a SR Strategy scenario where the Cloud keep an idle VM (golden circle) and an idle PM (vertical lined rectangle) ready to fulfill any workload.

- Pros: The strategy has been shown effective to deal with unexpected peak demands
- Cons: It showed the same behavior as OD strategy in cases where demand raised very rapidly; in other words, the idle feature was not enough to process the demand. Another negative point was the energy consumption; since it always had an idle resource, the consumption was greater than the OD strategy.

*3) Hybrid Strategy:* Seeking the merger of the strengths of the previous strategies and mitigating its shortcomings, we propose a hybrid strategy. This strategy aims to reduce the energy consumption on private Cloud and reduce the violation of SLAs.

As shown in Fig. 7, the Cloud enables the VMs when the service in question reaches its saturation threshold, just as the OD strategy. When a PM is unable to allocate more VMs, it uses the public Cloud to host the new VMs while a disabled PM is passing through the activation process. This way we fulfill requests that would be lost during the activation process.

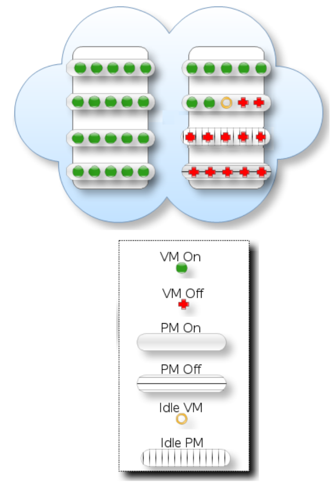


Fig. 6. Spare Resource Strategy

The deactivation process occurs just as the other strategies. However, it is considered that the public Cloud is paid by time (usually by hour of processing); so, it disables the VM hosted in the public Cloud only when:

- it is idle and;
- it is almost time to complete a full hour of hosting.

*4) Tests:* As previously mentioned, we performed some modifications to the CloudSim code in order to enable the simulation of scenarios using our proposed model. Before we started the simulations, we defined some variables, such as the saturation threshold and idleness. The variables considered in our experiments are shown in Table II.

The amount of requests per second was calculated based on the previously presented workload pattern (Fig. 4), using the formula $R_t * M_x$ where $R_t$ is the number of requests per second in time *t*, and $M_x$ is the stress multiplier of the experiment *x*.

To get an overview of how each strategy would behave in different scenarios, we ran a series of tests which varied the:

- **Amount of Requests**: To maintain the defined request

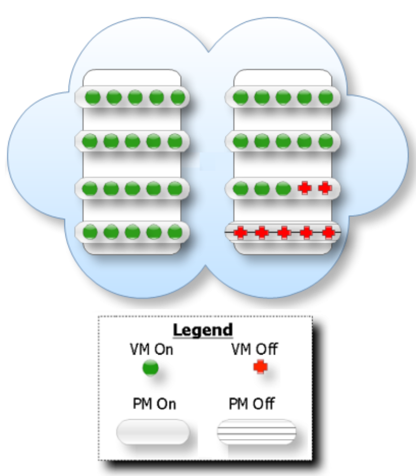


Fig. 5. On Demand Strategy

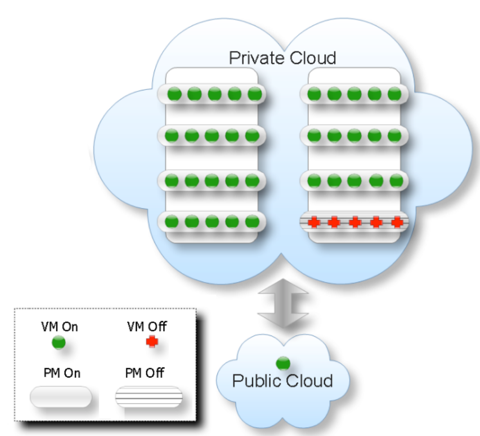


Fig. 7. Hybrid Strategy

TABLE II. SIMULATION'S VARIABLES

| Variable | Value |
|---|---|
| Saturation Threshold (Load 1 minute) | 1.0 |
| Idleness Threshold (Load 1 minute) | 0.1 |
| Activation VM time (seconds) | 10 |
| Activation PM time (seconds) | 120 |
| Size of Request (MI) | 1000 to 2000 |
| DVFS | On or Off |
| Number of PMs | 8 |
| Maximum number of VMs per PMs | 5 |
| SLA timeout threshold (seconds) | 10 |

distribution (explained in the beginning of Section V), we used multipliers to increase the number of requests. Those multipliers started from 2 to 20 in steps of 2 (2, 4, 6, etc.).

- **Size of Requests**: The size of requests ranged from 1000 to 2000 MI (Millions Instructions) to be executed, in steps of 100 (1000, 1100, 1200, etc.).

- **Utilization of DVFS**: Based on the previously tests, we compare the proposed hybrid strategy with and without DVFS.

This way, it was performed a total of 440 simulations being 330 simulations without DVFS and 110 with DVFS (just the hybrid strategy). These tests evaluated the power consumption of the private Cloud and the total number of timeouts (SLAs not accomplished) for the period.

*5) Results:* Figures 8, 9, and 10 show the results obtained while running the experiments described before. Each figure shows the timeout and the energy consumption variation of each experiment for every combination of the settings multiplier and request size variable (110 simulations each experiment).

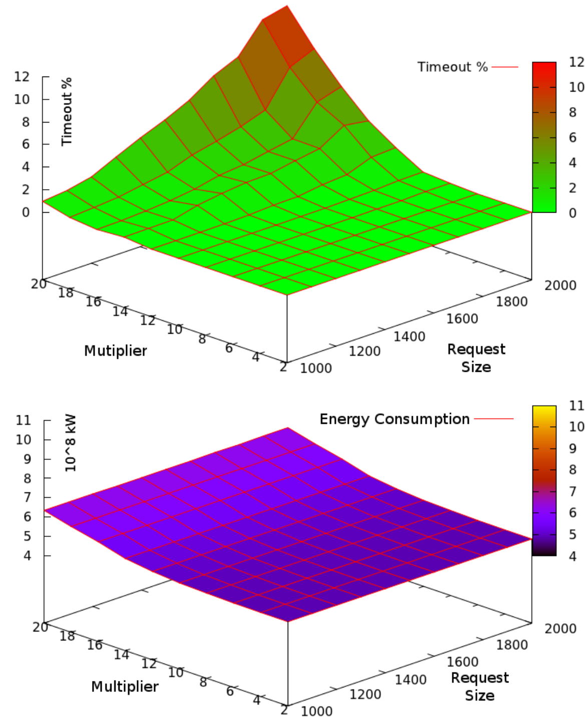


Fig. 8. Number of Timeouts (top) and Energy Consumption (bottom) using OD Strategy

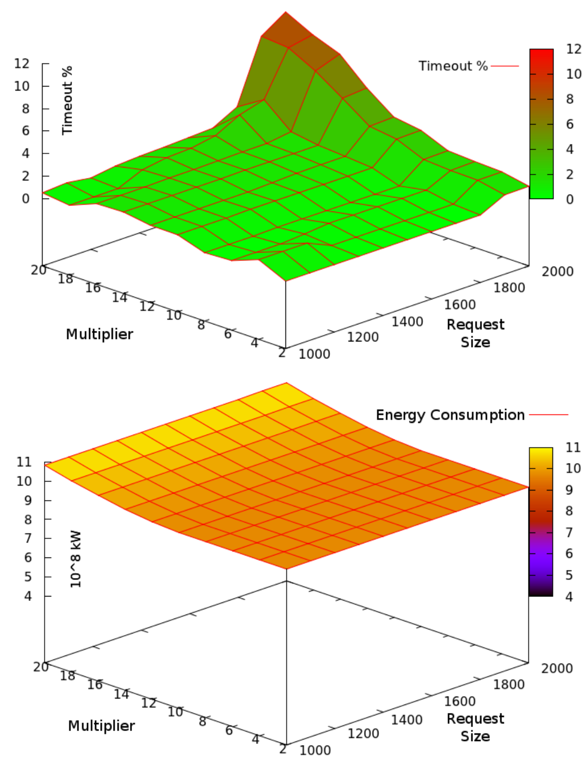


Fig. 9. Number of Timeouts (top) and Energy Consumption (bottom) using SR Strategy

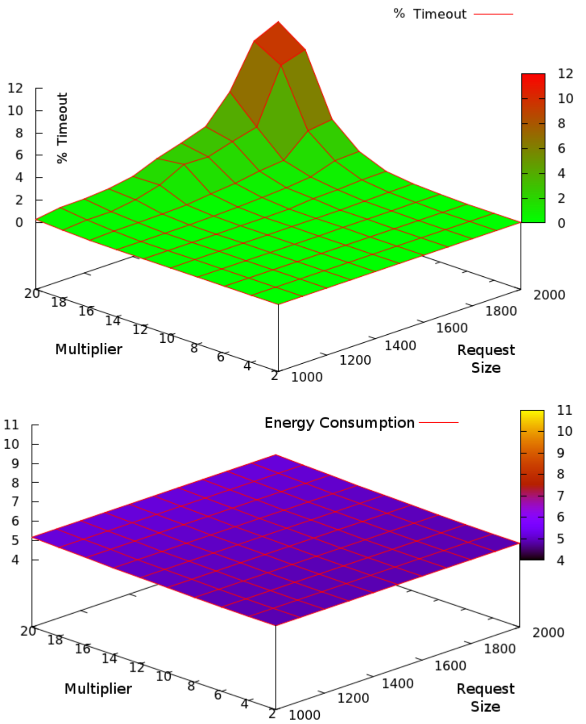


Fig. 10. Number of Timeouts (top) and Energy Consumption (bottom) using Hybrid Strategy

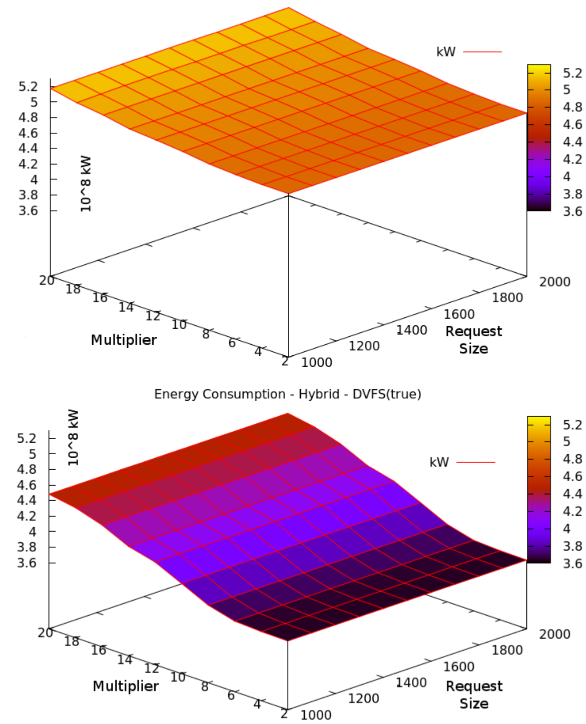


Fig. 11. Consumption with DVFS Off (top) and with DVFS On (bottom) using Hybrid Strategy

Table III shows the results obtained in the ”worst case scenario”, by definition, with the multiplier equal to 20 and the request size equal to 2000 MI. Regarding the results in Table III, it took the Hybrid Strategy as a basis of comparison. In this case, the values listed are for hybrid strategy. For example, the hybrid strategy presented 3% fewer request timeouts than the OD strategy.

TABLE III. HYBRID STRATEGY COMPARED TO THE OTHER STRATEGIES

| | OnDemand | Spare | Hybrid With DVFS |
|---|---|---|---|
| Timeouts | -3 % | +15 % | - |
| Consumption | -18 % | -52 % | -13 % |

Now, comparing the same Hybrid Strategy, with and without using DVFS, we got 13 % less energy consumption. To get a better view of the differences between the two simulations, the scale of the graph in Fig. 11 was zoomed. There were no significant difference on the timeout rate in this scenario.

## VI. Discussion & Conclusion

Based on what was presented in previous sections, and considering the objectives defined at the beginning of this paper, we consider that the intended goal was achieved. Two strategies for allocation and provisioning were proposed; both aimed at optimizing the energy consumption and resource utilization without sacrificing service availability.

The allocation strategy in private Clouds, compared to a normal Cloud, demonstrated an 87% reduction in energy consumption. Though, it was observed that this strategy is not effective in scenarios that have huge oscillations in workload. That is because it ends up generating too much reconfigurations and migrations which have a significant computational cost. Despite this, it still shows a significative improvement in energy savings when compared to a Cloud without any resource management strategy deployed. Should be mentioned that, part of the 87% reduction rate is derived from the fact that the energy consumption from the public Cloud is not considered in the graphs. This part represents approximately 3% of the final value.

Fig. 12 shows a comparison between the green Cloud provisioning strategies. The strategies are being compared with the SR strategy which is the most expensive since it always keeps spare resources to maintain SLAs for unpredicted increases in workloads. While the OD strategy achieves up to 47.05% of energy savings when compared to SR strategy, the proposed hybrid strategy shows up to 3.13% of improvement, achieving 50.13% of energy savings with fewer timeouts than the OD strategy. The energy saving rates were even bigger when we simulated an environment where the servers deployed had the DVFS enabled. This improved the energy savings to 59.87% while maintaining the timeouts rate for extreme situations, such as when the request load was multiplied by a factor of 20 and each request size was 2000 million of instructions to be processed.

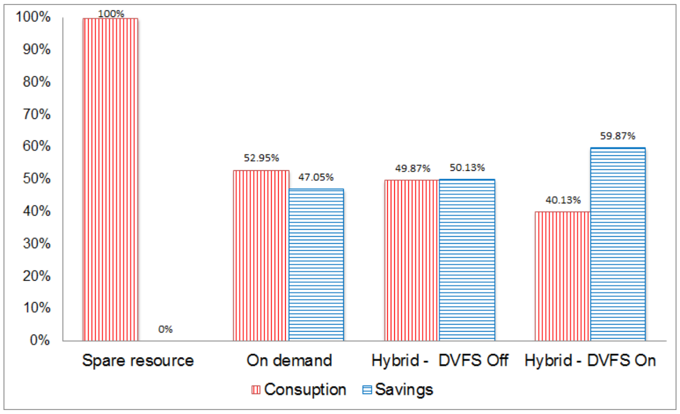


Fig. 12. Average energy consumption gain over the strategies

We should mention that we found (and fixed) some "bugs" in CloudSim DVFS module. The simulator bases the energy consumption directly on the use of the CPU, regardless of other components in the physical machine such as GPUs, NIC, memory, HD, which leads the energy consumption to lower rates than it should be.

As can be viewed in Figures 8, 9, and 10 the strategy that achieved the lowest timeout rate was the SR strategy followed directly by the hybrid strategy with a difference lower than 3%. It was expected that the SR strategy achieved better timeout rates since it always has a spare VM and PM to supply sudden spikes in workloads, though it comes with a high cost in energy consumption and resource optimization. So, if we consider the energy savings and resource optimization generated by the hybrid strategy and compare them with the expenses of the SR strategy, the 3% extra timeouts generated by the hybrid strategy is acceptable.

Thus, we conclude that the use of the hybrid strategy is recommended in situations where the activation time of resources affects directly the SLA (in other words, generates fines). This strategy is the most balanced strategy for resource provisioning for green Cloud environments. However, this approach is not recommended when access to public Cloud resources is poor or the Cloud provider lacks in resource quality, security or other factors that can affect directly the SLAs.

### A. Future Works

As future work, we aim at adding the strategy of Dynamic Reconfiguration of VMs in public Clouds. This way the public Cloud provider would be able to better manage its resource. This procedure was not adopted because, during the development of this work, this feature was not a market reality. We also intend to invest in new simulations of the Cloud extending the variables (e.g., adding UPS variable), exploring some artificial intelligence techniques [30] such as Bayesian networks, adding the recalculation of beliefs, repeating the simulation with different Cloud simulators such as GreenCloud [31], ICanCloud [32] or MDCSim [33]. This way we could compare the results and check if our proposed models show the same benefits in different simulation tools engines.

We also want to implement our proposed solutions in a real datacenter, in order to create an error factor between the results obtained with the use of simulation tools and the results of a real Cloud. This way we could measure how accurate the Cloud simulation tools are when compared with a real environment. Our PCMONS (Private Cloud Monitoring System), open-source solutions for Cloud monitoring and management, also will help to manage Green Clouds by automating the instantiation of new resource [34].

We foresee a way of working out unexpected workload peaks scenario. Prior knowledge of the behavior of hosted services could allow the management services to improve consolidation and energy consumption while maintaining the services' expected behaviors. It is believed to be necessary to develop a description language that represents the structure and behavior of a service, enabling and easing the exchange of information between application developers and Cloud provider for planning, provisioning, and managing the Cloud.

## ACKNOWLEDGMENT

The authors thank anonymous reviewers for their comments to improve the paper.

## REFERENCES

[1] G. Geronimo, C. Werner, J. Westphall, C. Westphall, and L. Defenti, "Provisioning and Resource Allocation for Green Clouds," in *ICN 2013 - The Twelfth International Conference on Networks*, Jan. 2013, pp. 244–289.

[2] J. Werner, G. A. Geronimo, C. B. Westphall, F. L. Koch, C. M. Westphall, R. R. Freitas, and A. Fabrin, "Aperfeiçoando a gerência de recursos para nuvens verdes," *INFONOR*, vol. 1, pp. 1–8, 2012.

[3] J. Werner, G. A. Geronimo, C. B. Westphall, F. L. Koch, R. R. Freitas, and C. M. Westphall, "Environment, services and network management for green clouds," *CLEI Electronic Journal*, vol. 15, no. 2, p. 2, 2012.

[4] Werner, J. and Geronimo, G. A. and Westphall, C. B. and Koch, F. L. and Freitas, R. R., "Simulator improvements to validate the green cloud computing approach," *LANOMS Latin American Network Operations and Management Symposium*, vol. 1, pp. 1–8, 2011.

[5] S. Murugesan, "Harnessing green it: Principles and practices," *IT professional*, vol. 10, no. 1, pp. 24–33, 2008.

[6] R. Buyya, A. Beloglazov, and J. Abawajy, "Energy-Efficient management of data center resources for cloud computing: A vision, architectural elements, and open challenges," in *Proceedings of the 2010 International Conference on Parallel and Distributed Processing Techniques and Applications (PDPTA 2010), Las Vegas, USA, July 12*, vol. 15, 2010.

[7] M. A. P. Leandro, T. J. Nascimento, D. R. dos Santos, C. M. Westphall, and C. B. Westphall, "Multi-tenancy authorization system with federated identity for cloud-based environments using shibboleth," in *ICN 2012, The Eleventh International Conference on Networks*, 2012, pp. 88–93.

[8] OpenCC, "Open cloud consortium," 2012, "[Online; Last access: 2013-01-15]". [Online]. Available: http://opencloudconsortium.org/

[9] OCCI, "Open cloud computing interface," 2012, "[Online; Last access: 2013-01-15]". [Online]. Available: http://www.occi-wg.org

[10] I. Foster, Y. Zhao, I. Raicu, and S. Lu, "Cloud computing and grid computing 360-degree compared," in *Grid Computing Environments Workshop, 2008. GCE 08*, nov. 2008, pp. 1–10.

[11] J. Werner, G. A. Geronimo, C. B. Westphall, F. L. Koch, and R. R. Freitas, "Um modelo integrado de gestão de recursos para as nuvens verdes," in *CLEI 2011*, vol. 1, 2011, pp. 1–15.

[12] G. Magklis, G. Semeraro, D. Albonesi, S. Dropsho, S. Dwarkadas, and M. Scott, "Dynamic frequency and voltage scaling for a multiple-clock-domain microprocessor," *Micro, IEEE*, vol. 23, no. 6, pp. 62–68, 2003.

[13] W. KIM, "Fast, per-core dvfs using fully integrated voltage regulators," "[Online; Last access: 2013-01-15]". [Online]. Available: http://www.eecs.harvard.edu/ wonyoung/research.html

[14] Q. Wang, Y. Kanemasa, J. Li, C. A. Lai, M. Matsubara, and C. Pu, "Impact of dvfs on n-tier application performance," in *Conference on Timely Results in Operating Systems (TRIOS)*. ACM, 2013.

[15] M. Basoglu, M. Orshansky, and M. Erez, "Nbti-aware dvfs: A new approach to saving energy and increasing processor lifetime," in *Low-Power Electronics and Design (ISLPED), 2010 ACM/IEEE International Symposium on*, 2010, pp. 253–258.

[16] W. Kim, M. Gupta, G.-Y. Wei, and D. Brooks, "System level analysis of fast, per-core dvfs using on-chip switching regulators," in *High Performance Computer Architecture, 2008. HPCA 2008. IEEE 14th International Symposium on*, 2008, pp. 123–134.

[17] G. von Laszewski, L. Wang, A. Younge, and X. He, "Power-aware scheduling of virtual machines in dvfs-enabled clusters," in *Cluster Computing and Workshops, 2009. CLUSTER '09. IEEE International Conference on*, 31 2009-sept. 4 2009, pp. 1 –10.

[18] C. Gunaratne, K. Christensen, B. Nordman, and S. Suen, "Reducing the energy consumption of ethernet with adaptive link rate (alr)," *Computers, IEEE Transactions on*, vol. 57, no. 4, pp. 448–461, 2008.

[19] C. Gunaratne, K. Christensen, and B. Nordman, "Managing energy consumption costs in desktop pcs and lan switches with proxying, split tcp connections, and scaling of link speed," *International Journal of Network Management*, vol. 15, no. 5, pp. 297–310, 2005.

[20] E. Pinheiro, R. Bianchini, E. Carrera, and T. Heath, "Load balancing and unbalancing for power and performance in cluster-based systems," in *Workshop on Compilers and Operating Systems for Low Power*, vol. 180. Citeseer, 2001, pp. 182–195.

[21] B. Urgaonkar, P. Shenoy, and T. Roscoe, "Resource overbooking and application profiling in a shared Internet hosting platform," *ACM Transactions on Internet Technology*, vol. 9, no. 1, pp. 1–45, Feb. 2009. [Online]. Available: http://portal.acm.org/citation.cfm?doid=1462159.1462160

[22] A. V. Do, J. Chen, C. Wang, Y. C. Lee, A. Y. Zomaya, and B. B. Zhou, "Profiling Applications for Virtual Machine Placement in Clouds," *2011 IEEE 4th International Conference on Cloud Computing*, pp. 660–667, Jul. 2011. [Online]. Available: http://ieeexplore.ieee.org/lpdocs/epic03/wrapper.htm?arnumber=6008768

[23] Z. Gong, X. Gu, and J. Wilkes, "Press: Predictive elastic resource scaling for cloud systems," in *Network and Service Management (CNSM), 2010 International Conference on*. IEEE, 2010, pp. 9–16.

[24] Z. Shen, S. Subbiah, X. Gu, and J. Wilkes, "Cloudscale: elastic resource scaling for multi-tenant cloud systems," in *Proceedings of the 2nd ACM Symposium on Cloud Computing*. ACM, 2011, p. 5.

[25] H. A. Franke, "Uma abordagem de acordo de nível de serviço para computação em nuvens," PPGCC/UFSC, 2010.

[26] W. Dawoud, I. Takouna, and C. Meinel, "Dynamic scalability and contention prediction in public infrastructure using internet application profiling," in *Cloud Computing Technology and Science (CloudCom), 2012 IEEE 4th International Conference on*. IEEE, 2012, pp. 208–216.

[27] M. N. Hulkury and M. R. Doomun, "Integrated green cloud computing architecture," in *Proceedings of the 2012 International Conference on Advanced Computer Science Applications and Technologies*, ser. ACSAT '12. Washington, DC, USA: IEEE Computer Society, 2012, pp. 269–274. [Online]. Available: http://dx.doi.org/10.1109/ACSAT.2012.16

[28] R. Buyya, "Modeling and simulation of scalable cloud computing environments and the cloudsim toolkit: Challenges and opportunities," in *HPCS 2009. International Conference on*. IEEE, 2009, pp. 1–11.

[29] T. Wood, P. Shenoy, A. Venkataramani, and M. Yousif, "Sandpiper: Black-box and gray-box resource management for virtual machines," *Comput. Netw.*, vol. 53, no. 17, pp. 2923–2938, Dec. 2009. [Online]. Available: http://dx.doi.org/10.1016/j.comnet.2009.04.014

[30] F. L. Koch and C. B. Westphall, "Decentralized network management using distributed artificial intelligence," *Journal of Network and Systems Management*, vol. 9, pp. 375–388, 2001, 10.1023/A:1012976206591. [Online]. Available: http://dx.doi.org/10.1023/A:1012976206591

[31] D. Kliazovich, P. Bouvry, Y. Audzevich, and S. U. Khan, "GreenCloud: A Packet-Level Simulator of Energy-Aware Cloud Computing Data Centers," *2010 IEEE Global Telecommunications Conference GLOBECOM 2010*, pp. 1–5, Dec. 2012. [Online]. Available: http://ieeexplore.ieee.org/lpdocs/epic03/wrapper.htm?arnumber=5683561

[32] A. Núñez, J. L. Vázquez-Poletti, A. C. Caminero, G. G. Castañé, J. Carretero, and I. M. Llorente, "icancloud: A flexible and scalable cloud infrastructure simulator," *Journal of Grid Computing*, vol. 10, no. 1, pp. 185–209, 2012.

[33] S.-H. Lim, B. Sharma, G. Nam, E. K. Kim, and C. R. Das, "Mdcsim: A multi-tier data center simulation, platform," in *Cluster Computing and Workshops, 2009. CLUSTER'09. IEEE International Conference on*. IEEE, 2009, pp. 1–9.

[34] S. A. de Chaves, R. B. Uriarte, and C. B. Westphall, "Toward an architecture for monitoring private clouds," *Communications Magazine, IEEE*, vol. 49, no. 12, pp. 130 –137, December 2011.

# Enhanced Adaptive Traffic Dependent Handover Decision System for Wireless Mobile Networks

Thanachai Thumthawatworn
Networking Technology Research Laboratory
Vincent Mary School of Science and Technology
Assumption University, Thailand
Email: thanachai@scitech.au.edu

Anjum Pervez
Faculty of Engineering, Science and the Built Environment
London South Bank University
United Kingdom
Email: perveza@lsbu.ac.uk

Pratit Santiprabhob
Networking Technology Research Laboratory
Vincent Mary School of Science and Technology
Assumption University, Thailand
Email: pratit@scitech.au.edu

***Abstract*—Integrated network architectures have the potential to provide ubiquitous and seamless services over wide areas of mobility, with adequate quality of service and favourable price. To fully exploit such architectures (heterogeneous networking environments) multiple handovers often become necessary. Furthermore, in view of the growing demand for real-time applications, the inclusion of QoS-related parameters in the handover decision process is essential. This requirement inevitably increases the overall number of decision parameters, leading to unacceptably long algorithm execution time for a typical monolithic fuzzy-based handover decision system (MHDS), which employs a single fuzzy decision engine. In this paper, an adaptive traffic dependent fuzzy-based handover decision system (ATDHDS), which employs multiple fuzzy decision engines, each dedicated to a specific traffic type, is presented. The results show that, comparing with the MHDS, the proposed ATDHDS significantly improves the network selection performance and algorithm execution time. The ATDHDS is then enhanced by introducing additional fuzzy engines, which perform a QoS aggregation process, with the aims to further improve the overall network selection performance and to further reduce the algorithm execution time. The simulation results suggest that the enhanced ATDHDS (EATDHDS) successfully achieves both objectives.**

***Keywords*-fuzzy logic; handover; traffic dependent; QoS aggregation; wireless mobile.**

## I. Introduction

Mobile users in the 'Information age' expect ubiquitous and seamless services over wide areas of mobility, with adequate quality of service and favourable price. It appears that integrated network architectures have the potential to satisfy the above requirements. Integrated network architectures (referred to as heterogeneous networking environments) require interconnections of various wireless technologies such as WLAN, WiMAX and Cellular networks as illustrated in Figure 1. To ensure continuous connection, required quality of service and acceptable usage price, over a wide area of mobility, multiple handovers (switching connection from one wireless network to another) often become necessary. A handover may take place in a homogeneous networking environment (horizontal handover) or in a heterogeneous networking environment (vertical handover). In either case some form of decision mechanism needs to exist within the mobile device.

A horizontal handover decision is normally a straightforward process as the decision is based simply on the received signal strength (RSS). However, due to varied characteristics of different wireless networks, a simple RSS based decision cannot achieve the required results in a vertical handover decision process. Clearly there is a need for a much more intelligent handover decision system (HDS) for heterogeneous networking environments. Several deterministic algorithms for handover decision engines have been proposed in the literature, however they suffered from two limitations: 1) inability to deal with imprecise data efficiently, 2) inconsistencies in the decision outcomes, due to the fact that the procedures used for assignment of parameter weight are subjective.

The fuzzy logic techniques are regarded to have the ability to deal with the above limitations. Thus, numerous fuzzy logic based solutions, which enhance intelligence of the vertical handover process, have been proposed in the literature. However, in most of the existing work the decision process is based on a single monolithic decision engine, and with no regard

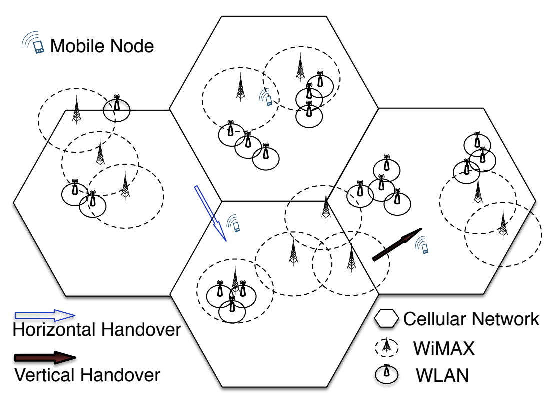


Figure 1. Architecture of Heterogeneous Wireless Mobile Networks

to the traffic type. Furthermore, only a limited number of decision parameters are generally considered. The restriction on the number of decision parameters seems to be due to the fact that as the number of decision parameters increases, the number of decision rules increases exponentially, which leads to computational complexity and very long algorithm execution time ($\tau$). Despite these constraints the QoS-related parameters (latency, jitter and packet loss) need to be included in the decision process, if real-time services (VoIP, video streaming, etc.) are demanded by the users (noting the global demand for real-time services).

To address the above issues, we proposed an adaptive traffic dependent fuzzy-based HDS (ATDHDS) in our previous publication [1]. The performance of the proposed ATDHDS was compared, in terms of the network selection and $\tau$, with monolithic fuzzy-based HDS (MHDS), tailored MHDS and Simple Additive Weighting (SAW). The simulation results showed that the ATDHDS gave an improvement in terms of network selection and a reduction in the value of $\tau$. However, the simulation model did not take into account the fact that the output scores generated by the fuzzy engines follow a random process (the input parameter values are randomly selected). In this paper a statistical averaging procedure is included, which produces more reliable results. In addition, the WiMAX data range is extended from (3 - 6 Mbps) to (1 - 6 Mbps) to represents a more realistic WiMAX capability.

The ATDHDS is further enhanced by introducing two new fuzzy engines, which perform a QoS aggregation process. The aims of the Enhanced ATDHDS are to improve the overall network selection performance and, at the same time, to further reduce $\tau$. The results suggest that the Enhanced ATDHDS gives some improvements in the network selection performance but huge benefit in reducing $\tau$.

Finally, the battery consumption analysis is carried out and the results suggest that the power consumption of the proposed fuzzy-based algorithm is unlikely to have a major impact on the battery life in real-life implementations.

The paper is organized as follows. Related vertical handover decision algorithms are given in Section II. In Section III, the design and development of a monolithic fuzzy-based HDS and the adaptive traffic dependent fuzzy-based HDS are presented. The simulation results and comparisons of performance are also given in Section III. The design and development of the enhanced adaptive traffic dependent HDS is presented in Section IV. A comparison between the ATDHDS and Enhanced ATDHDS and the battery life analysis are also given in Section IV. Section V gives conclusions and future work.

## II. Related Vertical Handover Decision Algorithms

Numerous vertical handover decision algorithms have been developed over the past several years [2]–[4]. They have varying degree of complexity and intelligence. These algorithms can be broadly classified into two categories: deterministic algorithms and heuristic algorithms. The former algorithms use mathematical functions to select the best candidate wireless network for handover, whilst decisions in the latter algorithms are made on the basis of some pre-defined decision (IF-THEN) rules, which identify the inter-relationships of the decision parameters considered. Mathematic-based algorithms are simple to use but suffer from two limitations: 1) it is often difficult to acquire very precise data [5], as a result, the network selection performance is degraded, 2) the methods used for assigning the parameter weight to individual decision parameters are subjective [6], as a result, the outcomes are often inconsistent.

Heuristic algorithms (e.g., rule-based, fuzzy logic, neural network and Adaptive Neural Fuzzy Inference System (ANFIS)) follow a different decision making approach and therefore avoid the drawbacks suffered by the deterministic algorithms. Fuzzy logic, in general, is regarded to have the ability to enhance intelligence in decision making processes. It has been widely used for decision making processes in many different areas, e.g., business forecasting [7] and stock trading [8]. More specific to handover in wireless networks, fuzzy-based algorithms have been used in a handover triggering algorithm [9]; pre-processing of imprecise input data for Analytic Hierarchy Process (AHP) [10] and Simple Additive Weighting (SAW) algorithms [11]. The use of fuzzy logic in all the above applications has been only to assist handover decision engines.

A number of researchers have focused their attention on developing fuzzy-based vertical handover decision algorithms [12], [13]. A fuzzy-based vertical handover decision algorithm, which assumes interconnection between WLAN and WMAN, is proposed in [14]. The decision parameters considered are: RSS, data rate, distance. The main aim of this work is to minimize the number of packet loss and the results presented are encouraging.

Authors in [15] have proposed a network selection algorithm based on fuzzy logic assuming three wireless technologies (Cellular, WiMAX and WLAN). The algorithm takes RSS, network load and available bandwidth into consideration. The results suggest that the proposed algorithm can select the most appropriate wireless network for handover in a given scenario.

In [16], a fuzzy-based algorithm between WWAN and WLAN is proposed. RSS, bandwidth, usage price are included in the decision process. The results show that the proposed algorithm makes accurate handover decisions, reduces the number of unnecessary handovers, balances network resources and improves network performance.

In all the above solutions, no QoS-related decision parameters (i.e., latency, jitter and packet loss) have been considered in the decision process. In view of the growing demand for real-time mobile applications, which require guaranteed QoS (defined by commonly used recommendations [17]), it has become necessary to include the QoS parameters in the decision process. More recently, efforts have been directed to evaluate the performance of a HDS in the presence of multiple QoS parameters.

In [18], bit error rate (BER) and RSS have been considered in their fuzzy-related decision algorithm. The results show improvement in terms of the number of handover reduction. In [19], a fuzzy-based vertical handover algorithm taking data rate, delay and BER (along with other parameters such as cost and security) into consideration is proposed. The algorithm improves the process of wireless network selection, thus avoiding unnecessary handovers. Authors in [20] have proposed a QoS aware fuzzy-based vertical handover mechanism that considers data rate, latency, jitter and BER. The proposed work is found to be effective for selecting a wireless network that meets the requirements of different applications. The results show a reduction in average end-to-end delay and yield a moderate average bandwidth.

The above work clearly suggests that including QoS-related parameters improves the overall decision performance. This inevitably increases the overall number of decision parameters, which generally leads to an unacceptably long algorithm execution time ($\tau$). The time delay as a result of long $\tau$ imposes a serious restriction on the number of decision parameters that can be used in fuzzy-based decision algorithms. Thus, a new approach is needed that allows a relatively large number of decision parameters to be included and, at the same time, minimizes $\tau$.

## III. Adaptive Traffic Dependent Fuzzy-based HDS Design

We introduced the idea of traffic dependency and proposed an adaptive traffic dependent fuzzy-based handover decision system design (ATD design) in our previous published work [1]. The network selection performance of the ATD design was compared with a conventional monolithic fuzzy-based handover decision system (MHDS design) and a tailored MHDS designs. The ATD design was shown to have given significant improvement for the network selection process as well as a hugh reduction in $\tau$.

In our previous work [1], the simulation model did not take into account the fact that the output scores generated by the fuzzy engines follow a random process (the input parameter values are randomly selected). In this paper a statistical averaging procedure has been used to produce more reliable results.

In the new procedure, for each of the three traffic types (i.e., CBR, VBR and ABR), 1000 runs of simulations (one trial, $T$) were carried out by each HDS design. The performance criterion chosen was the percentage success ($PS$), defined as the number of times (expressed as a percentage) the HDS selected the wireless network that had the highest score among the three wireless networks and fully satisfied the QoS requirements. The QoS requirements for CBR and VBR traffics were taken from [17]. In the case of ABR traffic, the packet loss of 7% or less was used. Ten trials were carried out for each traffic and the average of 10 trials was taken as the final outcome, as shown in Figures 2, 3 and 4.

In addition, the WiMAX data range was extended from (3 - 6 Mbps) to (1 - 6 Mbps) in the new simulation model, which represents a more realistic WiMAX capability. The simulation model assumed the following network and traffic scenarios:

(i) Three wireless network technologies, namely, WLAN, WiMAX and Cellular (supporting High Speed Packet Access (HSPA), which supports data rate up to 7.2 Mbps).

(ii) One WLAN, one WiMAX and one Cellular to represent a heterogeneous networking environment.

(iii) Three applications (VoIP, video streaming and file transfer to represent CBR, VBR and ABR traffics, respectively) - VoIP application with voice CODEC (G.711) and a data rate of 64 kbps, video streaming application in H.264 coding format with a bit rate of 0.8–1 Mbps along with an encoded (ACC) audio signal at 96 kbps and file transfer application with a bit rate of 1 Mbps.

The range of values for decision parameters in Tables I, II and III were taken either from real-life tests or commonly used standards [21]–[25].

The simulation results show that the ATD design gives an improvement of 17.2% compared with the MHDS (MD1) design in the case of VoIP traffic (CBR traffic), depicted in Figure 2. However, the performance of tailored MHDS (MD2) design is identical to that of ATD design. This is to be expected as the two designs use identical FMFs and decision rules [1].

For the video streaming traffic (VBR traffic), depicted in Figure 3, the performance of ATD design is 15.71% and 25.49% better than the MD1 and MD2 designs, respectively.

In the case of file transfer traffic (ABR traffic), the performance of ATD design is 4.09% and 13.04% better than the MD1 and MD2 designs, respectively (in Figure 4).

The network selection performance of Simple Additive Weighting (SAW) algorithm is also compared with the ATD design and the results are shown in Figures 5, 6 and 7. The results show that the ATD design is 19.08%, 18.9% and 10.45% better than the SAW design for VoIP (in Figure 5), video streaming (in Figure 6) and file transfer traffics (in

TABLE I
Decision Parameters for CBR Traffic

| Network | DR (Mbps) | LA (ms) | JI (ms) | PL (%) | BA (hrs) | PR (p/min) |
|---|---|---|---|---|---|---|
| WLAN | 1 - 8 | | | | 2.5 - 5 | 1 |
| WiMAX | 1 - 6 | 0-300 | 0-50 | 0-1.5 | 0.55x(2.5-5) | 2 |
| Cellular | 1 - 5 | | | | 0.74x(2.5-5) | 3 |

TABLE II
Decision Parameters for VBR Traffic

| Network | DR (Mbps) | LA (s) | JI (ms) | PL (%) | BA (hrs) | PR (p/min) |
|---|---|---|---|---|---|---|
| WLAN | 1 - 8 | | | | 2.5 - 5 | 1 |
| WiMAX | 1 - 6 | 0-7 | | 0-7 | 0.55x(2.5-5) | 2 |
| Cellular | 1 - 5 | | | | 0.74x(2.5-5) | 3 |

TABLE III
Decision Parameters for ABR Traffic

| Network | DR (Mbps) | LA (s) | JI (ms) | PL (%) | BA (hrs) | PR (p/min) |
|---|---|---|---|---|---|---|
| WLAN | 1 - 8 | | | | 2.5 - 5 | 1 |
| WiMAX | 1 - 6 | | | 0-7 | 0.55x(2.5-5) | 2 |
| Cellular | 1 - 5 | | | | 0.74x(2.5-5) | 3 |

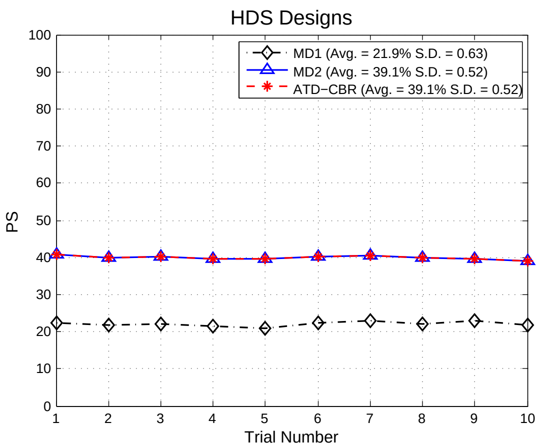


Figure 2. Network Selection Performance - VoIP

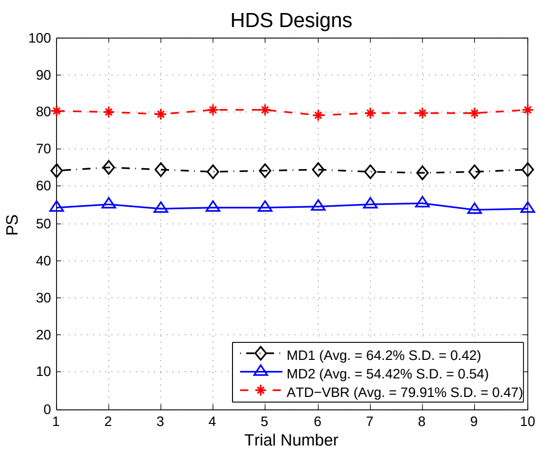


Figure 3. Network Selection Performance - Video Streaming

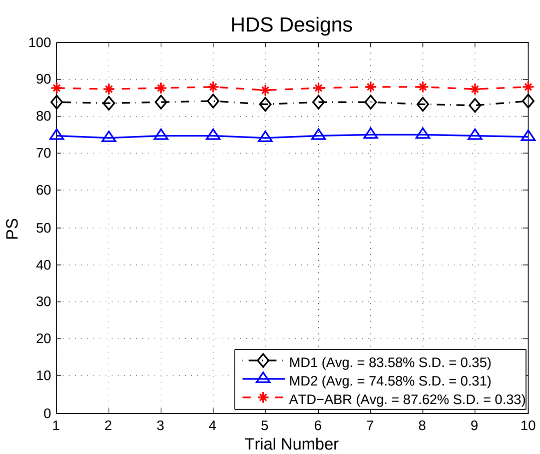


Figure 4. Network Selection Performance - File Transfer

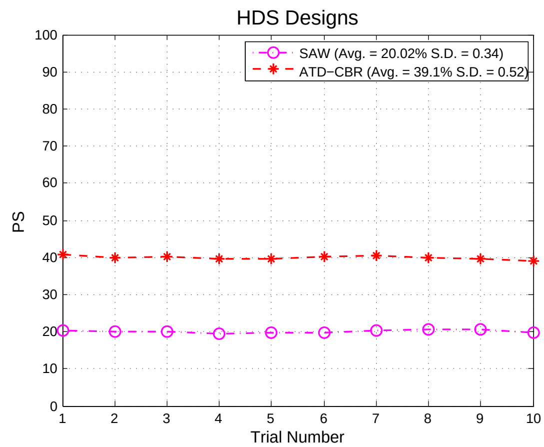


Figure 5. Network Selection Performance - VoIP

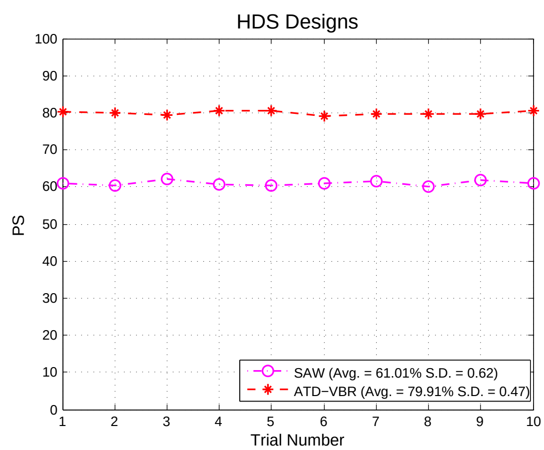


Figure 6. Network Selection Performance - Video Streaming

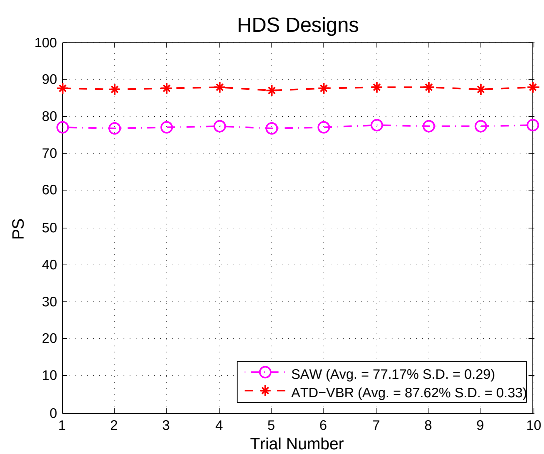


Figure 7. Network Selection Performance - File Transfer

Figure 7), respectively.

As has been mentioned in Section II, minimization of the algorithm execution time ($\tau$) is an important requirement for handover decision systems. The value of $\tau$ required for MD1, MD2, ATD and SAW designs was evaluted on a 2.13GHz Intel Core 2 Duo with 4GB memory. The simulation results (in Figure 8) show that the value of $\tau$ for MD1 and MD2 designs is 1.87 second for all the three traffic types. In the case of

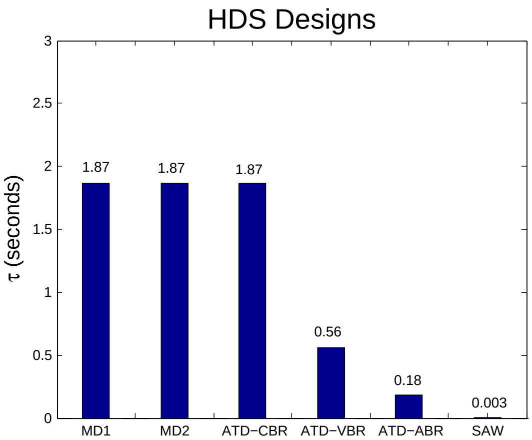


Figure 8. Algorithm Execution Time

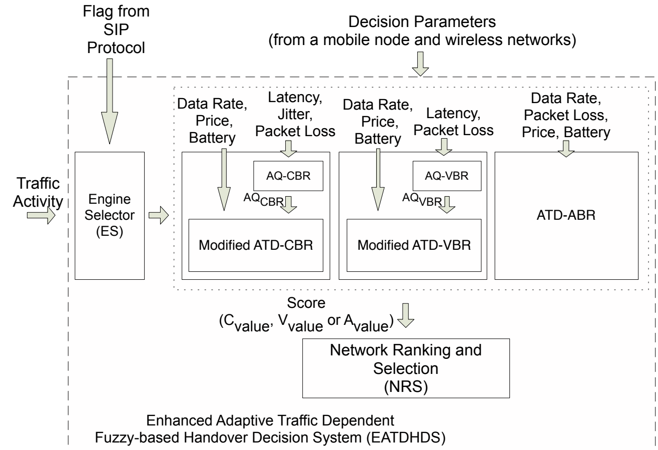


Figure 9. Architecture of EATDHDS

ATD design, the value of $\tau$ is 1.87 second, 0.56 second and 0.18 second for VoIP, video streaming and file transfer traffics, respectively.

The results clearly show that the proposed ATD design significantly reduces $\tau$ for video streaming (VBR) and file transfer (ABR) traffics when compared with MD1 and MD2 designs. The reduction in $\tau$ is 70.05% and 90.37% for video streaming and file transfer traffic, respectively. However, in the case of VoIP, there is no improvement in the value of $\tau$. It is to be expected as the three HDS designs (MD1, MD2 and ATD) employ the same number of decision rules.

Note that the $\tau$ of SAW design is lower than that of ATD design since SAW algorithm uses a simple mathematical function to calculate the score used for a decision making. Although, the value of $\tau$ in the case of SAW design is relatively low, the overall network selection performance of the ATD design is superior to SAW design. Therefore, it is more beneficial to use fuzzy-based algorithms for a handover decision.

## IV. Enhanced ATD Design (EATD Design)

The ATD design has been extended to include two additional fuzzy engines. The aims of the EATD design are: a) to improve overall network selection performance and b) to further reduce $\tau$. The network selection performance of ATD and EATD designs and the corresponding $\tau$ are compared.

The general architecture of enhanced adaptive traffic dependent fuzzy-based HDS (EATDHDS) is shown in Figure 9. The two new fuzzy engines, namely AQ-CBR and AQ-VBR, convert individual values of QoS parameters into an aggregated single value (AQ), i.e., $AQ_{CBR}$ and $AQ_{VBR}$ for CBR and VBR traffics, respectively. In the case of ABR traffic only one QoS parameter (packet loss) is relevant, thus no QoS aggregation is neccessary.

### A. AQ-CBR and AQ-VBR Engines

Each engine contains a specific set of FMFs and decision rules to match the corresponding traffic. The Engine Selector (ES) identifies the type of incoming traffic and the relevant engine is selected to perform a QoS aggregation process, which generates the corresponding AQ value ($AQ_{CBR}$ or $AQ_{VBR}$) as shown in Figure 10.

If VoIP (CBR) traffic is identified, three QoS parameters (latency (LA), jitter (JI) and packet loss (PL)), associated with the candidate wireless network, are directed to the AQ-CBR engine. The corresponding input fuzzy sets are denoted by $\widetilde{LA}$, $\widetilde{JI}$, and $\widetilde{PL}$. Each fuzzy set has three memberships (Low, Medium, High). The total number of decision rules required for this fuzzy engine is 27 (using equation 1 from [26]). Each decision rule is then assigned a decision output, which is based on expert knowledge. This process formulates an output fuzzy set, $\widetilde{AQ}_{CBR}$.

For video streaming (VBR) traffic, only two QoS parameters (i.e., latency (LA) and packet loss (PL)) are directed to the AQ-VBR engine. The corresponding input fuzzy sets for the VBR traffic are denoted by $\widetilde{LA}$, and $\widetilde{PL}$. Following the above principle, the total number of decision rules required for this fuzzy engine is 9 (using equation 1 from [26]) and the output fuzzy set is denoted by $\widetilde{AQ}_{VBR}$.

The crisp inputs (the values for each QoS parameter) are fuzzified and provided to fuzzy inference system (FIS). The aggregated fuzzified data, $\mu\widetilde{AQ}_{CBR}$ and $\mu\widetilde{AQ}_{VBR}$, are given by (equation 4 from [26]):

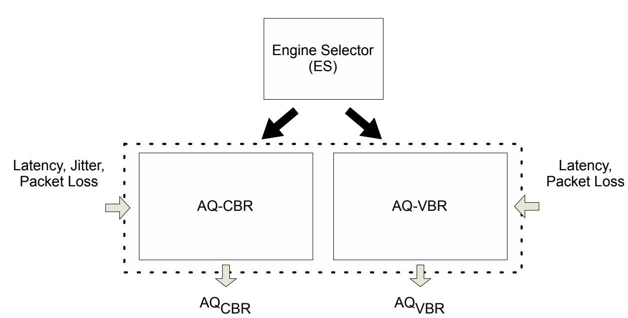


Figure 10. QoS Aggregation Engines

$$\mu\widetilde{AQ}_{CBR}(y) = max_k[min[\mu\widetilde{LA}^k(latency), \mu\widetilde{JI}^k(jitter), \mu\widetilde{PL}^k(packetloss)]], \text{ for k = 1, 2, \ldots, 27} \tag{1}$$

$$\mu\widetilde{AQ}_{VBR}(y) = max_k[min[\mu\widetilde{LA}^k(latency), \mu\widetilde{PL}^k(packetloss)]], \text{ for k = 1, 2, \ldots, 9} \tag{2}$$

Finally, defuzzifier converts the aggregated fuzzified data into crisp value. The values generated by AQ-CBR and AQ-VBR engines are $AQ_{CBR}$ and $AQ_{VBR}$, respectively (as shown in Figure 10). They are calculated using a centroid method, which are given by (equation 5 from [26]):

$$AQ_{CBR} = \frac{\int \mu\widetilde{AQ}_{CBR}(y).ydy}{\int \mu\widetilde{AQ}_{CBR}(y)dy} \tag{3}$$

$$AQ_{VBR} = \frac{\int \mu\widetilde{AQ}_{VBR}(y).ydy}{\int \mu\widetilde{AQ}_{VBR}(y)dy} \tag{4}$$

The $AQ_{CBR}$ and $AQ_{VBR}$ are then fed into the relevant decision engines (modified ATD-CBR or modified ATD-VBR) togerther with input decision parameters as shown in Figure 9.

Triangular and trapezoidal functions are used for fuzzy memberships in the design of input fuzzy sets for the AQ-CBR and AQ-VBR engines. The associated FMFs are shown in Figures 11 and 12. A small portion of the decision rules for the two AQ engines is shown in Tables IV and V.

TABLE IV
DECISION RULES FOR AQ-CBR ENGINE

| No. | Latency | Jitter | Packet Loss | Output |
|---|---|---|---|---|
| 1 | Low | Low | Low | High |
| 2 | Low | Low | Medium | MediumHigh |
| 3 | Low | Low | High | Low |
| 4 | Low | Medium | Low | MediumHigh |
| 5 | Low | Medium | Medium | Medium |
| : | : | : | : | : |
| 27 | High | High | High | Low |

TABLE V
DECISION RULES FOR AQ-VBR ENGINE

| No. | Latency | Jitter | Packet Loss | Output |
|---|---|---|---|---|
| 1 | Low | Low | Low | High |
| 2 | Low | Low | Medium | MediumHigh |
| 3 | Low | Low | High | Low |
| : | : | : | : | : |
| 9 | High | High | High | Low |

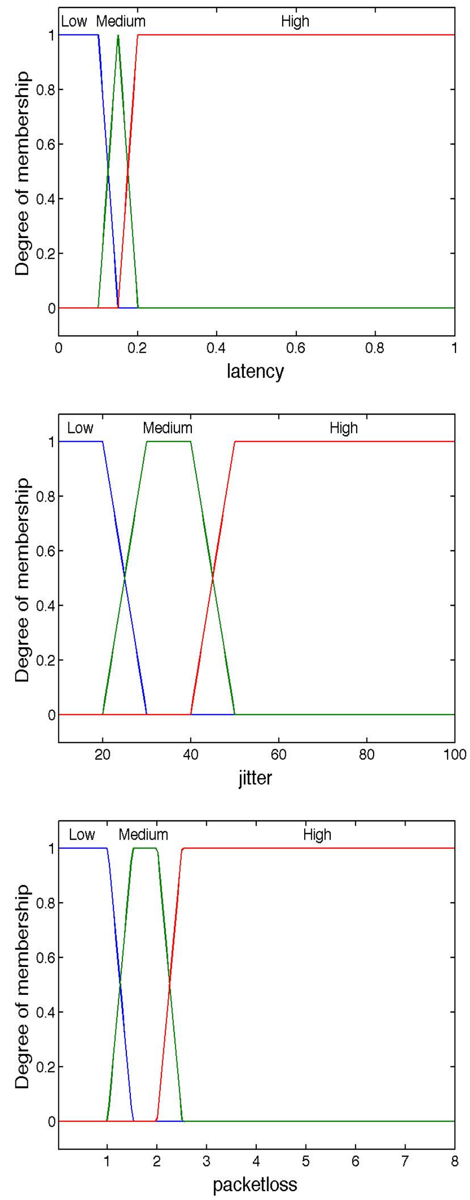


Figure 11. FMFs for AQ-CBR Engine

### B. Modified ATD-CBR, Modified ATD-VBR and ATD-ABR Decision Engines

As the QoS parameters are aggregated in the EATD design, fewer inputs are needed for the decision engines, i.e., data rate, usage price, battery life and $AQ_{CBR}$ for the ATD-CBR decision engine and data rate, usage price, battery life and $AQ_{VBR}$ for the ATD-VBR decision engine (as shown in Figure 9). As a result, the existing ATD-CBR and ATD-VBR decision engine designs needed to be modified. The ATD-ABR decision engine is identical to the ATD-ABR decision engine presented in the ATD design [1]. Note that due to the QoS aggregation process, the input parameters to the modified ATD-CBR and modified ATD-VBR decision engines have been reduced, which in turn

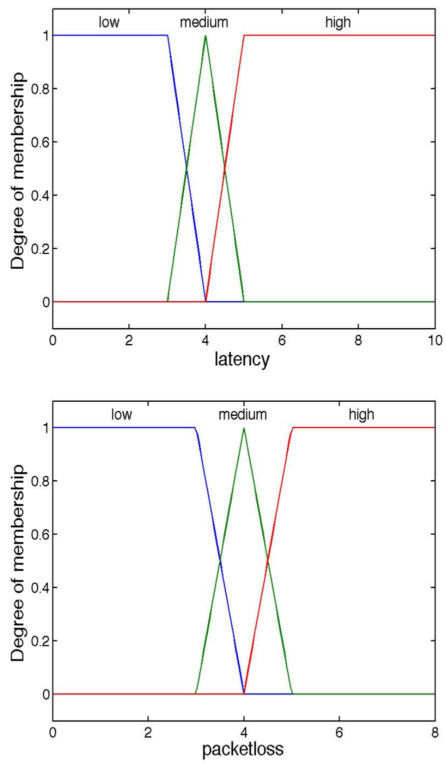


Figure 12. FMFs for AQ-VBR Engine

have reduced the total number of decision rules.

Then, the aggregrated fuzzified data generated by the modified ATD-CBR decision engine, $\mu\tilde{C}(y)$, modified ATD-VBR decision engine, $\mu\tilde{V}(y)$, and ATD-ABR decision engine, $\mu\tilde{A}(y)$, are given by (equation 4 from [26]):

$$\begin{aligned}\mu\tilde{C}(y) =& max_k[min[\mu\widetilde{DR}^k(datarate),\\ &\mu\widetilde{AQ}^k(AQ_{CBR}), \mu\widetilde{PR}^k(price),\\ &\mu\widetilde{BA}^k(battery)]],\\ &fork = 1, 2, 3, \ldots, 81\end{aligned} \tag{5}$$

$$\begin{aligned}\mu\tilde{V}(y) =& max_k[min[\mu\widetilde{DR}^k(datarate),\\ &\mu\widetilde{AQ}^k(AQ_{VBR}), \mu\widetilde{PR}^k(price),\\ &\mu\widetilde{BA}^k(battery)]],\\ &fork = 1, 2, 3, \ldots, 81\end{aligned} \tag{6}$$

$$\begin{aligned}\mu\tilde{A}(y) =& max_k[min[\mu\widetilde{DR}^k(datarate),\\ &\mu\widetilde{PL}^k(packetloss), \mu\widetilde{PR}^k(price),\\ &\mu\widetilde{BA}^k(battery)]],\\ &fork = 1, 2, 3, \ldots, 81\end{aligned} \tag{7}$$

where $k$ is the total number of rules.

The defuzzifier converts the aggregated fuzzified data into the score (i.e., $C_{value}$, $V_{value}$ and $A_{value}$ for the modified ATD-CBR, modified ATD-VBR and ATD-ABR decision engines, respectively) using the same principle as above (equation 3 and 4). The score (depending on the decision engine used) is then used by the NRS to rank the wireless networks. The wireless network with the highest score is selected for a handover.

The associated FMFs for the modified ATD-CBR, modified ATD-VBR and ATD-ABR decision engines are shown in Figures 13, 14 and 15, respectively. A small portion of the decision rules for the modified ATD-CBR and modified ATD-VBR decision engines is shown in Table VI. Table VII shows a small portion of the decision rules for the ATD-ABR decision engine.

### C. Simulation Results, Comparisons and Discussion

Based on the simulation procedure given in Section III, the performance of EATD design was evaluated. The results are compared with the ATD design in Figures 16 and 17 for VoIP and video streaming traffics, respectively.

The results in Figure 16 show that the network selection performance of the EATD design is 4.28% better than the ATD design for VoIP traffic. In the case of video streaming traffic (Figure 17), the improvement is 3.36%.

The algorithm execution time ($\tau$) of the ATD and EATD designs is also compared (shown in Figure 18) for the two traffic types (VoIP and video streaming). The results show that $\tau$ of the EATD design is reduced to 0.25 second for VoIP traffic. This gives a reduction of 86.6% when compared with the ATD design. In the case of video streaming traffic, $\tau$ is reduced to 0.21 second. A reduction of 62.5% is achieved.

The network selection performance is improved due to the fact that fewer decision rules facilitate relatively more accurate assignment of the corresponding decision outputs, which are based on expert knowledge. The reduction in $\tau$ is due to QoS

TABLE VI
DECISION RULES FOR THE MODIFIED ATD-CBR AND ATD-VBR DECISION ENGINES

| No. | DR | AQ | PR | BA | Output |
|---|---|---|---|---|---|
| 1 | Low | Low | Low | Low | Low |
| 2 | Low | Low | Low | Medium | Low |
| 3 | Low | Low | Low | High | Low |
| : | : | : | : | : | : |
| 79 | High | High | High | High | Medium |
| 80 | High | High | High | Medium | MediumHigh |
| 81 | High | High | High | High | High |

TABLE VII
DECISION RULES FOR THE ATD-ABR DECISION ENGINE

| No. | DR | AQ | PR | BA | Output |
|---|---|---|---|---|---|
| 1 | Low | Low | Low | Low | MediumLow |
| 2 | Low | Low | Low | Medium | Medium |
| 3 | Low | Low | Low | High | MediumHigh |
| : | : | : | : | : | : |
| 79 | High | High | High | High | VeryLow |
| 80 | High | High | High | Medium | VeryLow |
| 81 | High | High | High | High | Low |

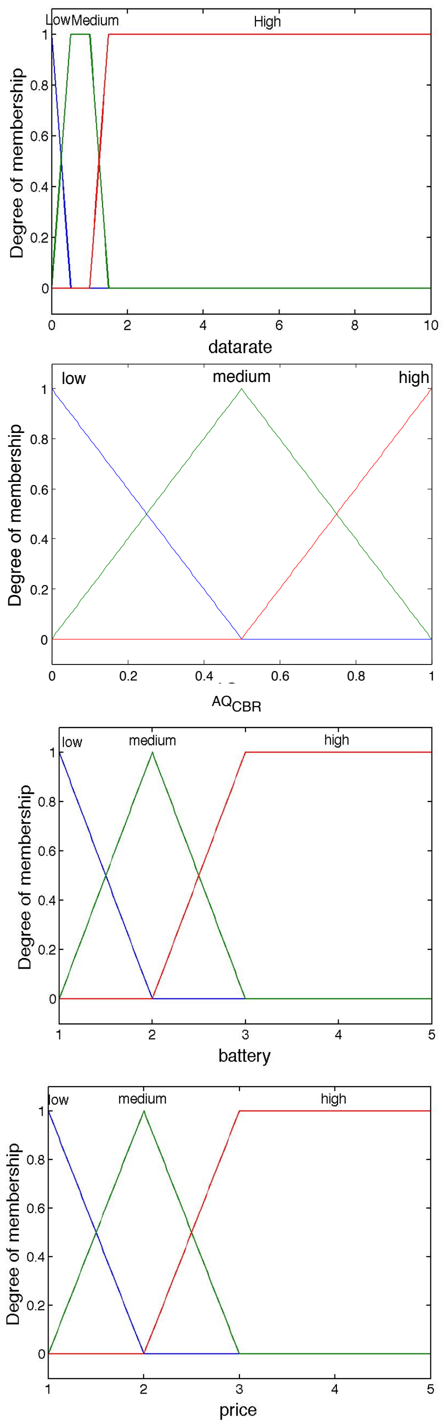


Figure 13. FMFs for The Modified ATD-CBR Decision Engine

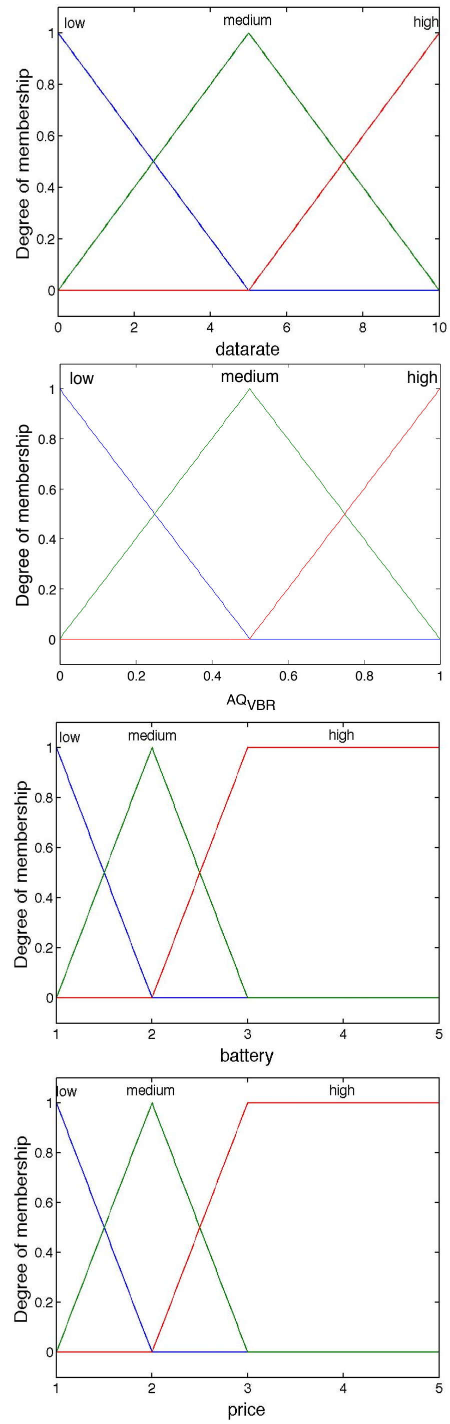


Figure 14. FMFs for The Modified ATD-VBR Decision Engine

aggregation process. The modified ATD-CBR and modified ATD-VBR decision engines require just 81 decision rules when compared with 729 and 243 decision rules required by the ATD-CBR and ATD-VBR decision engines, respectively.

### D. Battery Consumption Analysis

Our comparison of fuzzy-based algorithms with SAW algorithm reveals that the superiority of fuzzy-based algorithm comes at a price, i.e., the algorithm execution time of even the best (EATD) decision engine is higher than that required by the SAW. This raises the issue of power consumption and

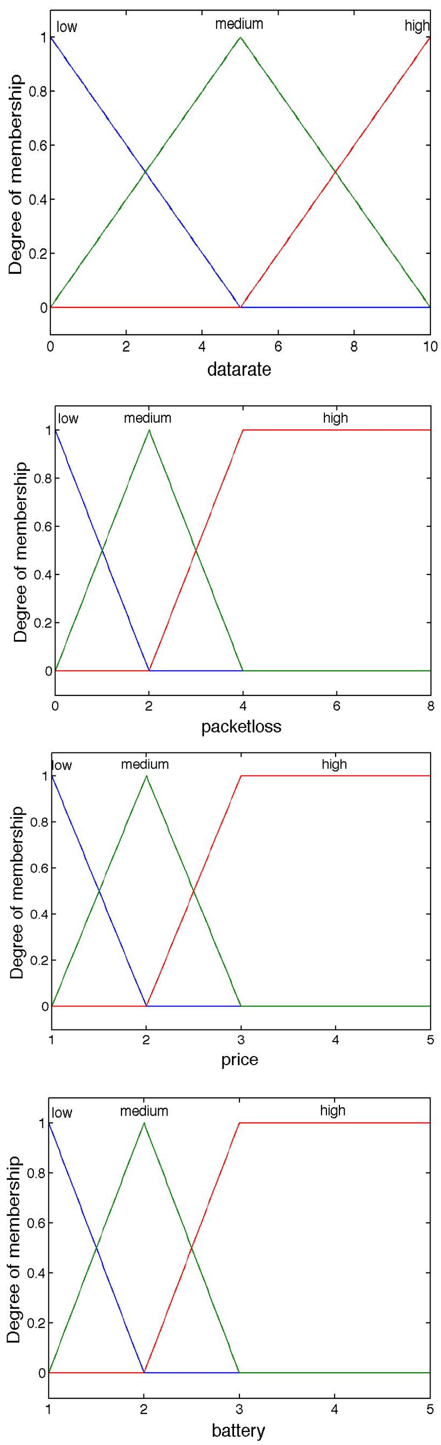


Figure 15. FMFs for the ATD-ABR Decision Engine

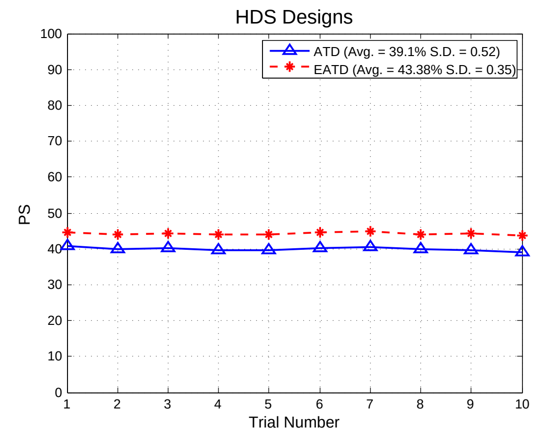


Figure 16. Network Selection Performance - VoIP

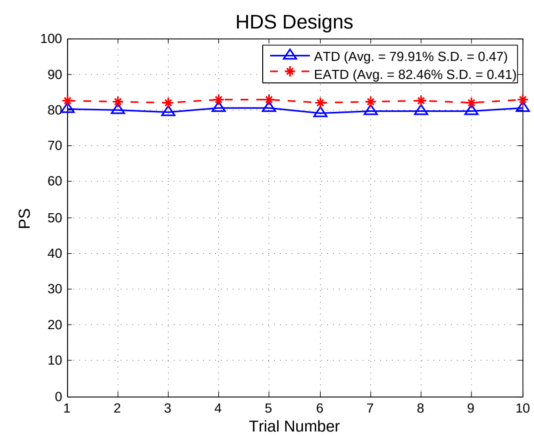


Figure 17. Network Selection Performance - Video Streaming

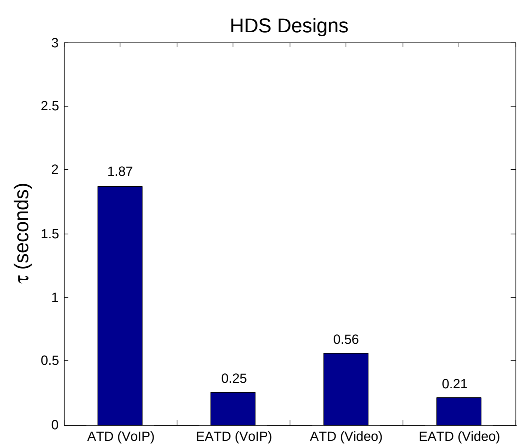


Figure 18. Algorithm Execution Time

the recharging frequency for the battery. In order to address these issues we have made some projections based on the data available to us.

Our simulations were carried out on MATLAB platform using Intel processor of 65watts rating. The longest $\tau$ required by the decision engine (worst case for the EATD design) is 0.25 seconds (shown in Figure 18). Therefore, the power consumption for the worst case = 65x0.25 = 16.25 watt-seconds or 0.0045 watt-hours. Now the battery capacity of a modern smart phone is around 5.5 watt-hour. Thus, a smart phone can execute the above algorithm around 1222 times

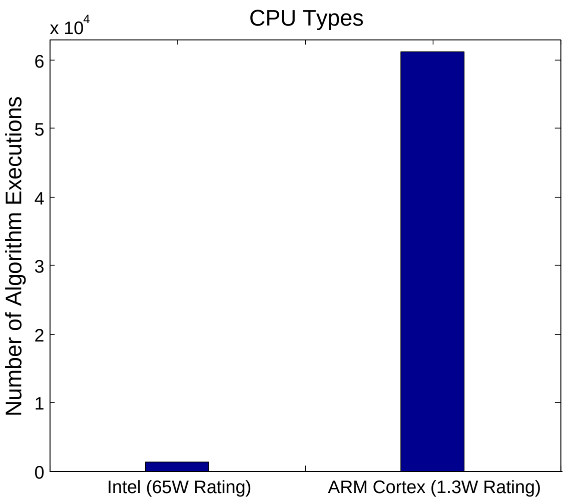


Figure 19. Intel-based vs. ARM-based Processor

as shown in Figure 19 (this does not include the power consumption of other components) before the battery needs recharging.

If we now consider a processor that is actually used in mobile devices (e.g., ARM Cortex A series of approximately 1.3 watts rating), the estimated power consumption reduces to 0.00009 watt-hour. Assuming the same battery as above, a smart phone can execute the algorithm for over 61,111 times (in Figure 19) before the need for recharging. Significant improvement in terms of battery consumption has been observed here. Further improvements will come from the fact that an actual mobile device is likely to use dedicated and embedded software, or dedicated hardware (e.g., FPGA [27], [28]) instead of MATLAB platform to run fuzzy algorithm. This will further reduce $\tau$ and hence the power consumption.

### *E. Discussion*

We have addressed the two main issues concerned with the vertical handover decision mechanisms that are widely proposed in the literature. In these mechanisms, a) a single monolithic fuzzy decision engine is generally proposed, and b) the decisions for network selection are made with no regard to traffic type. The former concern restricts the number of decision parameters that can be included in the decision process. This restriction arises due to the fact that as the number of decision parameters increases, the number of decision rules increases exponentially, resulting in computational complexity and an unacceptably long algorithm execution time ($\tau$). However, for real-time applications it becomes very important to include the QoS-related parameters in the decision process, which inevitably increases the overall number of decision parameters. The latter concern impairs the quality of network selection. This limitation on the network selection performance arises due to the fact that a single monolithic decision engine cannot possibly perform equally well for all the different types of traffics.

In order to deal with the above issues we have suggested an adaptive traffic dependent handover decision system (ATDHDS). In our approach multiple decision engines, each dedicated to a specific traffic type, have been proposed. This is achieved by tailoring FMFs to match the QoS requirements of each individual traffic type. As only those QoS parameters that are relevant to a given traffic type are included in the corresponding decision engines, the number of decision rules required for video streaming and file transfer traffics has been reduced, compared with a typical monolithic fuzzy-based handover decision system (MHDS). In the case of VoIP, the two HDS designs have the same number of decision rules. The simulation results show that the ATD design gives a significant improvement in terms of network selection performance and a reduction in $\tau$.

The ATD design has been further enhanced by introducing additional fuzzy engines, which perform a QoS aggregation process for the CBR and VBR traffics. The additional fuzzy engines allow the total number of decision rules required for the enhanced ATD design (EATD design) to be further reduced, which leads to further reduction in $\tau$. Furthermore, fewer decision rules facilitate relatively more accurate assignment of the decision outputs of fuzzy decision engines. As a result, the network selection performance has been enhanced and the value of $\tau$ has been further reduced (for the CBR and VBR traffics).

Finally, the battery life analysis has been carried out and it has been shown that the power consumption of the proposed fuzzy-based algorithm is unlikely to have a major impact on the battery life in real-life implementations.

## V. Conclusion and Future Work

In our previous work, we introduced the idea of traffic dependency and proposed an adaptive traffic dependent fuzzy-based handover decision system (ATDHDS). In this paper, a new simulation model, which includes a statistical averaging procedure, has been used in order to produce more reliable simulation results.

For evaluation and comparison purposes, three handover decision system designs, namely MHDS design 1 (MD1), MHDS design 2 (MD2) and ATD design, have been developed. Assuming a heterogeneous networking environment and three traffic types (CBR, VBR and ABR), simulation results have been produced to compare the network selection performance and the algorithm execution time of the three HDS designs. In addition, the performance of SAW design has also been compared with the ATD design.

In terms of the network selection performance, the simulation results show that the ATD design gives an improvement of 17.2%, 15.71% and 4.09% for VoIP, video streaming and file transfer traffics, respectively when compared with MD1, and 19.08%, 18.9% and 10.45% for VoIP, video streaming and file transfer traffics, respectively when compared with SAW design.

In the case of VoIP the network selection performance of ATD and MD2 is identical as the two designs use identical

FMFs and decision rules. However, the ATD design is 25.49% and 13.04% better than the MD2 design for video streaming and file transfer traffics, respectively. This result clearly suggests that comparing with MD1, the performance of MD2 has degraded for video streaming and file transfer traffics. The reason for this degradation is that the FMFs and decision rules used for the video steaming and file transfer traffics are in fact tailored to match the VoIP traffic. In other words, the MD2 design is biased towards VoIP traffic, hence rendering this design less attractive for the other two traffics. We conclude that for optimum performance the FMFs and the decision rules must be matched to each individual traffic type.

In terms of $\tau$, the results show that the ATD design gives an improvement of over 70% and 90% for video streaming and file transfer traffics, respectively when compared with MD1 and MD2 designs. In the case of VoIP, $\tau$ has the same value for all the three designs, since the three designs use the same number of decision rules for VoIP traffic.

The ATD design has been further enhanced to include a QoS aggregation process. The EATD design has been presented and the performance compared. The simulation results show that the network selection performance of EATD design is 4.28% and 3.36% better than that of the ATD design for VoIP and video streaming traffics, respectively. At the same time a reduction of 86.6% and 62.5% in the value of $\tau$ has been achieved by the EATD design for VoIP and video streaming traffics, respectively.

Future work will focus on further enhancement of intelligence of the decision mechanisms, especially when mobility related parameters are considered (e.g., velocity, coverage area, distance, direction of movement, etc.). It is envisaged that the algorithm execution time will be even a greater challenge when mobility related parameters are included in the decision process. Thus, development of new algorithms that require significantly reduced execution time will be part of our future work.

## ACKNOWLEDGEMENT

The authors would like to express their thanks to the Vincent Mary School of Science and Technology, Assumption University, Thailand and the Faculty of Engineering, Science and the Built Environment, London South Bank University, UK for the support provided to carry out this research.

## REFERENCES

[1] T. Thumthawatworn, A. Pervez, and P. Santiprabhob, "Adaptive traffic dependent fuzzy-based vertical handover for wireless mobile network," *12th International Conference on Networks (ICN)*, pp. 112–117, 2013.

[2] J. Oliveira Filho and E. Madeira, "A mechanism for vertical handover based on SAW using IEEE 802.21," *Mobile Networks and Management, vol. 68 of Lecture Notes of the Institute for Computer Sciences, Social Informatics and Telecommu- nications Engineering*, pp. 96 –108, 2011.

[3] Q. He, "A novel vertical handover decision algorithm in heterogeneous wireless networks," *IEEE International Conference on Wireless Communications, Networking and Information Security (WCNIS)*, pp. 566 –570, 2010.

[4] C. Kwong, S. Lee, and M. Sim, "Mobility management incorporating pattern recognition in the handover decision," *International Conference on Advanced Computer Control (ICACC)*, pp. 737 –741, 2009.

[5] W. Zhang, "Handover decision using fuzzy MADM in heterogeneous networks," *IEEE Wireless Communications and Networking Conference (WCNC)*, vol. 2, pp. 653–658, 2004.

[6] K. Savitha and C. Chandrasekar, "Vertical handover decision schemes using SAW and WPM for network selection in heterogeneous wireless networks," *Global Journal of Science and Technology*, vol. 11, pp. 19 –24, 2011.

[7] M. Ben Ghalia and P. Wang, "Intelligent system to support judgmental business forecasting: the case of estimating hotel room demand," *IEEE Transactions on Fuzzy Systems*, vol. 8, pp. 380–397, 2000.

[8] A. Esfahanipour and P. Mardani, "An ANFIS model for stock price prediction: The case of tehran stock exchange," *International Symposium on Innovations in Intelligent Systems and Applications (INISTA)*, pp. 44–49, 2011.

[9] A. Ezzouhairi, A. Quintero, and S. Pierre, "A fuzzy decision making strategy for vertical handovers," *Canadian Conference on Electrical and Computer Engineering (CCECE)*, pp. 583–588, 2008.

[10] P. Chan, Y. Hu, and R. Sheri, "Implementation of fuzzy multiple objective decision making algorithm in a heterogeneous mobile environment," *IEEE Wireless Communications and Networking Conference (WCNC)*, vol. 1, pp. 332–336, 2002.

[11] K. Radhika and A. Reddy, "Network selection in heterogeneous wireless networks based on fuzzy multiple criteria decision making," *3rd International Conference on Electronics Computer Technology (ICECT)*, vol. 6, pp. 136–139, 2011.

[12] F. Zhu and F. MacNair, "Optimizations for vertical handoff decision algorithms," *IEEE Wireless Communications and Networking Conference (WCNC)*, no. 2, pp. 867–872, 2004.

[13] C. G. Patil and M. T. Kolte, "An approach for optimization of handoff algorithm using fuzzy logic system," *International Journal of Computer Science and Communication*, vol. 2, no. 1, pp. 113–118, 2011.

[14] T. Jun, Z. Ying Jiang, Z. Zhi, Y. Zhi Wei, and C. Zhi Lan, "Performance analysis of vertical handoff in wifi and wimax heterogeneous networks," *International Symposium on Computer Network and Multimedia Technology (CNMT)*, pp. 1 –15, jan. 2009.

[15] M. Sharma and R. K. Khola, "An intelligent approach for handover decision in heterogeneous wireless environment," *International Journal of Engineering (IJE)*, vol. 4, no. 5, pp. 452–462, 2010.

[16] Q. He, "A fuzzy logic based vertical handoff decision algorithm between WWAN and WLAN," *International Conference on Networking and Digital Society*, pp. 561–564, 2010.

[17] T. Szigeti and C. Hattingh, "Quality of Service Design Overview," *CISCO Press*, [Online Access] Available: http://www.ciscopress.com/articles/article.asp?p=357102&seqNum=3

[18] K. C. Foong, C. T. Chee, and L. S. Wei, "Adaptive network fuzzy inference system (ANFIS) handoff algorithm," *Conference on Future Computer and Communication*, pp. 195–198, 2009.

[19] Y. Chen, J. Ai, and Z. Tan, "An access network selection algorithm based on hierarchy analysis and fuzzy evaluation," *International Conference on Wireless Communications and Signal Processing (WCSP)*, pp. 1–5, 2009.

[20] K. Vasu, S. Maheshwari, S. Mahapatra, and C. S. Kumar, "QoS aware fuzzy rule based vertical handoff decision algorithm for wireless heterogeneous networks," *17th National Conference on Communication (NCC)*, 2011.

[21] Real-life Speed Test for WLAN [Online Access] Available: http://www.pantip.com/cafe/mbk/topic/T11689772.html

[22] Real-life Speed Test for WiMAX [Online Access] Available: http://www.clear.com/coverage

[23] Real-life Speed Test for Cellular [Online Access] Available: http://www.pantip.com/cafe/mbk/topic/T11594482.html

[24] Battery Life Testing [Online Access] Available: http://www.anandtech.com/Show/Index/4643?cPage=3&all=False&sort=0&page=7&slug=htc-evo-3d-vs-motorola-photon-4g-best-sprint-phone

[25] QoS Concepts, [Online Access] Available: http://www.cisco.com/en/US/docs/net_mgmt/ip_solution_center/3.0/qos/user/guide/concepts.html

[26] T. Thumthawatworn, A. Pervez, and P. Santiprabhob, "Adaptive modular fuzzy-based handover decision system for heterogeneous wireless network," *International Journal of Networks and Communications*, vol.3, no.2, pp. 25-38, 2013.

[27] D.C. Sati, P. Kumar, and Y. Misra, "FPGA implementation of a fuzzy logic based handoff controller for microcellular mobile networks,"

*International Journal of Applied Engineering Research*, vol. 1, no. 1, pp. 52-62, 2011

[28] R. Sepulveda, O. Montiel-Ross, J. Quinones-Revera, and E. E. Quiroz, "WLAN cell handoff latency abatement using an FPGA fuzzy logic algorithm implementation," *Advances in Fuzzy Systems*, vol. 2012, Article ID 219602, 2012.


**www.iariajournals.org**

**International Journal On Advances in Intelligent Systems**

ICAS, ACHI, ICCGI, UBICOMM, ADVCOMP, CENTRIC, GEOProcessing, SEMAPRO, BIOSYSCOM, BIOINFO, BIOTECHNO, FUTURE COMPUTING, SERVICE COMPUTATION, COGNITIVE, ADAPTIVE, CONTENT, PATTERNS, CLOUD COMPUTING, COMPUTATION TOOLS, ENERGY, COLLA, IMMM, INTELLI, SMART, DATA ANALYTICS

issn: 1942-2679

**International Journal On Advances in Internet Technology**

ICDS, ICIW, CTRQ, UBICOMM, ICSNC, AFIN, INTERNET, AP2PS, EMERGING, MOBILITY, WEB

issn: 1942-2652

**International Journal On Advances in Life Sciences**

eTELEMED, eKNOW, eL&mL, BIODIV, BIOENVIRONMENT, BIOGREEN, BIOSYSCOM, BIOINFO, BIOTECHNO, SOTICS, GLOBAL HEALTH

issn: 1942-2660

**International Journal On Advances in Networks and Services**

ICN, ICNS, ICIW, ICWMC, SENSORCOMM, MESH, CENTRIC, MMEDIA, SERVICE COMPUTATION, VEHICULAR, INNOV

issn: 1942-2644

**International Journal On Advances in Security**

ICQNM, SECURWARE, MESH, DEPEND, INTERNET, CYBERLAWS

issn: 1942-2636

**International Journal On Advances in Software**

ICSEA, ICCGI, ADVCOMP, GEOProcessing, DBKDA, INTENSIVE, VALID, SIMUL, FUTURE COMPUTING, SERVICE COMPUTATION, COGNITIVE, ADAPTIVE, CONTENT, PATTERNS, CLOUD COMPUTING, COMPUTATION TOOLS, IMMM, MOBILITY, VEHICULAR, DATA ANALYTICS

issn: 1942-2628

**International Journal On Advances in Systems and Measurements**

ICQNM, ICONS, ICIMP, SENSORCOMM, CENICS, VALID, SIMUL, INFOCOMP

issn: 1942-261x

**International Journal On Advances in Telecommunications**

AICT, ICDT, ICWMC, ICSNC, CTRQ, SPACOMM, MMEDIA, COCORA, PESARO, INNOV

issn: 1942-2601